THE UNIVERSITY of ADELAIDE

Investigation of KLF5 Function in Normal Haemopoiesis

Nur Hezrin Shahrin, B. Sc (Biotechnology) (Hons.)

A thesis submitted for the degree of Doctor of Philosophy

in the School of Molecular & Biomedical Science

at the University of Adelaide

Acknowledgement

I would like to thank all of the staff and students at the Institute of Medical and Veterinary Science where this research was undertaken, and in particular my colleagues and friends in the Acute Leukaemia Laboratory for their help and support, both scientific and non-scientific, during my undertaking of this program. I also want to thanks the University of Adelaide for their financial support and resources. Thank you also to the staff and students at the University of Adelaide and the Discipline of Genetics.

A special thanks to my supervisors, Prof. Richard D'Andrea and Dr. Anna Brown in providing continuous support, encouragement, and scientific advice throughout my project.

To my parents; Mr Shahrin Osman and Mrs Ahmisa Abdul Salam, my in-laws; Mr Shamsudin and Mrs Jamaliah, my siblings; Harmimi Eni Liana, Nur Raihana and Nur Hafizah and close friends especially Dr Noor Alia Lokman, thanks a lot for all their encouragement and support over these years especially throughout the final year, I dearly appreciate the continuing motivation all of you have given to me.

I would like to say thanks to my lovely husband, Mohd Annas Shamsudin, I am truly appreciative of all that you have done for me over the years. I could not have reached my goals without your help and support at all times. You have made me feel special even when times were tough for me. You have been my pillar of strength through all my ups and downs. I feel blessed to be a part of your life, and am fortunate to be married to the most kind-hearted and generous person I have ever known.

Last but not least, thanks to my little boy, Adyan Hamzah for your patience when mama has to leave you all day in accomplishing this mission.

Contents

List of Figures

List of Tables

Abbreviations

ACK	Ammonium, Chloride, Potassium
AML	acute myeloid leukaemia
AngII	angiotensin II
APC	adenomatous polyposis coli
APL	acute promyelocytic leukaemia
ATF3	activating transcription factor 3
Atg	*Autophagy*
BM	Bone marrow
C/EBP	CCAAT-enhancer-binding proteins
CBC	complete blood counts
CFU	erythroid progenitor
CFU Assay	colony-forming unit assays
CFU-E/BFU-E	erythroid colony forming cells
CHO	Chinese hamster ovary
CLP	common lymphoid progenitors
CMP	common myeloid progenitors
Dpc	days postcoitum
DSS	dextran sodium sulphate
Egr-1	epidermal growth factor receptor
EKLF	Erythroid Krüppel-like factor
EKLFTAD2	transactivation domain 2 of KLF1
ER	estrogen receptor

ESCC	esophageal squamous cell cancer
ESCs	embryonic stem cells
FASN	fatty acid enzyme
FGF-BP	fibroblast growth factor binding protein 1
FISH	fluorescent in situ hybridization
FS	forward scatter
G-CSF	Granulocyte-colony stimulating factor
GM	Granulocyte-Macrophage
GMP	granulocyte-macrophage progenitors
Hct	Haematocrit
HE	haematoxylin and eosin
Hgb	Haemoglobin
HRP	horseradish peroxidase
HSC	haemopoietic stem cells
HSPC	haemopoietic stem and progenitor cell
IBD	inflammatory bowel disease
ICM	inner cell mass
JNK	c-Jun N-terminal kinase
Klf5-KO	*Klf5* knockout
KLFE	KLF-binding element
KLFs	*Krüppel-like factors*
KO	knockout
LOH	Loss-of-heterozygosity

LT-HSC	long-term HSC
MAPK	Ras-mitogen-activated protein kinase
MCH	Mean Corpuscular Haemoglobin
MCHC	Mean Corpuscular Haemoglobin Concentration
MCV	Mean Corpuscular Volume
MEP	megakaryocyte-erythrocyte progenitor
MkP	megakaryocyte progenitor
MPO	myeloperoxidase
MPP	potent progenitor
PAGE	SDS-Polyacrylamide Gel Electrophoresis
PAH	pulmonary arterial hypertension
PASMC	pulmonary artery smooth muscle cell
PB	Peripheral blood
PCR	Polymerase Chain Reaction
PE	primitive endoderm
PKC	lisophosphatidic acid and non-canonical Wnt signalling
preCFU	early erythroid progenitor
preGM	primitive granulocyte-macrophage progenitors
preMEGE	primitive erythroid/megakaryocyte progenitor
QIMR	Queensland Institute of Medical Research
QPCR	Quantitative reverse transcription PCR
Rb	*Retinoblastoma*
RBC	red blood cell

SDS	Sodium Dodecyl Sulfate
SID	Sin3a-interacting domain
SM	Sample Media
Socs3	*suppressor of cytokine signalling-3*
SS	side scatter
ST-HSC	short-term HSC
TAC	Tris Ammonium Chloride
TAD	transactivation domain
TAZ	PDZ-binding motif
TE	trophectoderm
TFs	transcription factors
VSMCs	vascular smooth muscle cells
WBC	white blood cell
YAP	Yes-associated protein

Abstract

Krüppel-like factor 5 (KLF5) is a zinc-finger transcription factor known to have regulatory roles in the growth and differentiation of many adult tissues. In humans, *KLF5* is located at 13q21-22, which is frequently lost in multiple tumour types, including tumours of the breast, endometrium, ovary and prostate where it is associated with loss of *KLF5* expression. Little is known about the potential role of KLF5 in the haemopoietic system. Previous work by us and others has shown that KLF5 has a functional role in induction of differentiation of the myeloid compartment. In acute myeloid leukaemia (AML), our group has previously show that *KLF5* expression is reduced relatively to normal $CD34^{+}$ cells and that reduction of expression is associated with hypermethylation in intron 1. We also found that hypermethylation of *KLF5* was associated with poor outcome, identifying KLF5 as an important target for further investigation in haemopoiesis and particularly the myeloid compartment. To extend the functional analysis of *Klf5*, an *in vivo* gene-ablation model was generated. As non-conditional *Klf5* knockout mice (KO) die at embryonic day 8.5, pan-haemopoietic *Klf5* conditional gene KO mice were generated by crossing $Klf5^{fl/fl}$ mice with *Vav-cre* transgenic mice. The $Klf5^{fl/fl}Vav\text{-}cre^{+/-}$ and $Klf5^{fl/fl}$ mice were analysed at 3, 9 and 12 month of age for defects in steady state haemopoiesis. Peripheral blood (PB) analysis of 9 and 12 month old mice revealed that $Klf5^{fl/fl}Vav\text{-}cre^{+/-}$ animals displayed significantly higher values for total white blood cell (WBC) count. To further characterise the changes in blood cell populations, flow cytometry was used with a range of different lineage antibody markers. The peripheral blood data indicated a decrease in the granulocytes of $Klf5^{fl/fl}Vav\text{-}cre^{+/-}$ mice as well as an increase in the T-cell compartment.

Interestingly, we also showed that the *Klf5*$^{fl/fl}$*Vav-cre*$^{+/-}$ mice have increased numbers of blood and bone marrow eosinophils compared to *Klf5*$^{fl/f}$ mice. Consistently, we found significantly increased numbers of eosinophils in the lungs of *Klf5*$^{fl/fl}$*Vav-cre*$^{+/-}$ mice compared to *Klf5*$^{fl/fl}$ mice. The spleen weight of *Klf5*$^{fl/fl}$*Vav-cre*$^{+/-}$ mice was significantly higher compared to *Klf5*$^{fl/fl}$ mice. In addition, clonal assays conducted from the spleen of 9 and 12 month old mice showed a significant increase in colony number in the *Klf5*$^{fl/fl}$*Vav-cre*$^{+/-}$ mice compared to *Klf5*$^{fl/fl}$ mice. This correlated with the flow cytometry data which showed a significant increase in haemopoietic stem cell (HSC) populations; short-term HSC (ST-HSC) and multipotent progenitor (MPP) in the spleen of *Klf5*$^{fl/fl}$*Vav-cre*$^{+/-}$ mice. In summary, this study revealed multiple functional roles for Klf5 in haemopoiesis. Firstly, these studies demonstrated that as predicted losing *Klf5* leads to alterations in the development of the myeloid compartment. Secondly, we showed that the stem cell compartments (ST-HSC and MPP) were significantly increased in the spleen of *Klf5*$^{fl/fl}$*Vav-cre*$^{+/-}$ mice compared to *Klf5*$^{fl/fl}$ mice, which also correlated with extra-medullary splenic haemopoiesis and increased spleen size. Finally, the increase in T-cells for the *Klf5*$^{fl/fl}$*Vav-cre*$^{+/-}$ mice suggests a possible previously unidentified functional role for Klf5 outside the myeloid compartment.

Declaration

This work contains no material which has been accepted for the award of any other degree or diploma in any university or other tertiary institution to Nur Hezrin Shahrin and, to the best of my knowledge and belief, contains no material previously published or written by another person, except where due reference has been made in the text. With respect to my relative contribution in each of the experimental Chapters, I certify that I carried out all of the experimentation described except where duly noted in the text.

I give consent to this copy of my thesis, when deposited in the University Library, being made available for loan and photocopying, subject to the provisions of the Copyright Act 1968.

I also give permission for the digital version of my thesis to be made available on the web, via the University's digital research repository, the Library catalogue, the Australasian Digital Theses Program (ADTP) and also through web search engines, unless permission has been granted by the University to restrict access for a period of time.

NUR HEZRIN SHAHRIN

November 2014

Chapter 1: Literature Review

1.1 Haemopoiesis

Haemopoiesis is a continuous process that produces blood cellular components throughout life. All blood cells are generated from multipotent haemopoietic stem cells (HSC) in the haemopoietic organs, mainly the bone marrow (reviewed in *Seke et al.*) [1]. HSC have a unique property where they can either sustain a certain number of HSC by self-renewal as well as having the potential to differentiate into either common lymphoid (CLP) or myeloid (CMP) progenitors that subsequently commit to further development along a particular pathway (Figure 1.1) (reviewed in *Seita and Weissman*) [2]. Many models have been proposed suggesting that this process involves irreversible determination of the fate between myeloid and lymphoid lineages (reviewed in *Ceredig et al.*) [3]. Haemopoietic lineage specification is determined by intrinsic (transcription factors) and extrinsic factors (haemopoietic growth factors) [4, 5]. In normal conditions, both of these factors should act in a lineage-specific manner to support the growth and survival of haemopoietic progenitors or to alter mature cell function [6, 7]. Interestingly, lineage specificity is also conferred by the restricted expression of the cognate cytokine receptors [8-10]. Moreover, differentiation of normal haemopoietic stem cells into their mature progeny also depends on a fine-tuned interplay of haemopoietic transcription factors (TFs) [6]. Thus, co-ordination of the cytokine-induced signalling events with the activity of lineage specific TFs will result in specific proliferation and differentiation programs which if perturbed can occur amplification of particular lineages and lead to unwanted events such as the leukaemic development of diseases.

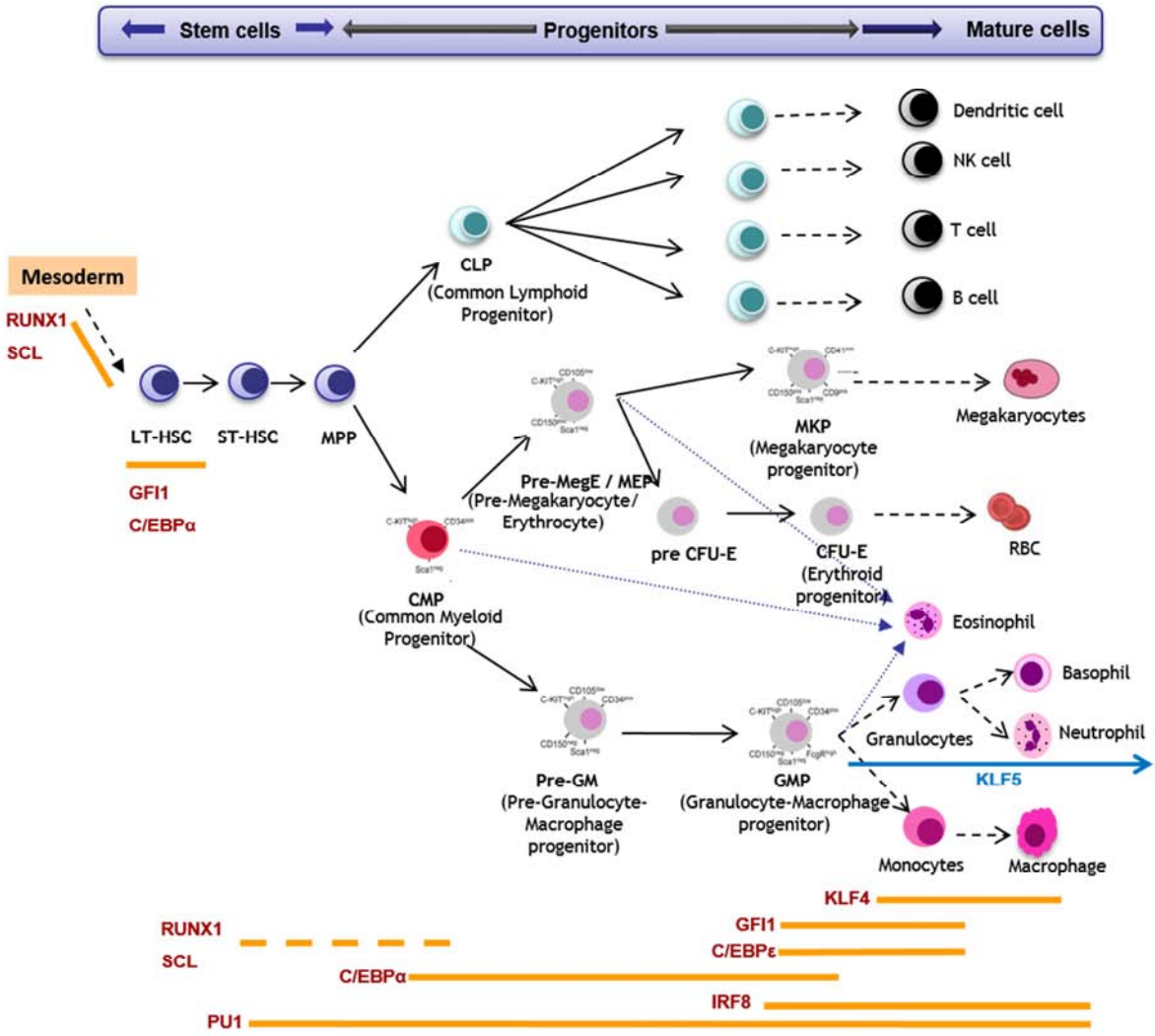

Figure 1.1: Schematic diagram of the process of haematopoietic differentiation

Haemopoietic stem cells (HSC) can be functionally defined as either long-term (LT-HSC) or short-term repopulating stem cells (ST-HSC) by their capacity to provide life-long or transient haemopoiesis. HSC can either self-renew or generate multilineage progenitors that are restricted to either the myeloid or lymphoid lineages (the CMP, common myeloid progenitor and the CLP, common lymphoid progenitor). Further differentiation of these pluripotent cells will generate mature erythroid, megakaryocytic, myeloid or lymphoid cells. **This diagram also outlines the stepwise requirement for transcription factors during myeloid differentiation.** The differentiation of stem cells into the two main myeloid lineages, the monocytic and the neutrophilic lineages, is orchestrated by a hierarchical network of transcription factors (RUNX1, SCL, C/EBPα, C/EBP□, GFI1, IRF8 and PU1). Individual transcription factors are essential for specific steps GMP, granulocyte-macrophage progenitor; LMPP, late multipotent progenitor; MEP, megakaryocyte erythroid progenitor; MkEP, megakaryocyte/erythroid progenitor.

1.2 Transcription factors play critical roles in directing haemopoietic lineage commitment

Transcription factors (TFs) are specialised nuclear proteins with the ability to bind to DNA and control gene transcription. TFs have various *trans*-activation or repressor domains [11], and may also induce chromatin remodelling to facilitate the entry of additional activator or repressor complexes in order to activate or inactivate specific gene transcription [12, 13]. By binding to discrete *cis*-regulatory elements, individual TFs can control expression of multiple target genes [14]. Many TFs can form complexes as they cooperatively bind to their cognate DNA sequences and are also able to cooperatively recruit transcriptional cofactors. Numbers of studies using various computational methods have identified the cooperative interactions among TFs based on predicted binding sites in DNA (reviewed in [15-18]). This cooperation therefore provides the mechanistic basis for reading out combinatorial expression patterns of TFs in tissue specific manner which also allow TFs to play a major role in cellular differentiation, including differentiation of the various haemopoietic lineages.

In normal haemopoiesis, pluripotent HSC have the ability to either self-renew or differentiate through successive symmetric and asymmetric divisions to a committed progenitor cell of either the lymphoid (CLP) or myeloid lineage (CMP) (reviewed in, [19]). Although both CLP and CMP possess stem-cell like properties, they are more limited in their differentiation potential as they have the capability to differentiate towards mature lymphoid or erythroid, megakaryocytic, granulocyte and monocytic cells respectively. Throughout this process, TFs act as the key regulators in lineage commitment as they will render the cells responsive to environmental signals including

physiological stimuli, such as growth factors, hormones, and cytokines [20]. Regulation of gene expression throughout haemopoiesis controls cellular differentiation and TFs play a role in this through activation of some gene while simultaneously silencing others [21, 22].

As shown in Figure 1.1, individual transcription factors are essential for specific steps involved during myeloid formation and the specific functions for those TFs are summarised in Table 1.1. *C/EBPα* and *Growth-factor independent 1* (*GFI1*), for example have been identified as TFs that function in self-renewal of existing HSCs [23, 24]. In the haemopoietic system, *C/EBPα* is expressed in stem and myeloid progenitor cells and up-regulated during granulocytic differentiation [25]. Early investigation in mice has revealed that disruption of the *C/EBPα* gene in mice results in a specific loss of granulocyte development and the accumulation of early myeloid blasts in the foetal liver [23] uncovering a critical role for *C/EBPα* in granulopoiesis. This shows that TF expression levels in cells play an important role in the establishment of cell fate [26]. As well, macrophage production depends on *PU.1* and *Interferon-regulatory factor 8* (*IRF8*) [21, 27]. In this process, *PU.1* seems to be essential for all intermediate steps starting from HSCs, whereas *IRF8* fulfils a role in later progenitors. Since all of these transcription factors play important roles in myeloid formation, dysregulation of any of these may potentially lead to aberrant formation of myeloid cells.

In addition to the above TFs which are known to regulate cell fate determination during haemopoiesis, *KLF5* has also been reported to act as a promoter of differentiation in the myeloid lineage (Figure 1.1) [28]. *In vitro* studies have revealed that loss of *Klf5* expression was associated with attenuated neutrophil differentiation [28]. This was

Transcription Factors	Specific steps involved during myeloid formation	References
C/EBPα	Self-renewal of existing HSCs Conferring the transition of common myeloid progenitors (CMPs) into granulocyte/monocyte progenitors (GMPs)	[23]
C/EBPε	Crucial for late-stage neutrophil production	[29]
GFI1	Self-renewal of existing HSCs Crucial for late-stage neutrophil production	[24]
IRF8	Macrophage production	[27]
RUNX1	Generation of *foetal* liver HSCs from the mesoderm	[30]
KLF4	Key regulator for monocyte differentiation	[31]
PU.1	Macrophage production	[21]
SCL	Generation of *foetal* liver HSCs from the mesoderm	[32]

Table 1.1: Specific transcription factors involved in different cell stages during myeloid cell formation

shown in the murine myeloid cell line, 32D, where knockdown of *Klf5* expression was associated with an increase in cell expansion and attenuated granulocyte differentiation in response to G-CSF [28]. A similar finding was also observed in the acute promyelocytic leukemia, APL cell line (NB4) where knocking down *KLF5* significantly attenuated neutrophil differentiation [33]. Interestingly, *KLF5* expression was also reported to be reduced in multiple subtypes of AML and this may be a common event associated with development of the AML blast and stem cell populations [28, 33]. These findings lead to a suggestion that KLF5 acts as a potential regulator of myeloid differentiation.

1.2.1 Studies of altered transcription factor function in normal and malignant myelopoiesis

Very frequently, alterations in the structure or regulation of TFs that participate in normal blood cell development have an association with leukaemogenesis. These alterations can occur at any stage either at the gene or protein level. Mutations can involve small or large sections of specific DNA sequence. Small scale mutations include point mutations which can result in amino acid changes through missense mutation or introducing of an early stop codon through a nonsense mutation which can lead to the production of a truncated protein as reviewed in *Barnes M.R.* [34]. In addition, an insertion or deletion of one nucleotide can lead to alteration of the reading frame. Large scale genomic alteration such as chromosomal rearrangements or translocations may result in deletion or disruption of the genes or the generation of fusion protein witch affect functions and hence contribute to the transformation of a normal cell into a

cancerous cell (reviewed in *Van De Peer et al.*) [35]. In addition, gene amplification, if it involves a proto-oncogene, can result in the formation of many copies of a proto-oncogene hence, each copy of the proto-oncogene produces protein that is involved in stimulating cell growth (*reviewed in Hastings et al.*) [36]). In addition, deregulation of functional TFs can also be due to other mechanism such as epigenetic regulation via DNA methylation changes [37].

Mutations in transcriptional regulatory elements have been found to be associated with numerous human diseases. This includes mutations that cause a *C/EBPα* loss of function which is well known to be associated with development of AML [38, 39]. Most commonly, *C/EBPα* mutations found in patients with AML involve the selective loss of *p42* expression due to frameshift mutations in the part of the coding sequence unique to this isoform [40, 41]. Furthermore, studies in knockout mice have shown that conditional ablation of *C/EBPα* in the bone marrow of mice results in a block at the transition from the CMP to GMP, resulting in the accumulation of immature myeloid blast cells in the marrow, similar to that observed in AML [40, 42]. Mechanistically, it has been shown the loss of *C/EBPα* in AML leads to increased expression of the oncogene *SOX4* demonstrating it as a key target gene of repression [43].

In addition to small scale mutations found in association with AML, a variety of cancer causing genes were also ascertained as a result of identification of chromosomal rearrangements (translocation) involving TFs. The rearrangements commonly involve fusion of a TF and another protein which can cause production of a chimeric protein having a new or altered activity. For example the t(8:21) translocation which is observed in 12 to 15% of AML cases, produces the fusion protein *AML1-ETO* a fusion of two

different transcription factors [44]. Studies with mouse models have shown that *AML1* (also known *RUNX1*) is a transcription factor that is widely expressed in multiple haemopoietic lineages and regulates the expression of a variety of haemopoietic genes [30, 45]. Both *in vitro* and *in vivo* studies show that AML1-ETO may cause abnormal myeloid development through blocking the normal function of AML1-dependent transcription [22]. *AML1* can also be modified by gene amplification. Analysis through fluorescent *in situ* hybridization (FISH) has shown that *AML1* amplification is found in different clones of bone marrow cells and confirmed in lineage conversion of childhood B-cell acute lymphoblastic leukaemia to acute myelogenous leukaemia [46]. In addition, *AML1* amplification was also found in childhood acute lymphoblastic leukaemia [47].

DNA methylation is one of the frequent mechanisms associated with deregulation of TFs in AML. For example, deregulation of *C/EBPα* expression is influenced by promoter methylation which was identified in 12.5% of AML patients [48-51]. Later studies have confirmed that *C/EBPα* promoter methylation in AML demonstrates shared phenotypic features with *C/EBPα* double mutation AML [48-51]. Interestingly, it has been shown that reduced expression of *KLF5* in AML is associated with hypermethylation in intron 1 of *KLF5* [28, 52]. It was reported that hypermethylation in intron 1 of *KLF5* is a relatively frequent occurrence and was found in 50% of patients [52]. Importantly, this methylation of *KLF5* in AML was also shown to be an independent predictor of poorer overall survival [52].

Such examples show that many forms of genetic alteration may occur to TF genes that change the normal activity of the TFs where such alterations of specific TFs might lead to aberrant blood cell development.

1.3 The role of the Klf family in cellular development

Krüppel-like factors (*KLFs*) are a family of transcription factors with various regulatory functions in cell growth, proliferation, differentiation, apoptosis and embryogenesis. They are involved in regulating gene expression in a tissue specific context. In mammalian cells, 17 members of the *KLF* family have been identified [53]. All *KLF*s share sequence homology with the DNA-binding domain of the Drosophila embryonic pattern regulator *Krüppel*. This consists of a conserved region of three Krüppel-like zinc fingers which bind to CACCC elements and GC-rich regions in promoters of target

genes [54]. As shown in

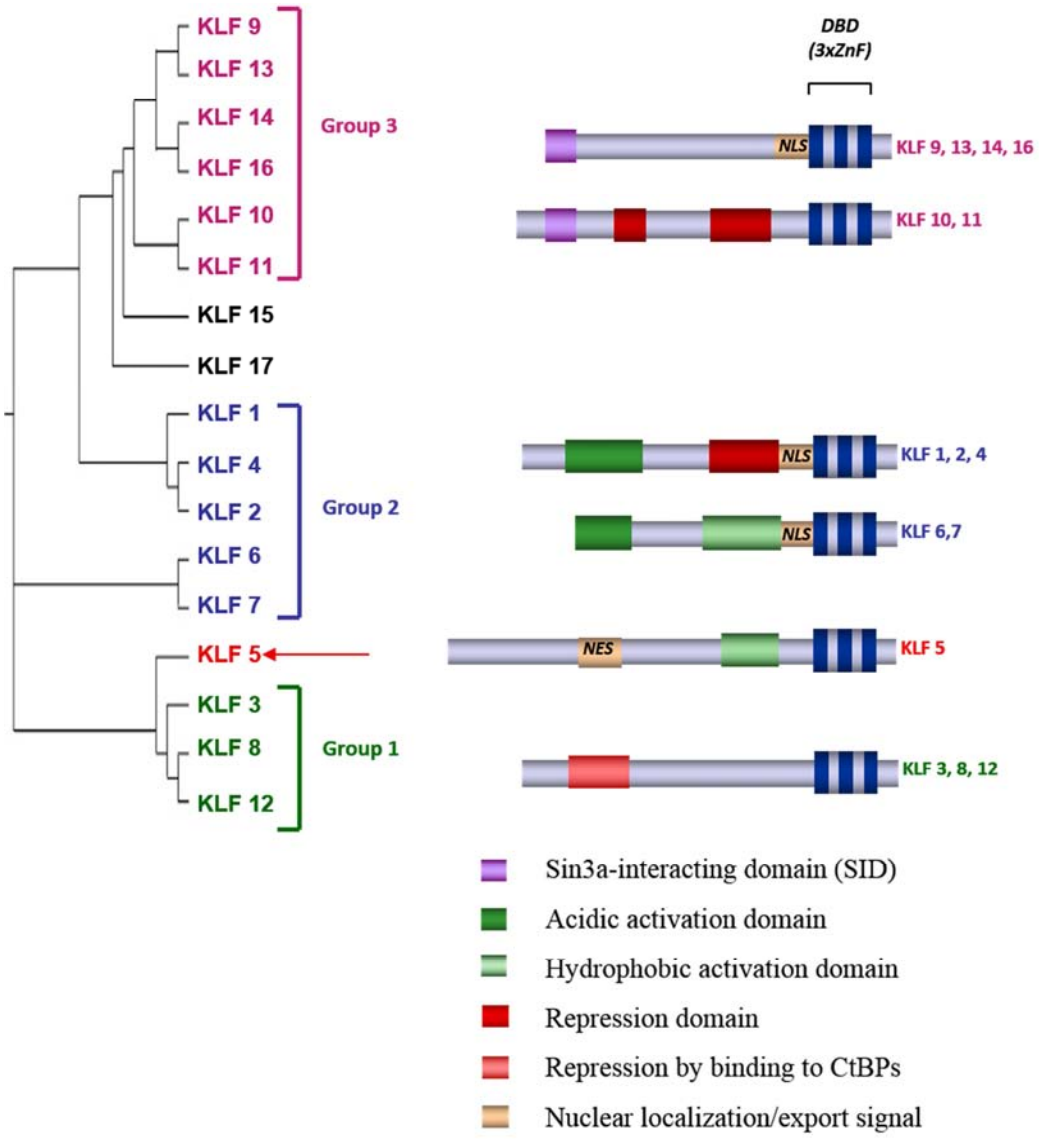

Figure 1.2, the zinc finger domains of all KLFs are localised in the extreme carboxyl terminus and followed by an additional one to three amino acids residues before the

termination codon [55]. However, also as shown in

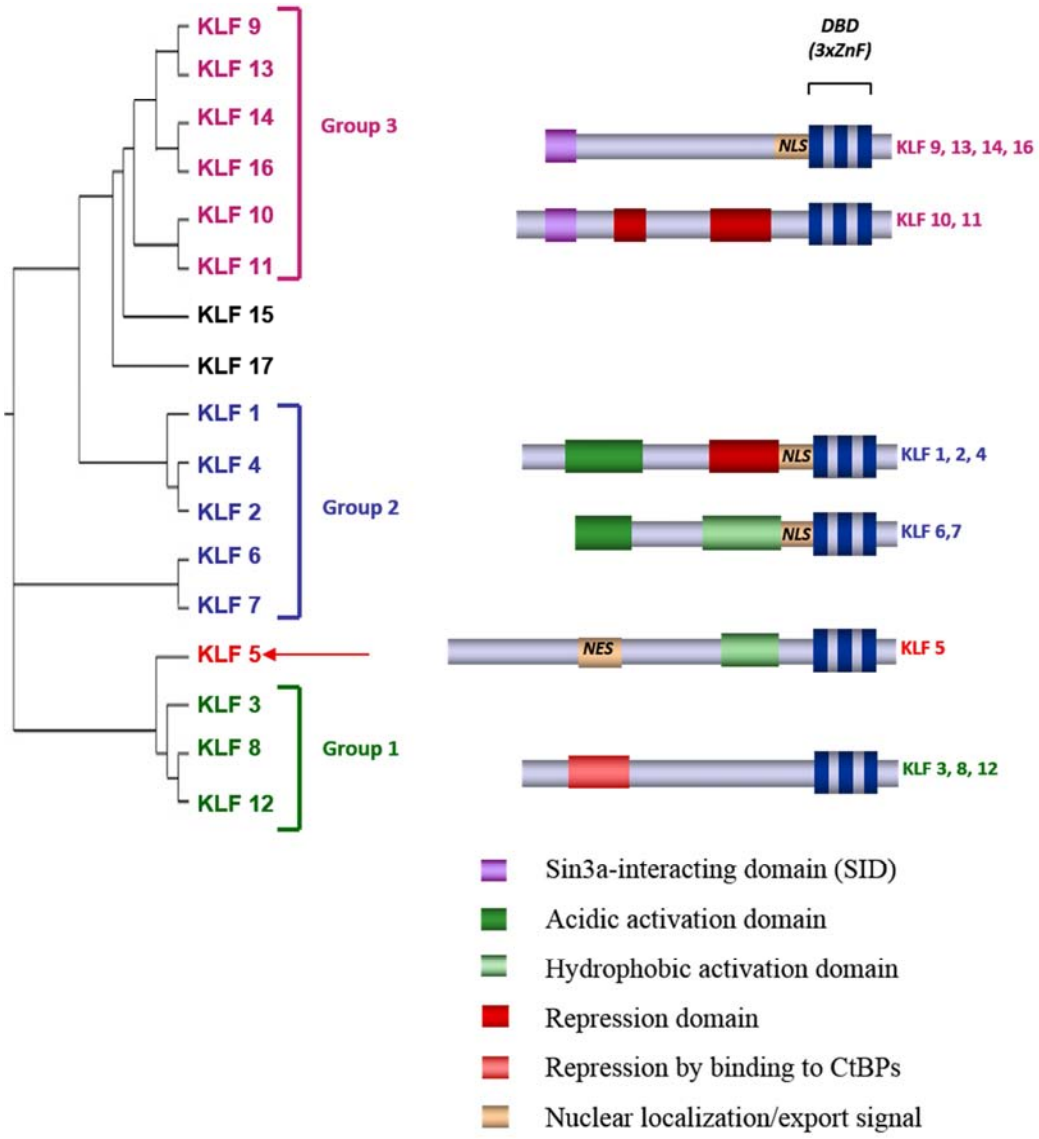

Figure 1.2, although the proteins are highly related in their zinc finger region they contain relatively limited homology elsewhere. Reviewed in *Knoedler JR and Denver RJ* [56], the phylogenetic relationship among the 17 mammalian KLFs were grouped

into three major subfamilies based on similarities in their N-terminal domains (

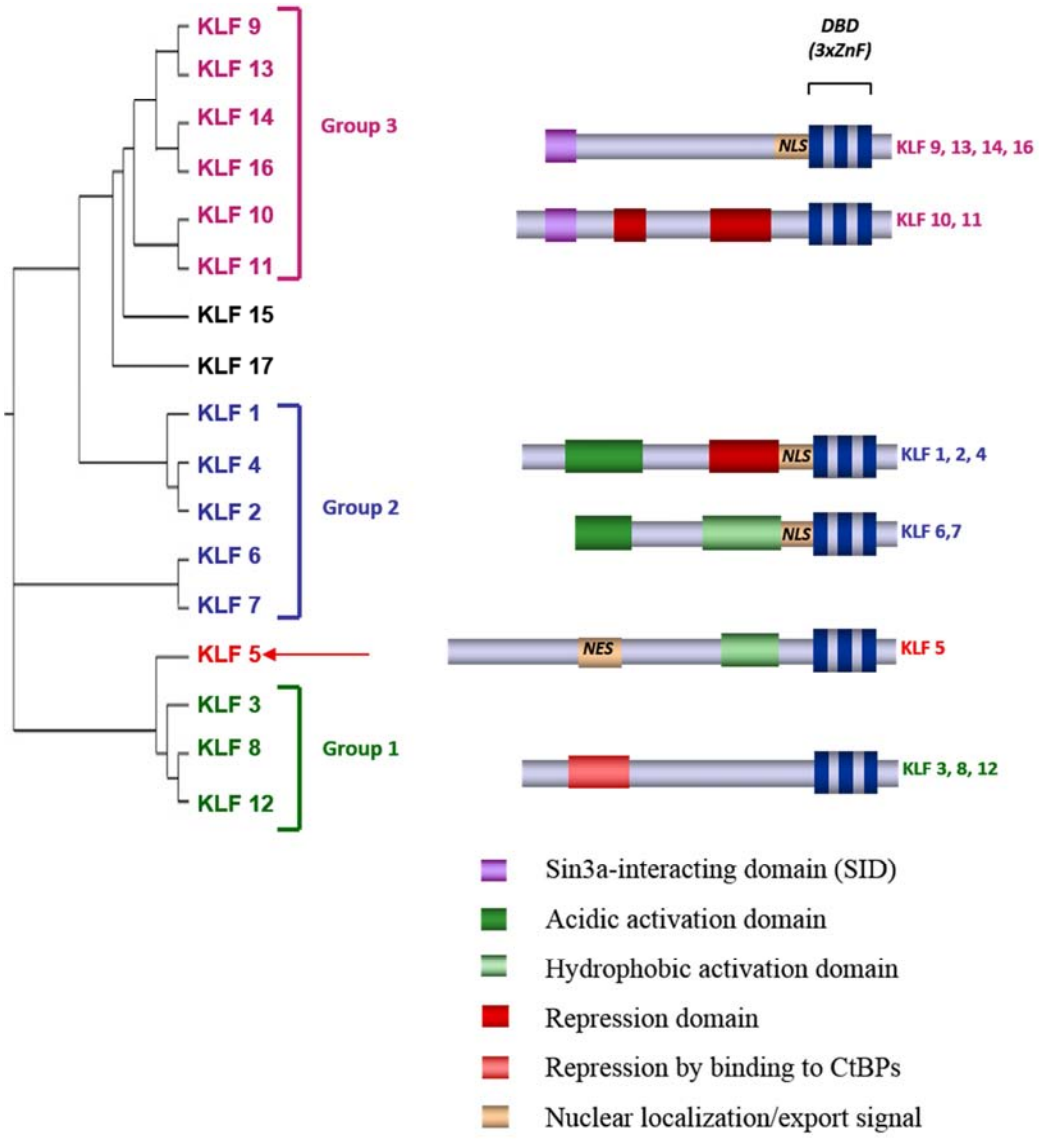

Figure 1.2). The first group included KLFs 3, 8, and 12 which are characterised by classical repressor function via binding to the C-terminal binding proteins (CtBPs) [57]. In contrast, the second group of KLFs, KLFs 1, 2, 4, 6 and 7, typically act as transcriptional activators as they share acidic activation domains. Finally, the third group (KLFs 9, 10, 11, 13, 14 and 16) share a Sin3a-interacting domain (SID), an α-helical motif that interacts with the repressor protein Sin3a [58]. Interestingly, KLF5 does not

fall into any of these family groups based on the presence of identifiable protein–protein interaction motifs [56].

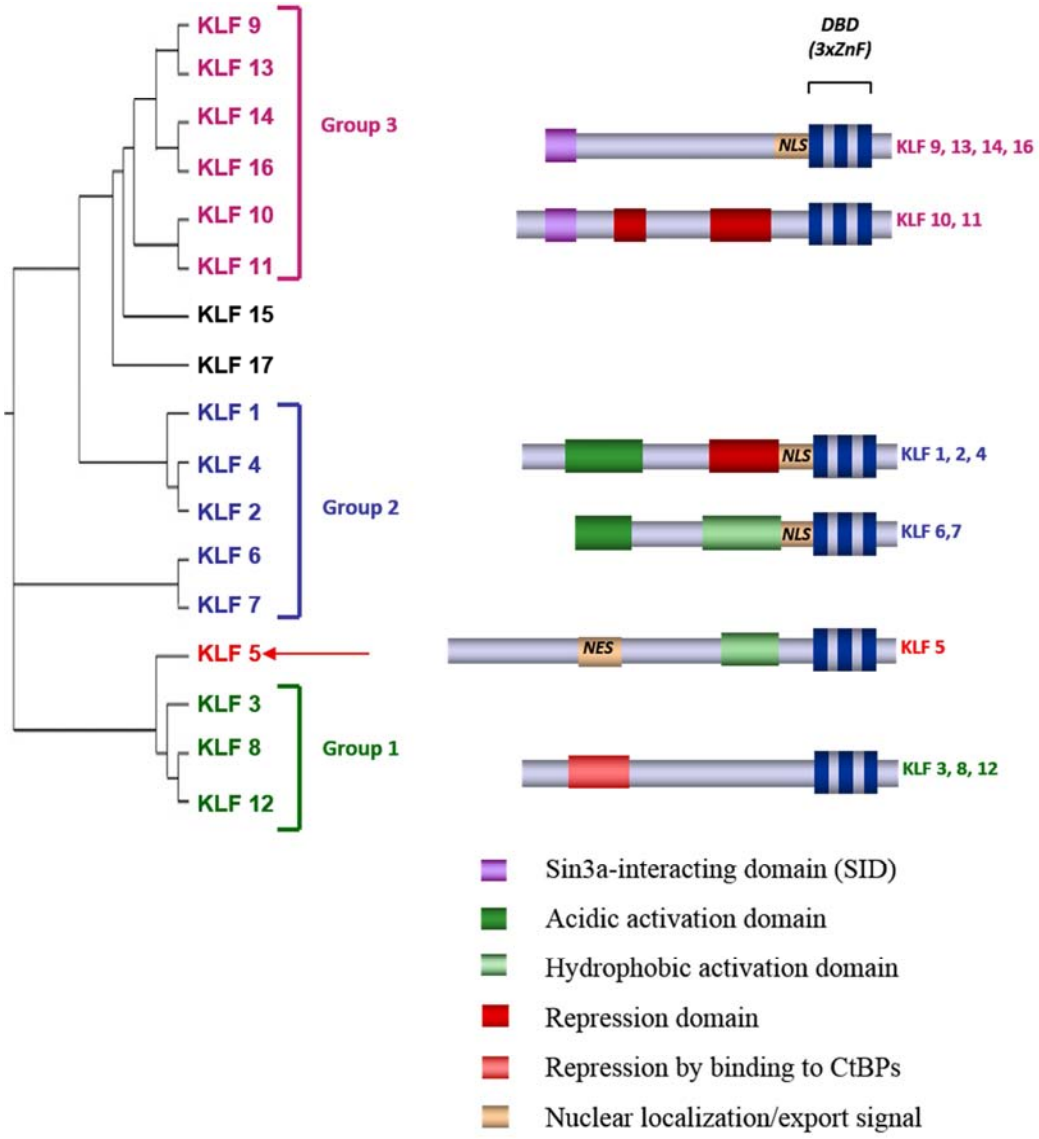

Figure 1.2: The Krüppel-like transcription factor family

The phylogenetic tree of the KLF family showing the various family members and their evolutionary relationship based on amino acid conservation. All members share conserved region of three Krüppel-like zinc fingers. All 17 KLFs genes in mammals were grouped into three major subfamilies based on similarities in their N-terminal domains. KLF5 (pointed with red arrow) did not fall into any of these family groups based on the presence of identifiable protein–protein interaction motifs. KLFs 3, 8, and 12 (Group 1) typically repress gene transcription by binding to the C-terminal binding proteins (CtBPs)(light red) [57]. KLFs 1, 2, 4, 6 and 7 (Group 2) share acidic activation

domains and thus typically act as transcriptional activators (dark green). KLFs 9, 10, 11, 13, 14 and 16 (Group 3) share a Sin3a-interacting domain (SID), an α-helical motif that interacts with the repressor protein Sin3a (purple) [58]. Adapted from *Knoedler JR and Denver RJ, 2014* [56].

However, KLF5 has a hydrophobic activation domain, similar to KLF6 and 7 and located before the three ZF domains, which is involved in transcriptional activation or repression and protein-protein interaction [55].

KLFs are known to play critical roles in the development of organs and tissues (including cancer development) as reviewed in *Pearson et al.*, *Nagai et al.*, *Dang et al.*, *Nandan et al.*, *Black et al.* and *Simmen et al.* [55, 59-61].

1.4 Transcriptional regulation by KLF family members

This topic has been the subject of many reviews [63-67] and will not be covered in detail here except to mention some common features shared between KLF family members that also apply directly to KLF5. Although most of the KLFs have a single activity in a particular tissue-specific context (for example KLF1 and KLF4 act as activators while KLF3 and KLF5 act as repressors [68, 69]), there are some KLFs which can act as both activators and the repressors. For example, based on the *in vitro* studies in the human endometrial carcinoma cell line RL95, KLF5 is known to have a dual modulator role where it can activate or repress specific target genes depending on the cellular environment [70] (this will be discussed in more details in Section 1.7). In addition, KLF4 has been shown to have dual functional roles in the immune system,

Table 1.2: The phenotypes of *Klf* knockout mice

Gene name	Alternative names	Knockout phenotype	Other functional roles	References
Klf1	*Eklf*	Lethal β-thalassemia at E14.5	Many roles in erythrocyte differentiation	[71]
Klf2	*Lklf*	Lethal cardiac failure at E12.5 to E14.5	Erythroid differentiation; T-cell differentiation; migration and homing; adipogenesis	[72, 73]
Klf3	*Bklf*	Viable with impaired B-cell development	Smaller in size and have defect in adipogenesis	[74, 75]
Klf4	*Gklf*	Peri-natal failure of skin barrier leading to lethal dehydration	Gut differentiation; Reduced number of monocytes	[31, 76, 77]
Klf5	*Iklf; Bteb2*	Early embryonic death before E8.5	Cardiovascular development and response to injury; Gut development; Adipogenesis	[78, 79]
Klf6	*BCD1*	Lethal failure of erythropoiesis and yolk sac vascularisation at E12.5		[80]
Klf7	*Uklf*	Severe neurological defects lead to death within 2 days of birth		[81]
Klf9	*Bteb1*	Viable with impaired uterine development and defective embryo implantation	Mild behavioural defects	[82, 83]
Klf10	*Tieg1*	Viable with bone defects, impaired skeletal development	Aged cardiac defects	[84]
Klf11	*Fklf; Tieg2*	Viable with no phenotype observed		[85]
Klf13	*Fklf2; Bteb3; Rflat-1*	Viable with defects in T cell differentiation	Heart development	[86]
Klf15	*Kklf*	Viable with increased susceptibility to cardiac hypertrophy	Adipogenesis	[87]

where it functions as a transcription factor to activate the IL-6 promoter at specific binding sites and also has a role in the chromatin remodeling of the IL-6 promoter [88].

KLFs family members have similar binding characteristics [89]. KLFs expressed in the same cell may have to compete for a given binding site as they have the capability of binding to the same promoter region. An interesting example for Klf competitive activity was shown in an *in vivo* study of a mouse model where *Klf8* is activated by Klf1 and repressed by Klf3 [69]. Interestingly, these activating and repressing KLFs, Klf1 and Klf3, were competing for the same binding site on the *Klf8* promoter [69]. On a larger scale, Klf3 has been shown to repress a subset of Klf1 activated target genes during erythropoiesis [90]. An *in vitro* study in Chinese hamster ovary (CHO) cells shows that two KLFs, KLF4 and KLF5 could compete for the same DNA *cis*-elements in the *KLF4* promoter but have opposing effects in regulating *KLF4* expression. While KLF4 activated its own expression, KLF5 repressed the *KLF4* promoter [68]. Recently, a study conducted in embryonic stem cells has shown that Klf4 and Klf5 play distinct roles in the control of pluripotency by differentially inhibiting mesoderm and endoderm differentiation respectively in murine ES cells [91].

shows individual KLFs and their specific role in tissue development based on knockout mouse studies for each KLF family members. Since it is known that KLFs are highly conserved across species, this suggests that the functions of the mouse and human KLFs may be conserved as well [62]. Hence, gene knockout studies in the mouse are highly relevant to determine the specific functions of each KLF.

1.4 Transcriptional regulation by KLF family members

This topic has been the subject of many reviews [63-67] and will not be covered in detail here except to mention some common features shared between KLF family members that also apply directly to KLF5. Although most of the KLFs have a single activity in a particular tissue-specific context (for example KLF1 and KLF4 act as activators while KLF3 and KLF5 act as repressors [68, 69]), there are some KLFs which can act as both activators and the repressors. For example, based on the *in vitro* studies in the human endometrial carcinoma cell line RL95, KLF5 is known to have a dual modulator role where it can activate or repress specific target genes depending on the cellular environment [70] (this will be discussed in more details in Section 1.7). In addition, KLF4 has been shown to have dual functional roles in the immune system,

Table 1.2: The phenotypes of *Klf* knockout mice

Gene name	Alternative names	Knockout phenotype	Other functional roles	References
Klf1	*Eklf*	Lethal β-thalassemia at E14.5	Many roles in erythrocyte differentiation	[71]
Klf2	*Lklf*	Lethal cardiac failure at E12.5 to E14.5	Erythroid differentiation; T-cell differentiation; migration and homing; adipogenesis	[72, 73]
Klf3	*Bklf*	Viable with impaired B-cell development	Smaller in size and have defect in adipogenesis	[74, 75]
Klf4	*Gklf*	Peri-natal failure of skin barrier leading to lethal dehydration	Gut differentiation; Reduced number of monocytes	[31, 76, 77]
Klf5	*Iklf; Bteb2*	Early embryonic death before E8.5	Cardiovascular development and response to injury; Gut development; Adipogenesis	[78, 79]
Klf6	*BCD1*	Lethal failure of erythropoiesis and yolk sac vascularisation at E12.5		[80]
Klf7	*Uklf*	Severe neurological defects lead to death within 2 days of birth		[81]
Klf9	*Bteb1*	Viable with impaired uterine development and defective embryo implantation	Mild behavioural defects	[82, 83]
Klf10	*Tieg1*	Viable with bone defects, impaired skeletal development	Aged cardiac defects	[84]
Klf11	*Fklf; Tieg2*	Viable with no phenotype observed		[85]
Klf13	*Fklf2; Bteb3; Rflat-1*	Viable with defects in T cell differentiation	Heart development	[86]
Klf15	*Kklf*	Viable with increased susceptibility to cardiac hypertrophy	Adipogenesis	[87]

where it functions as a transcription factor to activate the IL-6 promoter at specific binding sites and also has a role in the chromatin remodeling of the IL-6 promoter [88].

KLFs family members have similar binding characteristics [89]. KLFs expressed in the same cell may have to compete for a given binding site as they have the capability of binding to the same promoter region. An interesting example for Klf competitive activity was shown in an *in vivo* study of a mouse model where *Klf8* is activated by Klf1 and repressed by Klf3 [69]. Interestingly, these activating and repressing KLFs, Klf1 and Klf3, were competing for the same binding site on the *Klf8* promoter [69]. On a larger scale, Klf3 has been shown to repress a subset of Klf1 activated target genes during erythropoiesis [90]. An *in vitro* study in Chinese hamster ovary (CHO) cells shows that two KLFs, KLF4 and KLF5 could compete for the same DNA *cis*-elements in the *KLF4* promoter but have opposing effects in regulating *KLF4* expression. While KLF4 activated its own expression, KLF5 repressed the *KLF4* promoter [68]. Recently, a study conducted in embryonic stem cells has shown that Klf4 and Klf5 play distinct roles in the control of pluripotency by differentially inhibiting mesoderm and endoderm differentiation respectively in murine ES cells [91].

1.5 KLFs in cancer development and progression

In relation to the important roles played by KLFs in normal cell growth and differentiation, any disruption to their activity or expression may lead to the development of disease and aberrant cell growth such as cancer. This has been evidenced in a number of studies done over the past several years, suggesting a significant role for KLFs in carcinogenesis by enhancing or repressing transcription of

many genes related to cell cycle, and angiogenesis among others (reviewed in *Tetreault et al. and Limame et al.*) [92, 93]. Error! Reference source not found. summarises the involvement of specific KLFs in different types of cancer. Various studies on KLFs and their association with cancer have shown that they may act as positive regulators of cell proliferation and also as tumour suppressors. Apart from the important roles of KLFs in regulating cell cycle associated proliferation, KLFs also promote cancer progression through the regulation of invasion and metastasis in malignancies (reviewed in *Tetreault et al.*) [92].

1.5.1 KLFs as oncogenes

Consistent with their roles as promoters of proliferation and survival, a number of KLFs have been implicated as oncogenes in selected epithelial tissues. For example, increased *KLF8* expression has been observed in several cancer tissues compared to that in normal tissues [94-101]. As such, a study conducted *in vitro* and *in vivo* has shown that up-regulation of *KLF8* promotes tumour invasion and indicates poor prognosis for hepatocellular carcinoma [97]. In addition, microarray analysis showed that a reduction of *KLF8* expression in hepatocellular carcinoma cells down-regulated expression of multiple genes involved in tumour progression and metastasis [97]. KLF8 has also been reported as inducing pro- tumourigenic mammary stem cells via miR-146a potentially by activating Notch signalling and thereby promoting human breast cancer invasion [98, 99]. The function of *KLF8* over-expression in bone cancer has also revealed its role in the regulation of the cell cycle and a critical role in oncogenic transformation and

epithelial to mesenchymal transition (EMT) [100]. An initial study of KLF8 examining its association with ovarian cancer has revealed a functional role of KLF8 expression in

KLF2	• Down-regulated in AML	[33]
KLF3	• Down-regulated in AML	[33]
KLF4	• Loss of expression in intestinal, colon, gastric and breast cancer • Down-regulation in esophageal cancer and skin cancer • Tumor suppressor in B-cell malignancies • Hypermethylated in ATL	[102-104] [105, 106] [107] [108]
KLF5	• Promotes proliferation and colon cancer progression • Reduced expression in gastric cancer • Oncogene in bladder cancer • Loss of expression in breast and prostate cancer • Promotes breast cancer proliferation • Up-regulated in skin and lung cancer • Promoting survivin expression in ALL • Down-regulated and hypermethylated in AML	[109-112] [113] [114] [115] [116] [117-119] [120] [28, 33, 52]
KLF6	• Loss of expression in intestinal and colon tumour, gastric cancer and hepatocellular carcinoma • Loss of expression in prostate, pancreatic cancer and lung cancer and central nervous system tumor • Lack in transactivation in breast cancer • Reduced expression in ovarian cancer	[121, 122] [123-127] [128] [129]
KLF7	• Hypomethylated in gastric cancer	[130]
KLF8	• Oncogene in ovarian, renal, breast and ovarian cancer	[95, 97]
KLF9	• Down-regulation in intestinal and colon tumours	[131]
KLF10	• Tumour suppressor in pancreatic cancer	[132-134]
KLF11	• Tumour suppressor in pancreatic cancer	[135, 136]
KLF12	• Higher expression in gastric cancer	[66]
KLF13	• Over-expression in oral cancer	[67]
KLF17	• Reduced expression in breast, gastric, liver and lung cancer	[137-142]

Table 1.3: Klf5 roles in various cancers

promoting tumour formation through mediating responses to FAK via PI3K-Akt signalling [95, 96]. Very recently, it has been shown that *KLF8* over-expression is associated with human ovarian carcinoma pathogenesis, identifying it as a potential molecular biomarker for ovarian cancer [101]. As well, *KLF8* expression has been proposed to give the poor prognostic effect in pancreatic cancer and gastric cancer [143-145].

Another example for Klfs in association with oncogenic activity is KLF4 [104, 146-148]. In breast cancer, increased *KLF4* expression has been observed in neoplastic cells compared to adjacent uninvolved epithelium [146]. *KLF4* was also shown to be activated prior to invasion through the basal membrane [146]. In addition, its nuclear localization is associated with an aggressive phenotype in early-stage breast cancer [148]. Recently, it has been shown that KLF4 plays a potent oncogenic role in mammary tumourigenesis likely by maintaining stem cell-like features and by promoting cell migration and invasion [104]. In colon cancer, it has been shown that *KLF4* expression is important in tumour generation as well as in regulating cancer cell migration and invasion [147]. Interestingly, numbers of studies have also shown the association of KLF5 and cancer progression and malignancies (details for KLF5 as a key regulator in cancer cells will be discussed later in this chapter at Section 1.7).

1.5.2 KLFs as tumour suppressors

KLF family members have been implicated to act as tumour suppressor genes in cancer, and an imbalance in expression or modulation of activity is intimately implicated in the onset and progression of tumours in a tissue-specific manner. For instance, a loss

of *KLF4* expression or down regulation of *KLF4* has been reported in a number of cancerous tissues such as gastric and esophageal cancer [105, 149, 150]. In gastric cancer, loss of *KLF4* expression in primary tumours is associated with poor survival [149]. As well, *Klf4* mutant mice have dramatic changes in their gastric epithelia characterised by increased proliferation and altered differentiation [150]. Accordingly, an *in vitro* study has shown that *KLF4* is down-regulated in esophageal squamous cell carcinoma [105]. *Wang et al.* also suggested that down-regulation of *KLF4* may contribute to the malignant phenotype of esophageal cancer via increased proliferation and decreased adhesion which was observed in the esophageal cancer cell line with down-regulated *KLF4* [105]. In addition, *KLF4* was identified as a putative tumour suppressor in B-cell malignancies [107]. *Yasunaga et al.* identified that *KLF4* was aberrantly hypermethylated in adult T-cell leukemia (ATL) and that restoring *KLF4* expression in ATL-derived cell lines induced cell death by apoptosis [108].

KLF6 has also been marked as a tumour suppressor in various forms of cancer including prostate, colon, lung and gastric cancer [121-124, 151-156]. Loss-of-heterozygosity (LOH) analysis revealed that one *KLF6* allele is deleted in 77% of primary prostate tumours [123]. Functional studies have confirmed the tumour suppressor role of *KLF6* in prostate cancer. Introducing wildtype *KLF6* in prostatic carcinoma cell lines (DU145) effectively inhibited the growth and significantly reduced cell proliferation, probably through up-regulation of *p21* [123, 151]. Later, knockdown of *KLF6* showed a loss of induction of apoptosis in prostate cancer cells via up-regulation of *ATF3* (*activating transcription factor 3*) expression [152]. As well, the single nucleotide polymorphism-increased splice isoform, *KLF6 SV1* is demonstrated to be essential for prostate cancer cell growth and spread [124]. In colon cancer, the *KLF6*

locus was found to be deleted in at least 55% of tumours, and mutations were identified in 44% [121]. *Reeves et al.* also described that a KLF6 mutant was shown to lose the ability to induce p21WAF1/CIP1, and failed to inhibit CRC-derived cell growth [121]. In addition, 48.3% of LOH of *KLF6* was found in nonpolypoid-type colorectal carcinoma thus implicating it in development from an intra-mucosal to an invasive carcinoma [153, 154]. *KLF6* LOH is also observed in 16 of 37 informative cases in gastric cancer [155]. Interestingly, four missense mutations, S155R, P172T, S180L, and R198K, were also detected in the transactivation domain of the *KLF6* gene when a set of 80 sporadic gastric cancers were screened for mutations and allele loss of the *KLF6* gene [155]. An *in vivo* study also showed that *KLF6* mutants increase tumourigenicity in gastric cancer [122]. Collectively, these findings suggest that genetic alterations of the *KLF6* gene are involved in the development and/or progression of sporadic gastric cancer [122, 155]. The role of *KLF6* as a tumour suppressor was also reported in lung cancer studies [126, 156]. It was shown that the expression of *KLF6* mRNA was down-regulated in 85% of primary tumours compared with normal lung tissue [126]. LOH analysis using the laser capture microdissection technique also revealed that 34% of informative samples had LOH of the *KLF6* gene locus [126]. In parallel, over-expression of *KLF6* in the lung cancer cell lines (NCI-H1299 and NCI-H2009) also suggested that KLF6 induced apoptosis [126]. Later, it was shown that KLF6 induction was important for PMA-mediated cancer cell growth arrest via PKC activation [156].

In addition to KLF4 and KLF6, KLF9 also exerts effects in modulating cancer cell proliferation and progression in a tumour suppressor manner [131, 157-159]. Initially, KLF9 was identified as an important transcriptional regulator of progesterone-responsive genes in endometrial epithelial cells and was shown to be a key regulator of

cellular proliferation and differentiation in reproductive tissues [83, 160, 161]. An extended study then showed that attenuated expression of *KLF9* correlated with high endometrial tumour grade, thereby suggesting the potential involvement of KLF9 dys-regulation in both pregnancy failure and endometrial pathogenesis [157]. In colon cancer, 86% of the 50 cancerous tissues examined expressed lower levels of *KLF9* mRNA than individually matched normal mucosa [131]. In addition, KLF9 protein expression was reduced or absent in 65% of the samples [131]. Thus, this study suggested that loss of *KLF9* expression may have an association in the carcinogenesis of human colorectal cancer [131]. Supporting the role of *KLF9* as a strong anti-proliferative gene regulator, a recent study showed that over-expression of *KLF9* inhibits AKT activation and abrogates tumour growth of prostate cancer cells lines [159].

Lastly, studies have demonstrated that loss of *KLF11* is also involved in oncogenesis [135, 162]. KLF11 is an early response transcription factor that mediates TGF-β-induced growth inhibition in untransformed epithelial cells and this KLF was demonstrated to be deregulated by oncogenic ERK-MAPK in pancreatic cancer cells [162]. Later, it was shown that aberrant activation of ERK-MAPK interferes with KLF11 activity thus resulting in impaired *c-myc* repression and loss of growth inhibition by TGFβ in pancreatic cancer cells [135]. In addition, KLF11 was also reported to functionally regulate uterine leiomyoma where an *in vitro* study revealed that siRNA knockdown of *KLF11* increased leiomyoma cell proliferation [136, 163]. Based on genome-wide analysis of DNA methylation, it was shown that DNA methylation of the promoter *KLF11* leads to gene silencing in uterine leiomyoma in African American women, thus establishing a mechanism for its tumour suppressor role [163].

1.6 The role of KLFs in haemopoiesis

In haemopoiesis, a number of different KLF family members have been identified to play critical roles in both the myeloid or lymphoid lineages during mature blood cell development. A number of independent studies have shown some Klf involvement during mature lymphoid cell development. Klf2, for example, has been shown to be involved in T lymphocyte activation and migration [164, 165]. Another Klf study has shown that the *KLF4* promoter possesses dense methylation in T-cell leukaemia compared to normal cells suggesting that KLF4 also has a role in T-cell activity [108]. In addition, a study on Klf10 has shown dual roles of Klf10 in the T-cell compartment, firstly as a key transcriptional regulator of TGF-β1 in peripheral T regulatory cell differentiation and secondly in $CD4^{+}CD25^{-}$ T-cell activation [166]. In a *Klf13*$^{-/-}$ model, the percentage of $CD4^{+}CD8^{+}$T-cells in the thymus were consistently increased, indicating that Klf13 has a functional role in regulating these cells [86]. In addition to the involvement of Klfs in T-cell regulation, several independent studies have also shown the important roles of Klfs in B-cell development and function. For instance, deletion of *Klf2* specifically in B-cells caused a loss of phenotypic markers associated with B cell identity which identified a role for Klf2 in maintaining the mature B-cell phenotype [167]. Furthermore, a *Klf3* knockout mouse study has shown that deleting *Klf3* results in decreased immature B-cell formation but an increase in circulating mature cells [74]. In contrast, enforced expression of *Klf4* and *Klf9* results in delaying B cells from entering into cell division hence reducing the number of proliferating cells [168].

In addition to regulating lymphoid lineages, studies of Klfs in the myeloid lineage during mature cell development have been conducted. Initially, an *in vitro* study showed

that *KLF4* was expressed in a monocyte-restricted and stage-specific pattern during myelopoiesis and functions to promote monocyte differentiation through over-expression and knockdown of *KLF4* expression in HL-60 cells [169]. Later, it has been reported that in normal wildtype mice, *Klf4* has high expression in bone marrow monocytic cells and activated macrophages [31]. Additionally, this study showed that in chimeras, monocytic precursor cells with the *Klf4* knockout genotype were only present at half the number of wildtype cells, which suggests Klf4 is a key regulator for monocyte differentiation or survival [31].

In the erythroid lineage, Klf1 has been shown to directly activate the *Klf* genes in erythroid cells [170]. Originally, KLF1 was globally marked as an important regulator during erythroid maturation and it was described to specifically bind CAACC element in the *β-globin* promoter [170, 171]. *Klf1*-null embryos die at embryonic day E14.5 diagnosed with anaemia because definitive erythroid cells fail to produce *β-globin* transcripts *in vivo* hence lead to a profound β-thalassemia [71, 172]. Further studies have shown that together with Klf1, Klf2 also regulates gene expression during erythropoiesis [173-175]. In addition, the *Klf3* knockout model identified that Klf3 represses a subset of *Klf1* target genes and is required for proper erythroid maturation [90]. Interestingly, Klf8 has also been shown to interact with Klf3 during erythropoiesis [176]. Mice with homozygous disruption of *Klf8* are viable but crossing these mice with *Klf3*-null mice results in embryonic lethality at embryonic day 14.5 (E14.5), indicative of a genetic interaction between these two factors [176]. A study in the foetal liver revealed that *Klf3* and *Klf8* operated as a pair of transcriptional regulators that operate in an erythroid transcriptional network downstream of Klf1 and double mutant embryos exhibited a greater deregulation of gene expression than either of the two single mutants in the

Ter119^{+}-erythroid foetal liver cells [176]. Additionally, KLF4 has also been shown to play a significant role during red blood cell formation [177] by regulating the *HBA* gene [178, 179]. Interestingly, a study on the regulation of human *γ-globin* gene through the CACCC promoter element in human erythroid models, in K562 and HEL cells shows that the expression of the *KLF2*, *4*, *5* and *12* mRNAs changed significantly upon erythroid differentiation [180], which shows the involvement of other KLF family members depending on the cell stage and different cues.

Since our interest is in the functional role of KLF5 in regulating haemopoiesis, a detailed description about KLF5 and its functional role in a tissue-specific context will be described later in this review.

1.7 Krüppel-like factor 5

1.7.1 *KLF5* gene and protein

KLF5 (also known as *IKLF* and *BTEB2*) is located at 13q21 and encompasses 4 exons which span approximately 18.5 kb of DNA (Figure 1.3-A). Mouse *Klf5* was mapped on chromosome 14 and spans 16.38 kb of DNA, also encompassing 4 exons (Figure 1.3-B). *KLF5* was first identified from a human placenta cDNA library, and the KLF5 protein was reported to be 219 amino acid (aa) long with three contiguous zinc finger (ZF)-binding domains in the carboxyl terminus [181]. However, later KLF5 was characterised to have 457 aa for human and 446 aa for mouse [70, 182] (Figure 1.3). It is known that the *KLF5* gene is highly-conserved among species (from human to

drosophila) and the coding region of mouse *Klf5* is 88% identical to the human sequence [181].

1.7.2 KLF5 protein modification

The KLF5 protein undergoes modification following translation which extends the range of its function by changing the chemical nature of constituent amino acids or by making possible structural changes, such as the formation of disulfide bridges. Numerous studies have demonstrated that KLF5 protein modifications can change its activity [183-186]. KLF5 post-translational modification includes phosphorylation, acetylation, methylation, ubiquitination and sumoylation at specific sites (Figure 1.3). KLF5 is known to be phosphorylated at the CBP interaction region which enhances its transactivation function [187]. Interestingly, it has been shown that KLF5 is phosphoryalated in vascular smooth muscle cells (VSMCs) by angiotensin II (Ang II) via the ERK1/2 pathway that subsequently leads to increased interaction of KLF5 with c-Jun resulting in *p21* transcriptional repression [188].

KLF5 has been shown to be acetylated by p300 and deacetylated by HDAC1 and SET where KLF5 acetylation has been shown to alter protein interactions which then result in a mode of binding where KLF5 transcriptional activity is changed from repressive to active [185, 186, 189]. A recent study in prostate epithelial cells has reported that while acetylated Klf5 (Ac-Klf5) functioned in the differentiation of prostate epithelial cells, unacetylated Klf5 (unAc-Klf5) functioned in the proliferation of prostate epithelial cells, showing that Klf5 function can be modulated by post-translational modification [190]. This has been supported by a recent finding

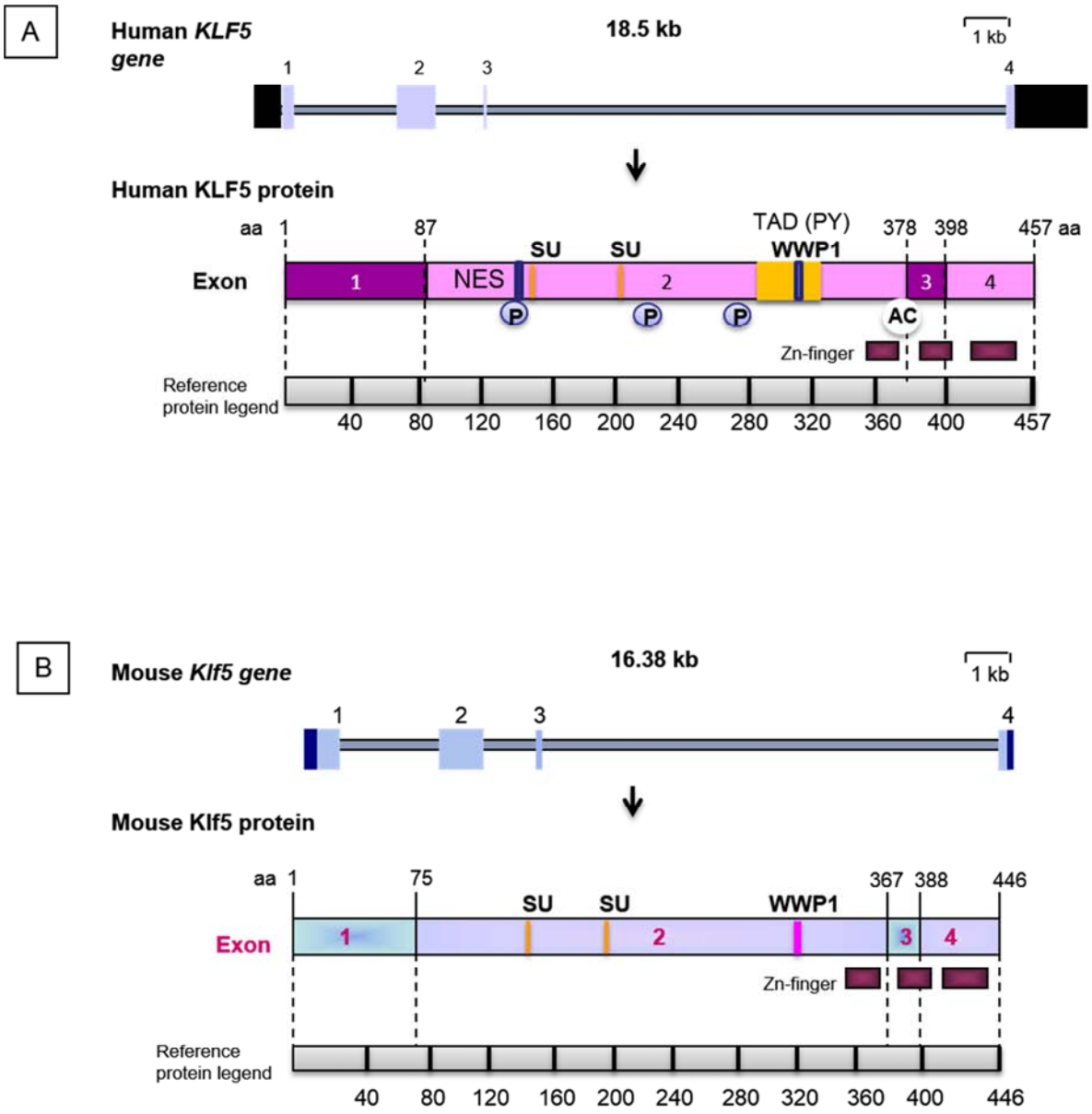

Figure 1.3: Schematic diagram for *Klf5* gene and protein structures

A) Human *KLF5* gene and protein structure. The human *KLF5* gene contains four exons (exon 1, 573 bp; exon 2, 874 bp; exon 3, 60 bp; and exon 4, 1839 bp). The KLF5 protein contains three zinc-finger (*ZF*) domains, one major transactivation domain (*TAD*) with PY motif (*PPSY*328), and a nuclear export signal (*NES*). The KLF5 protein undergoes different types of post-translational modifications, including phosphorylation (*P* at S153, T227 and S292), acetylation (*Ac* at K369) and sumoylation (*Su* at K162 and K209) [191]. **B)** Mouse *Klf5* gene and protein structures. The mouse *Klf5* genome span 16.38 kb contains four exons (exon 1, 532 bp; exon 2, 873 bp; exon 3, 59 bp and exon 4, 261 bp). The mouse Klf5 protein also contains three *ZF* domains in the N-terminal domain, one major *TAD* with a WWP1 motif predicted at 313 to 317 aa. Sumoylation sites for mouse Klf5 protein were identified at K151 and K202.

demonstrating that KLF5 inhibits cancer cell proliferation *in vitro* and suppressed tumourigenesis in nude mice in an acetylation-dependent manner [192].

KLF5 has also been demonstrated to be SUMOylated at two consensus lysine sites, 151 and 202 of mouse KLF5 and 162 and 209 of human KLF5 which leads to functional modification of KLF5 and regulates its nuclear export [183, 193]. This SUMOylation of KLF5 has been reported to stimulate anchorage-independent growth in a colorectal cancer cell line [183]. Consistent with other studies where SUMOylation of proteins is also involved in the progression of malignant cell transformation [194, 195]. Furthermore, in breast and prostate cancer studies, it has been shown that the KLF5 protein is ubiquitinated and targeted to the proteosome for degradation [196]. Multiple studies have reported that the KLF5 protein is targeted for ubiquitin-degradation by Fbw7 and WWP1 which then results in suppression of cell proliferation [197, 198].

1.7.3 *KLF5* activation

KLF5 expression is known to be regulated via several pathways triggered by specific signals including Ras-mitogen-activated protein kinase (MAPK), non-canonical Wnt signalling (PKC), retinoid, and androgen (reviewed in *Diakiw et al.*) [199]. In the context of acting as a promoter of cell growth, *KLF5* is most frequently reported to be regulated via MEK/ERK pathways. It has been shown that *KLF5* expression is activated downstream of MEK/ERK pathways via Ras activation or early growth response protein 1 (Egr-1) signalling [109, 200]. *KLF5* expression is also activated via the MEK/ERK pathway by up-regulation of PKC [201, 202]. *KLF5* has been identified as one of the Wnt-responsive genes from both *in vitro* and *in vivo* enforced expression of *Wnt-1* [201,

202]. These studies have reported that the regulation of *KLF5* by the Wnt-1 signaling is β-catenin-Lef/TCF-independent but related to PKC [202]. Additionally, numerous studies have shown that KLF5 can promote cell proliferation in association with up-regulation of the cell cycle-promoting proteins Cyclin D1, Cyclin B1 and Cdc2 via the MEK/ERK pathway [203]. *KLF5* expression is also reported to be activated by mitogenic or angiogenic factors including PMA, bFGF, and angiotensin II (Ang II) [79, 204]. In VSMCs, it has been shown that KLF5 is phosphorylated by Ang II via the ERK1/2 pathway that subsequently leads to increased interaction of KLF5 with c-Jun and to *p21* transcriptional repression [188]. It was reported that the ERK1/2 inhibitor PD98059 markedly attenuated KLF5 phosphorylation and hence interfered with the interaction between KLF5 and c-Jun induced by Ang II in VSMCs [188]. Concurrently, KLF5 has been shown to bind to the promoter of the *EGFR* gene which further activates the MEK/ERK pathway and *KLF5* expression itself [205]. *KLF5* transcription is also known to be regulated by Sp1, CBFa, and NF-1 binding on its promoter region, where it has been shown that the *KLF5* promoter element consists of a GC box, a CCAAT box, and an NF-1 binding site [206, 207].

1.7.4 KLF5 target genes and interacting proteins

Similar to other KLFs, the KLF5 ZF DNA binding domain binds to GC/GT rich sequences, widely regulating eukaryotic gene expression [55, 57, 79]. A number of independent studies have identified direct target genes of *Klf5* in regulating cell proliferation, renewal, survival and differentiation as well as in other biological processes (reviewed in *Dong and Cheng*) [191]. Table 1.3 summarises direct target

genes of *Klf5* and whether those genes are activated or repressed. Ample studies have also shown that in regulating gene expression, KLF5 also interacts with other proteins and forms complexes at the promoter regions of target genes [208]. KLF5 has a proline rich transactivation domain (TAD) N-terminal to the three ZF domains which is involved in transcriptional activation or repression and protein-protein interaction [55]. Table 1.4 summarises the KLF5 interacting proteins including coactivators or corepressor (reviewed in *Diakiw et al.*) [199].

1.7.5 The role of KLF5 in cancer progression and disease

KLF5 is expressed in many different tissues and evidence suggests that *KLF5* might play context-dependent roles in different tissues [109, 188, 209, 210]. Interestingly, various studies conducted on cancer initiation and progression have reported diverse roles of KLF5 during cancer cell progression in a range of cancers type (reviewed in *Diakiw et al.* and *Dong and Chen*) [191, 199]. The *KLF5* gene has been shown to undergo frequent genetic deletions which are associated with a reduction in *Klf5* expression in various cancers suggesting it plays a tumour suppressor role (reviewed in *Diakiw et al.* and *Dong and Chen*) [191, 199]. Oppositely, *KLF5* was also identified as a positive regulator of cell proliferation in some cancer cell types where it is expressed mainly in cancerous cells but not in the normal unproliferative cell types [211-213]. As such, KLF5 has been implicated to play roles in a variety forms of cancer and human diseases by either inducing differentiation and cell cycle arrest and/or promoting proliferation and self-renewal depending on the cellular context [214].

Regulation by *KLF5*	Gene Symbol	References
Activated	*CCNB1, CCND1, CDK1 (CSC2), DAF, EGFR, EGR1, FASN, FGFBP1, HBG1, IGF1, ILK, LAMA1, LTF, MIR146A, MMP9, MYH10, NANOG, OCT3, OCT4, SERPINE1, PDGFA, PDGFB, PIM1, PPARG, TAGLN, SURVIVIN, TCL1, TRB, VEGFA*	[79, 111, 116, 120, 180, 193, 203, 205, 215-230]
Repressed	*ABCG2, CDKN1A (p21), KLF4, MAOB*	[68, 188, 231, 232]
Both (activated and repressed)	*CDKN2B (p15), CPT1B, MYC, UCP2, UCP3*	[78, 128, 203, 215, 220]

Table 1.3: KLF5 target genes

Function	Protein Symbol	References
Transcriptional coactivator	C/EBPß, C/EBPδ, JUN, NFκB, PPARδ, RAR/RXR, SREBP1	[78, 79, 118, 120, 188, 221, 228, 233]
Transcriptional corepressor	NCoR1, NCoR2, JUN, PPARδ	[188, 193, 221]
Transcription factor	ß-catenin, ERα, HIF1α,	[234-236]
Basal transcriptional component	TFIIB, TFIIEß, TFIIFß,	[237]
Activator of apoptosis	PARP1	[238]
Basal transcription component	TBP	[237]

Table 1.4: KLF5 interacting proteins

1.7.6 Tissue-specific roles of KLF5

1.7.6.1 Breast

KLF5 has been identified as a key regulator in normal breast cell proliferation and survival [116, 217, 235]. KLF5 was shown to promote breast cell proliferation through fibroblast growth factor binding protein 1 (FGF-BP) [116]. KLF5 also interacts with estrogen receptor (ER) to play a role in the normal development and epithelial homeostasis of the breast [235].

In breast cancer, *KLF5* was first suggested to act as a tumour suppressor from the observation of frequent hemizygous deletion or loss of expression found in several breast cancer cell lines and the observation that over-expression of *KLF5* in one breast cancer line inhibits tumour cell growth [115, 239]. Interestingly, *KLF5* loss of expression was observed from the cases with hemizygous deletion and no homozygous deletion was identified, indicating that *KLF5* haploinsufficiency may contribute to cancer progression [115]. *Guo et.al.*, believed that *KLF5* acts as a tumour suppressor and reported that KLF5 inhibits the function of ERα (approximately 70% of human breast cancers express *ER*; including *ERα* and *ERβ* [240]) in gene regulation and cell proliferation through protein interaction that interrupts the binding of ERα to the promoter of its target genes and subsequent target gene induction [235]. In contrast, a later study showed that gene expression of *KLF5* is directly correlated with cell proliferation *in vivo* and is a prognostic factor for patients with breast cancer where patients with higher *KLF5* expression have shorter disease-free survival and overall survival compared to patients with lower *KLF5* expression [241]. *KLF5* was also reported to be one of the nine genes that are over-expressed in high-grade and poorly

differentiated aggressive breast tumours [242]. A *KLF5* knock-down and over-expression study has shown that KLF5 promotes breast cancer cell proliferation *in vitro* [116]. This study also demonstrated that KLF5 promotes breast cell proliferation by activating its downstream gene, *FGF-BP* [116]. In addition, KLF5 was demonstrated to promote breast tumourigenesis *in vivo* [116]. This was shown by injecting populations of the breast cancer cell line, MCF7 overexpressing *KLF5* and *lacZ* (*MCF7-KLF5* and *MCF7-lacZ*) into nude mice and it was reported that the mean tumor weight from *MCF7-KLF5* is about three times of that from *MCF7-lacZ* after 40 days of growth *in vivo* [116]. Whether *KLF5* is an oncogene or tumour suppressor gene is still debatable. Accumulatively, studies have revealed that KLF5 promotes the proliferation and survival of breast cancer cells hence *KLF5* was defined as an oncogenic transcription factor in breast cancer [197, 198, 243-246]. As such, studies have shown that *KLF5* was found to be induced by progesterone and androgen to contribute to progesterone/androgen-induced breast cancer cell proliferation [243, 245, 246]. KLF5 also promotes breast cell survival partially through pERK-mediated MKP-1 phosphorylation and stabilization [243]. In addition, the KLF5 protein was shown to be targeted for degradation by Fbw7 and WWP1 which then suppresses breast cell proliferation [197, 198]. While the KLF5 protein was shown to be targeted for degradation, studies on the role of KLF5 in breast cancer have shown that Yes-associated protein (YAP) and PDZ-binding motif (TAZ) stabilise the KLF5 protein and protect it from WWP1-targeted degradation hence promoting breast cancer proliferation and progression [198, 244]. These studies revealed that KLF5 protein is stabilised by TAZ antagonizing WWP1 activity providing KLF5 with an oncogenic role in promoting breast cell growth [198, 244].

1.7.6.2 Prostate

KLF5 has been identified as an important regulator of prostate cell differentiation and survival [190]. Analysis of prostate morphology and cell proliferation in *Klf5* knockout mice confirmed that losing one allele of *Klf5* leads to increases in cell proliferation and causes hyperplasia, however loss of both alleles causes cell death [190]. This study also revealed that while acetylated Klf5 (Ac-Klf5) functioned in the differentiation of prostate epithelial cells, unacetylated Klf5 (unAc-Klf5) functioned in the proliferation of prostate epithelial cells showing that Klf5 function is modulated by post-translational modification [190].

KLF5 was suggested as a tumour suppressor in prostate cancer since it was initially observed that the 13q21 region was frequently deleted in various human cancers including prostate cancer [239, 247]. *KLF5* deletion in prostate cancer was confirmed by deletion mapping analysis conducted in human tumour samples, xenograft models, and cancer cell lines [239, 247]. The proposed tumour suppressor role for KLF5 was functionally supported by *KLF5* over-expression in prostate cancer cell lines which resulted in decreased colony numbers and enhanced differentiation and reduced tumour weight *in vivo* on subcutaneous injection [247, 248]. Conversely, *KLF5* knockdown enhanced tumour growth in these cells both *in vitro* and *in vivo* [247, 248]. One of these studies also demonstrated that in response to treatment with estrogen antagonists, KLF5 positively cooperates with ERβ to enhance expression of *FOXO1* which promotes apoptosis and prevents anchorage-independent tumour growth [248].

It is likely that KLF5 may also play different roles in various stages of prostate tumourigenesis as an independent study has identified that KLF5 may alternatively have

a role in promoting prostate cancer progression and metastasis [210]. KLF5 was also reported to interact with sterol regulatory element-binding protein-1 (SREBP) to synergistically induce expression of the *fatty acid enzyme* (*FASN*) in prostate cancer cells where FASN is known to act as an important oncogenic protein in cancer cell growth and proliferation [233]. A gene profiling study also identified *KLF5* gene expression to have an association with prostate cancer growth [249]. Similar to the findings of KLF5 acetylation altering its function in normal prostate epithelium, a recent finding has shown that KLF5 inhibits cancer cell proliferation *in vitro* and suppressed tumourigenesis in nude mice in an acetylation-dependent manner [192]. Interestingly, *Li et al.* also reported that KLF5-deacetylation, possibly in association with multiple molecules (including RELA, p53, CREB1, MYC, JUN, ER, AR and SP1), converted KLF5 from having tumour-suppressive to tumour-promoting function [192].

1.7.6.3 Bladder

Initial observation in bladder cancer cell lines showed that over-expression of *KLF5* did not inhibit cell growth or induce apoptosis [250]. Consistent with this, enforced expression of *KLF5* in the bladder cancer cell line, TSU-Pr1, leads to increased proliferation potentially via G1 to S phase transition [114]. This study also reported that KLF5 promotes G1 to S phase transition via up-regulation of cyclin D1 expression, phosphorylation of MAPK and Akt proteins, and inhibition of p27 and p15 expression [114]. Recently, it has been shown that lentivirus-based knockdown of *KLF5* inhibits bladder cancer cell growth and targeting KLF5 for proteosome-dependent degradation through knockdown of YAP/TAZ (which normally protect KLF5 from degradation) in

bladder cancer cells confirmed the potent inhibitory effects on tumour growth and the pro-proliferative effect of KLF5 [251].

1.7.6.4 Colon

KLF5 (also known as intestine enriched *krüppel-like factor, IKLF*), appears to play a central role in the regulation of intestinal epithelial renewal in both the small intestine and colon [182, 252]. Numbers of studies have described that *KLF5* is expressed mainly in the proliferating cells of the crypt [182, 252, 253], suggesting that it plays a positive growth regulatory role in this tissue. An inducible *Klf5*-gene ablation model has revealed that *Klf5* loss from the adult colon leads to the disruption of epithelial homeostasis followed by a regenerative response led by Sox9 and the Reg family of proteins [253]. In addition, gene expression analysis showed that functional loss of *KLF5* was detected in Crohn's Disease and Ulcerative Colitis [254]. Interestingly, a study of inflammatory bowel disease (IBD), has demonstrated KLF5 as a potential therapeutic agent as over-expression of *KLF5* in mice led to less colonic injury development and significantly reduced disease activity when mice were treated with dextran sodium sulphate (DSS) to induce colitis [255].

In a colon cancer study, analysis of colon cancer cell lines and patient samples provided direct evidence that *KLF5* expression was down-regulated in cancer cells suggesting a potential *KLF5* growth inhibitory role on colon cancer cells [215]. These findings once again highlight the context-dependent role of KLF5 during tumour progression. On the other hand, KLF5 was then found to play an important role in proliferation of colon cancer cells by LPA-mediated signaling and that the induction of

KLF5 is mediated via MEK and PKCδ-dependent pathways [110]. It has also been shown that KLF5 plays an important role in colon cancer progression in association with the *adenomatous polyposis coli* (*APC*) mutations (the *APC* gene is an important tumour suppressor for colorectal cancer and is mutated in 80% of colorectal cancer, which is also reported to act as a component of the WNT signaling pathway that targets β-catenin for degradation) [211]. KLF5 has also been reported to facilitate nuclear localisation of β-catenin as a downstream target of mutant APC [234]. This study also revealed that KLF5/β-catenin increased *CCND1* and *MYC* gene transcription, where these β-catenin target genes are known to be associated with promoting proliferation [234]. KLF5 was also reported to have an association with KRAS activation (leading to aberrant activation of proliferative signaling pathways) in colon cancer progression [112]. Supporting an oncogenic role for KLF5 in colon cancer, a genomic analysis of colorectal cancer tissues has identified a somatic mutation (P301S) in *KLF5* within the phosphodegron sequence [256]. Interestingly, a recent study by *Bialkowska et al.* revealed that the P301S KLF5 protein has greater stability compared to wt-KLF5 protein [257]. It was reported that phosphorylation of serine residue 303 by GSK3β is important for FBW7α facilitated proteosomal degradation of WT KLF5 protein [257]. This study revealed that a somatic mutation (P301S) found in *KLF5* led to an increased KLF5 stability with elevated protein levels and enhanced transcriptional activity [257]. Thus, these studies provided multiple lines of evidence for a role of KLF5 as an oncogene in colon cancer.

1.7.6.5 Esophagus

KLF5 is expressed in proliferating cells of the gastrointestinal tract, including the esophagus and it has been demonstrated that KLF5 is a regulator for cell growth and proliferation [213]. Over-expression of *Klf5 in vivo* demonstrated that Klf5 promotes proliferation in esophageal basal cells but not sufficient to maintain proliferation in the esophageal epithelium [213]. KLF5 was first evidenced as a tumour suppressor when enforced expression of *KLF5* in a poorly differentiated esophageal squamous cancer cell line TE2 was observed to inhibit proliferation and invasion [258]. KLF5 also upregulates the cdk inhibitor p21 (waf1/cip1) and pro-apoptotic protein BAX following UV irradiation in cancer cells [258]. As well, in response to DNA damage from UV irradiation, cell viability is decreased in KLF5 transduced cells indicating the role of *KLF5* in regulating apoptosis in esophageal cancer cells [258]. Although an *in vivo* transgenic study of Klf5 function in regulating epithelial homeostasis has shown that *Klf5* expression is important for esophageal epithelial cell proliferation, this was not evidenced to accommodate KLF5 as an oncogene since *Klf5* over-expression in this model was not sufficient to maintain proliferation in these cells [213]. However, numbers of studies have suggested an anti-proliferative role for KLF5 in esophageal cancer [259-261]. For example, *KLF5* loss together with a *p53* mutation is reported as a key determinant of invasive squamous cell cancer by loss of *NOTCH1* transactivation [259, 260]. This study reported that in normal epithelia, p53 preferentially bound *NOTCH1*, but in precancerous dysplasia (in which *p53* mutations are found), KLF5 will transactivate *NOTCH1* [259, 260]. However, subsequent loss of *KLF5* leads to failure to transactivate *NOTCH1* hence transformed primary human keratinocytes harboring

mutant p53 to the formation of invasive tumours [259, 260] suggesting an anti-proliferative role of KLF5 in cancer invasion. In addition, over-expressing *KLF5* in human esophageal squamous cell cancer (ESCC) cell lines, results in increased apoptosis and decreased viability [261]. Interestingly, restoring KLF5 in ESCC also activated c-Jun N-terminal kinase (JNK) signalling, an important upstream mediator of proapoptotic pathways including BAX [261]. Together, this data suggests that KLF5 plays a pro-proliferative role in normal cells but anti-proliferative in cancer cells.

1.7.6.5 Gastric

Similar to some of the cancers discussed previously, it has also been observed that *KLF5* expression is altered in gastric carcinomas with higher expression in early-staged gastric cancer, small gastric cancer tissues and in gastric cancer without lymph node metastasis [113]. In this study, a favourable survival rate after surgery was correlated with KLF5-postive expression [113]. In contrast, a clinical study conducted on 76 surgical human gastric specimens in Taiwan revealed that higher KLF5 expression was significantly associated with a higher tumour grade, lymph node status and poorer survival which lead to the suggestion of KLF5 oncogenic role in gastric carcinogenesis [212]. Also of relevance to this tissue, it has been shown that CDX1-induced (CDX1 and CDX2 are key transcription factors that are known to play roles in inducing *Helicobacter pylori* gastric intestinal metaplasia) SALL4 and KLF5 which then converted gastric epithelial cells into tissue stem-like progenitor cells which may be part of the transformation process leading to gastric neoplasia [262]. Very recently, genome-wide binding profiles have revealed cooperation between *KLF5*, *GATA4* and *GATA6* in

gastric cancer [263]. This study reported that these factors act in an intimate, cross-regulatory and collaborative manner, to target common downstream genes for example *HNF4α*, relevant to gastric cancer development and proliferation [263].

1.7.6.6 Lung

Through a conditional *Klf5*-gene knockout model, it has been shown that Klf5 controls lung development in differentiation and lung morphogenesis [78, 264]. It was reported that Klf5 is required for regulation of lung epithelial cell maturation, proximal airway epithelial cell maturation and also influences paracrine signaling between lung epithelium and mesenchyme [264]. Interestingly, a recent study has reported that *KLF5* expression is up-regulated in lung cancer tissues and cell lines [119]. *Li et al*. also reported that while over-expression of *KLF5* promotes cell growth and proliferation, knockdown of *KLF5* expression inhibits proliferation of lung carcinoma cell lines [119]. Interestingly, this study also revealed that KLF5 positively regulates Sox4, identifying a downstream mechanism that KLF5 uses to mediate the growth effect [119]. Consistent with this finding, an independent study conducted in non-small cell lung cancer recently has also shown a functional role for KLF5 in promoting lung carcinoma [265]. KLF5 was demonstrated to cooperate with HIF-1α in promoting hypoxia-induced survival and inhibition of apoptosis in non-small cell lung cancer cells via cyclin B1/survivin/caspase-3 [265].

1.7.6.7 Epithelium/Skin

KLF5 expression has been identified in human skin and specifically in the matrix and the inner root sheath cuticle layer of the hair follicle [266]. Further investigation demonstrated that over-expression of *KLF5* at the basal layer of the epidermis leads to abnormal epidermal development and differentiation, and disrupts epithelial-mesenchymal interactions necessary for skin adnexae formation as well as craniofacial morphogenesis [266]. In epithelial homeostasis, *KLF5* has been shown to encompass a pro-proliferative role where it is highly expressed in proliferating cells [184, 267]. In addition, over-expression of *KLF5* was found to stimulate fibroblast cell growth and at the same time enhance their transformation [268]. In addition, KLF5 has been identified as a transcription factor that has an association with the NF-κB factors in regulating skin morphogenesis and carcinogenesis [118]. Most interestingly, an *in vitro* study on HaCaT epidermal epithelial cells showed that KLF5 regulation of MYC transcription could be modified from activation to repression by TGFβ, illustrating the importance of context in cellular response to particular factors [224].

1.7.6.8 Female reproductive tissue

Within the female reproductive system, a small amount of evidence exists suggesting that KLF5 may have several distinct roles. For example, an *in vivo* study has reported that *Klf5* is persistently expressed in the uterine epithelium throughout the preimplantation period and that deletion of uterine *Klf5* confers female infertility due to implantation failure [269].

KLF5 has been found to be highly expressed in an ovarian cancer cell line, where *KLF5* expression was correlated with survivin expression [270]. It was shown that silencing of *KLF5* by small interfering RNA down-regulated survivin expression, which also sensitised the cells to apoptosis induced by chemotherapeutic drugs [270].

Lastly, it has been shown that KLF5 is a potential molecular marker in cervical cancer such that over-expression of *KLF5* was detected in cervical cancer compared to normal tissue [271].

1.7.6.9 Cardiac muscle

A study of a conditional knockout mouse for *Klf5* has shown that KLF5 is one of the key regulators in cardiac hypertrophy, potentially making it a therapeutic target for treating heart failure [218]. KLF5 has been reported to play roles in phenotypic modulation of vascular smooth muscle cells by activating specific genes which have an association with vascular diseases including restenosis [216, 272, 273]. Specifically KLF5 has been reported to be important during cardiovascular remodelling [54] and such KLF5 was also reported to have an association with pulmonary arterial hypertension (PAH) development (PAH is a vascular remodelling disease characterized by enhanced proliferation of pulmonary artery smooth muscle cell (PASMC) and suppressed apoptosis) [274]. KLF5 was reported to be expressed in human PAH in a STAT3 dependent manner and PAH could be improved through KLF5 inhibition which inhibited proliferation and induced apoptosis [274]. It was reported that KLF5 inhibition

through siRNA in PAH-pulmonary artery smooth muscle cell (PAH-PASMC) results in decreased proliferation to the level seen in control-PASMC [274].

1.7.7 The function of KLF5 in haemopoiesis

As KLF5 has been reported to play significant roles in various forms of cancer and diseases, studies on KLF5 activity in tissue-specific contexts are rapidly growing, attracting interest as a therapeutic target in several settings. However, the role of KLF5 in haemopoiesis is not well studied and our preliminary data supporting a role in myelopoiesis drove our interest to investigate the functional role of KLF5 in this system. In relation to our particular interest in KLF5, this section of this review will be focusing on the roles of KLF5 in haemopoiesis.

Since this project was started one study has been published using a *Klf5* conditional knockout model to examine some aspects of the functions of Klf5 in haemopoiesis. In this study, Klf5 was demonstrated to play an important role for adhesion and bone marrow homing through Rab5-dependent post-translational regulation of β1/β2 integrins [275]. *Ishikawa et al.* also reported that *Klf5*-deficient HSC and progenitors fail to engraft after transplantation [275]. In the lymphoid compartment, microarray gene expression analysis has revealed that *Klf5* expression is down-regulated in natural killer cells, B-cell and T-cells relative to normal HSC (Figure 1.4) [276]. On the other hand, KLF5 was shown to potentially contribute to lineage-specific regulation of germline T-cell receptor (TCR) transcription since *KLF5* expression was identified in a restricted manner with highest expression in pro–T-cell lines [277]. In the erythroid compartment, KLF5 was found as a potential candidate to regulate human gamma-

globin gene expression through its CACCC element [180]. *KLF5* mRNA expression was identified in human and mouse erythroid cell lines and that mRNAs expression changed significantly upon erythroid differentiation [180].

1.7.7.1 KLF5 function in the myeloid compartment and AML

Microarray studies of the FDB1 myeloid cell line here at the Acute Leukaemia Laboratory, IMVS identified *KLF5* as a transcription factor of interest in the myeloid compartment [278]. In response to GM-CSF and IL-3, the FDB1 cell line undergoes Granulocyte-Macrophage (GM) differentiation or continued proliferation respectively [279, 280]. Microarray gene expression profiling over a time-course of GM-CSF-induced differentiation was performed to identify a number of potential novel transcriptional regulators of the GM lineage by using this model system [278]. Detailed analysis of *KLF5* expression in FDB1 cells by Q-RT-PCR has confirmed the initial microarray data [278]. These data indicated that *KLF5* mRNA is up-regulated at 12 hours in FDB1 cells undergoing GM differentiation [278]. As shown in Figure 1.4, microarray gene expression profiling in primary mouse and human haemopoietic cells also confirms this observation of up-regulation of *Klf5* expression in myeloid lineages. Thus the expression profile of *KLF5* is consistent with a role as a transcriptional regulator of GM differentiation in both mouse and human systems.

Functional characterisation of Klf5 in the myeloid system using retroviral transduction to express *KLF5* in the FDB1 cell line showed that under growth-promoting conditions (IL-3), FDB1 cells transduced with a MSCV-*mKLF5*-IRES-GFP retrovirus display a decreased rate of proliferation due to a significant increase in apoptosis G0/G1

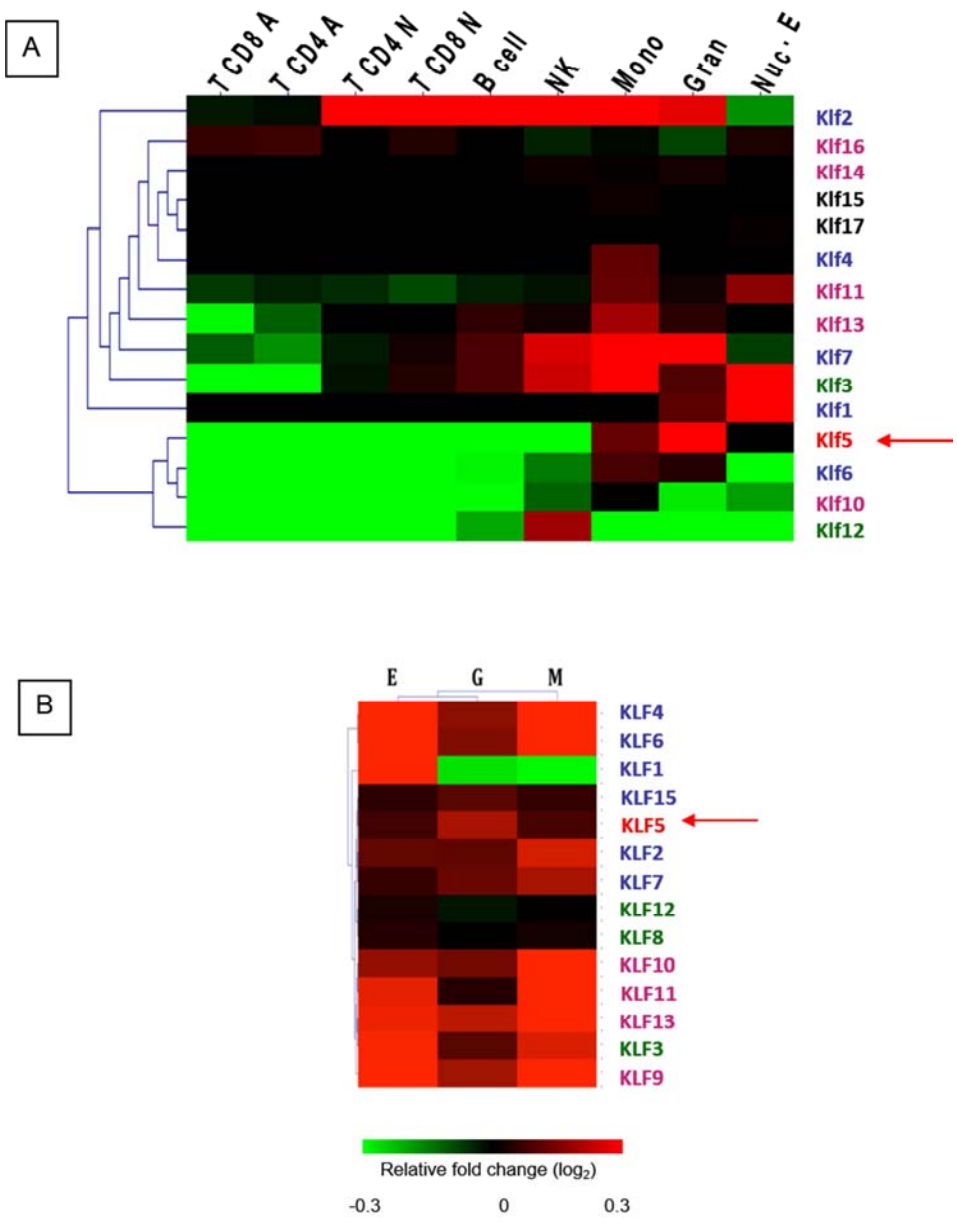

Figure 1.4: Expression of KLF family members in mouse and human haemopoietic lineages

A) Heat maps showing expression of mouse *klf5* (red arrow) and other family members in mouse haemopoietic lineages. Data was extracted from a study by *Chambers et al.* in which mature haemopoietic cell populations and haemopoietic stem cells were freshly harvested from bone marrow or peripheral blood [281]. **B)** Heatmap showing expression of human *KLF* family members during *in vitro* differentiation of human CD34+ cells along erythroid (E), granulocyte (G) and monocytic lineages (M). Data was extracted from Tonk et. al. followed by gene expression analysis for each population by microarray [282]. Heat map colours represent fold change relative to haemopoietic stem cells as indicated by the colour scale (log2). Red=increase, green=decrease [276].

and cell cycle arrest [276]. This was accompanied by a significant increase in the maturation markers Gr-1 and c-Fms, indicating that *KLF5* over-expression was inducing growth arrest and changes associated with GM differentiation in these cells [276].

The effects of forced *KLF5* expression in primary murine haemopoietic cells has also been tested [276]. Expression of *KLF5* in bone marrow cells significantly reduced their capability to form colonies in semi-solid media. Similar experiments have also shown that *KLF5* expression can induce markers of maturation in human leukaemic cell lines [28]. Further evidence supporting a functional role for KLF5 as a growth suppressor in myeloid cells was obtained where *Diakiw et al.* demonstrated that knockdown of *KLF5* expression was associated with an increase in cell expansion and attenuated granulocyte differentiation in response to G-CSF [28]. Interestingly, an independent study conducted in acute promyelocytic leukaemia (APL) cells has shown similar results in which knocking down *KLF5* in the APL cell line (NB4) significantly attenuated neutrophil differentiation [33]. Additionally, both groups have shown similar findings where *KLF5* expression is reduced in multiple subtypes of acute myeloid leukaemia (AML) suggesting that this may be a common event associated with development of the AML blast and stem cell populations [28, 33]. In addition, KLF5 has been reported to be hypermethylated in the intron 1 region, contributing to reduced expression, which is correlated with inferior survival in AML [28, 52].

Recent research has shown that upregulation of *Klf5* expression during neutrophil differentiation of APL cells is *CEBPA*-dependent [283]. *C/EBPα*, is a known transcription factor which codes for a critical regulator during formation of granulocyte-monocyte progenitors and neutrophil differentiation [283, 284]. Global gene expression

analysis has revealed that *Klf5* expression is reduced in the *C/EBPα* knockdown lineage-negative marrow cells [284]. This study also reported that higher levels of *C/EBPα* are required for granulocyte lineage and lower levels for monocyte lineage specification [284]. Since it has been reported that *Klf5* expression level is associated with *C/EBPα* [284], this further suggested that *Klf5* in association with *C/EBPα* plays a key functional role in regulating granulocyte development.

As a whole, the expression and functional data generated supports the proposal that *KLF5* is acting as a growth suppressor and promoter of differentiation in the myeloid lineage, and the prediction is that it will have a role as a tumour suppressor in AML. However, the role of *KLF5* as a regulator of myeloid cell growth and differentiation has not been investigated extensively *in vivo*.

1.7.8 KLF5 mouse knockout phenotypes

Klf5 knockout (KO) mice (*Klf5*$^{-/-}$) are embryonic lethal at 8.5 days postcoitum (dpc) [79], making the study of KLF5 function in the adult via homozygous KO impossible. A study on mouse embryonic stem cells (ESCs) has shown that *KLF5* regulates their proliferation and self-renewal and that loss of *KlF5* expression interrupts normal embryonic development [285, 286]. Recent studies have also identified that Klf5 is important in regulating mouse embryo implantation and that Klf5 is required for the formation of the trophectoderm (TE) and the inner cell mass (ICM), whilst repressing primitive endoderm (PE) development [269, 287]. However, the heterozygous littermates, *Klf5*$^{+/-}$ mice survive until adulthood and are apparently normal and fertile, with expression of KLF5 reduced to about half that in wild-type mice [79].

Several *in vivo* studies conducted on *Klf5*$^{+/-}$ mice revealed different roles of Klf5 function in tissue-specific contexts. For example, while *Shindo et al.*, showed that Klf5 is important in the activation and proliferation of smooth-muscle cells in cardiovascular remodelling [79], *Oishi et al.,* have shown that KLF5 is a key regulator of the transcription factor network that governs adipocyte differentiation [78]. Additionally, several groups have generated conditional knockout models (Cre/*LoxP* recombination system) to study Klf5 in various tissues, for example in the study of cardiac hypertrophy and heart failure, as well in studies to assess the role of KLF5 in lung development and function [218, 264]. In haemopoiesis, *Ishikawa et al.* had generated an inducible *Klf5*-gene ablation model using the Mx1-*Cre* system and shown that Klf5 has a functional role in the homing and retention of haemopoietic stem cell (HSC) in the bone marrow but did not present a detailed analysis of Klf5 in committed lineages [275]. Combined with *in vitro* data suggesting Klf5 as a myeloid regulator generated by us and others, this suggests that *Klf5* might be involved in multiple aspects of blood cell formation during haemopoiesis. Thus, further investigations on the consequences of loss of *Klf5* on haemopoietic stem and progenitor cell (HSPC) function and committed lineage progenitors are warranted. Hence, we generated a haemopoietic *Klf5* conditional knockout mouse model by using the Cre/*LoxP* recombination system for the *in vivo* study of *Klf5* function in the haemopoietic system.

1.7.8.1 The use of the Cre/LoxP recombination system to generate a conditional knockout mouse model.

The Cre/*LoxP* recombination system has been widely used as an efficient tool for generating site-specific DNA recombination in transgenic mice where the genome was altered in a tissue-specific manner [288, 289]. Cre recombinase is an enzyme of the PI bacteriophage that integrates DNA in a site-specific manner where it catalyses the recombination between two of the recognition sites, *LoxP* [290]. A *LoxP* site consists of two 13 bp inverted repeats separated by an 8 bp asymmetric spacer region [291] (Figure 1.5). When a single Cre recombinase molecule binds to each palindromic half of a *LoxP* site and forms a tetramer, two *LoxP* sites are brought together and recombination occurs within the spacer area of the *LoxP* sites [292]. The Cre/*LoxP* recombination system allows both the knock-out and knock-in of specific genes in a range of diseases and developmental studies. As reviewed in *Zhao et al.* and *Daria et al.*, [293, 294], there are two mouse lines required; firstly a conventional transgenic mouse line with Cre targeted to a specific tissue or cell type through use of a cell specific promoter. Secondly, a mouse strain engineered to have a target gene for example *Klf*5,

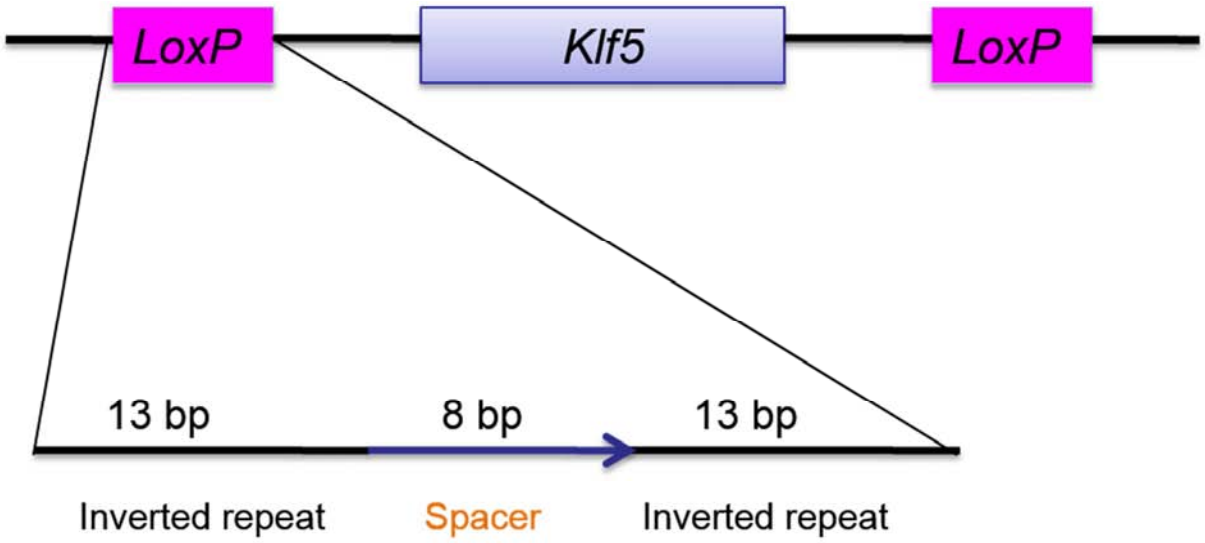

Figure 1.5: Two loxP sites flanking exon 2 of *Klf5* to be targeted by Cre recombinase

The schematic diagram represents a target gene for an exon of *Klf5*, flanked by two *LoxP* sites in a direct orientation where a *LoxP* recombination site is 34 bp long and consists of two 13 bp inverted repeats separated by an asymmetric 8 bp spacer region.

flanked by two *LoxP* sites in a direct orientation. Mating of these two transgenic mice allow the recombination event to occur in the progeny in those cells expressing Cre recombinase. As the recombination event occur only in a tissue-specific manner, the targeted gene (deleted in specific cells) remains active in other cells and tissues which do not express Cre (reviewed in *Georgiades et al.*, [295]). This genetic tool is being improved and expanded indicating its potential benefits in a broader area of studies, especially in a larger scale of DNA manipulation [296, 297].

1.7.8.2 The *Vav* promoter drives Cre-mediated gene knockout throughout the blood system.

In the haemopoietic system, *vav* promoter elements have been used in a transgenic vector to drive transgene expression throughout the haemopoietic compartment [298]. *Vav* is a proto-oncogene that was described to be ubiquitously expressed in the haemopoietic compartment [299] and subsequent studies in an *in vivo* model showed that *vav* expression is restricted to haemopoietic tissues and endothelial tissues [300]. The *vav-Cre* transgenic mice have now become a widely used tool for mutagenesis in all haemopoietic lineages [295, 301]. The *vav-Cre* transgenic mice have been successfully used to generate a conditional haemopoietic KO of the gene *Autophagy (Atg)* allowing the investigation of its role in haemopoietic cells and its association with anaemia [302]. Additionally, a *Retinoblastoma* (*Rb*) gene conditional KO was generated using *vav-Cre* techniques and used to assess the role of Rb in HSC development and function [294]. In addition, the role of *suppressor of cytokine signalling-3* (*Socs3)* in the regulation of

haemopoietic growth factor signalling has been investigated using a tissue-specific deletion in the haemopoietic system, generated using *vav-Cre* techniques [303].

1.8 Research Proposal

1.8.1 HYPOTHESIS

1. Based on the previous findings [28, 33, 52, 276, 278], we hypothesise that *KLF5* is acting as a growth suppressor and promoter of differentiation in the myeloid lineage.

1.8.2 EXPERIMENTAL AIMS and DESIGNS

1. *Generating a Klf5 conditional knockout mouse model for study in the haemopoietic system.*

We proposed to generate a *Klf5* pan-haemopoietic gene-ablation model by crossing $Klf5^{flox/flox}$ mice with *Vav-Cre* transgenic mice. Details on the procedure used to construct this mouse will be described in Chapter 3.

2. *Analysing peripheral blood of Klf5 conditional knockout mice*

Peripheral blood (PB) will be drawn through orbital eye-bleed under halothane anaesthesia at 3, 6, 9 or 12 months old. PB will be measured for white blood cell (WBC) and red blood cell parameters (including haemoglobin, haematocrit, mean corpuscular volume, mean corpuscular concentration and mean corpuscular concentration) counts. This will be performed using automated blood cell count. Next, PB phenotype will be

analysed by flow cytometry analysis using cell surface marker specific to mature cells type (e.g. CD11b, Gr-1, B220, CD3, and TER119).

3. Analysing bone marrow of Klf5 conditional knockout mice

Mice will be sacrificed by cervical dislocation followed by extracting the bone marrow from both femur and tibia of each mouse. Flow cytometry will also be used to measure cell populations from BM for the expression of various lineage differentiation markers. The stem and progenitor cell compartments will also be assessed by multicolour flow cytometry (Lin^-, $Sca\text{-}1^+$, $c\text{-}Kit^+$ and Lin^-, $Sca\text{-}1^-$, $c\text{-}Kit^+$ cells respectively). Flow cytometry will also be used to measure the percentages of HSC, CMP, CLP and GMP as described in [304]. Colony assay (CFU assay) and serial replating assay in a range of different cytokines will be conducted to detect and quantify the capability of haemopoietic progenitor cells in bone marrow to form colonies [305].

4. Analysis of haemopoietic organs from Klf5 conditional knockout mice

Following bone marrow analysis, post-morterm analyses will also be conducted on other haemopoietic organs (including rib cage, liver and spleen). Haemopoietic organs from *Klf5*-KO mice will be physically visualised next to control littermate for any defects or differences (such as colour, size and appearance). Next, sections of tissues will be stained with haematoxylin and eosin (HE) and/or myeloperoxidase (MPO) for histology analysis.

5. Analysis of spleen from Klf5 conditional knockout mice

Extended analyses will be conducted on spleen of *Klf5*-KO mice. Spleen cells will be extracted and percentages of specific cell types were measured by flow cytometry. The stem and progenitor cell compartments will also be assessed by multicolour flow cytometry using specific cell surface markers. CFU assay will also be conducted to monitor the frequency of haemopoietic progenitor cells in spleen.

1.8.3 Ethical Considerations

Ethical approvals for all experiments have been approved by the Animal Ethics Committees of SA Pathology and the University of Adelaide. All procedures complied with the "The Australian Code of Practice for the Care and Use of Animals for Scientific Purposes, 2004 and the South Australian Animal Welfare Act, 1985.

1.8.4 Location

The experiments were mainly conducted at the Institute of Medical and Veterinary Science (IMVS). Mice were raised and bred in the animal house of Hanson Institute, SA Pathology, Frome Road whereas dissecting and analysis of the mice were held in the Acute Leukaemia Laboratory in the division of Haematology department, IMVS, Frome road, Adelaide. Other experiments involving *in vitro* analysis were conducted in the Acute Leukaemia Laboratory in the division of Haematology, IMVS, Frome Rd, Adelaide.

Chapter 2: Materials and methods

2.1 Materials

Supplier	Reagent
Alpha Diagnostic Int.	Antibody stripping solution
Applied Biosystem - USA	BigDye Terminator v3.1 sequencing reagent
BD Pharmingen™	Alexa Fluor 488® rat anti-mouse CD125 antibody FITC rat anti-mouse CD41 antibody PE-Cy™5 rat anti-mouse CD45 antibody PE rat anti-mouse CD117 antibody PE rat anti-mouse CD16/32 antibody PE rat anti-mouse Siglec-F antibody
Biolegend – USA	APC anti-mouse CD11b antibody APC anti-mouse CD150 (SLAM) antibody Biotin anti-mouse CD127 (IL-7Rα) antibody FITC anti-mouse CD48 antibody Pacific Blue™ anti-mouse CD3ε antibody Pacific Blue™ anti-mouse Ly-6A/E (Sca-1) antibody PE/Cy5 anti-mouse CD3ε antibody PE/Cy5 anti-mouse CD11b antibody PE/Cy5 anti-mouse CD45R/B220 antibody PE/Cy5 anti-mouse Ly-6G/Ly-6C (Gr-1) antibody

	PE/Cy5 anti-mouse TER-119/Erythroid Cells antibody PE/Cy7 anti-mouse CD105 antibody Strepavidin-PE/Cy7
eBioscience –USA	Anti-human/mouse CD45R (B220) PE-Cy7 antibody Anti-mouse CD117 (c-Kit) APC-eFluor® antibody Anti-mouse CD135 (Flt3) PE antibody Anti-mouse CD45.2 FITC antibody Anti-mouse CD45.1 PE antibody Anti-mouse Ly-6G (Gr-1) APC-eFluor® 780
Geneworks – Australia	Oligonucleotide primers
Invitrogen - USA	0.5 -10 Kb RNA ladder 1 Kb plus DNA ladder BenchMark™ pre-stained protein ladder Proteinase K Trizol solution Trypan blue solution
Merck Australia - Australia	Ethanol, absolute Isopropanol
Millipore	Anti-KLF5 antibody (#07-1580)
Miltenyi Biotec - Germany	AutoMACS™ rinsing solution CD117 MicroBeads mouse MACS Multistand MiniMACS Separator

	MS Columns Pre-separation filters, 30 µm
Peprotech	G-CSF (mouse)
Pierce	SuperSIgnal WestPico substrate SuperSIgnal WestDura substrate ImmunoPure Goat Anti-Mouse IgG HRP ImmunoPure Goat Anti-Rabbit IgG HRP
Progen Industries Ltd – Australia	Agarose
Qiagen – USA	DNeasy Blood & Tissue kit QIAquick Gel Extraction kit QIAquick PCR Purififcation kit QuantiTect Rev. Transcription kit RNeasy Micro kit
Roche – Australia	Complete™protease inhibitor cocktail FastStart Taq reagents Glygocen Pefabloc™
Sigma-Aldrich - USA	1X Phosphate buffered saline (PBS) 1X TAE buffer (tris-acetate-EDTA) Bovine serum albumin Dimethyl sulfoxide (DMSO) Dextran from Leuconostoc spp. –Mr ~500,000

	(#31392) EDTA (ethylenediamine-tetraacetic acid) Ethidium bromide Foetal calf serum (FCS) lot #3A0561 Glucose IMDM (Iscove's Modified Dulbecco's Medium with L-glutamine and 25Mm HEPES) L-glutamine-penicillin-streptomycin solution for cell culture TEMED Ammonium Persulphate Polybrene Puromycin
StemCell Technologies – Canada	Methylcellulose-Based Medium with Recombinant Cytokines and EPO for mouse cells (#M3434) Methylcellulose-Based Medium with EPO (without cytokines) for mouse cells (#M3334) Methylcellulose-Based Medium without cytokines for mouse cells (#M3234)
Veterinary Services of Australia – Australia	Isofluorane inhalation anaesthetic

2.1.1 Oligonucleotide PCR Primers

NAME	DETECTS	USE	FORWARD PRIMER	REVERSE PRIMER	DESIGN by
Actb	*Actb*	Q-PCR (control)	AGTGTGACGTTGACATCCGTA	GCCAGAGCAGTAATCTCCTTCT	Dr Sonya Diakiw
CRE 1	*Cre*	Cre PCR	CTGACCGTACACCAAAATTTGCCTG	GATAATCGCGAACATCTTCAGGTTC	Warren Alexander
CRE 2	*Cre*	Cre PCR	CATTTGGGCCAGCTAAACATG	GCAATCCCCAGAAATGCCAG	N.H. Shahrin
SD41/42	*FLPE*	Flpe PCR	GTGGATCGATCCTACCCCTTGCG	GGTCCAACTGCAGCCCAAGCTTCC	Dr Ian D Tonks
Primer set 1	Downstream flox	Flox PCR	CCAAGTTGCAGGCATAAGC	CCGTATGAGTCCTCAGGTGA	Dr Ian D Tonks
Primer set 2	Upstream flox	Flox PCR	CTGGTTCAAGTGAACATTTGG	CAAAGGGCTTTTGTGTGTGGAC	Dr Ian D Tonks
Primer set 3 **Primer R2** **Primer R2**	Downstream flox	Flox PCR Klf5-deleted PCR Sequencing	CGTGACCCAAAATATAATTGGATGG	GTAAATGGAGAGCAATCGTGGGAC GTAAATGGAGAGCAATCGTGGGAC GTAAATGGAGAGCAATCGTGGGAC	N.H. Shahrin
Primer set 4 **Primer F** **Primer R1**	Upstream flox	Flox PCR Klf5-deleted PCR Sequencing	GAGGGTGCAATTGTTTTGTATC GAGGGTGCAATTGTTTTGTATC GAGGGTGCAATTGTTTTGTATC	CTTGAAAACTAAAACCTGTGC CTTGAAAACTAAAACCTGTGC	N.H. Shahrin
Klf5	*Klf5*	Q-PCR	AGCTCAGAGCCTGGAAGTC	TGAGTCCTCAGGTGAGCTTT	Dr Sonya Diakiw

Table 2.1: Oligonucleotide sequences

2.1.2 Media and solutions

TAC (Tris Ammonium Chloride): erythrocyte lysis buffer for bone marrow

13mM Tris and 13.5 mM ammonium chloride (NH_4CL) was made up to 500 ml in PBS. The PH was adjusted to 7.2 with concentrated HCl and subsequently autoclaved and stored at room temperature.

ACK (Ammonium, Chloride, Potassium): RBC lysis buffer for peripheral blood

To make up 10x ACK, 150mM NH_4CL, 10mM $KHCO_3$ and 0.1mM NaEDTA of final concentration were made up to 500 ml in miliQ water. The PH was adjusted to 7.4 with concentrated HCl and subsequently autoclaved and stored at room temperature.

2% Dextran for RBC separation

2% dextran was made up with PBS and stock were store at 4°C.

Sample media (SM) for flow cytometry

Made up with PBS (490 ml) with 2% FCS (10ml) and 0.5 mM EDTA.

Solution 2 for tail genomic DNA prep

50 mM Tris with pH 8.0, 20 mM EDTA with pH 8.0, 2% SDS and water to make an 80 ml stock solution.

2.2 Generating conditional *Klf5* knockout mice

Details on the strategy used to generate pan-haemopoietic *Klf5* conditional gene knockout mice by using *Vav-Cre* transgenic mice were explained in Chapter 3

of this study. The *Klf5*-floxed mice (*Klf5*$^{fl/fl}$) were generated by a commercial provider; Queensland Institute of Medical Research (QIMR). The *Flp* recombinase mice used in this study are driven by *ACTB* promoter which allows complete excision of the NEO selection cassette in the germ line [306]. This was performed at QIMR and we were provided with *Klf5*$^{fl/fl}$*Flpe*$^{+}$ mice on a 129/C57BL6 mixed background. We had already established a local colony of *Vav-cre* transgenic mice for this study in the SA Pathology animal care facility (Kind gift of Warren Alexander, WEHI) [303].

2.3 Genotyping from genomic DNA

2.3.1 Extracting genomic DNA from mice

2.3.1.1 Tail genomic DNA preparation

700 µl of Solution 2 was added into each eppendorf tube containing an individual tail tip. Using sharp scissors, each tail was chopped into small pieces. Then, 35 µl of 10 mg/ml proteinase K was added into each tube and mixed by inversion. The mixtures were then incubated for at least 6 hours or overnight at 56°C. Following incubation, the mixtures were chilled on ice for 10 minutes. Next, 250 µl of NaCl was added and inverted to mix. The mixtures were chilled on ice for 5 minutes followed by centrifugation at 13.4 rcf for 5 minutes. Supernatants were then transferred into a new eppendorf tube and DNA was precipitated by adding 700 µl of isopropanol. The mixtures were mixed by inverting followed by centrifugation at 13.4 rcf for 5 minutes. Later, DNA pellets were washed with 70% ethanol. Dried pellets were then resuspended in 50 µl of TE buffer containing 0.2 mg/ml RNAseA.

2.3.1.2 Bone marrow genomic DNA preparation

Genomic DNA from whole bone marrow cells was extracted by using DNeasy Blood & Tissue Kits from Qiagen according to manufacturer's instructions.

2.3.2 Polymerase Chain Reaction (PCR)

2.3.2.1 Flpe, Flox and Klf5 deleted PCR method

Oligonucleotides used for these PCR reactions are listed in **Table 2.1**. PCR reactions and cycles used for Flpe-PCR, Flox-PCR and Klf5 deleted-PCR were the same using the Roche FastStart Taq PCR kit according the manufacturer's protocols. However, primers used in each polymerase chain reaction (PCR) were designed individually according to the detection of desired gene. PCR was performed in 50 µl of total reaction with 100 ng of genomic DNA as the template, 10x Reaction Buffer, 4 µl of $MgCl^2$, 5x GC-rich solution and 10 mM dNTPs. Amplification parameters were as follow; 96°C for 2 minutes (1 cycle), then 2 cycles of 96°C for 30 seconds, 64°C for 30 seconds and 72°C for 1 minute. Then the annealing temperature was decreased by 2°C/step and 2 cycles/step were performed until the annealing temperature of 58°C was reached. Then, 35 cycles of 96°C for 30 seconds, 55°C for 30 seconds and 72°C for 1 minute. Followed by 72°C for 2 minutes and lastly, hold at 4°C.

2.3.2.2 Cre PCR method

PCR was performed using the Roche FastStart Taq PCR kit according the manufacturer's protocols with 1 µg of gDNA template. Cycling parameters used for Cre PCR were as follow; the initial denaturation was at 95°C for 4 minutes (1 cycle). Then, the following denaturation step was at 95°C for 30 seconds, followed by

annealing at 60°C for 30 seconds and extension at 72°C for 1 minute (25 cycles). The final extension was at 72°C for 10 minutes (1 cycle). PCR was performed on a Corbett Gradient Palm-Cycler. 5 µl of each PCR reaction was separated and visualised using gel electrophoresis. Oligonucleotide primer sequences are shown in Table 2.1.

2.4 RNA isolation and cDNA production

Total RNA was isolated from whole bone marrow cell pellet using the Qiagen RNEasy Micro kit according to the manufacturer's instructions. Quantitation of RNA was performed using a NanoDrop Spectrophotometer. RNA was stored in aliquots at -80°C. For production of cDNA, 1 µg of RNA was treated with DNAse and reverse-transcribed using the Qiagen QuantiTect Reverse Transcription kit as per the manufacturer's protocol. cDNA samples were stored at -20°C.

2.5 Quantitative reverse transcription PCR

Quantitative reverse transcription PCR (Q-PCR) reactions were carried out using the following conditions per reaction: 1.25 U/µl Roche FastStart Taq, 1x Taq Buffer (without magnesium), 2.5 mM magnesium chloride, 200 µM each dNTP, 1x EvaGreen fluorescent nucleic acid dye, 450 nM each forward and reverse PCR primers, and 1 µl cDNA template. Q-PCR was performed on a Corbett RotorGene 6000 instrument with the following cycling conditions: 95°C for 10 minutes (1 cycle), 95°C for 25 seconds - 60°C for 25 seconds - 72°C for 30 seconds (40 cycles – acquiring to green), 72°C for 1 minute (1 cycle). Products of Q-PCR were analysed by melt curve analysis as follows: Increments of 1°C for 5 seconds each from 72°C -

99°C, acquiring to green. For each sample duplicate reactions were performed for detection of the gene of interest and a control gene (Beta-actin, ACTB). QGene software was used for analysis of relative mRNA expression levels313. Oligonucleotide primer sequences are shown in Table 2.1.

2.6 Preparation of Cell lysates and Protein assay

Cells were pelleted by centrifugation at 287 rcf for 5 minutes and then resuspended in ice cold Phosphate buffered saline (PBS). The cells were then centrifuged at 3.3 rcf for 3 minutes at 4°C. Cells were lysed in Modified RIPA Lysis Buffer (MRLB) (1% Np-40, 0.1% SDS, 0.1% NaDeoxycholate, 100 mM NaCl, 2.5 mM EDTA, 2.5 mM EGTA, 50 mM Hepes pH 7.4) with inhibitors (Pefabloc (50x), Complete (25x) and PhosSTOP (10X)) (Roche) on ice for 30 minutes. Cells were then centrifuged at 13.4 rcf for 1 minute at 4°C and the supernatants were transferred to new tubes. Protein concentrations were determined using the Biorad D^C protein assay as in the manufacturer's instructions.

2.7 Western Blot

Samples with 5X Sodium Dodecyl Sulfate (SDS) load buffer (including 2-mecapto-ethanol @ 50 µl/ml) were run on 8% SDS-Polyacrylamide Gel Electrophoresis (PAGE) with 1X SDS running buffer, followed by wet transfer on nitrocellulose membrane run with 1X towbin buffer (200 ml 10X Towbin buffer (0.25M Tris, 1.92M Glycine, water), 1.6 ml milliQ and 200 ml methanol). To see an even transfer for each lane, Ponceau S was used to stain the membrane. 5% milk in PBS-tween 20 was used for 1 hour blocking. The membranes were then incubated with the primary antibody and left overnight. Primary antibody binding was detected

with a horseradish peroxidase (HRP) conjugated secondary antibody (Pierce) followed by chemiluminescence detection (SuperSignal West Pico Chemiluminescent Substrate and SuperSignal West Dura Chemiluminescent Substrate; Pierce) and developed on LAS4000. For stripping, 10 ml of 1:10 antibody stripping solution (cat#90101, Alpha Diagnostic Int.) and milliQ was used. The intensity of the band which represented the protein amount was quantified using ImageQuant.

2.8 Isolation and Preparation of Mouse Bone Marrow Cells

Mice were first euthanized by cervical dislocation. The skin was then disinfected with 70% ethanol. For necroscopy purposes, the abdominal area was transversely cut to open the abdominal cavity. Prior to fixation, spleen from each individual mouse was weighed, measured and inspected for any signs of disease. Later, spleen, liver and rib cage of each mouse were removed from the body and put into 10% formaldehyde for at least overnight followed by paraffin embedding before sectioning and staining for histology analysis. Both feet were then cut and removed from the body. Femur and tibia were then dissected and transferred into the cold buffer (IMDM+15%FCS).

After isolation of all bone fragments, the bones were transferred to a mortar and gently crushed. Next, the bones were flush crushed with isolation buffer and pipetted up and down with cold buffer (IMDM+15%FCS), followed by filtering the suspension using the 80-mm cup filter into an appropriately sized collection tube. The cell suspension was centrifuged at 400 × *g* for 10 min followed by resuspending the cell pellet in 200 µL/mouse of 1× TAC lysis buffer. For washing step, 1 ml/mouse cold buffer (IMDM+15%FCS) was added followed by filtering to get rid

clumps of cell debris. Next step was centrifuged again at 400 × *g* for 10 min followed by resuspending in an appropriate volume of (IMDM+15%FCS) buffer.

2.9 C-Kit enrichement using MACS

2.9.1 Magnetic Labelling

2 x 10^7 of whole bone marrow cells were centrifuged at 400 × *g* for 10 minutes and supernatant was removed. Cells were then resuspended in 100 µl of cold MACS buffer (provided by Miltenyi Biotec). 3.5 µl of CD 117 (c-Kit) micro beads (Miltenyi Biotec – Cat #130-091-224) were added into the samples. Samples were then incubated on ice for 30 minutes in the dark. Later, 10 mL MACS buffer added followed by centrifugation of those cells for 10 minutes at 300 x g. Cells were then resuspended in 500 µl of MACS buffer and placed on ice.

2.9.2 Magnetic separation

MS columns (Miltenyi Biotec – Cat # 130-042-201) were placed in the magnetic field of a suitable MACS Separator (Miltenyi Biotec Midi Macs separation unit #130-042-302) and rinsed with 3 ml Macs buffer. C-Kit stained cells were applied onto the column through a 30 µm nylon mesh filter (pre-separation filter, #130-041-407). Unlabelled cells that pass through were collected in a separate tube (kept aside) and columns were washed with an appropriate amount of Macs buffer (MS: 500 µl) three times. To elute cells, columns were removed from the separator and placed on a suitable collection tube. 1 ml MACS buffer was used to flush out the magnetically labelled cells

2.10 Retro orbital blood collection

For blood cell phenotyping, blood was collected through the peri-orbital sinus of the mouse. Animals were first anaesthetised with isofluorane 2% by inhalation. When the animals were no longer moving, a mask was placed on to continue anaesthetic stage with isofluorane 1%. Under the halothane anaesthetic condition, the forefinger of the operator's hand was used to pull the facial skin taut and cause the eye to protrude slightly. Breathing and colour were monitored throughout the procedure to ensure that the restraint did not compromise the airway. Using the other hand, the tip of a haematocrit tube was gently inserted below the eye at an approximately 45 degree angle into the space between the globe and the lower eye lid. When the tip of the pipette contacts the bony floor of the orbit it was gently twisted to rupture the capillary sinus. Blood was allowed to flow by capillary action into the haematocrit tube and collected blood was transferred into an EDTA coated collection tube straight away. After the required amount of blood was obtained (approximately 150 µl), the tube was withdrawn and bleeding was ceased by direct pressure with sterile gauze over the eyelids. Normal colour and respiration were rechecked before returning the animals into their cages for recovery. The animals were checked at the end of the day and 24 hours later for complication such as squinting or bulging of the eye.

2.11 Cell blood count

To do the CBC, the Sysmex XE analyser automated blood cell counted was used. The minimum volume required for the analyser to run each sample by manual open mode setting was 200 µl. Since we were collecting a small amount of blood

from each mouse, we made a 1:5 dilution of each blood sample in cell pack buffer to make 200 µl of the final volume prior running the samples on the analyser.

2.12 Flow Cytometry

2.12.1 Peripheral blood cell preparation prior to flow cytometry analysis

For flow cytometry analysis, at least 50 µl of whole blood is required prior to cell preparation. In each blood sample, 250-500 µl of 2% dextran/PBS* was added per blood sample depending on the blood volume and mixed by pipetting up and down followed by 30 minutes incubation at 37°C. After incubation, RBC centrifuged to the bottom of an eppendorf tube, and the top layer (~700 ul vol) pipetted into a fresh FACS tube. Then, 1 ml of sample media (SM) was added and the sample centrifuged at 287 rcf for 5 minutes and aspirated. Samples were then treated with 200 µl ACK per sample for 3 minutes at room temperature followed by additional of 1 ml of SM and centrifugation at 1200 rpm for 5 minutes and aspirated. 100 µl of SM media was added into each sample with the desired antibodies.

2.12.2 Flow cytometry from peripheral blood

Mature Marker panel – Following ACK treatment, the antibodies required for the mature marker panel were CD45.1-PE, CD45.2-Alexa488 (FITC), B220-PECy7, Mac1-APC, Gr1-APC/AL780, CD3ϵ-PB and TER119-PECy5. Then, samples were incubated for 30 minutes on ice in the dark in 100 µl SM. The incubated samples were then washed twice with 1 ml SM and centrifuged at 287 rcf for 5 minutes. Finally, cells were re-suspended in 180 µl SM and 20 µl of Fluorogold added prior to FACS analysis. Analysis was done with an Aria R/S. Single stained

controls for compensation and fluorescence minus one (FMO) controls for gating strategy were prepared in parallel with samples preparations.

2.12.3 Flow cytometry from Bone Marrow and Spleen cells

Mature Marker panel – 8 x 10^5 bone marrow cells were stained with CD45.1-PE, CD45.2-Alexa488 (FITC), B220-PECy7, Mac1-APC, Gr1-APC/AL780, CD3ϵ-PB, and TER119-PECy5 in 200 µl SM. Then, samples were incubated for 30 minutes on ice in the dark. The incubated samples were then washed twice with 1 ml SM and centrifuged at 287 rcf for 5 minutes. Finally, cells were re-suspended in 180 µl SM and 20 µl of Fluorogold added prior to FACS analysis. Analysis was done with an Aria R/S. Single stained controls for compensation and fluorescence minus one (FMO) controls for gating strategy were prepared in parallel with samples preparations.

Myeloid progenitor panel – 8 x 10^5 of c-Kit enriched bone marrow cells or 8 x 10^5 of unfractionated spleen cells were stained with desired antibodies; CD41-FITC, CD16/32-PE, CD150-APC, c-Kit-APCAL780, Sca-1-PB, CD105-PECy7 and lineage antibodies (CD3e-PECy5, B220-PECy5, Gr1-PECy5, Mac1-PECy5 and TER-119-PECy5). Then, samples were incubated for 30 minutes on ice in the dark. The incubated samples were then washed twice with 1 ml SM and centrifuged at 287 rcf for 5 minutes. Finally, cells were re-suspended in 180 µl SM and 20 µl of Fluorogold added prior to FACS analysis. Analysis was done with an Aria R/S. Single stained controls for compensation and fluorescence minus one (FMO) controls for gating strategy were prepared in parallel with sample preparations.

Stem cell and lymphoid progenitor panel – 8 x 10^5 of c-Kit enriched bone marrow cells or 8 x 10^5 of unfractionated spleen cells were stained with desired

antibodies; CD48-FITC, FLT3-PE, CD150-APC, c-Kit-APCAL780, Sca-1-PB, IL7Rα-biotinylated and lineage antibodies (CD3e-PECy5, B220-PECy5, Gr1-PECy5, Mac1-PECy5 and TER-119-PECy5). Then, samples were incubated for 30 minutes on ice in the dark. Later, the incubated samples were washed twice with 1 ml SM and centrifuged at 287 rcf for 5 minutes. After that, StrepAvidin-PECy7 was added and incubated for another 30 minutes on ice in the dark. Again, samples were washed twice with 1 ml SM. Finally, cells were re-suspended in 180 µl SM and 20µl of Fluorogold added prior to FACS analysis. Analysis was done with an Aria R/S. Single stained controls for compensation and fluorescence minus one (FMO) controls for gating strategy were prepared in parallel with sample preparations.

2.12.4 Eosinophil analysis by Flow Cytometry

Peripheral blood (PB) and bone marrow (BM) – Antibodies required for the eosinophil panel were SiglecF-PE, CD45.2-Alexa488 (FITC), Mac1-APC and TER119-PECy5. BM and PB cells were prepared as detailed in Section 2.8 and 2.12.1 respectively. Both BM and PB samples were then incubated with desired antibodies in FACS wash buffer for 30 minutes on ice in the dark. . Later, the incubated samples were washed twice with 1 ml SM and centrifuged at 287 rcf for 5 minutes. Finally, cells were re-suspended in 180 µl SM and 20 µl of Fluorogold added prior to FACS analysis. Analysis was done with an Aria R/S. Single stained controls for compensation and fluorescence minus one (FMO) controls for gating strategy were prepared in parallel with samples preparations.

Lung – In this study, lung cells were extracted by mashing the lung from at least 5 mice from each genotype group at 12 months old. Again, flow cytometry were used for the analysis. In this analysis, the antibodies used were SiglecF-PE,

CD45.2-Alexa488 (FITC) and Mac1-APC for cell surface marker detection. Cells were stained for 30 minutes on ice followed by two times washes with FACS media. Cells were then fixed with FACS media contained 10% formaldehyde and kept in the fridge (4°C). The next day, samples were run on a Gallios Flow Cytometer. For analysis, FCS4 express was used.

2.13 Colony Assays

Methylcellulose colony forming assays were performed using either MethoCult™ GF M3434 (with recombinant cytokine and EPO for mouse cells) or MethoCult™ M3234 (incomplete medium) or MethoCult™ M3334 with (with EPO for mouse cells) according to the manufacturer's protocol. 1 x 10^4 bone marrow cells or 2 x 10^5 spleen cells were seeded in each plate in triplicate plates for each condition. Colonies greater than 50 cells in size were counted at Day 7 post-seeding. Representative photographs for colony morphology were taken using an Olympus CK2 microscope and DP11 camera system at an original magnification of 100x. For serial replating assays, cells from triplicate at Day 7 post-seeding were harvested and resuspended with IMDM media to wash away the methocult. Cells were centrifuged at 287 rcf for 5 minutes and the supernatant were removed. Again, 1 x 10^4 bone marrow cells or 2 x 10^5 spleen cells were seeded in each triplicate plate for each condition. At Day 7 post-seeding, colonies were scored and the same procedures were repeated.

2.14 Mouse monitoring protocol

For this, we monitored the visual characteristics of the animals. All breeding was performed in the clean barrier facilities in the SA Pathology animal care facility

to provide pathogen-free conditions. All mice from the *Klf5*$^{+/fl}$ X *Klf5*$^{+/fl}$, *Klf5*$^{fl/fl}$ X *Vav-cre*$^{+/-}$ and *Klf5*$^{+/fl}$, *Vav-cre*$^{+/-}$ X *Klf5*$^{fl/fl}$ or *Klf5*$^{+/fl}$, *Vav-cre*$^{+/-}$ X *Klf5*$^{+/fl}$ breeding pairs were monitored for physical appearance until adult stage. The pregnant mice were also monitored. Mice were born at the expected Mendelian ratios as shown in **Table 3.1**. Upon weaning at day 21, mice were marked with an ear notch for identification (ID), followed by tail tipping for genotyping. We continued physical monitoring every week until mice reached 12 months of age. Mice were monitored for their behaviour, physical activity and for any sign of disease. Since these genetic monitoring involved daily observations, they were conducted together with the animal care facility staff members on the first few littermates while the animal care facility staffs have undertook the rest of the daily routine on monitoring.

Chapter 3: Generating a *Klf5* conditional knockout mouse model for study in the haemopoietic system.

3.1 Introduction

Klf5 knockout (KO) mice (*Klf5*$^{-/-}$) are embryonic lethal at 8.5 days postcoitum (dpc) [79], making the study of KLF5 function in the adult impossible. Thus, generating a conditional *Klf5* gene KO model by using Cre/*LoxP* recombination has become a necessary and important approach for tissue-specific studies (as discussed in Chapter 1, Section 1.7.8.1). In this study, we used *vav* promoter elements to drive *Cre* expression throughout the haemopoietic compartment hence targeting *Klf5*-exon 2 removal in the haemopoietic compartment. This system will enable a detailed *in vivo* analysis of the effect of *Klf5* deletion on haemopoiesis, and will further elucidate any specific roles KLF5 may have in granulocyte versus macrophage lineage determination

In this chapter, we outline the generation of a *Klf5* haemopoietic gene-ablation model by crossing *Klf5*-floxed mice with *Vav-Cre* transgenic mice, generating *Klf5*$^{flox/flox}$*Vav-Cre* mice.

3.2 Results

3.2.1 Generating a pan-haemopoietic *Klf5* conditional gene knockout mice

For this study, we used *Klf5*-floxed mice (*Klf5*$^{fl/fl}$) which were generated by a commercial provider; Queensland Institute of Medical Research (QIMR). The *Klf5*$^{fl/fl}$ mice were targeted for exon 2 deletion as outlined in
Figure 3.1. The removal of exon 2 should delete the protein-coding region from amino acid 77 until 367,

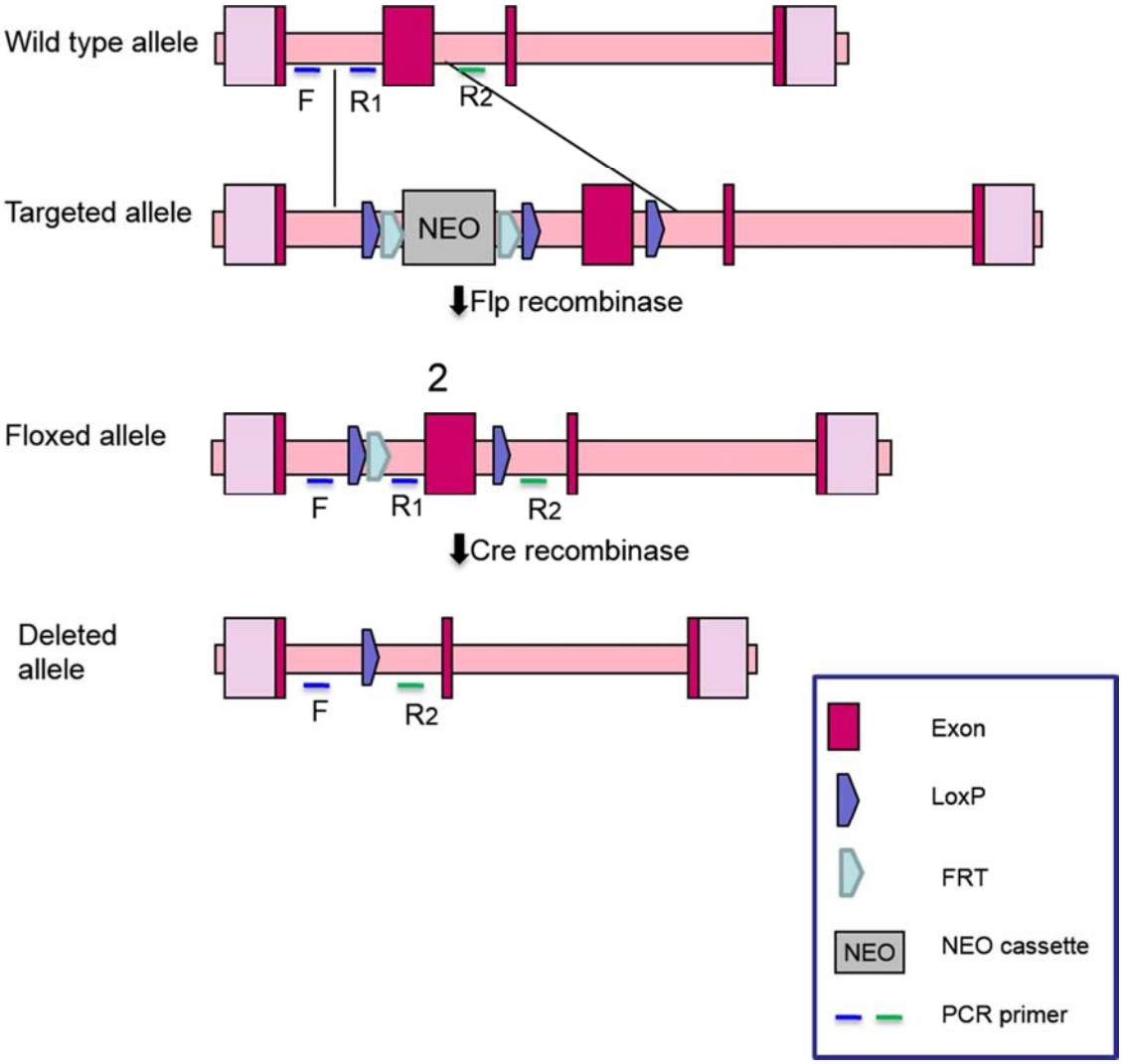

Figure 3.1: Strategy for targeting deletion of *Klf5* exon 2

Indicated are structures of the wildtype *Klf5* allele, targeted allele with NEO selection cassette, floxed inserted *Klf5* allele and exon 2 deleted *Klf5* allele. Genomic PCR with specific primer pairs allowed detection of each specific allele. As indicated on the diagram above, using primer F, R1 and R2 allowed amplification of wildtype *Klf5* determined by band at 189 bp (F and R1) or *Klf5*-floxed allele with 279 bp in size (F and R1) and the deleted-*Klf5* allele determined as the 389 bp (F and R2).

including the transactivation domain of the Klf5 protein (see Figure 1.3 in Chapter 1). Interestingly, this is predicted to generate a truncated Klf5 protein of 87 amino acids since removal of exon 2 results in a change in reading frame after exon 1 (Figure 3.2) [307]. As shown in Figure 3.3, a nucleotide from the end of exon 2 was part of the codon for the amino acid across the splice junction between exon 2 and exon 3 [308, 309]. Hence, exon 2 deletion will affect the reading frame of Klf5 protein translation. *Shindo et. al*., have shown that removal of this protein section was enough to interrupt normal function of Klf5 protein which led to an embryonic lethal phenotype at 8.5 days post-coitum (dpc) for homozygous *Klf5* deleted mice [79]. Thus, the *Klf5* gene was modified by the insertion of two *loxP* sites in a direct orientation flanking exon 2 of *Klf5* gene (floxed), which is the largest exon of the *Klf5* gene as shown in
Figure 3.1. It also harbours an FRT flanked neo selection cassette that lies upstream of the most 5' loxP site for neomycin selection of targeted clones and for subsequent removal of the cassette. Crossing the targeted (construct for *Klf5* conditional KO) and *Flp* recombinase mice will result in recombination between the introduced loxP sites to give $Klf5^{fl/fl}$ mice as shown in Figure 3.4. The *Flp* recombinase is driven by *ACTB* promoter which allows complete excision of the NEO selection cassette in the germ line [306]. This was performed at QIMR and we were provided with $Klf5^{fl/fl}$, $Flpe^{+}$ mice on a 129/C57BL6 mixed background (detail reports on generating $Klf5^{fl/fl}$, $Flpe^{+}$ mice are attached in the **Appendix A** and **B**). To remove the *Flpe* gene, we crossed *Klf5*-floxed ($Flpe^{+}$) mouse with a wildtype C57/BL6 mouse and the progeny were genotyped for the $Klf5^{fl/fl}$ allele and *Flpe* allele. We first extracted the gDNA from tail as described in Chapter 2, Section 2.3.1. Klf5-flox PCR and Flpe PCR were conducted on each gDNA obtained from

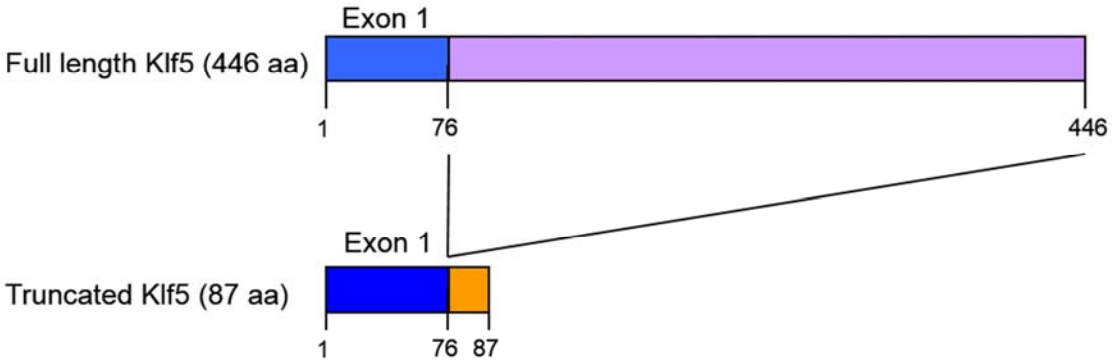

Translation of full length Klf5 (446 aa):

MPTRVLTMSARLGPLPQPPAAQDEPVFAQLKPVLGAANPARDAALFSGDDLKHAHHHPPAPPPAAGPRLP
SEELVQTRCEMEKYLTPQLPPVPIISEHKKYRRDSASVVDQFFTDTEGIPYSINMNVFLPDITHLRTGLY
KSQRPCVTQIKTEPVTIFSHQSESTAPPPPPAPTQALPEFTSIFSSHQTTAPPQEVNNIFIKQELPIPDL
HLSVPSQQGHLYQLLNTPDLDMPSSTNQTAVMDTLNVSMAGLNPHPSAVPQTSMKQFQGMPPCTYTMPSQ
FLPQQATYFPPSPPSSEPGSPDRQAEMLQNLTPPPSYAATIASKLAIHNPNLPATLPVNSPTLPPVRYNR
RSNPDLEKRRIHFCDYNGCTKVYTKSSHLKAHLRTHTGEKPYKCTWEGCDWRFARSDELTRHYRKHTGAK
PFQCMVCQRSFSRSDHLALHMKRHQN

Translation of truncated Klf5 (87 aa):

MPTRVLTMSARLGPLPQPPAAQDEPVFAQLKPVLGAANPARDAALFSGDDLKHAHHHPPAPPPAAGPRLP
SEELVQVAQKFIQSRLT

Figure 3.2: Alteration of the *Klf5* protein predicted after removal of exon 2

This diagram visualises the size of a putative truncated protein isoform relative to the full length Klf5 isoform. The top sequence shows full Klf5 protein sequence while the bottom sequence is the protein sequence translated after removal of exon 2. Blue encoded exon 1, purple indicates the original protein sequence from exon 2, 3 and 4 while orange shows the protein translated after removal exon 2 [307].

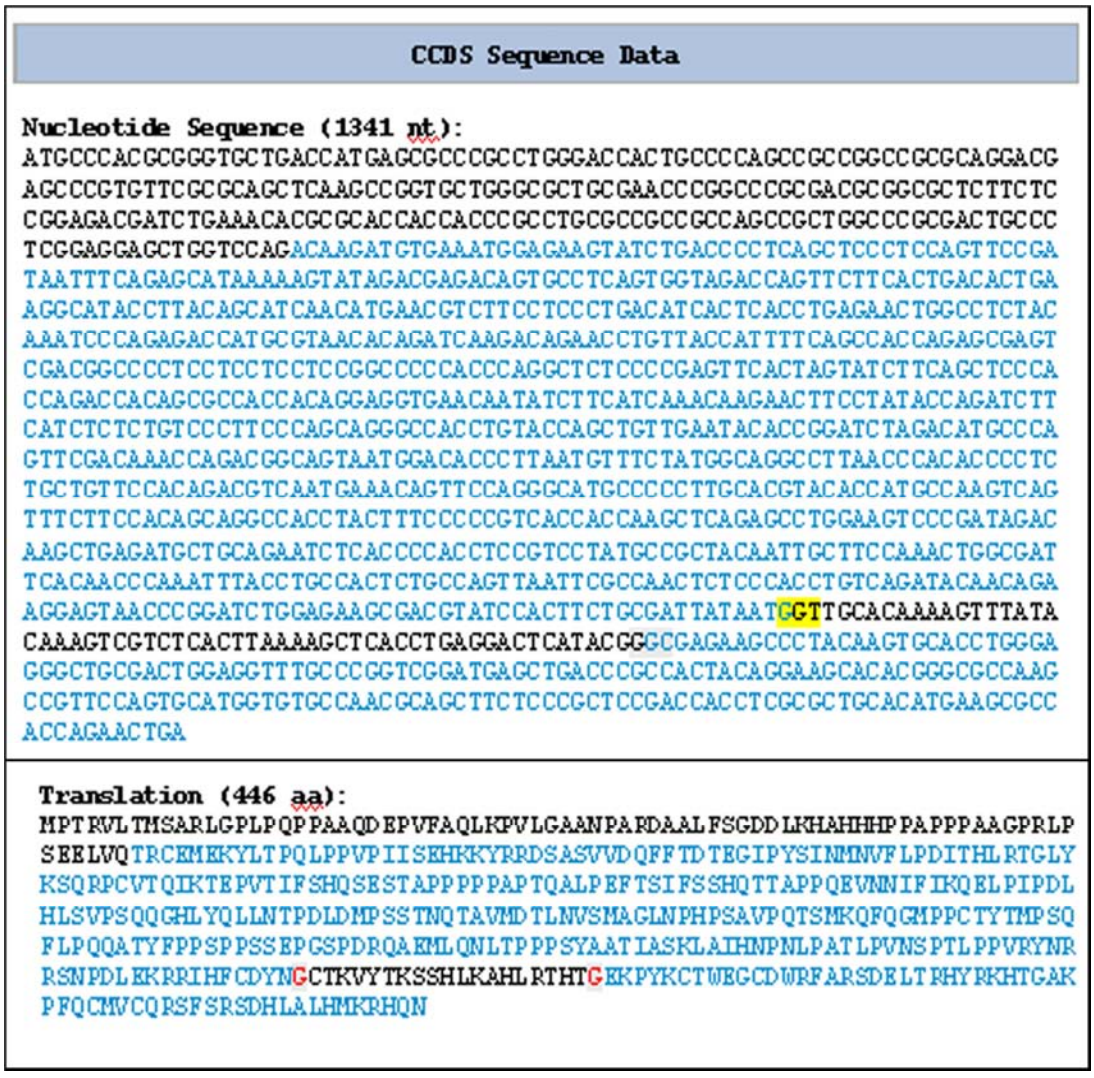

Figure 3.3: Mus musculus *Klf5* Consensus Coding Sequence, (CCDS)

Data was generated from National Center for Biotechnology Information (NCBI) (gene & data). Given on the top is the nucleotide sequence while the bottom shows amino acid translated sequence. Black text represents exon 1 and 3 nucleotide and protein sequence, blue text shows the exon 2 and 4 nucleotide and protein sequences and red text shows the amino acids encoded across the splice junction. Codon highlighted in yellow represent the nucleotide encoded for G amino acids encoded across the splice junction which wil be affected when exon 2 is deleted [308, 309].

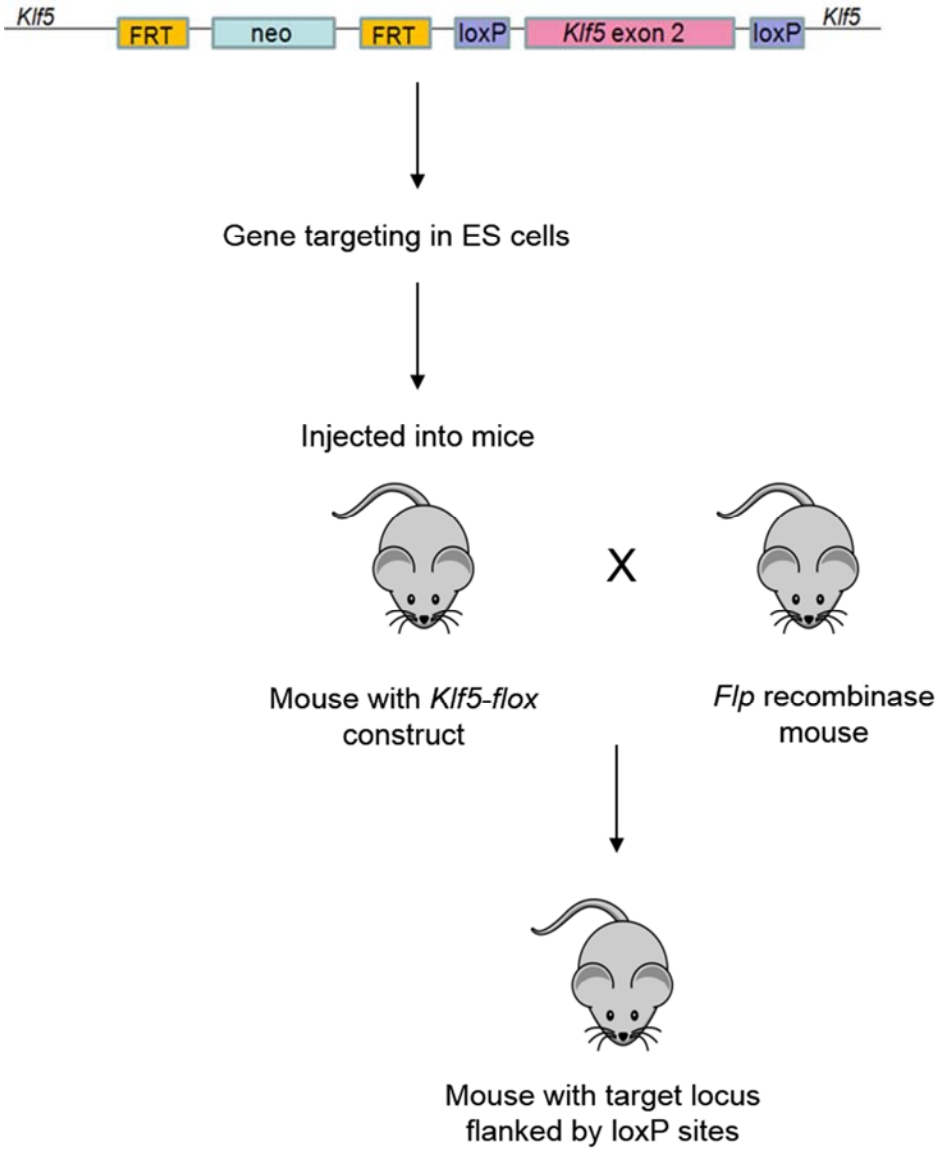

Figure 3.4: Removal of the neomycin selection from *Klf5*-floxed mice using a Flpe transgenic mouse

The construct for *Klf5* conditional knockout contains exon 2 of *Klf5* flanked by unidirectional loxP sites to perform Cre mediated deletion. It harbours a FRT flanked neo selection cassette that lies upstream of the most 5' loxP site for antibiotic selection of targeted clones and for subsequent removal of the cassette. Crossing the floxed (construct for *Klf5* conditional KO) and *Flp* recombinase mice will result in recombination between the introduced FLP mice use FRT sites to give *Klf5* floxed mice lacking the neomycin selection gene. These steps were conducted by the QIMR transgenic facility.

each litter mate (
Figure 3.5). The *Klf5*-flox allele was also confirmed by sequencing (**Appendix C**). Details of the primers and the PCR reaction used for these experiments are described in Chapter 2, section 2.3.2.
Figure 3.5 shows representative of gel electrophoresis diagram from PCR results obtained to show presence of $Klf5^{fl/fl}$ allele or wiltdtype *Klf5* allele (
Figure 3.5-A). As shown in

Figure 3.5-B, band at 700 bp represents *Flpe* positive mice. On the basis of these results, we then selected mice which were positive for $Klf5^{wt/fl}$ allele and negative for *Flpe* allele (mice ID: CR4, CR10, CR11) for the next breeding step in order to generate homozygous *Klf5*-floxed mice ($Klf5^{fl/fl}$).

These $Klf5^{fl/fl}$ mice were then mated to the homozygous *Vav-cre* transgenic mice ($Vav\text{-}cre^{+/+}$). We had already established a local colony of *Vav-cre* transgenic mice for this study in the SA Pathology animal care facility (Kind gift of Warren Alexander, WEHI) and the presence of *Cre* allele have been confirmed by genotyping PCR from tail gDNA (**Appendix D**). As shown in Figure 3.6, we did an initial cross to generate heterozygous conditional haemopoietic *Klf5*-KO mice ($Klf5^{fl/+}Vav\text{-}cre^{+/-}$) followed by a backcross to generate homozygous conditional haemopoietic *Klf5*-KO mice ($Klf5^{fl/fl}Vav\text{-}cre^{+/-}$). At this stage, this transgenic line was generated and maintained by crossing the female $Klf5^{fl/+}Vav\text{-}cre^{+/-}$ to male $Klf5^{fl/+}$. It was important to use female $Klf5^{fl/+}Vav\text{-}cre^{+/-}$ mice for breeding as it has been reported that *Vav* is also expressed in the male germline [301] hence by using male $Klf5^{fl/+}Vav\text{-}cre^{+/-}$ mouse might lead to a non-conditional *Klf5*-KO via the germline. Throughout breeding, the genotypes of mice from each generation were confirmed by PCR from the tail gDNA. Two independent PCR reactions were conducted to determine the presence of the $Klf5^{fl/fl}$ and *Cre* alleles in each litter mate. Details of the primers and PCR reactions used were as described in Chapter 2.

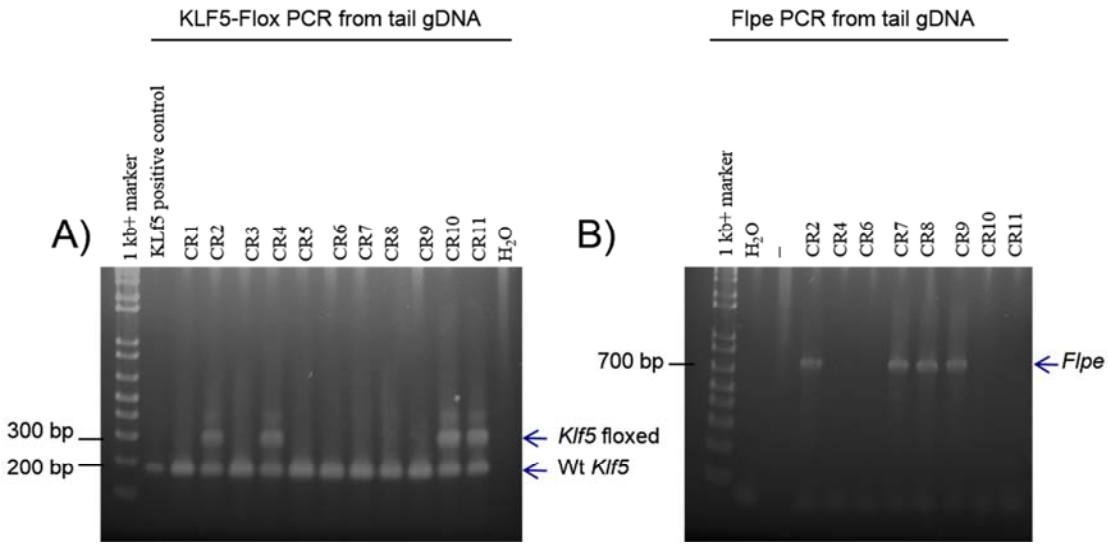

Figure 3.5: *Klf5*-flox and *Flpe* genotyping PCRs

A) Klf5-flox PCR results on littermates with ID: CR1 until CR12 on lane 3 until lane 13 respectively. Lane 14 of this gel shows the negative template control. Top band at 300 bp represents the Klf5-flox allele while the lower band at 200 bp represents the wildtype Klf5 allele. B) Flpe PCR results on littermates with ID: CR2, CR4, CR6 until CR11 (from the same gDNA used on (A)) on lane 4 until lane 12 respectively. Lane 2 of this gel shows the negative template control, while lane 3 was an empty lane. The observed band at 700 bp represents positive Flpe allele.

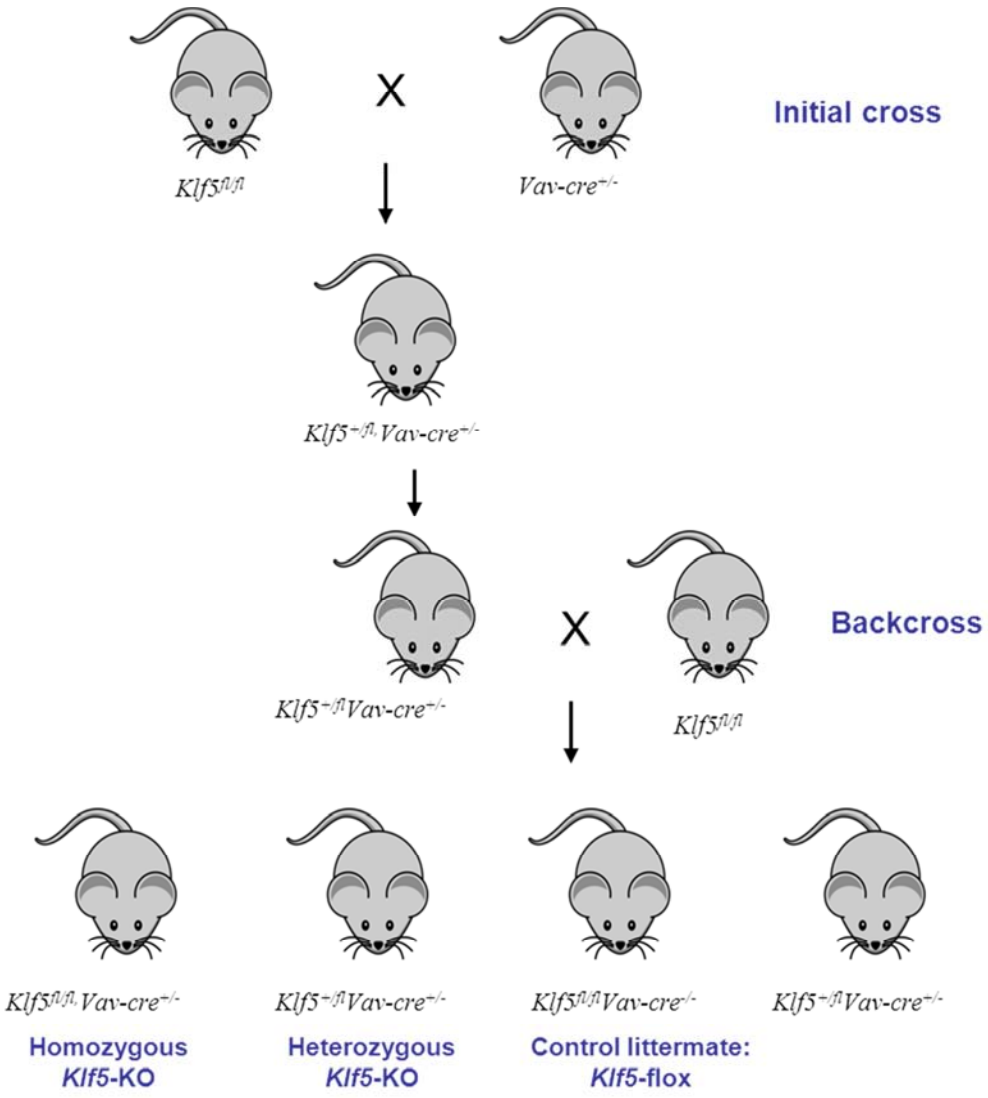

Figure 3.6: Flow chart of generation of conditional haemopoietic *Klf5* gene knockout mice

An initial cross between *Klf5*-floxed ($Klf5^{fl/fl}$) mice and *Vav-Cre* ($Vav\text{-}cre^{+/-}$) mice was conducted to generate heterozygous conditional haemopoietic *Klf5* knockout mice ($Klf5^{fl/+}Vav\text{-}cre^{+/-}$). These mice were then backcrossed to $Klf5^{fl/fl}$ mice to generate homozygous conditional *Klf5* knockout mice ($Klf5^{fl/fl}Vav\text{-}cre^{+/-}$).

Figure 3.7 shows PCR products representative of each genotype. The initial cross was set up between a *Klf5*$^{fl/fl}$ mouse and *Vav-cre*$^{+/-}$ mouse to generate a *Klf5*$^{fl/+}$*Vav-cre*$^{+/-}$ mouse. For the sequential backcross, progeny from the initial cross which were heterozygous *Klf5*-KO (*Klf5*$^{fl/+}$*Vav-cre*$^{+/-}$) were crossed with a homozygous *Klf5* floxed (*Klf5*$^{fl/fl}$) mouse to generate mice with genotypes including the homozygous conditional haemopoietic *Klf5*-KO (*Klf5*$^{fl/fl}$*Vav-cre*$^{+/-}$) (refer Figure 3.6). Mice with homozygous *Klf5*$^{fl/fl}$ and positive for *Vav-cre* were confirmed by PCR as shown in Figure 3.7. To confirm that those mice not only carried the *Klf5*$^{fl/fl}$ and *Cre* allele, but were appropriately deleting exon 2 of *Klf5*, we conducted further PCR on the gDNA of whole bone marrow using a different set of primers (*Klf5*-deletion specific PCR method and primers as described in the Chapter 2 and also shown in Figure 3.1) from mice confirmed as either homozygous *Klf5*-KO; (*Klf5*$^{fl/fl}$*Vav-cre*$^{+/-}$), heterozygous *Klf5*-KO; (*Klf5*$^{+/fl}$, *Vav-cre*$^{+/-}$) or *Klf5* floxed (*Klf5*$^{fl/fl}$). Figure 3.8 shows the Klf5-deleted PCR results from the gDNA of the bone marrow. Homozygous *Klf5*-KO mouse have two bands at 389 bp and 279 bp that represent the deleted *Klf5* and the *Klf5*$^{fl/fl}$ alleles respectively. The primer combinations used in this PCR reaction, which were primers F, R1 and R2 (see Figure 3.1) allowed amplification of three *Klf5* alleles which for wildtype-*Klf5* allele is determined by a product of 189 bp and the *Klf5*-floxed allele a product of 279 bp amplified by primers F and R1. The *Klf5*-deleted allele is determined by a 389 bp product amplified by primers F and R2. A product from wildtype or floxed-*Klf5* allele amplified by primers F and R2 was not expected or observed presumably due to our PCR conditions not allowing the amplification of such a large size product (2053 and

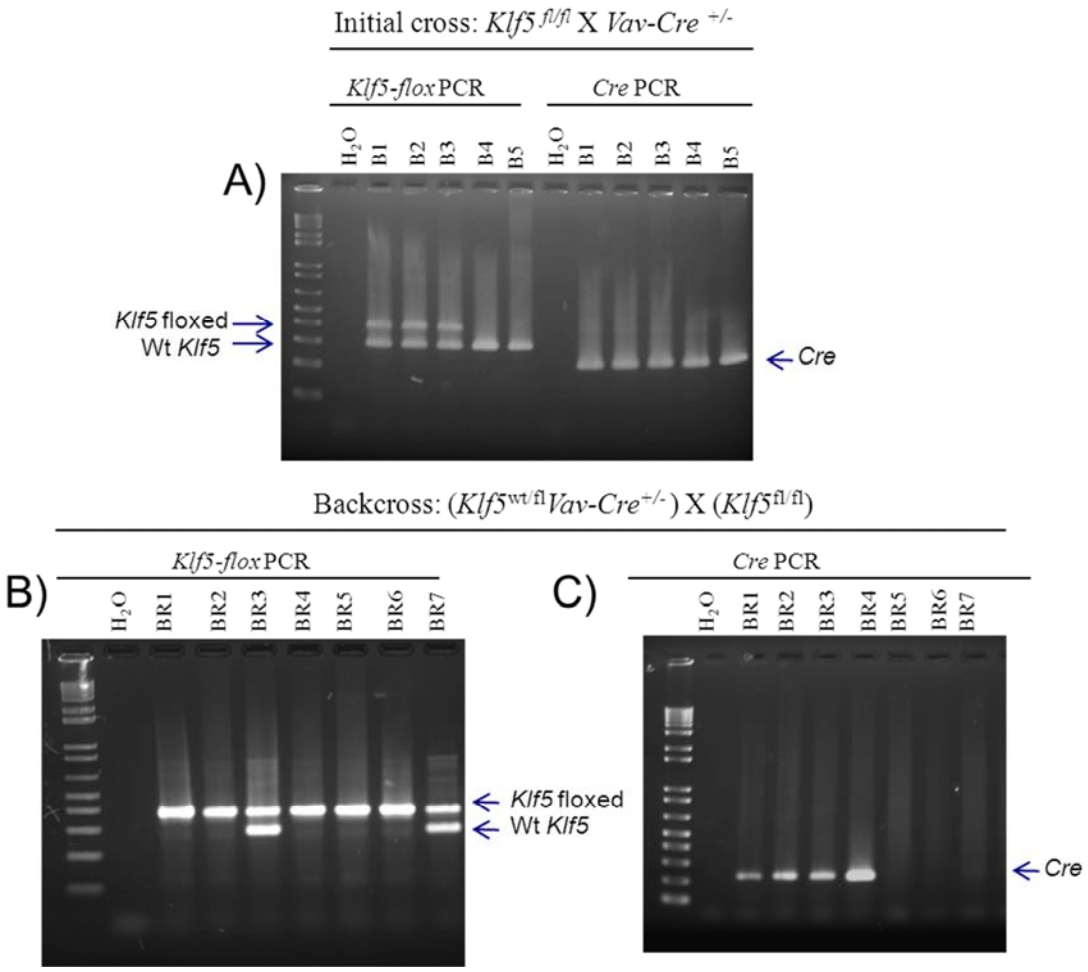

Figure 3.7: *Klf5* and *Cre* genotyping of mice used to generate the *Klf5* conditional haemopoietic knockout

A) Genotyping results of the progeny obtained from an initial cross of *Klf5*-floxed mouse with *VavCre* mouse to generate single copy blood cell specific *Klf5* knockout mice (*Klf5* $^{fl/+}$*Vav-cre*$^{+/-}$). Lanes 3 to 7 show PCR products obtained from Klf5-flox PCR while lanes 9 to 13 represent the Cre PCR product. Lane 3, 4 and 5 shows mice with heterozygous *KLf5-floxed* allele while lane 6 and 7 represents mice with wildtype *Klf5* allele. The Cre PCR results indicated all mice were positive for Cre allele. Lane 2 and 8 were no template controls used for Klf5-flox PCR and Cre PCR reactions respectively. B) and C) Represents the Klf5-flox PCR and Cre PCR of the progenies obtained from the sequential backcross to generate double copy blood cell specific *Klf5* knockout mice (*Klf5* $^{fl/fl}$*Vav-cre*$^{+/-}$) respectively. The marker used on lane 1 for was 1kb+ marker. B) Lane 3, 4, 6-8 represents mice with double *Klf5*-floxed allele. Lane 5 and 9 shows mice that have both *Klf5*-floxed and wildtype *Klf5* allele. C) Lane 3-6 show positive Cre allele with band at 210 bp. Lane 2 shows the negative control with no template indicated no template contamination while handling the PCR reactions.

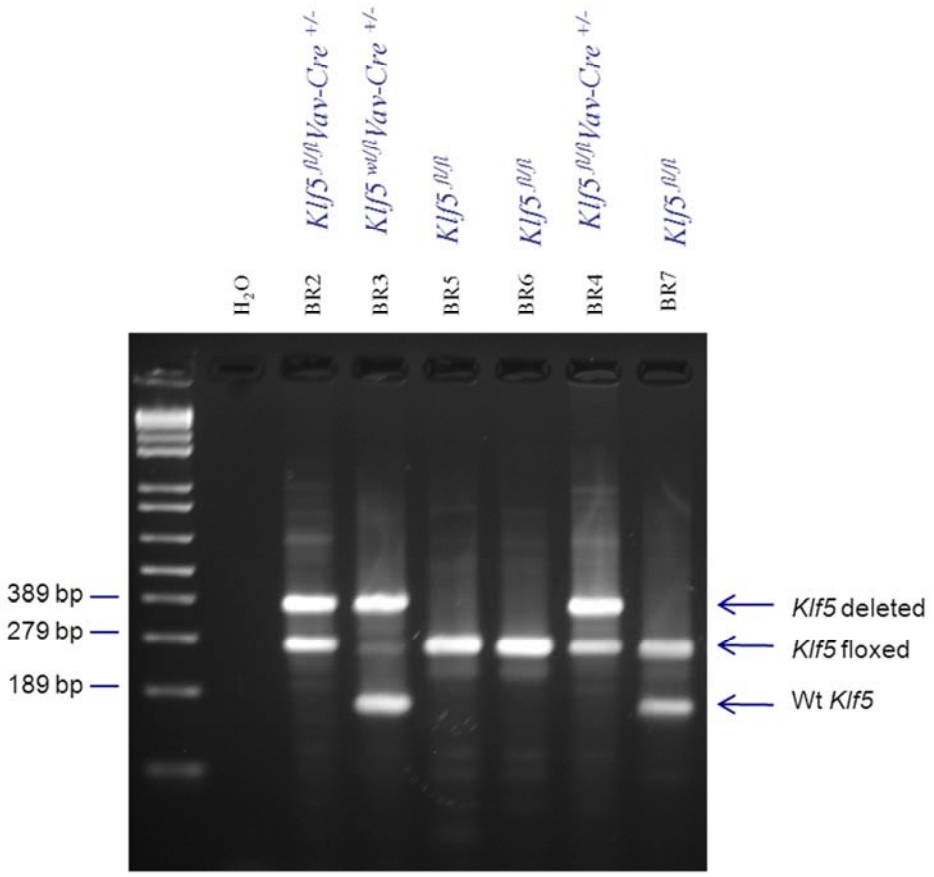

Figure 3.8: Representative PCR for detection of the *Klf5* exon 2 deleted allele in the bone marrow

PCR analysis on the genomic DNA from whole bone marrow detected the presence of *Klf5*-deleted allele (389 bp), *Klf5*-floxed allele (279 bp) and wildtype *Klf5* allele (189 bp). The marker used on lane 1 for was 1kb+ marker, followed by the no template control for Klf5-deleted PCR reaction. Next lane shows the $Klf5^{fl/fl}$, *Vav-*$Cre^{+/-}$ mouse (BR2) with two bands (*Klf5*-deleted allele and *Klf5*-floxed allele), followed by $Klf5^{wt/fl}$, *Vav-*$Cre^{+/-}$ mouse (BR3) with three bands (*Klf5*-deleted, *Klf5*-floxed and wt *Klf5* allele) and $Klf5^{fl/fl}$ (BR5 and BR6) with one *Klf5*-floxed allele. Next is $Klf5^{fl/fl}$, *Vav-*$Cre^{+/-}$ mouse (BR2) with two bands (*Klf5*-deleted allele and Klf5-floxed allele), followed by $Klf5^{fl/fl}$ (BR7) with one *Klf5*-floxed allele and wt *Klf5* allele.

2121 bp respectively). The sequence for *Klf5*-deleted allele obtained from PCR was also confirmed by sequencing as shown in **Appendix C**. Taken together, our initial aim to generate the conditional *Klf5*-KOmice (*Klf5*$^{fl/fl}$*Vav-cre*$^{+/-}$) was shown to be successful at the DNA level.

Next, we determined the level of *Klf5* gene expression in the haemopoietic system. To determine this, again whole bone marrow cells were collected from femur and tibia of mice; confirmed as homozygous *Klf5*-KO (*Klf5*$^{fl/fl}$*Vav-cre*$^{+/-}$), heterozygous *Klf5*-KO (*Klf5*$^{wt/fl}$*Vav-cre*$^{+/-}$) or Klf5-floxed (*Klf5*$^{fl/fl}$) based on initial PCR genotyping results. RNA was extracted from the whole bone marrow and levels of *Klf5* mRNA expression were determined by QPCR (details on the methods and primers used as explained in Chapter 2, section 2.5). As shown in Figure 3.9**,** the *Klf5* mRNA expression in the *Klf5*$^{fl/fl}$*Vav-cre*$^{+/-}$ marrow was significantly decreased compared to *Klf5*$^{fl/fl}$ marrow. Interestingly, QPCR analysis also showed that the *Klf5* mRNA expression was significantly reduced in the *Klf5*$^{wt/fl}$*Vav-cre*$^{+/-}$ marrow compared to *Klf5*$^{fl/fl}$ marrow.

Finally we also conducted western blot analysis to measure Klf5 protein level in our *Klf5*$^{fl/fl}$*Vav-cre*$^{+/-}$ mice. The *Vav-Cre* system is reported to lead to pan-haemopoietic gene ablation hence we predicted disappearance of full length Klf5 protein in BM cells of our *Klf5*$^{fl/fl}$*Vav-cre*$^{+/-}$ mice. To isolate haemopoietic cells from the whole BM cells, cells were stained with anti-mouse CD45 antibody and CD45-positive (CD45^{+}) cells were sorted by FACS. Western blot analyses were then conducted on the CD45^{+} cells. Figure 3.10 shows the results obtained from western blot analysis. The reduction of Klf5 protein was clearly observed in CD45^{+} cells from *Klf5*$^{fl/fl}$*Vav-cre*$^{+/-}$ mice when compared to *Klf5*$^{fl/fl}$ mice. Klf5 protein was also reduced in the *Klf5*$^{+/fl}$*Vav-cre*$^{+/-}$ mice when compared to *Klf5*$^{fl/fl}$ mice. Quantitation of three

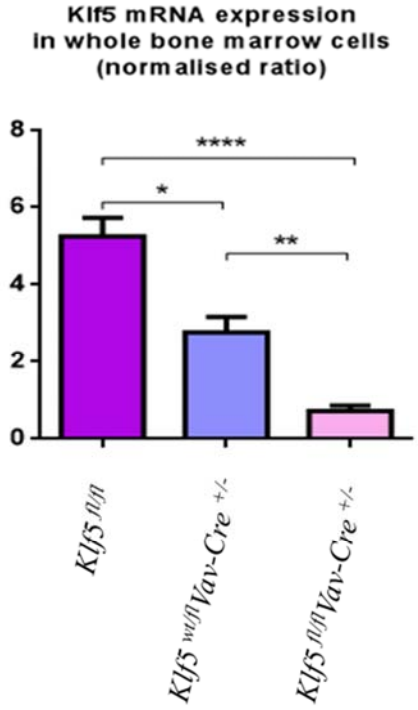

Figure 3.9: Quantitative PCR (qPCR) reaction to determine level of *Klf5* mRNA expression in the bone marrow cells

Q-PCR on mRNA from whole bone marrow shows significant decrease of *Klf5* expression in $Klf5^{fl/fl}$, $Vav\text{-}Cre^{+/-}$ mice compared to $Klf5^{fl/fl}$ mice, $Klf5^{fl/fl}$; n=4, $Klf5^{wt/fl}$, $Vav\text{-}Cre^{+/-}$; n=3 and $Klf5^{fl/fl}$, $Vav\text{-}Cre^{+/-}$; n=5. P-value obtained from t-test conducted between each genotype group using Graphpad Prism. Significantly different between $Klf5^{fl/fl}$ and $Klf5^{fl/fl}$, $Vav\text{-}Cre^{+/-}$ mice ****($P< 0.001$), significantly different between $Klf5^{fl/fl}$ and $Klf5^{+/fl}$, $Vav\text{-}Cre^{+/-}$ mice *($P< 0.05$), significantly different between $Klf5^{fl/fl}$ and $Klf5^{fl/fl}$, $Vav\text{-}Cre^{+/-}$ mice **($P< 0.01$).

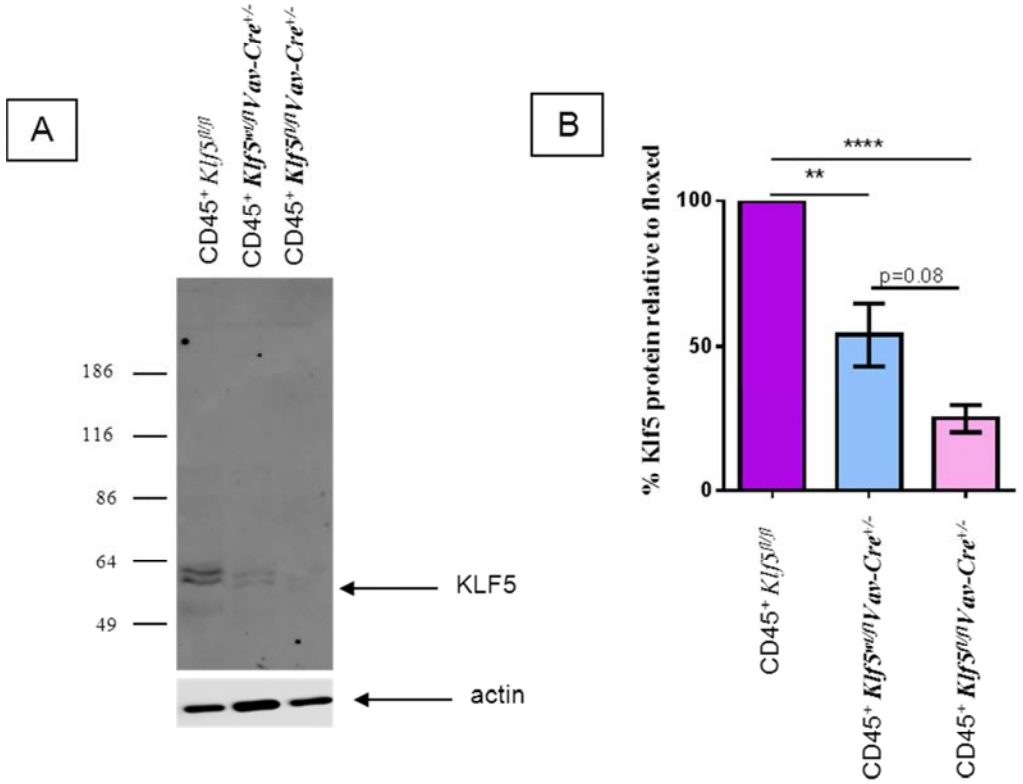

Percentage of protein knockdown	
Klf5$^{wt/fl}$Vav-Cre$^{+/-}$	46.06% ± 10.75%, n=3
Klf5$^{fl/fl}$Vav-Cre$^{+/-}$	75.07% ± 4.661%, n=3

Figure 3.10: Western blot to show the knockdown of *Klf5* protein in the CD45+ bone marrow leukocytes

A) Representative blot showing the disappearance of Klf5 protein in the sorted CD45^{+} cells from *Klf5$^{fl/fl}$Vav-Cre$^{+/-}$* and faint band observed in the sorted CD45^{+} cells from *Klf5$^{wt/fl}$Vav-Cre$^{+/-}$*. **B)** Quantification of Klf5 protein normalised to ß-actin and shown relative to the floxed level. The average percentages of Klf5 protein knockdown were genrated three individual mice from each genotype. 75.07% ± 4.661% of Klf5 protein were knockdown in the *Klf5$^{fl/fl}$Vav-Cre$^{+/-}$* while 46.06% ± 10.75% of Klf5 protein were knockdown in the *Klf5$^{wt/fl}$*, *Vav-Cre$^{+/-}$*. P-value obtained from t-test conducted between each genotype group using Graphpad Prism. Significantly different between *Klf5$^{fl/fl}$* and *Klf5$^{fl/fl}$Vav-Cre$^{+/-}$* mice ****(P< 0.001), significantly different between *Klf5$^{fl/fl}$* and *Klf5$^{+/fl}$Vav-Cre$^{+/-}$* mice **(P< 0.05).

independent experiments on different mice showed that Klf5 protein was reduced by 75.07% ± 4.661% in the *Klf5*$^{fl/fl}$*Vav-cre*$^{+/-}$ mice while 46.06% ± 10.75% of Klf5 protein was reduced in the *Klf5*$^{wt/fl}$*Vav-cre*$^{+/-}$ mice. In addition, we saw a higher molecular weight band above the predicted Klf5 band. This higher molecular isoform immunoreactive to the Klf5 antibody was also observed in the technical data sheets obtained from the commercial provider of KLF5 antibody (shown in the **Appendix E**) however, they did not comment on the identity of this higher molecular weight band detected. As shown in Figure 3.10, the intensity of this higher molecular weight immunoreactive band was almost the same as the predicted Klf5 molecular weight and quantification of both these immunoreactive bands also showed reduction in the *Klf5*$^{fl/fl}$*Vav-cre*$^{+/-}$ mice by 75% and 45% in the *Klf5*$^{+/fl}$*Vav-cre*$^{+/-}$ mice (data not shown). Consistent with the Klf5 protein structure, we predict this to be the post-translationally modified Klf5 protein as it is known to be target of multiple post-translational modifications (see Chapter 1, section 1.7.2). Together, these results are consistent with other pan-hameopoietic knockout mice model by using the Cre/LoxP recombination system.

3.2.2 Phenotypic monitoring on the newly generated *Klf5* conditional gene knockout mice

Klf5 is known to have a critical role during embryonic development [79], as well as known to be involved in the fat tissue formation [78] and other processes discussed in Chapter 1, section 1.7. Mice were monitored closely to establish any physical or behaviour phenotype. In order to determine this we first performed monitoring on this strain of mice.

For this, we monitored the visual characteristics of the animals. All breeding was performed in the clean barrier facilities in the SA Pathology animal care facility to provide pathogen-free conditions. All mice from the *Klf5*$^{+/fl}$ X *Klf5*$^{+/fl}$, *Klf5*$^{fl/fl}$ X *Vav-cre*$^{+/-}$ and *Klf5*$^{+/fl}$*Vav-cre*$^{+/-}$ X *Klf5*$^{fl/fl}$ or *Klf5*$^{+/fl}$*Vav-cre*$^{+/-}$ X *Klf5*$^{+/fl}$ breeding pairs were monitored for physical appearance until adult stage. The pregnant mice were also monitored. Mice were born at the expected Mendelian ratios as shown in Table 3.1.

Upon weaning at day 21, mice were marked with an ear notch for identification (ID), followed by tail tipping for genotyping. We continued physical monitoring every week until mice reached 12 months of age. As shown in Figure 3.11-A, there was no significant difference observed in weight between genotypes at 3, 6 and 9 months old. However, at 12 months age, *Klf5*$^{fl/fl}$*Vav-cre*$^{+/-}$ and *Klf5*$^{+/fl}$*Vav-cre*$^{+/-}$ mice showed a trend (p=0.05) for reduced weight when compared to *Klf5*$^{fl/fl}$ mice. We then compared the change of body weight with ages for each genotype (Figure 3.11-B). Mice from each group significantly increased in weight up to 9 months. However, only *Klf5*$^{fl/fl}$ mice were observed to have a further increase in body weight after 9 months.

Mice were also monitored for their behaviour, physical activity and for any sign of disease. Based on the observations, all mice displayed normal behaviour or ill health as measured by observation of grooming or coat condition, hunched posture, visible weight loss, decreased activity, development of masses or decreased motion when the mouse is returned to the cage. Since these genetic monitoring involved daily observations, they were conducted together with the animal care facility staff members on the first few littermates while the animal care facility staff have undertook the rest of the daily routine on monitoring (data not shown).

Litter	*Klf5*$^{fl/fl}$*Vav-cre*$^{-/-}$	*Klf5*$^{wt/fl}$*Vav-cre*$^{-/-}$	*Klf5*$^{wt/fl}$*Vav-cre*$^{+/-}$	*Klf5*$^{fl/fl}$*Vav-cre*$^{-/-}$	Female	Male
1d	1	3	1	0	5	
	1	1	1	0		3
3c	1	1	2	0	4	
	2	1	0	1		4
2d	1	2	1	1	5	
	1	1	1	2		5
1e	1	0	0	0	1	
	3	3	1	1		8
2e	0	0	2	2	4	
	0	0	3	2		5
1f	0	1	1	0	2	
	2	1	1	2		6
4a	1	1	1	0	3	
	2	2	0	2		5
4b	1	0	1	0	2	
	1	1	1	2		5
Total	18	18	17	15	26	41
Expected	16.75	16.75	16.75	16.75	33.5	33.5

Table 3.1a: *Klf5*$^{fl/fl}$*Vav-cre*$^{+/-}$ mice are born at the expected Mendelian ratio

The number of mice of various genotypes obtained by the *Klf5*$^{+/fl}$*Vav-cre*$^{+/-}$ X *Klf5*$^{fl/fl}$ intercross is shown. The expected number of mice was calculated according to the total number of mice born and based on the expected Mendelian ratio 1:1:1:1 for *Klf5*$^{fl/fl}$*Vav-cre*$^{-/-}$: *Klf5*$^{wt/fl}$*Vav-cre*$^{-/-}$: *Klf5*$^{wt/fl}$*Vav-cre*$^{+/-}$: *Klf5*$^{fl/fl}$*Vav-cre*$^{+/-}$.

Litter	*Klf5*$^{fl/fl}$*Vav-cre*$^{-/-}$	*Klf5*$^{wt/fl}$*Vav-cre*$^{-/-}$	*Klf5*$^{wt/wt}$*Vav-cre*$^{-/-}$	*Klf5*$^{wt/wt}$*Vav-cre*$^{+/-}$	*Klf5*$^{wt/fl}$*Vav-cre*$^{+/-}$	*Klf5*$^{fl/fl}$*Vav-cre*$^{-/-}$	Female	Male
4a	0	0	0	0	3	0	3	
	0	1	1	0	0	0		2
3a	0	1	0	1	1	0	2	
	0	0	0	0	1	0		1
1a	1	0	0	1	2	1	5	
	0	0	0	0	0	1		1
2d	1	0	1	1	0	0	3	
	0	2	0	0	1	0		3
7a	1	0	0	1	1	0	3	
	1	3	0	0	1	0		5
5a	1	1	1	1	1	1	6	
	0	1	0	0	0	1		2
7c	0	0	0	0	1	0	1	
	1	4	1	2	0	1		9
5c	1	1	1	1	0		4	
	1	1	1	1	0	2		6
6d	1	2	1	0	1	1	6	
	0	0	0	1	2	0		3
Observed	9	17	7	10	15	8	33	32
Expected	8.13	16.25	8.13	8.13	16.25	1.00	32.5	32.5

Table 3.1b: *Klf5*$^{fl/fl}$*Vav-cre*$^{+/-}$ mice are born at the expected Mendelian ratio

The number of mice of various genotypes obtained by the *Klf5*$^{+/fl}$*Vav-cre*$^{+/-}$ X *Klf5*$^{+/fl}$ intercross is shown. The expected number of mice was calculated according to the total number of mice born and based on the expected Mendelian ratio 1:2:1:1:2:1 for *Klf5*$^{fl/fl}$*Vav-cre*$^{-/-}$: *Klf5*$^{wt/fl}$*Vav-cre*$^{-/-}$: *Klf5*$^{wt/wt}$*Vav-cre*$^{-/-}$: *Klf5*$^{wt/wt}$*Vav-cre*$^{+/-}$: *Klf5*$^{wt/fl}$*Vav-cre*$^{+/-}$: *Klf5*$^{fl/fl}$*Vav-cre*$^{+/-}$.

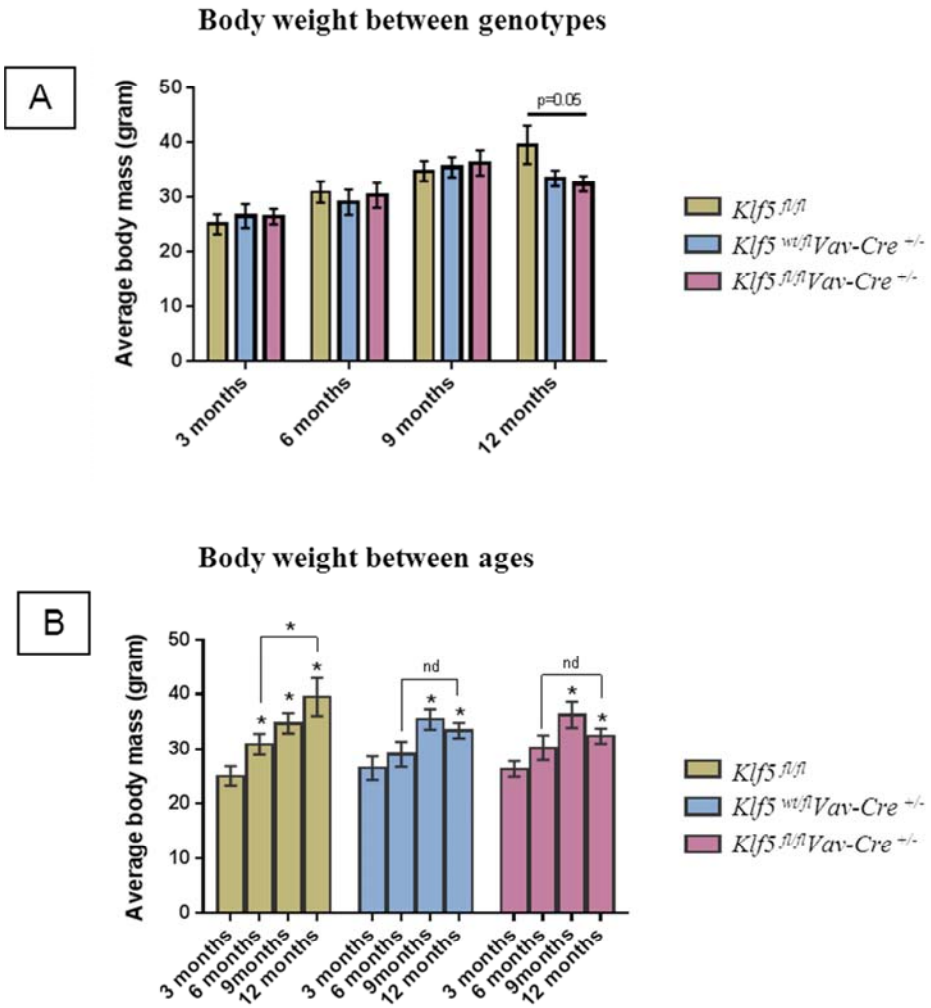

Figure 3.11: Average of body weight at 3, 6, 9, 12 months

A) Bar chart shows the average body weight compared between genotypes at each time point. **B)** Bar chart shows the average body weight compared between ages for each genotype. At least 6 individual mice from each genotype were weight at each time point. P-value obtained from t-test conducted between 3 months to 6, 9 and 12 months aged in each genotype using Graphpad Prism. *($P< 0.05$) shows significant weight gain from 3 months old. As well, *($P< 0.05$) shows significant weight gain from 6 to 12 months age in $Klf5^{fl/fl}$ but no difference (nd) of weight from 6 to 12 months age in $Klf5^{fl/fl}Vav\text{-}Cre^{+/-}$ mice and $Klf5^{fl/fl}Vav\text{-}Cre^{+/-}$ mice.

3.3 Discussion

This chapter describes the successful generation of a new transgenic conditional *Klf5*-KO mouse model for analysis in the haemopoietic system. We used the Cre/LoxP recombination system to remove exon 2 of the *Klf5* gene which encodes the largest exon. Removal of exon 2 of the *Klf5* gene, was predicted to produced non-functional Klf5 protein [79] with the deleted Klf5 allele translated into a truncated 87 residue protein with a frame shift after exon 1 (Figure 3.2) [307]. This method of generating *Klf5* gene ablation has been used in other studies in combination with the Cre/LoxP recombination system. This includes studies of Klf5 function in intestinal epithelial homeostasis, ocular surface pathologies, cardiac hypertrophy and heart failure [218, 264, 310, 311]. In each of these independent studies, different types of promoters have been used to drive tissue-specific Cre recombinase expression.

Genotyping PCR confirmed those exons 2 of *Klf5* were successfully removed at the genomic level. Although PCR on bone marrow of gDNA showed that recombined *Klf5* allele was still detectable in the homozygous KO mice (Figure 3.8), QPCR and western blot analysis indicated that Klf5 mRNA and protein was significantly reduced in the haemopoietic system specifically we observed significantly reduced *Klf5* mRNA expression in the bone marrow cells from $Klf5^{fl/fl}Vav\text{-}Cre^{+/-}$ mice compared to $Klf5^{fl/fl}$ mice. Western blot analysis also showed a large reduction of Klf5 protein in the sorted bone marrow $CD45^{+}$ cell populations from $Klf5^{fl/fl}Vav\text{-}Cre^{+/-}$ mice. We confirmed that 75.07% ± 4.661% of Klf5 protein reduction in the $Klf5^{fl/fl}Vav\text{-}cre^{+/-}$ mice. This is consistent with the other studies used *Vav-Cre* knockout model where 60-70% protein reduction has been observed in haemopoietic populations [295]. While we cannot rule out that there is significant

residual function of Klf5 in our knockout model, based on other reports of Klf5 conditional knockouts we believe that this 75% Klf5 protein reduction (Figure 3.10) observed by us is sufficient to reveal a loss of function phenotype. For example, *Xing et al.* have shown that approximately 80% Klf5 deletion in prostatic epithelial cells is enough to promote the development and severity of prostate tumorigenesis [312]. This Klf5 deletion was obtained by using a *PB-Cre4* transgenic strain where expression of Cre recombinase is driven by the prostatic epithelial specific probasin promoter [312]. In addition, another study has shown that conditional disruption of Klf5 derived by mating *Klf5-LoxP* and *Le-Cre* mice results in approximately 25% of Klf5 protein remaining and causes defective eyelids, malformed meibomian glands, abnormal cornea and loss of conjunctival goblet cells [311]. The most effective Klf5 knockout model so far is the inducible *Mx1-Cre;Klf5*$^{flox/flox}$ model as reported by *Ishikawa et al*. where approximately 10% of *Klf5* mRNA is expressed in the *Mx1-Cre;Klf5*$^{flox/flox}$ mice [275]. However, this system also allows partial gene inactivation in other tissues [313], which potentially results in indirect phenotype.

We also monitored our *Klf5*-KO mice and showed that our *Klf5* deleted allele was not interfering with non-haemopoietic organs or systems. The initial study on complete Klf5 knockout has shown that Klf5 is a key regulator during blastocyst development [285]. Subsequently, another study has shown that Klf5 is also important for normal embryonic implantation [269]. We observed the expected Mendelian ratio for each genotype indicating that our *Klf5*-KO model was not interfering with the embryonic development or implantation of the embryo. None of the *Klf5*$^{fl/fl}$*Vav-Cre*$^{+/-}$ mice shows signs of stress or disease from newborn pups until adulthood, although the *Klf5*$^{fl/fl}$*Vav-Cre*$^{+/-}$ and *Klf5*$^{+/fl}$*Vav-Cre*$^{+/-}$ mice did not increase body weight after 9 months in comparison to *Klf5*$^{fl/fl}$ mice.

Chapter 4: Analysis of the circulating blood and bone marrow of *Vav-Cre, Klf5* knockout mice

4.1 Introduction

KLF5 expression was first identified as up-regulated in the granulocyte lineage, and a role for Klf5 has been defined in granulocyte differentiation in response to G-CSF [278]. In addition, Q-RT-PCR analysis demonstrated that average *KLF5* expression was significantly (2.3-fold) lower in a local cohort of *de novo* AML patient samples than in $CD34^+$ cells from healthy controls [28]. In addition, microarray analysis conducted on AML patient samples has shown that *KLF5* expression is reduced in AML patients compared to $CD34^+$ control samples [28]. *In vitro Klf5* knockdown experiments also showed reduced granulocyte differentiation in response to cytokine simulation [28]. In addition, an independent study by *Humbert et al*. also supports the initial finding of a functional role for Klf5 in regulating myeloid cell development [33].

To extend this functional analysis of *Klf5*, an *in vivo* tissue-specific gene-ablation model was generated as outlined in the previous chapter (Chapter 3). The aim was to gain a detailed understanding of *Klf5* function in haemopoiesis. Thus, the specific aim for this chapter was to characterise in detail the blood cell types in peripheral blood and bone marrow. As such, complete blood counts (CBC) were performed. In addition, flow cytometry with a range of different lineage-specific cell surface markers was used to characterise blood cell populations (including mature cell types, progenitor cells and stem cell population) in *Klf5*-deficient mice and *Klf5*-floxed littermates. Finally, colony-forming unit assays (CFU assay) were conducted

to provide a quantitative assay of haemopoietic progenitor cells. Replating of haemopoietic colonies was used to provide an indicator of self-renewal capacity.

In this chapter, parallel analyses were conducted on homozygous *Klf5*-KO (*Klf5*$^{fl/fl}$*Vav-cre*$^{+/-}$), heterozygous KO (*Klf5*$^{wtl/fl}$*Vav-cre*$^{+/-}$) and *Klf5*-floxed (*Klf5*$^{fl/fl}$) littermates as the control group. Mice of these genotypes were compared at 3 months, 9 months and 12 months of age. Hereafter mice will be referred to as *Klf5*$^{\Delta/\Delta}$ for homozygous *Klf5*-KO, *Klf5*$^{wt/\Delta}$ for heterozygous *Klf5*-KO and *Klf5*$^{fl/fl}$ for wildtype control.

4.2 Results

4.2.1 Peripheral Blood Analysis

4.2.1.1 Complete blood count and differential counts on peripheral blood

CBC on peripheral blood (PB) showed that *Klf5*$^{\Delta/\Delta}$ mice displayed a small but significant reduction in values compared to *Klf5*$^{fl/fl}$ mice for red blood cell count (RBC), haemoglobin and haematocrit ($p<0.05$) at 3 months although this was not observed at other time points Figure 4.1-A, B and C). No significant differences were observed in other red blood cell parameters (MCV, MCH and MCHC) (Figure 4.1-D, E and F). Total white blood cell counts were also measured with the blood cell analyser. Interestingly, as shown in Figure 4.2-A the average white cell counts were significantly higher in *Klf5*$^{\Delta/\Delta}$ mice compared to *Klf5*$^{fl/fl}$ mice at 9 and 12 months ($p<0.05$). This difference was not observed between *Klf5*$^{\Delta/\Delta}$ mice and *Klf5*$^{fl/fl}$ mice at 3 and 6 months. The average white cell counts of *Klf5*$^{\Delta/\Delta}$ mice consistently increased with age with significant increases at 3 to 9 and 12 months ($p<0.05$)

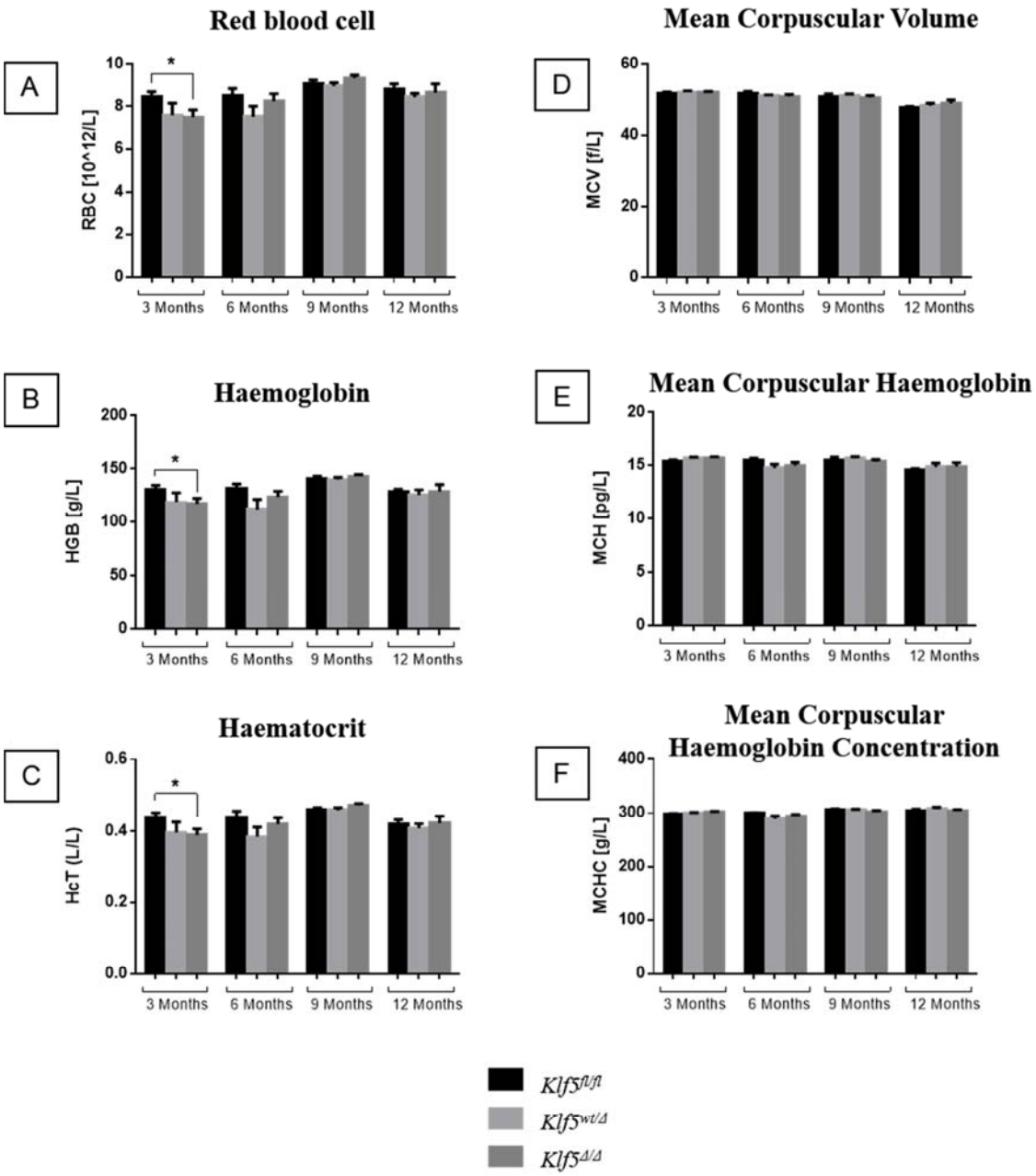

Figure 4.1: Red blood cell parameters from peripheral blood using automated blood analysis at 3, 6, 9 and 12 months of age

A) Red blood cells (RBC), **B)** Haemoglobin (Hgb), **C)** Haematocrit (Hct), **D)** Mean Corpuscular Volume (MCV), **E)** Mean Corpuscular Haemoglobin (MCH) and **F)** Mean Corpuscular Haemoglobin Concentration (MCHC). Results obtained from n=12 for *Klf5*$^{fl/fl}$, n=12 for *Klf5*$^{wt/\Delta}$ and n= 14 for *Klf5*$^{\Delta/\Delta}$ mice at 3 months, n=7 for *Klf5*$^{fl/fl}$, n=7 for *Klf5*$^{wt/\Delta}$ and n=8 for *Klf5*$^{\Delta/\Delta}$ mice at 6 months, n=8 for *Klf5*$^{fl/fl}$, n=8 for *Klf5*$^{wt/\Delta}$ and n= 10 for *Klf5*$^{\Delta/\Delta}$ mice at 9 months and n=8 for *Klf5*$^{fl/fl}$, *Klf5*$^{wt/\Delta}$ and *Klf5*$^{\Delta/\Delta}$ mice at 12 months. Shown are mean values plus or minus SEM. P-value were obtained from t-tests conducted between each genotype. *Significantly different between *Klf5*$^{fl/fl}$ and *Klf5*$^{\Delta/\Delta}$ mice ($P< 0.05$).

(Figure 4.2-B). In contrast, in *Klf5*$^{fl/fl}$ mice show a trend of decreased average white cell count with increased aged (p=0.05).

4.2.1.2 Flow cytometry analysis to assess different leukocyte populations in peripheral blood

To further characterise the changes in blood cell populations, we used flow cytometry with a range of different cell surface antibody markers. Detailed staining procedures are described in Chapter 2, section 2.10. Figure 4.3 shows the gating strategy used to determine the percentage of each cell population defined by different combinations of cell surface markers. Firstly, the live cells were selected based on the elimination of the fluorogold positive cells, followed by selection based on the forward (FS) and side (SS) scatter (Figure 4.3-A and B). The TER119-negative cells (TER119^{-}) were selected to remove erythroid cells from the analysis (Figure 4.3-C). This was followed by selecting for CD45 positive cells (CD45^{+}) (Figure 4.3-D). Following this, sequential antibody panels were used for determining different cell types. For example anti-CD3ε (T-cells) and anti-B220 (B-cells) antibodies were used to define the mature lymphoid cells and the anti-Gr1 and anti-Mac1 antibodies were used to define the mature myeloid cells. Since the initial studies conducted in this lab have shown a functional role for Klf5 in the granulocyte lineage, the primary interest in this analysis was the myeloid compartment [28, 33]. Each cell population was back-gated onto the FS versus SS (FS/SS) plot to define the distinct population in the live cell gate. Figure 4.4 shows the different cell populations that are identified by Gr1 and Mac1 cell surface markers [314]. Figure 4.4-F-J shows the five different

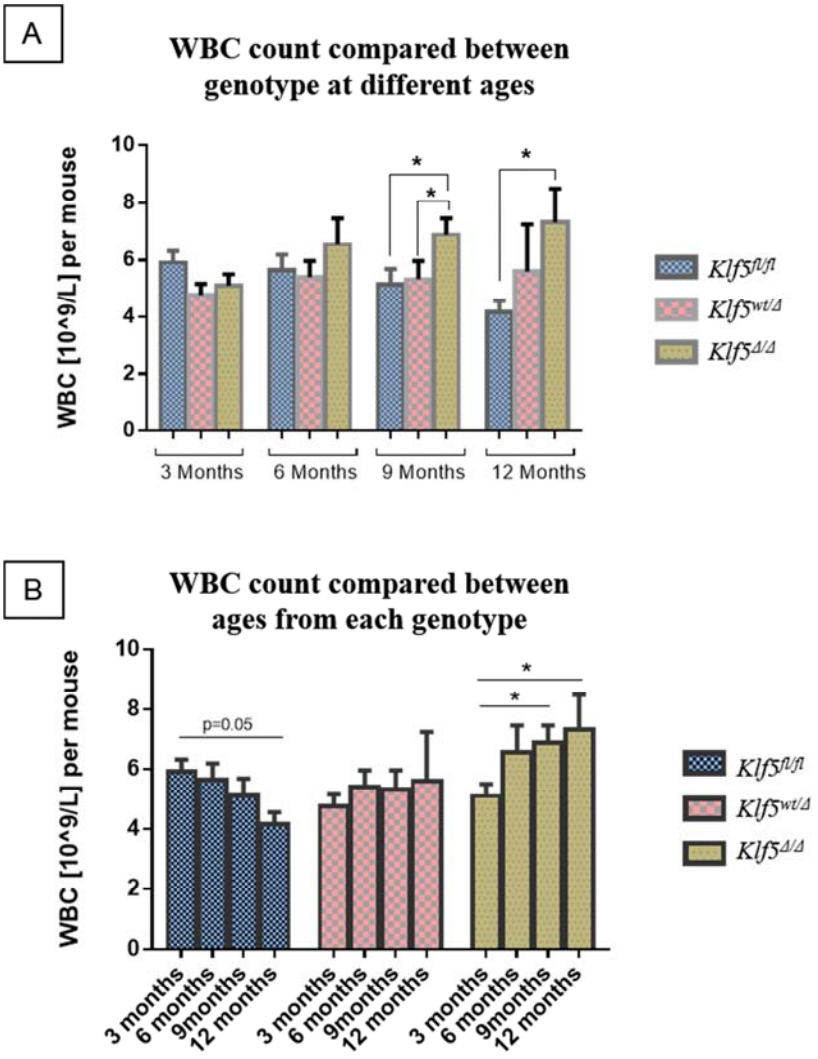

Figure 4.2: Figure 4.2: Total white blood cell counts from peripheral blood using automated blood analysis at 3, 6, 9 and 12 months of age

A) Shown are mean values plus or minus SEM across the genotype grouped by age or **B)** grouped by genotype. Results obtained from n=12 for $Klf5^{fl/fl}$, n=12 for $Klf5^{wt/\Delta}$ and n=14 for $Klf5^{\Delta/\Delta}$ mice at 3 months, n=7 for $Klf5^{fl/fl}$, n=7 for $Klf5^{wt/\Delta}$ and n= 8 for $Klf5^{\Delta/\Delta}$ mice at 6 months, n=8 for $Klf5^{fl/fl}$, n=8 for $Klf5^{wt/\Delta}$ and n= 10 for $Klf5^{\Delta/\Delta}$ mice at 9 months and n=8 for $Klf5^{fl/fl}$, $Klf5^{wt/\Delta}$ and $Klf5^{\Delta/\Delta}$ mice at 12 months. P-value were obtained from t-tests conducted between each genotype. *Significantly different between $Klf5^{fl/fl}$ and $Klf5^{\Delta/\Delta}$ mice ($P< 0.05$, t-test).

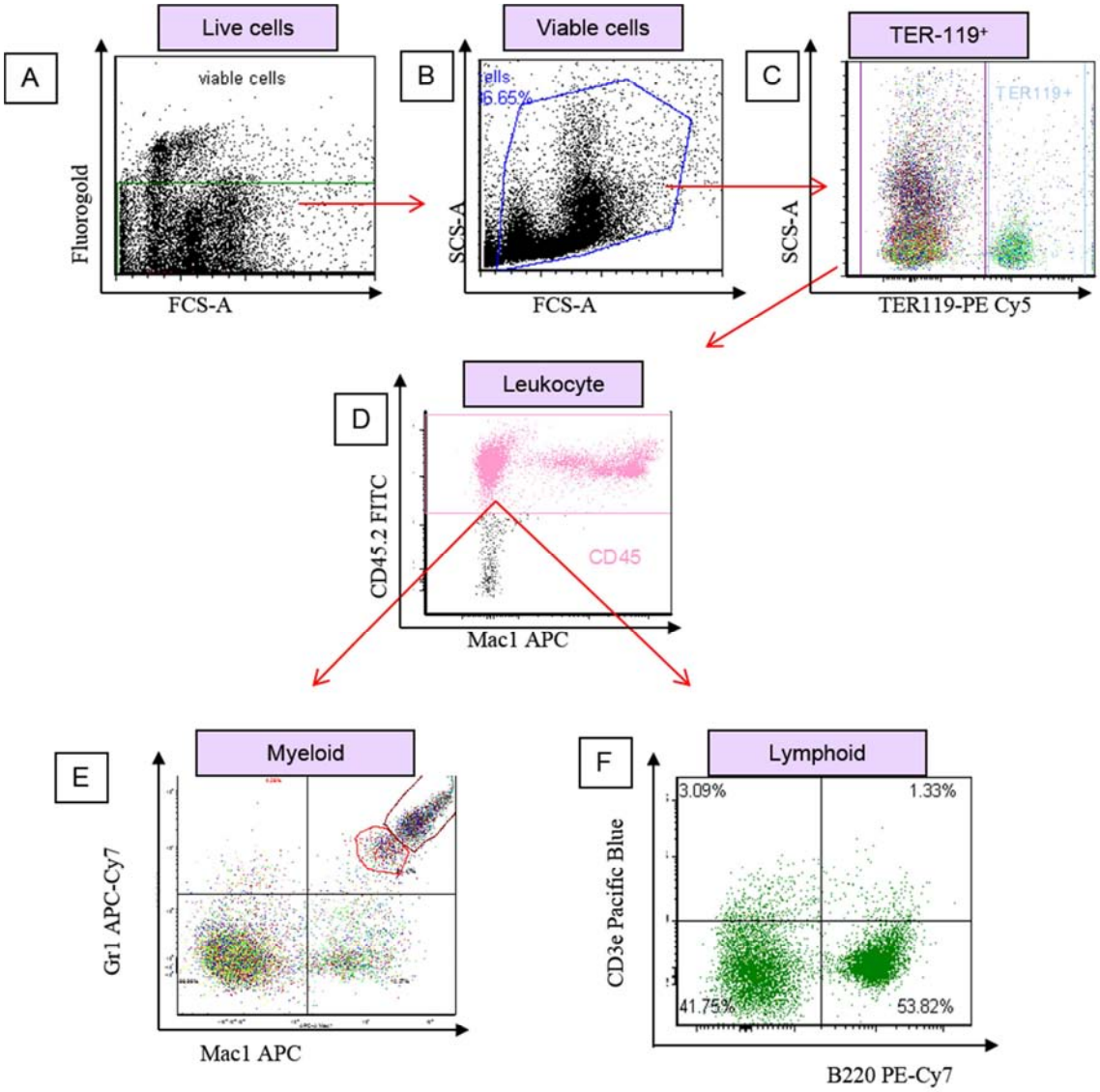

Figure 4.3: Schematic diagram of the sequential gating strategy for cell surface marker flow cytometry analysis of mature myeloid and lymphoid cell types from peripheral blood

(A) Fluorogold negative cells were first gated as live cells **(B)** Exclusion of debris based on the forward and side scatter. **(C)** Selection of TER119 negative cells (removal of red blood cells). **(D)** Selection of CD45 positive cells (leukocytes). **(E)** Gr1 and Mac1 for selection of mature myeloid cell population and **(F)** and CD3e and B220 marker for selection of mature lymphoid cells type.

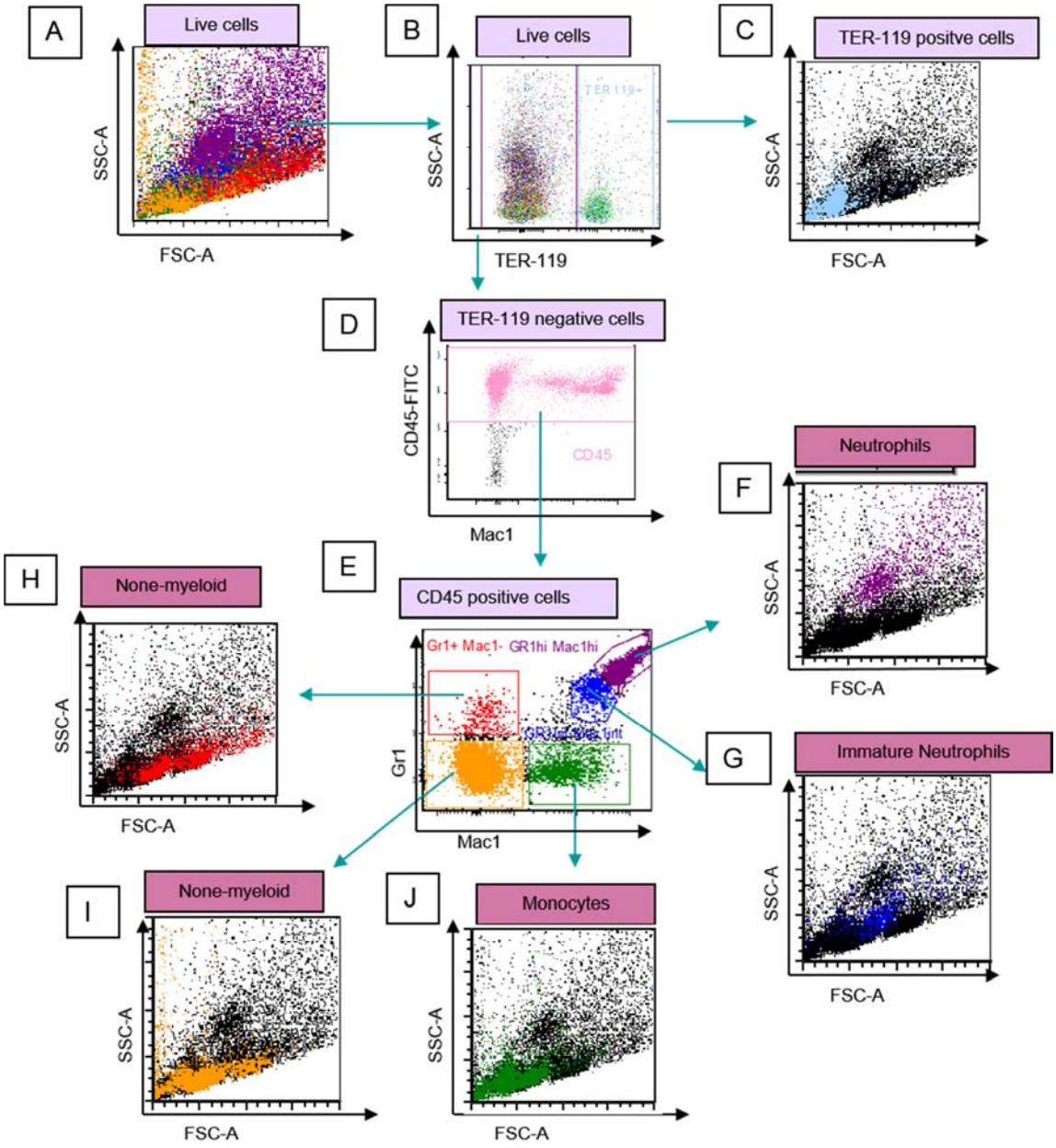

Figure 4.4: Different cell types from peripheral blood can be differentiated by forward and side scatter

(A) Forward and side scatter of all live cells. **(B)** Cells separated between TER119 positive and negative populations. **(C)** Backgating of $TER119^{+}$ cells on the FS versus SS plot. **(D)** The $TER119^{-}$ cells were then plotted on the CD45 versus Mac1 cell surface marker and gate was set on the CD45+ cell population. **(E)** $CD45^{+}$ cells were plotted based on the GR1 versus Mac1 cell surface markers and specific gates were drawn based on the specific marker selection, followed by backgating each cell type onto the FS versus SS plot to see specifically the granularity of each cell to identify cell type. **(F)** $Gr1^{hi}Mac1^{hi}$ (neutrophils), **(G)** $Gr1^{int}Mac1^{int}$ (immature neutrophils), **(H)** $Gr1^{+}Mac1^{-}$ (non-myeloid) , **(I)** $Gr1^{-}Mac1^{-}$ (none-myeloid), **(J)** $Gr1^{-}Mac1^{+}$ (monocytes).

cell types that can be identified based on the Gr1 and Mac1 cell surface markers. Two distinct $Gr1^{+}Mac1^{+}$ populations can be identified in the peripheral blood cells. The $Gr1^{hi}Mac1^{hi}$ cell population corresponds to mature neutrophils (and will be referred as neutrophils in this study) while the $Gr1^{int}Mac1^{int}$ cell population defines immature neutrophils [315-319]. The $Gr1^{-}Mac1^{hi}$ cell population will be referred to as monocytes in this study.

For this flow cytometry analysis on peripheral blood (PB), data was obtained from 3 and 9 month old mice. The results shown in Figure 4.5 and Figure 4.6 were generated from the same groups of mice and the data are presented as the average percentage of specific cell types from the $CD45^{+}$ (leukocyte) population. As shown in Figure 4.5-A, we observed a significant decrease of the neutrophil ($Gr1^{hi}Mac1^{hi}$) population at 3 and 9 months for the $Klf5^{\Delta/\Delta}$ mice and a trend of decreasing neutrophils in the $Klf5^{wt/\Delta}$ mice compared to $Klf5^{fl/fl}$ mice (t-test, $p<0.05$ and $p=0.05$ respectively). However, there were no significant differences observed in the immature neutrophil ($Gr1^{int}Mac1^{int}$) population (Figure 4.5-B). The monocyte ($Gr1^{-}Mac1^{+}$) population was found to be decreased in 3 month but not 9 month old $Klf5^{\Delta/\Delta}$ mice compared to $Klf5^{fl/fl}$ mice (Figure 4.5-C).

As described in Figure 4.3-C, T-cells were defined as the percentage of $CD3\varepsilon^{+}$, $B220^{-}$ cells in the $TER119^{-},CD45^{+}$ population and B-cells as the percentage of $CD3\varepsilon^{-}$, $B220^{+}$ cells from $TER119^{-},CD45^{+}$ population. Interestingly, we observed a significant increase in the T-cell population in PB of $Klf5^{\Delta/\Delta}$ mice in comparison to $Klf5^{fl/fl}$ mice at 3 and 9 months ($p<0.05$) (Figure 4.6-A). In contrast, as shown in Figure 4.6-B, we found that B-cells in PB of $Klf5^{\Delta/\Delta}$ mice were decreased at 3

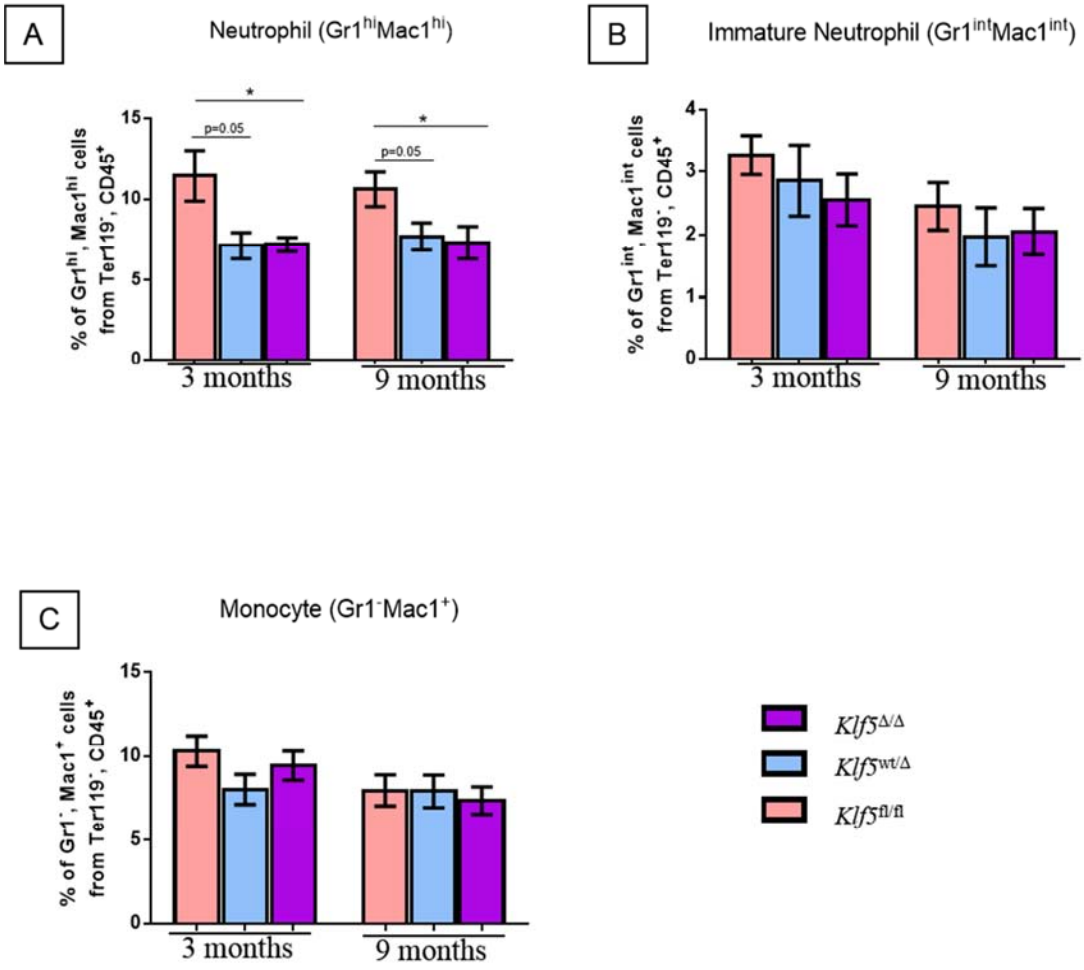

Figure 4.5: Characterisation of mature myeloid cells in peripheral blood using flow cytometry

Each graph represents the percentage of specific cell type determined by the specific cell surface marker from the peripheral blood of 3 and 9 month old mice. Each plotted are mean values plus or minus SEM of **(A)** Neutrophils ($Gr1^{hi}Mac1^{hi}$), **(B)** Immature neutrophils ($Gr1^{int}Mac1^{int}$) and **(C)** monocytes ($Gr1^{-}Mac1^{+}$) cells respectively. The p-value was obtained from a t-test conducted between the $Klf5^{fl/fl}$ and $Klf5^{\Delta/\Delta}$ groups. *Significantly different between $Klf5^{fl/fl}$ and $Klf5^{\Delta/\Delta}$ mice ($P<0.05$). Results obtained from n=10 for $Klf5^{fl/fl}$, n=6 for $Klf5^{wt/\Delta}$ and n=10 for $Klf5^{\Delta/\Delta}$ mice at 3 month, and n=8 for $Klf5^{fl/fl}$, n=8 for $Klf5^{wt/\Delta}$ and n=10 for $Klf5^{\Delta/\Delta}$ mice at 9 months.

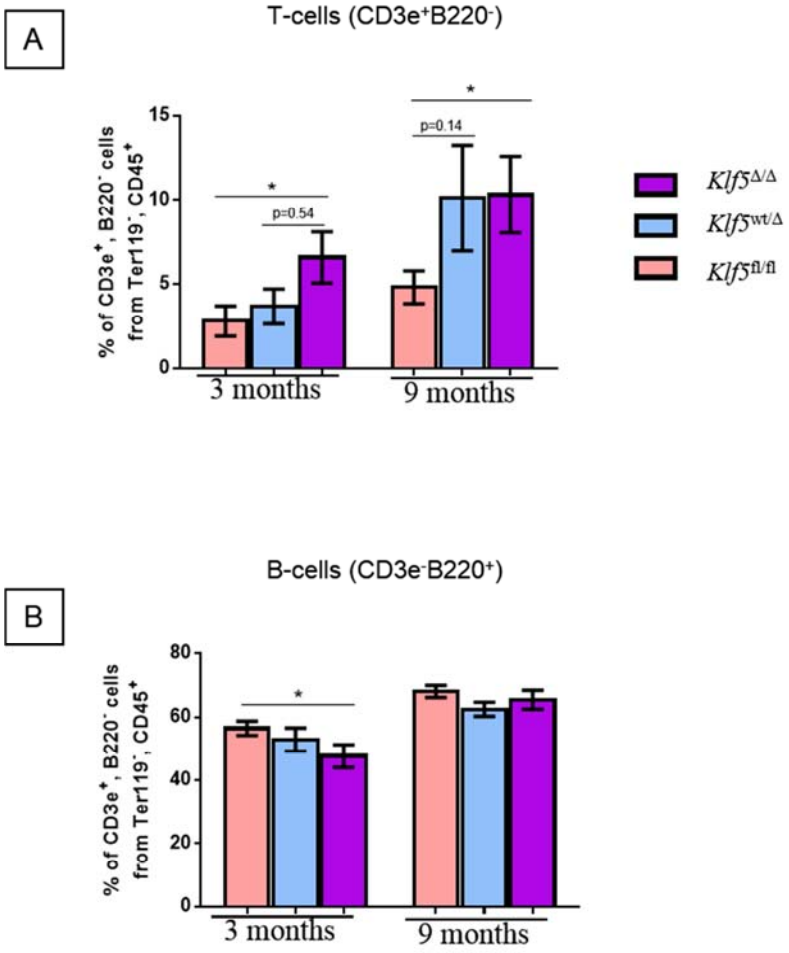

Figure 4.6: Characterisation of mature lymphoid cells in the peripheral blood using flow cytometry

Each graph represents the percentage of specific cell type determined by the lymphoid specific cell surface marker from the peripheral blood of 3 and 9 month old mice. Plotted are mean values plus or minus SEM of **(A)** T-cells ($CD3e^{+}B220^{-}$) and **(B)** B-cells ($CD3e^{-}B220^{+}$) respectively. The p-value was obtained from a t-test conducted between the $Klf5^{fl/fl}$ and $Klf5^{\Delta/\Delta}$ groups using Graphpad Prism. *Significantly different between $Klf5^{fl/fl}$ and $Klf5^{\Delta/\Delta}$ mice ($P< 0.05$). Results are obtained from n=10 for $Klf5^{fl/fl}$, n=6 for $Klf5^{wt/\Delta}$ and n=10 for $Klf5^{\Delta/\Delta}$ mice at 3 months, and n=8 for $Klf5^{fl/fl}$, n=8 for $Klf5^{wt/\Delta}$ and n=10 for $Klf5^{\Delta/\Delta}$ mice at 9 months.

months when compared to *Klf5*$^{fl/fl}$ mice ($p < 0.05$), but this difference was not observed at 9 months.

4.2.2 Flow Cytometry Analysis on Bone Marrow

4.2.2.1 Flow cytometry analysis to assess different leukocyte types in bone marrow

The data collected on peripheral blood (PB) suggests that Klf5 contributes to regulating the granulocyte and T-cell compartments. In this section, further testing was performed on the *Klf5* conditional KO model to define the changes in the bone marrow (BM) compartment. The same flow analysis as conducted for the PB analysis was used to assess mature cell types in the bone marrow. A representative plot of the gating strategy is attached in **Appendix F**. The methods used for bone marrow cell extraction from femur and tibia and for flow cytometry staining are described in Chapter 2, section 2.8. The average cell count was not significantly different between genotypes and consistently increased with age across all genotypes (Figure 4.7). Except for the *Klf5*$^{\Delta/\Delta}$ mice where it decreased between 9 and 12 months although this was not significant, and this is potentially due to the size of these mice (see Figure 3.11).

For flow cytometry analysis, firstly, the proportion of CD45 positive ($CD45^+$) cells present in the BM was determined. As shown in Figure 4.8, 80-100% of $TER119^-$ cells from bone marrow were $CD45^+$ (leukocyte) and this percentage was consistent between the aged-matched genotype groups. Combined with the data in Figure 4.7, this indicates that there are no large overall differences in bone marrow cellularity or leukocyte numbers between different genotypes. To assess mature

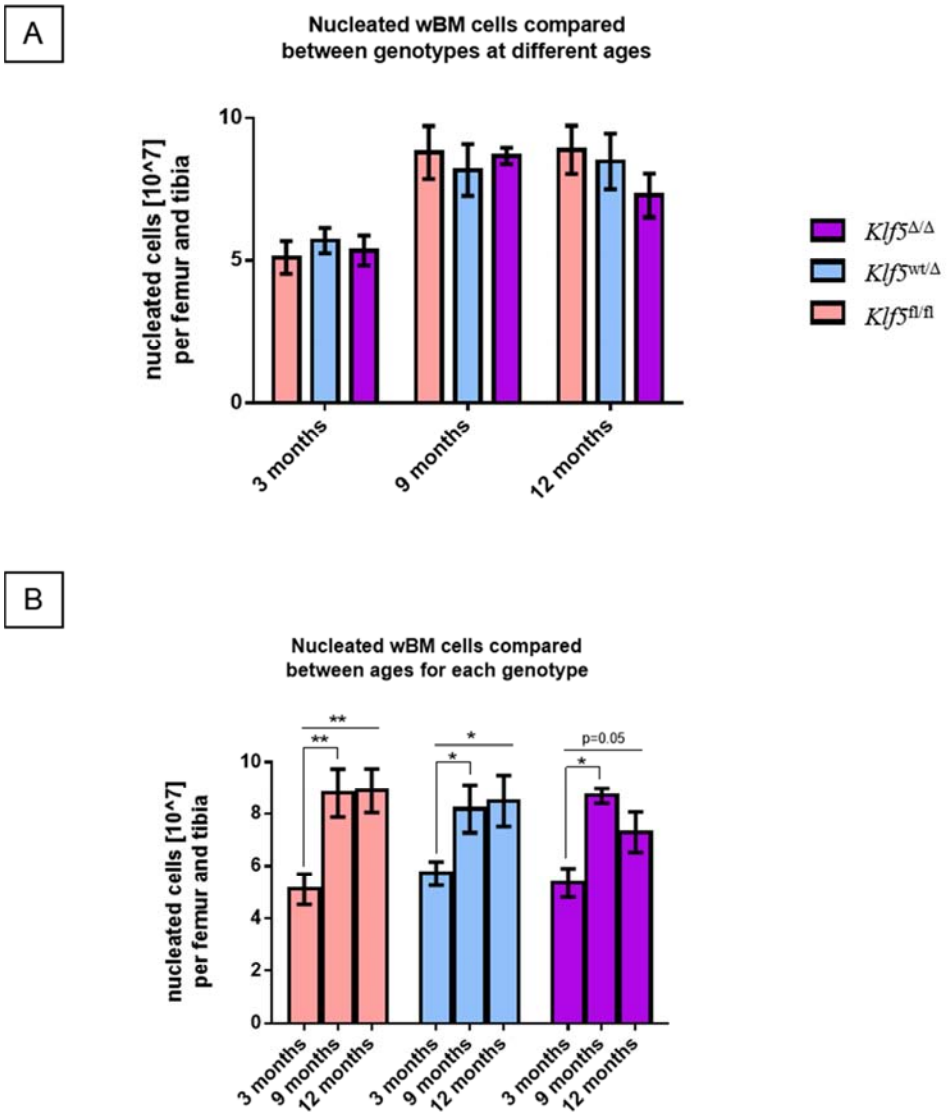

Figure 4.7: Nucleated cell numbers determined from bone marrow after red cell lysis

Nucleated cell counts for the different genotypes at 3, 9 and 12 months and **(B)** represents data comparing between age for each genotype. A minimum of 6 mice were used for each genotype group. The p-value was obtained from a t-test conducted between each genotype or age group using Graphpad Prism. Significantly different between age *($P< 0.05$) and **($P< 0.01$). Results were obtained from n=8 for $Klf5^{fl/fl}$, n=7 for $Klf5^{wt/\Delta}$ and n=8 for $Klf5^{\Delta/\Delta}$ mice at 3 months, n=9 for $Klf5^{fl/fl}$, n=8 for $Klf5^{wt/\Delta}$ and n=8 for $Klf5^{\Delta/\Delta}$ mice at 9 months and n=8 for $Klf5^{fl/fl}$, n=6 for $Klf5^{wt/\Delta}$ and n=7 for $Klf5^{\Delta/\Delta}$ mice at 12 months.

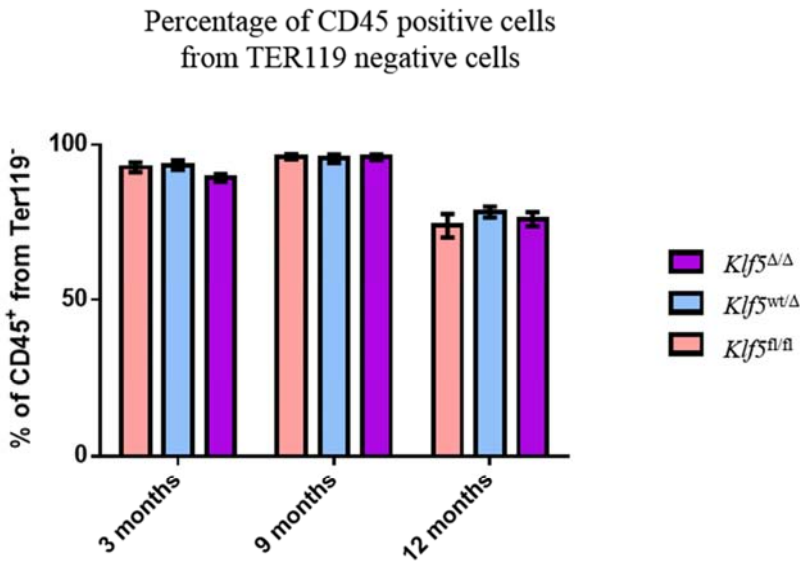

Figure 4.8: The proportion of CD45 positive cells in whole bone marrow as determined by flow cytometry

The bar chart shows the percentage of gated CD45 positive cells determined after selection of the TER119 negative cell population. The flow cytometry analysis was conducted on the fresh whole bone marrow cells from mice of the indicated ages and genotypes. The p-value obtained from t-tests conducted between each genotype group on age based using Graphpad Prism. Results obtained from n=7 for *Klf5*$^{fl/fl}$, n=7 for *Klf5*$^{wt/\Delta}$ and n=8 for *Klf5*$^{\Delta/\Delta}$ mice at 3 months, n=8 for *Klf5*$^{fl/fl}$, n=8 for *Klf5*$^{wt/\Delta}$ and n=9 for *Klf5*$^{\Delta/\Delta}$ mice at 9 months and n=7 for *Klf5*$^{fl/fl}$, n=6 for *Klf5*$^{wt/\Delta}$ and n=8 for *Klf5*$^{\Delta/\Delta}$ mice at 12 months

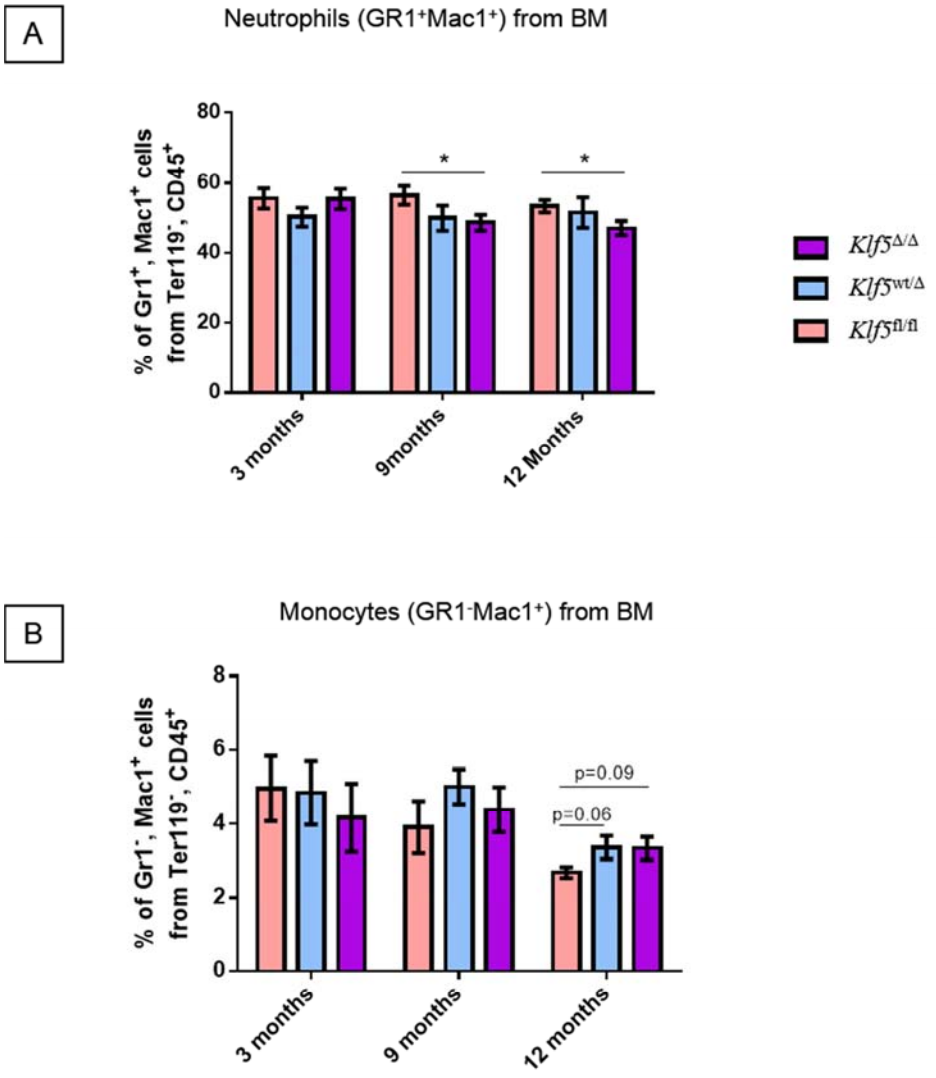

Figure 4.9: Characterisation of mature myeloid cells in the bone marrow using flow cytometry

Shown are mean values plus or minus SEM of **(A)** Neutrophils ($Gr1^{+}Mac1^{+}$) and **(B)** monocytes ($Gr1^{-}Mac1^{+}$). The p-value was obtained from t-tests conducted between each genotype group base on age *($P< 0.05$). Results obtained from n=7 for $Klf5^{fl/fl}$, n=7 for $Klf5^{wt/\Delta}$ and n=8 for $Klf5^{\Delta/\Delta}$ mice at 3 months, n=8 for $Klf5^{fl/fl}$, n=8 for $Klf5^{wt/\Delta}$ and n=9 for $Klf5^{\Delta/\Delta}$ mice at 9 months and n=7 for $Klf5^{fl/fl}$, n=6 for $Klf5^{wt/\Delta}$ and n=8 for $Klf5^{\Delta/\Delta}$ mice at 12 months.

myeloid cells in the bone marrow, the TER119$^-$CD45$^+$ cells were stained with Gr1 and Mac1 cell surface markers. Since we did not observe two distinct Gr1$^+$Mac1$^+$ populations in the bone marrow as for PB (see Figure 4.3 and compared to **Appendix F**), the neutrophil population was assessed based on the entire Gr1$^+$Mac1$^+$ population. Interestingly, neutrophils were found to be significantly decreased in the *Klf5*$^{\Delta/\Delta}$ mice compared to *Klf5*$^{fl/fl}$ mice at 9 and 12 months while no differences were observed at 3 months (Figure 4.9-A). Conversely, monocytes (Gr1$^-$Mac1$^+$) showed a trend towards an increase in the *Klf5*$^{\Delta/\Delta}$ mice at 12 months old (Figure 4.9-B).

Figure 4.10 shows the results obtained from bone marrow flow cytometry analysis with mature lymphoid cell markers. Using the T-cell and B-cell specific cell surface markers (CD3ε and B220 respectively), it was found that the T-cell population of *Klf5*$^{\Delta/\Delta}$ mice was significantly higher than *Klf5*$^{fl/fl}$ mice at 12 months with no difference observed at 3 or 9 months. In addition, the B-cell population was found to be significantly higher in *Klf5*$^{\Delta/\Delta}$ mice compared to *Klf5*$^{fl/fl}$ mice only at 9 months, with a trend towards an increase at 12 months.

4.2.2.2 Flow cytometry analysis to assess myeloid progenitor cell populations in bone marrow

In addition to analysis of mature cell types, further analysis was conducted to assess changes in the myeloid progenitor cell compartment from bone marrow using multi-colour flow cytometry. Details of procedures and antibodies used for this analysis are described in Chapter 2, section 2.12.3.

The gating strategy described by *Pronk et. al.* was used for the detection of immature myelo-erythroid progenitor subsets from c-Kit$^+$ enriched bone marrow

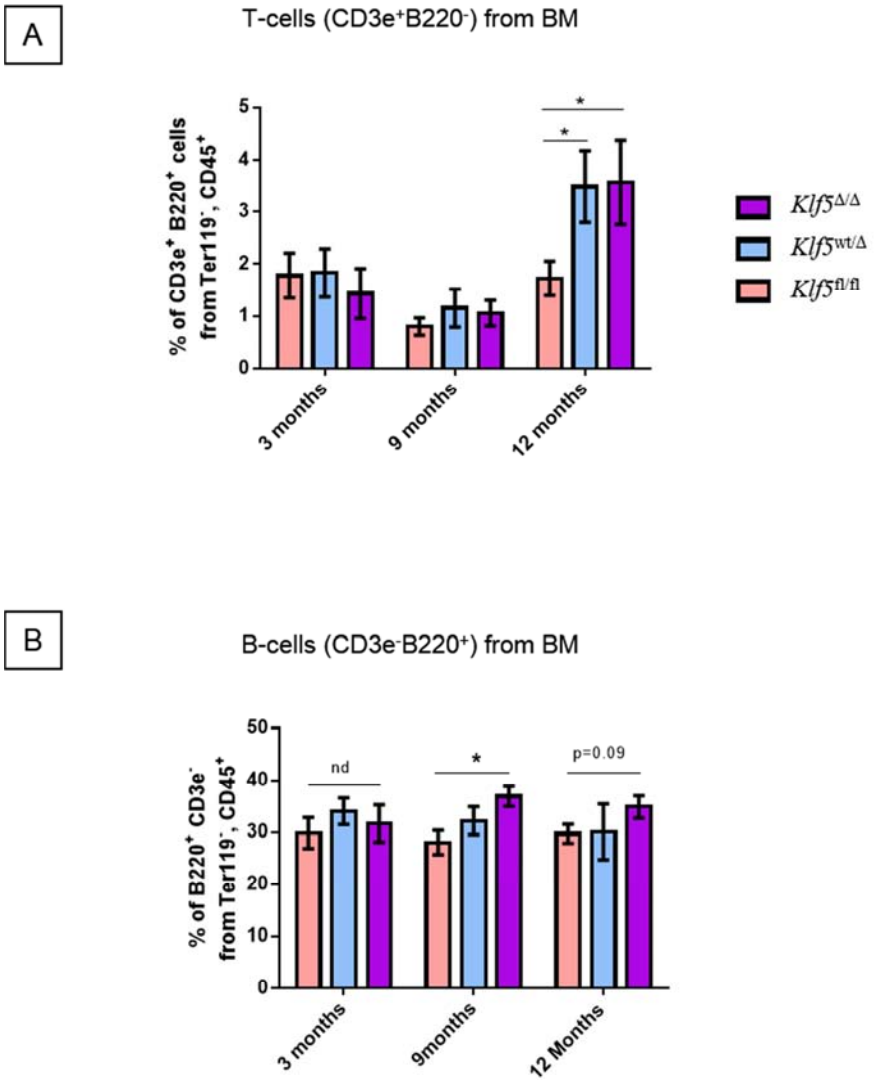

Figure 4.10: Characterisation of mature lymphoid cells in the bone marrow using flow cytometry

Shown are mean values plus or minus SEM **(A)** T-cells ($CD3e^{+}B220^{-}$) and **(B)** B-cells ($CD3e^{-}B220^{+}$) respectively. The flow cytometry analysis was conducted on the whole bone marrow cells from mice of the indicated ages and genotypes. P-values were obtained from t-tests conducted between each genotype group based on age. Significantly different between $Klf5^{fl/fl}$ and $Klf5^{\Delta/\Delta}$ mice *($P< 0.05$). Results obtained from n=7 for $Klf5^{fl/fl}$, n=7 for $Klf5^{wt/\Delta}$ and n=8 for $Klf5^{\Delta/\Delta}$ mice at 3 months, n=8 for $Klf5^{fl/fl}$, n=8 for $Klf5^{wt/\Delta}$ and n=9 for $Klf5^{\Delta/\Delta}$ mice at 9 months and n=7 for $Klf5^{fl/fl}$, n=6 for $Klf5^{wt/\Delta}$ and n=8 for $Klf5^{\Delta/\Delta}$ mice at 12 months.

cells (Figure 4.11) [320]. Briefly, an initial gating of the live cells was followed by eliminating unwanted particles including dead cells and debris, based on the forward (FS) and side (SS) scatter to further enrich live cells (Figure 4.11-A and B). For myeloid progenitor cell analysis, mature cells were excluded using positivity for a cocktail of lineage markers (Figure 4.11-C) and selection of Sca-1 negative cells (Figure 4.11-D). Consecutively, the next three plots show the purified myelo-erythroid progenitor subsets including early bipotent progenitors for the erythroid/megakaryocyte lineages (preMegE), early erythroid (preCFU-E and CFU-E), megakaryocyte progenitors (MkP), and primitive granulocyte/macrophage progenitors (preGM and GMP) (Figure 4.11-E) [320]. In this study, data are presented as the percentage of myelo-erythroid progenitor cells from the c-Kit^{+}, Lin^{-} cell population.

Prior to performing the progenitor analysis, we showed that there is a consistent percentage of myeloid progenitors (Sca-1^{-}) as the percentage of c-Kit^{+}, Lin^{-} cells for each genotype at 3 and 9 months (Figure 4.12-A). The LSK fraction (defined as the percentage of Sca-1^{+} from c-Kit^{+}, Lin^{-}) also did not show any difference in the *Klf5*$^{\Delta/\Delta}$ mice when compared to control age-match littermates (Figure 4.12-B). A more extensive analysis of the HSC compartment is discussed in this chapter in section 4.2.2.3.

The CD150 SLAM marker was next used to define myeloid progenitor cells [320, 321]. The granulocyte-macrophage progenitor (GMP) population which was defined as CD16/32^{+}, CD150^{-} (refer Figure 4.11-E) showed no significant changes as a percentage of the c-Kit^{+}, Lin^{-} population (Figure 4.13-A). We further investigated the primitive granulocyte-macrophage progenitor (preGM) cells which

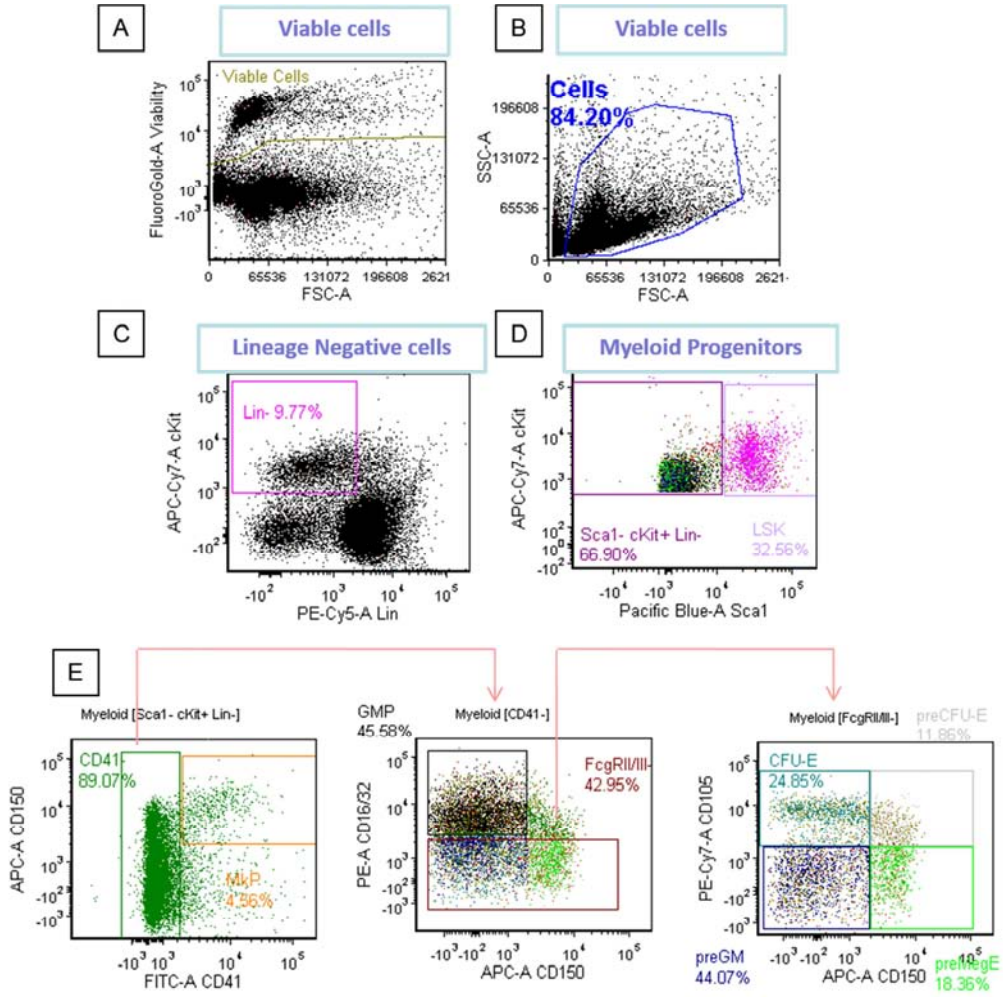

Figure 4.11: Schematic diagram of the sequential gating strategy for flow cytometry analysis of myeloid progenitor cells

(A) The live cell population was determined by fluorogold negativity. **(B)** Debris was excluded from the analysis based on forward and side scatter. **(C)** Selection for the c-Kit positive, lineage negative cells. **(D)** Sca-1 negative cells for the specific selection of myeloid progenitor cells. **(E)** The last three plots show the purified myelo-erythroid progenitor subsets including early bipotent progenitors for the erythroid/megakaryocyte lineages (preMegE), early monopotent erythroid (preCFU-E and CFU-E) and megakaryocyte progenitors (MkP), and primitive granulocyte/macrophage progenitors (preGM and GMP).

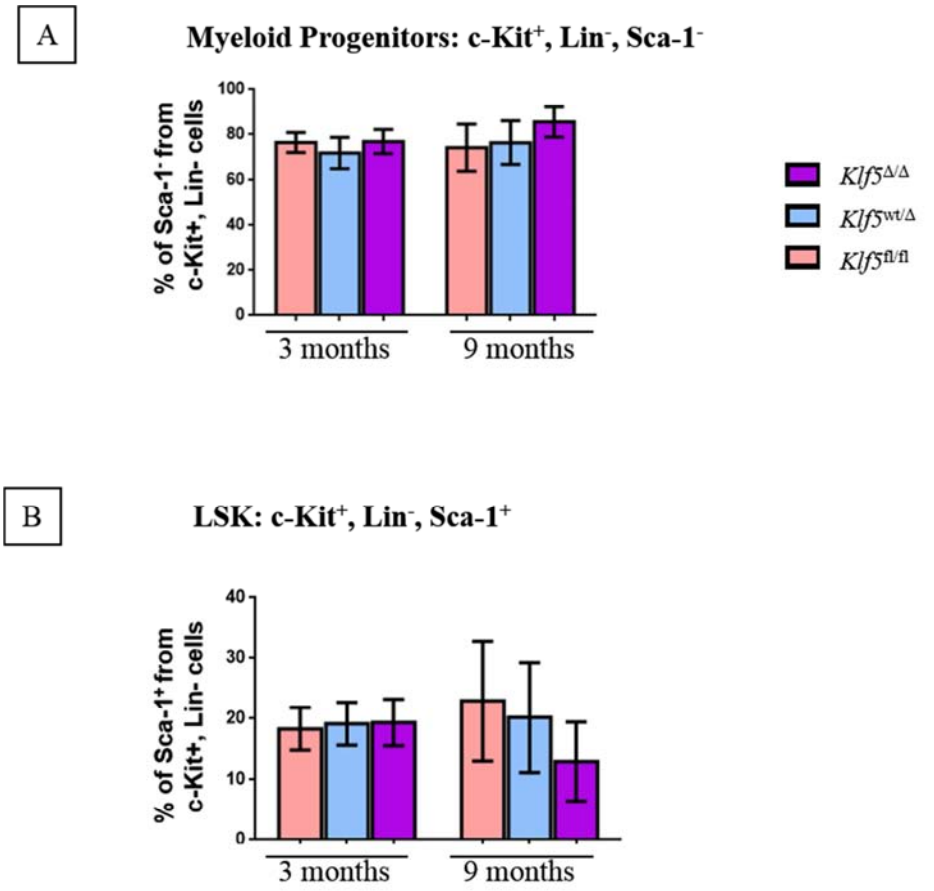

Figure 4.12: Characterisation of haemopoiesis stem and myeloid progenitor cells in the bone marrow using flow cytometry

(A) Percentage of Sca-1$^-$ from c-Kit$^+$, Lin$^-$, population and **(B)** Percentage of Sca-1$^+$ from c-Kit$^+$, Lin$^-$ population (also known as LSK cells). Results obtained from n=11 for *Klf5*$^{fl/fl}$, n=7 for *Klf5*$^{wt/\Delta}$ and n=10 for *Klf5*$^{\Delta/\Delta}$ mice at 3 months and n=8 for *Klf5*$^{fl/fl}$, n=8 for *Klf5*$^{wt/\Delta}$ and n=11 for *Klf5*$^{\Delta/\Delta}$ mice at 9 months.

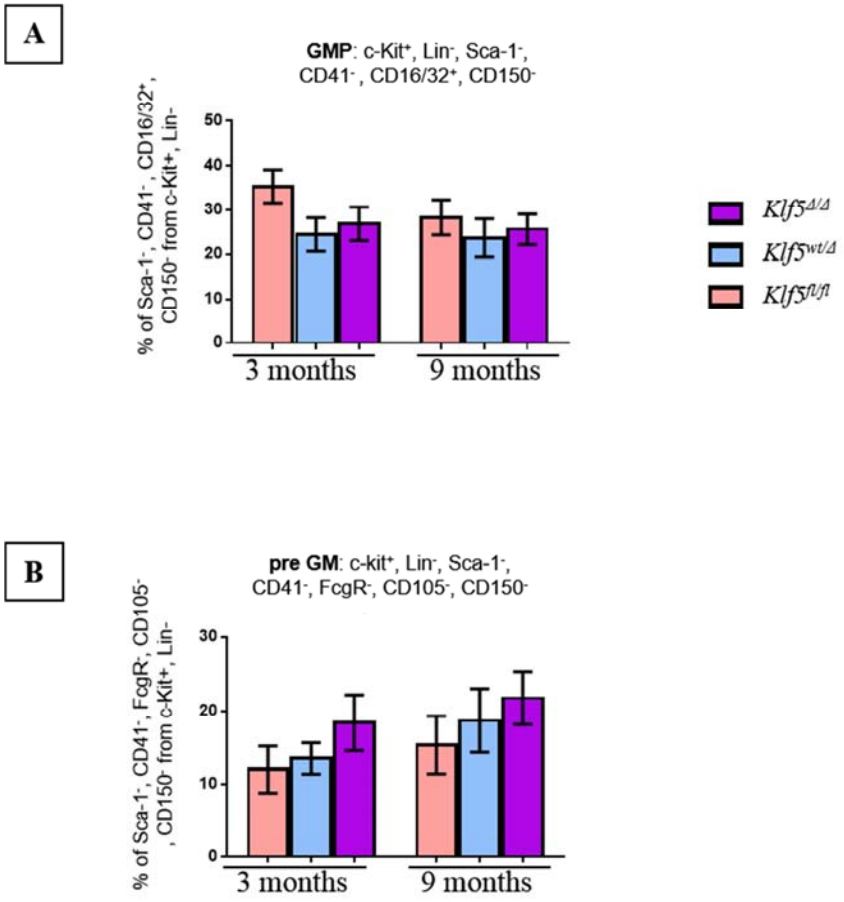

Figure 4.13: Characterisation of granulocyte-macrophage progenitors in the bone marrow using flow cytometry

(A) Percentage of granulocyte/macrophage progenitors (GMP) obtained from the flow cytometry analysis (defined by c-Kit^{+}, Lin^{-}, Sca-1^{-}, CD41^{-}, CD16/32^{+}) and **(B)** represents the percentage of primitive granulocyte/macrophage progenitors (preGM) (defined by c-Kit^{+}, Lin^{-}, Sca-1^{-}, CD41^{-}, CD16/32^{-}, CD105^{-}, CD150^{-}). Mean and SEM are shown. P-value obtained from t-test conducted between each genotype group on age based. *Significantly different between *Klf5*$^{fl/fl}$ and *Klf5*$^{\Delta/\Delta}$ mice ($P< 0.05$). Results obtained from n=11 for *Klf5*$^{fl/fl}$, n=7 for *Klf5*$^{wt/\Delta}$ and n=10 for *Klf5*$^{\Delta/\Delta}$ mice at 3 months and n=8 for *Klf5*$^{fl/fl}$, n=8 for *Klf5*$^{wt/\Delta}$ and n=11 for *Klf5*$^{\Delta/\Delta}$ mice at 9 months.

can be defined as $CD105^+$, $CD150^+$ [320, 321]. From the results obtained, the percentage of the preGM population was not significantly different between genotypes at either age analysed (3 and 9 months) (Figure 4.13-B). We also characterised erythroid progenitor populations, CFU-E and pre CFU-E cells which can be defined as $CD105^+$, $CD150^-$ and $CD105^+$, $CD150^+$ respectively [320, 321]. However, there was no difference observed between genotypes in the average percentage of CFU-E and pre CFU-E population from c-Kit^+, Lin^- population (Figure 4.14). In addition, we analysed the MkP and preMEGE populations and did not observe any significant differences (Figure 4.15).

4.2.2.3 Flow cytometry analysis to assess the stem cell compartment in bone marrow

To measure short-term and long-term HSC in the bone marrow, we used flow cytometry to define LSK cells and then further delineation of this population was performed using SLAM families marker CD48 and CD150 [322]. The gating strategy used for this analysis is summarised in Figure 4.16 and was based on the approaches described by *Pronk et al.*, *Karsunky et al.* and *Adolfson et al.* [320, 321, 323, 324]. An initial gating of live cells was performed by selecting the fluorogold negative population followed by eliminating unwanted particles including dead cells and debris base on the forward (FS) and side (SS) scatter. Applying a similar approach as described above for the myeloid progenitor cell analysis, we selected for the c-Kit positive cells and removed the lineage positive cells from the analysis in order to increase the sensitivity to measure immature cell types. The subsequent plot

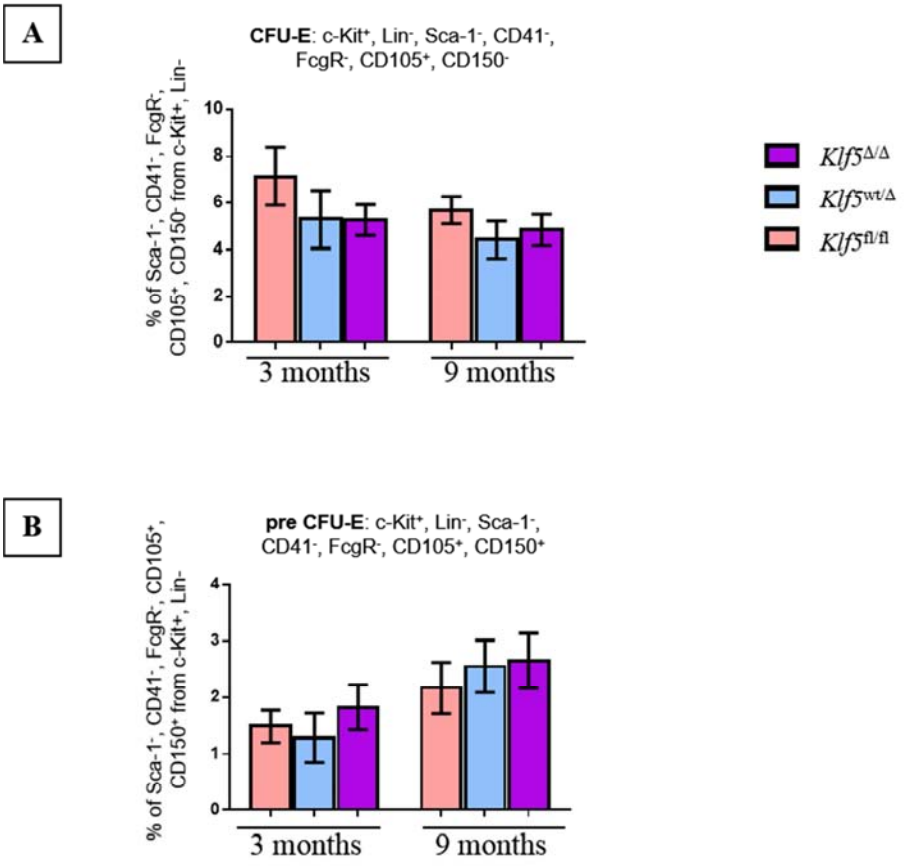

Figure 4.14: Characterisation of erythroid progenitors in the bone marrow using flow cytometry

(A) Percentage of erythroid progenitors (CFU-E) obtained from the flow cytometry analysis (defined by c-Kit^{+}, Lin^{-}, Sca-1^{-}, CD41^{-}, CD16/32^{-}, CD105^{+}, CD150^{-}) and **(B)** the percentage of primitive erythroid progenitors (pre CFU-E) (defined by c-Kit^{+}, Lin^{-}, Sca-1^{-}, CD41^{-}, CD16/32^{-}, CD105^{+}, CD150^{+}). Mean and SEM are shown. P-value were obtained from t-tests conducted between the *Klf5*$^{fl/fl}$ and *Klf5*$^{\Delta/\Delta}$ groups using Graphpad Prism. *Significantly different between *Klf5*$^{fl/fl}$ and *Klf5*$^{\Delta/\Delta}$ mice ($P< 0.05$). Results obtained from n=11 for *Klf5*$^{fl/fl}$, n=7 for *Klf5*$^{wt/\Delta}$ and n=10 for *Klf5*$^{\Delta/\Delta}$ mice at 3 months and n=8 for *Klf5*$^{fl/fl}$, n=8 for *Klf5*$^{wt/\Delta}$ and n=11 for *Klf5*$^{\Delta/\Delta}$ mice at 9 months.

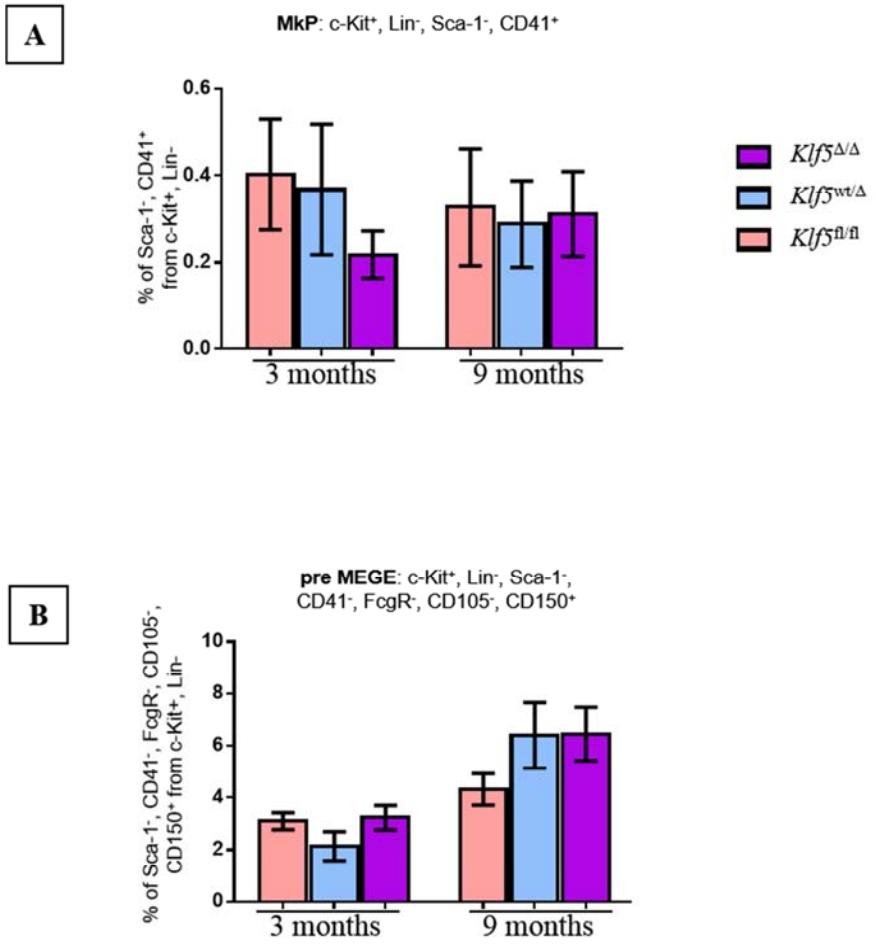

Figure 4.15: Characterisation of myelo-erythroid progenitors in the bone marrow using flow cytometry

(A) The percentage of megakaryocyte progenitors (MkP) obtained from the flow cytometry analysis (defined by c-Kit^{+}, Lin^{-}, Sca-1^{-}, CD41^{+}, CD150^{+}) and **(B)** the percentage of erythroid/megakaryocyte lineages (preMegE), (defined by c-Kit^{+}, Lin^{-}, Sca-1^{-}, CD41^{-}, CD16/32^{-}, CD105^{-}, CD150^{+}). Mean and SEM are shown. Results obtained from n=11 for *Klf5*$^{fl/fl}$, n=7 for *Klf5*$^{wt/\Delta}$ and n=10 for *Klf5*$^{\Delta/\Delta}$ mice at 3 months and n=8 for *Klf5*$^{fl/fl}$, n=8 for *Klf5*$^{wt/\Delta}$ and n=11 for *Klf5*$^{\Delta/\Delta}$ mice at 9 months.

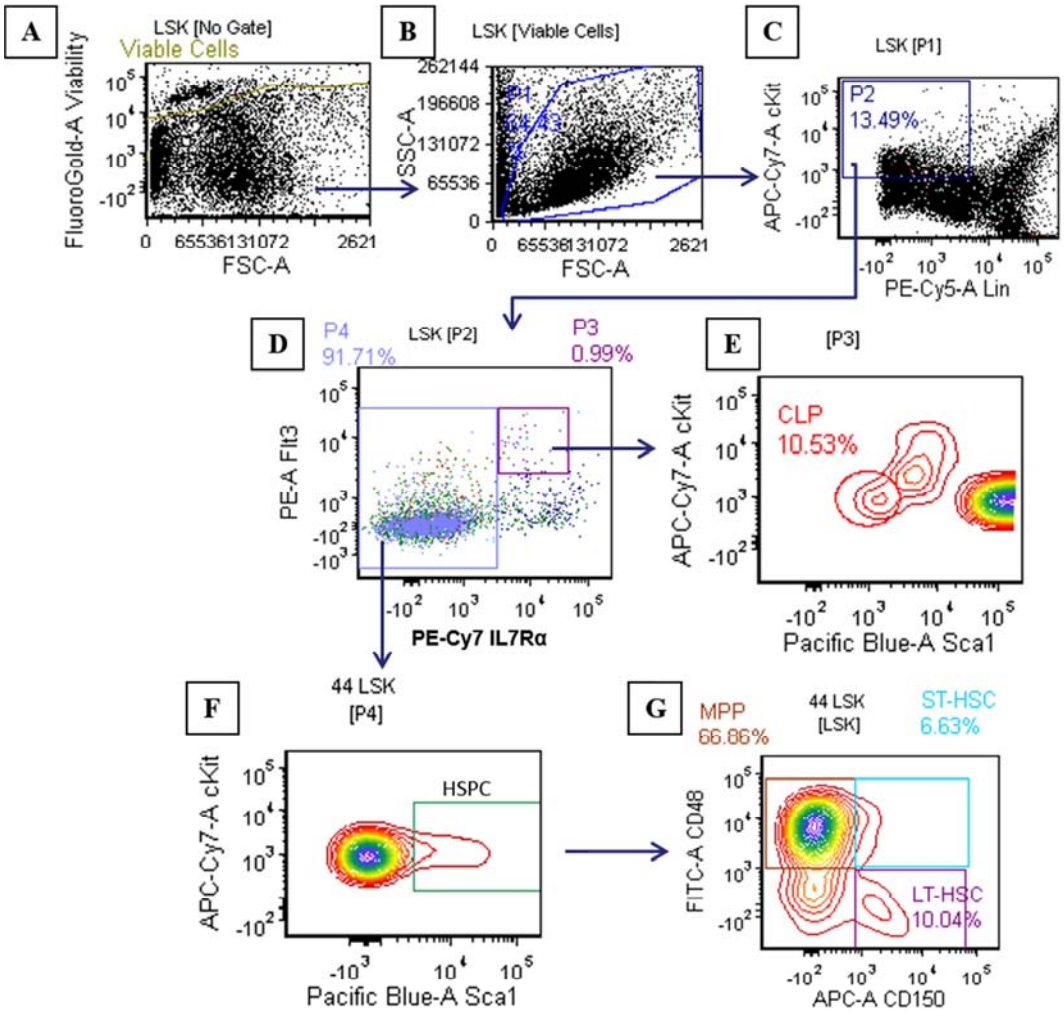

Figure 4.16: Schematic diagram of the sequential gating strategy for flow cytometry analysis of stem and lymphoid progenitor cells

(A) The live cell population was determined by fluorogold negativity. **(B)** Debris was excluded from the analysis using forward and side scatter. **(C)** Lineage negative and c-Kit positive cells were. **(D)** Cell were gated on either IL7Rα positive (P3) or IL7Rα negative cells (P4) as for specific selection for common lymphoid progenitor (CLP) or stem cell population (HSC). **(E)** The CLP population was determined out of the P3 gate based on c-Kit intermediate and Sca-1 intermediate signals. **(F)** The total HSPC population was defined out of the P4 gate by selection of Sca-1 positive cells. **(G)** Long-term HSC (LT-HSC), short-term HSC (ST-HSC) and multi-potent progenitor (MPP).

with Flt3 versus IL7-Rα cell surface markers was used to determine the common lymphoid (CLP) and HSC progenitor (HSCP) populations. Consecutively, more primitive stem cell populations including long-term HSC (LT-HSC), short-term HSC (ST-HSC) and multi potent progenitor (MPP) cells were defined based on the subsequent plot with CD48 versus CD150 cell surface markers.

The average percentage of total HSPC defined by gating the c-Kit^{+}, Sca-1^{+} population within the c-Kit^{+}, Lin^{-} cells was significantly decreased in the 9 month old *Klf5*$^{\Delta/\Delta}$ mice compared to *Klf5*$^{fl/fl}$ mice (Figure 4.17). However, subsequent measurement of the primitive stem cell compartments including LT-HSC, ST-HSC and MPP did not reveal significant differences between genotypes (Figure 4.18). In addition to this HSPC subset analysis, the combination of surface markers used enabled measurement of CLP as shown in Figure 4.16. Interestingly, as shown in Figure 4.19 the average percentage of CLP defined as Flt3^{+}, IL7Rα^{+}, c-Kit^{lo}, Sca-1^{lo} cells in the c-Kit^{+}, Lin^{-} population was significantly lower at 9 months for *Klf5*$^{\Delta/\Delta}$ mice compared to *Klf5*$^{fl/fl}$ mice with no significant difference observed at 3 months.

4.2.3 Colony Forming Unit Assays on Bone Marrow

4.2.3.1 Colony assays for the quantification of haemopoietic progenitor cells in bone marrow

Haemopoietic progenitor cells in BM of mice were also analysed using clonal assays to measure colony forming units (CFU). The CFU assay was originally developed by *Bradley and Metcalf* [325] as a measure of haemopoietic progenitor cell proliferation potential in the presence of particular lineage-specific cytokines (**Appendix G** shows different colonies that can be enumerated during CFU assays).

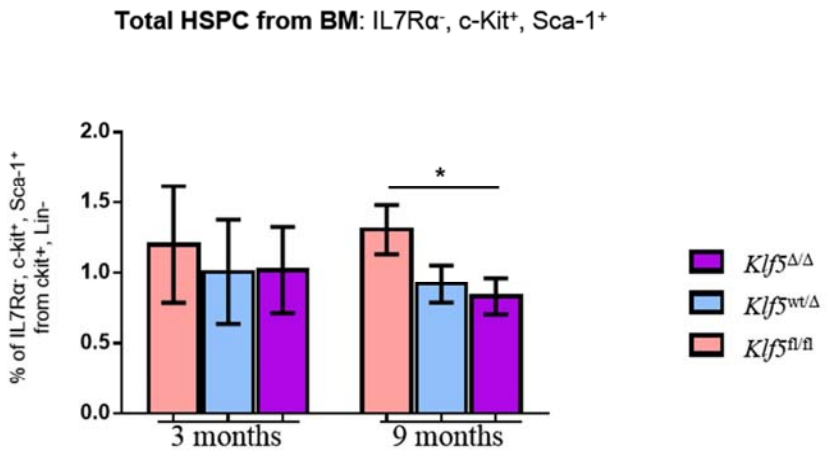

Figure 4.17: Characterisation of HSPC in the bone marrow using flow cytometry

Total HSPC were defined as shown in Figure 4.16F. The bar chart shows the percentage of total HSPC cells from c-Kit^{+}, Lin^{-} population. Mean and SEM are shown. The p-value was obtained from t-tests conducted between each genotype group on age based. Results obtained from n=11 for *Klf5*$^{fl/fl}$, n=7 for *Klf5*$^{wt/\Delta}$ and n=10 for *Klf5*$^{\Delta/\Delta}$ mice at 3 months and n=8 for *Klf5*$^{fl/fl}$, n=8 for *Klf5*$^{wt/\Delta}$ and n=11 for *Klf5*$^{\Delta/\Delta}$ mice at 9 months.

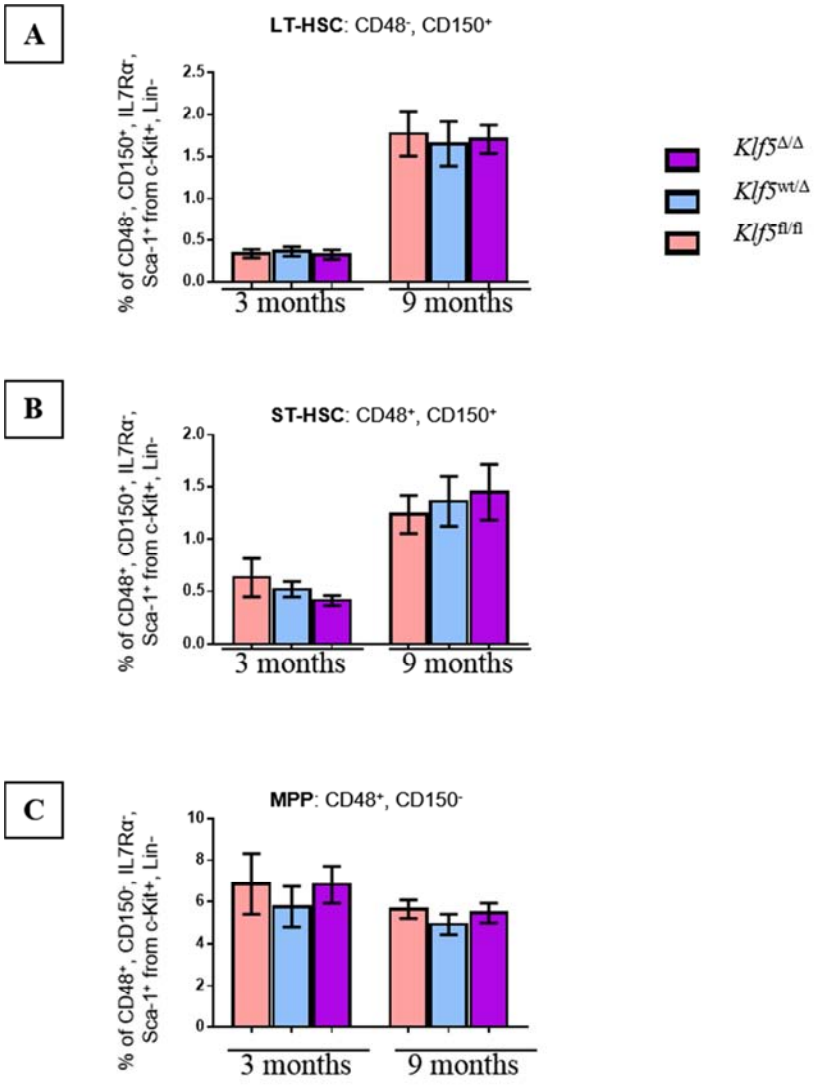

Figure 4.18: Characterisation of long-term and short-term haemopoietic stem cells and multi potent progenitor in the bone marrow using flow-cytometry

Stem cell compartments were defined as shown in Figure 4.16G. **(A)** Bar charts represent the percentage of long-term HSC (LT-HSC) obtained from the flow cytometry analysis which were defined by c-Kit^{+}, Lin^{-}, IL7Rα^{-}, Sca-1^{+}, CD16/32^{-}, CD48^{-}, CD150^{+}, **(B)** represents the percentage of short-term HSC (ST-HSC) which were defined by c-Kit^{+}, Lin^{-}, IL7Rα^{-}, Sca-1^{+}, CD16/32^{-}, CD48^{+}, CD150^{+} and **(C)** represents the percentage of multi potent progenitors (MPP) which were defined by c-Kit^{+}, Lin^{-}, IL7Rα^{-}, Sca-1^{+}, CD16/32^{-}, CD48^{+}, CD150^{-}. Mean and SEM are shown. Results were obtained from n=11 for *Klf5*$^{fl/fl}$, n=7 for *Klf5*$^{wt/\Delta}$ and n=10 for *Klf5*$^{\Delta/\Delta}$ mice at 3 months and n=8 for *Klf5*$^{fl/fl}$, n=8 for *Klf5*$^{wt/\Delta}$ and n=11 for *Klf5*$^{\Delta/\Delta}$ mice at 9 months.

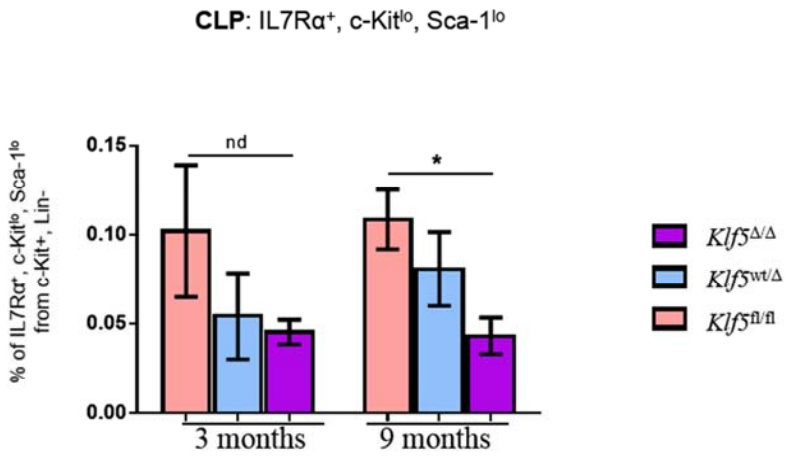

Figure 4.19: Characterisation of common lymphoid progenitors in bone marrow using flow cytometry

Common lymphoid progenitor (CLP) population were defined as shown in Figure 4.16E. The bar chart represents the percentage of CLP population normalised to c-kit^{+}, Lin^{-} population. Mean and SEM are shown. The p-values obtained are from t-tests conducted between each genotype group based on age. Results obtained from n=11 for *Klf5*$^{fl/fl}$, n=7 for *Klf5*$^{wt/\Delta}$ and n=10 for *Klf5*$^{\Delta/\Delta}$ mice at 3 months and n=8 for *Klf5*$^{fl/fl}$, n=8 for *Klf5*$^{wt/\Delta}$ and n=11 for *Klf5*$^{\Delta/\Delta}$ mice at 9 months.

Serial replating of colonies can be used as a measure of self-renewal capacity [326]. Figure 4.20 shows the CFU and the serial replating assay results from whole bone marrow cells of 3 and 9 month old mice seeded in methylcellulose containing SCF, IL3, IL6, EPO and GM-CSF. Interestingly, there was a small but significant increase in CFU frequencies of *Klf5*$^{\Delta/\Delta}$ mice at 3 months compared to *Klf5*$^{fl/fl}$ mice (Figure 4.20-A). In addition, the results obtained for 9 month old mice showed a decrease in CFU replating potential in the *Klf5*$^{\Delta/\Delta}$ mice compared to *Klf5*$^{fl/fl}$ mice revealed on the secondary and tertiary replating (Figure 4.20-B). The individual colonies were also typed and scored as described in methods, however, there were no significant changes observed for the individual progenitor types between the genotypes (**Appendix H**).

To test whether *Klf5* has a significant role in granulocyte-macrophage cell growth or differentiation in response to GM-CSF alone, 1 x 10^4 whole bone marrow cells from 3 and 9 months old mice were seeded in methylcellulose containing GM-CSF only. Figure 4.21 shows that there was a trend to decreasing CFU frequencies at 3 and 9 months for *Klf5*$^{\Delta/\Delta}$ mice compared to *Klf5*$^{fl/fl}$ mice (p=0.05 and p=0.07 respectively). Scoring of individual colonies showed that a significant reduction in CFU-G and CFU-M was contributing to the total decrease of colonies for *Klf5*$^{\Delta/\Delta}$ mice compared to *Klf5*$^{fl/fl}$ mice, with no significant difference observed for the CFU-GM.

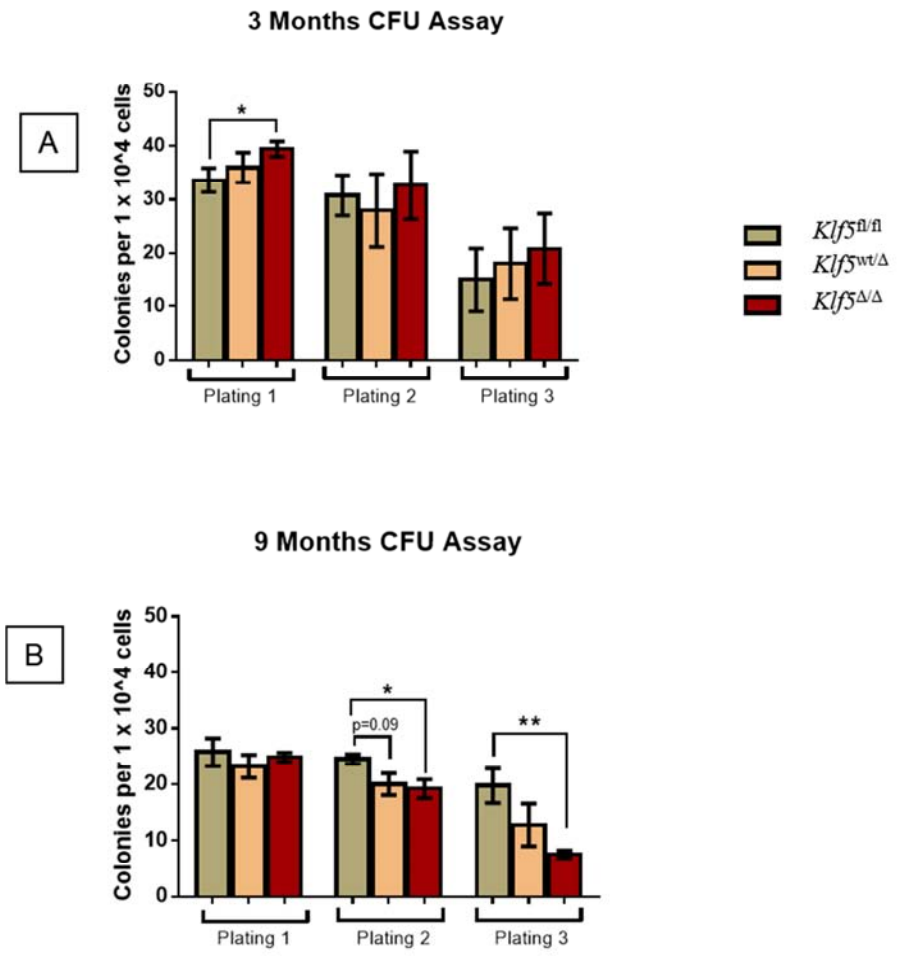

Figure 4.20: Quantification of myelo-erythroid progenitor self-renewal in a cytokine cocktail from bone marrow using serial colony forming assay

1 x 10^4 whole bone marrow cells were seeded in methylcellulose containing SCF, IL3, IL6, EPO and GM-CSF. The bar chart shows the total number of colonies obtained after 8 days (labelled as plating 1). At day 8, cells were harvested and reseeded in methylcellulose containing SCF, IL3, IL6, EPO and GM-CSF and cultured again for 8 days (labelled as plating 2). Plating 3 was the subsequent replating. **A)** Colonies scored for CFU-assay of 3 months old mice of n=6 for *Klf5*$^{fl/fl}$, n=6 for *Klf5*$^{wt/\Delta}$ and n=7 for *Klf5*$^{\Delta/\Delta}$ mice. **B)** Colonies scored for CFU-assay of 9 months old mice of n=4 for *Klf5*$^{fl/fl}$, n=5 for *Klf5*$^{wt/\Delta}$ and n=5 for *Klf5*$^{\Delta/\Delta}$ mice. The p-values were obtained from t-tests conducted between genotype group. Significantly different between *Klf5*$^{fl/fl}$ and *Klf5*$^{\Delta/\Delta}$ mice *($P< 0.05$) or **($P< 0.01$).

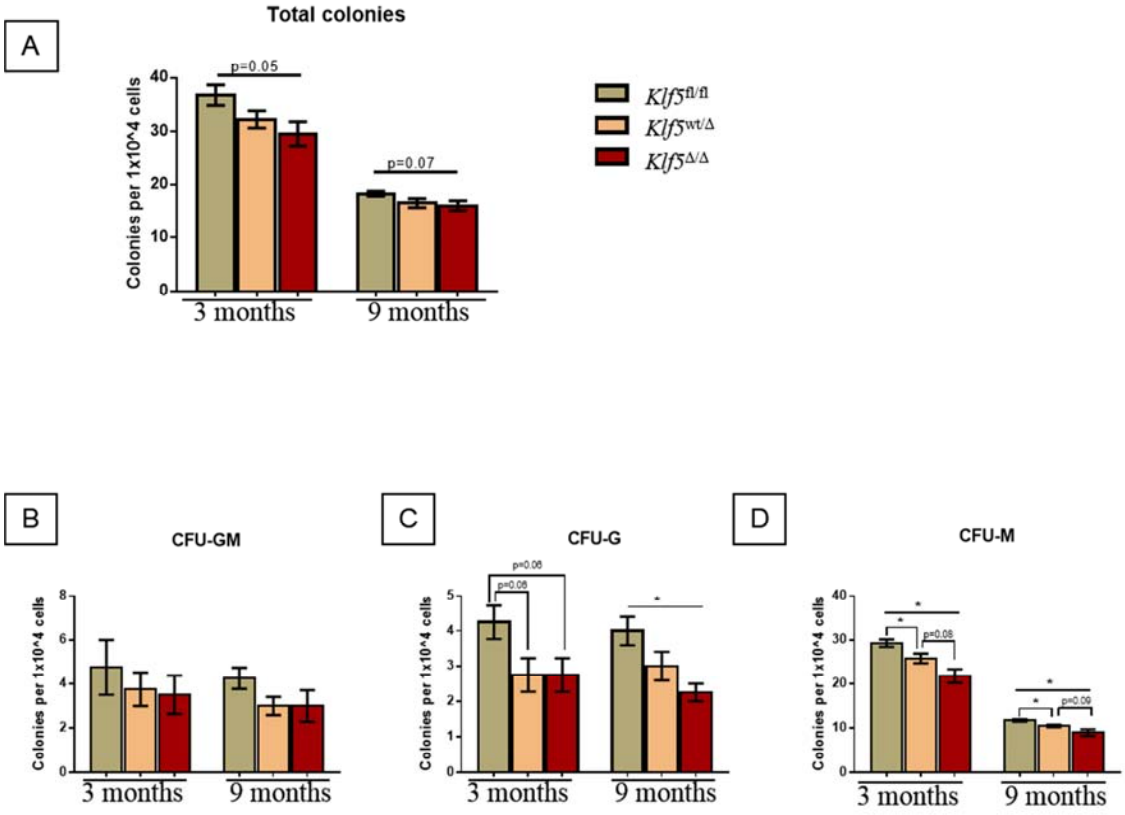

Figure 4.21: Quantification of myeloid progenitors in the bone marrow using colony forming assays in response to GM-CSF

1 x 10^4 whole bone marrow cells from 3 and 9 month old mice were seeded in methylcellulose containing GM-CSF only. **A)** Total colonies scored after 8 days. **B)** Individual colony type scored from each genotype after 8 days. Mean and SEM are shown. For 3 months old mice; n=4 for $Klf5^{fl/fl}$, n=3 for $Klf5^{wt\Delta}$ and n=5 for $Klf5^{\Delta/\Delta}$ mice. For 9 months old mice; n=4 for $Klf5^{fl/fl}$, n=4 for $Klf5^{wt/\Delta}$ and n=4 for $Klf5^{\Delta/\Delta}$ mice. P-values were obtained from t-tests conducted between the $Klf5^{fl/fl}$ and $Klf5^{\Delta/\Delta}$ groups using Graphpad Prism. *Significantly different between $Klf5^{fl/fl}$ and $Klf5^{\Delta/\Delta}$ mice ($P< 0.05$).

4.2.3.2 Colony assays for the quantification of CFU-E and BFU-E in bone marrow

To functionally characterise the erythroid progenitor compartment in bone marrow we performed assays for erythroid colony forming cells (CFU-E and BFU-E). As shown in Figure 4.22 both CFU-E and BFU-E colonies were significantly reduced in the *Klf5*$^{\Delta/\Delta}$ mice compared to the *Klf5*$^{fl/fl}$ mice.

4.3 Discussion

Since multiple studies have shown roles for several Klf family members during both myeloid and lymphoid cell development (as discussed in Chapter 1, section 1.8), it was important for us to conduct a comprehensive analysis to determine if Klf5 has a non-redundant role during haemopoiesis. In this study, an analysis was conducted using the Vav-cre mouse model, described in the previous chapter, to investigate if conditional *Klf5* ablation in the haemopoietic system leads to defects in steady-state haemopoiesis, and if so, at which stage and lineage(s) the defect occurs. Thus, *Klf5*$^{\Delta/\Delta}$ mice were analysed at 3, 9 and 12 months of age and compared with age-matched *Klf5*$^{wt/\Delta}$ mice and *Klf5*$^{fl/fl}$ mice. Signs of alterations in the haemopoietic system were observed when CBC on the PB of *Klf5*$^{\Delta/\Delta}$ mice was compared with the age-matched *Klf5*$^{wt/\Delta}$ and *Klf5*$^{fl/fl}$ mice littermates. At 9 and 12 months of age the total WBC scored in *Klf5*$^{\Delta/\Delta}$ mice was significantly higher than *Klf5*$^{fl/fl}$ mice. The RBC, HgB and HcT were found to be significantly decreased in *Klf5*$^{\Delta/\Delta}$ mice only at 3 months of age suggesting an early developmental defect in erythropoiesis.

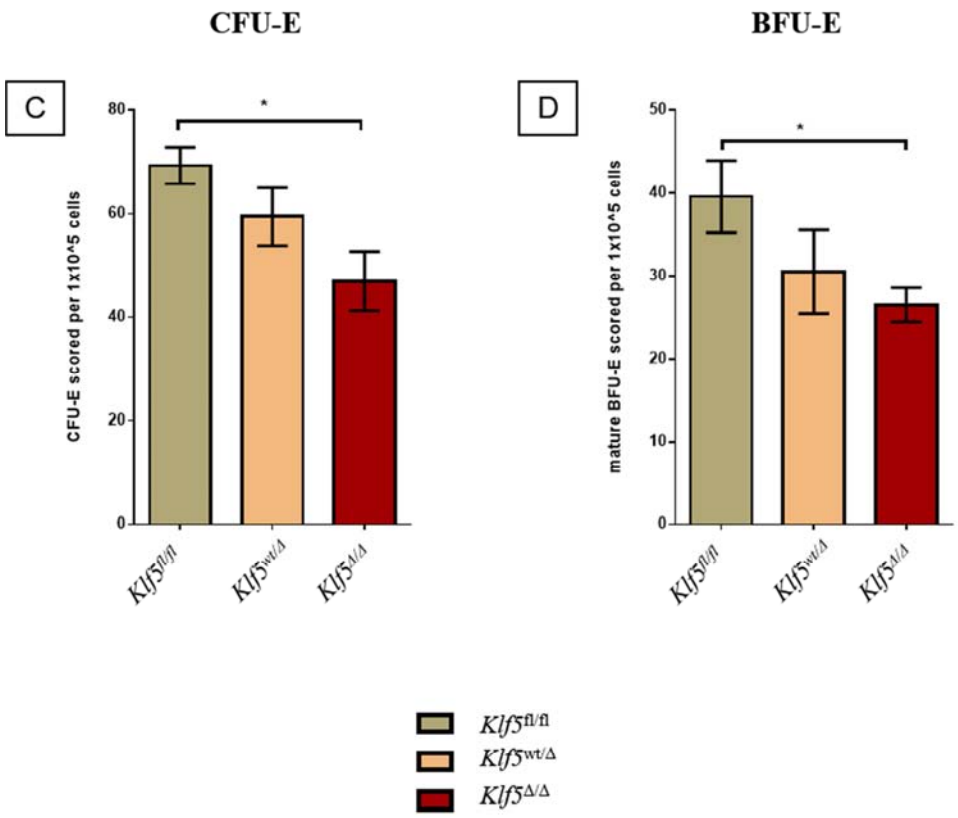

Figure 4.22: Quantification of CFU-E and BFU-E in bone marrow at 9 months of age using colony forming assay

1 x 10^5 whole bone marrow cells from 9 month old mice were seeded in methylcellulose containing EPO without other cytokines and cultured for 5 days. The CFU-E colonies were scored on day 3 while the mature BFU-E colonies were scored on day 5. Mean and SEM are shown. n=5 for *Klf5*$^{fl/fl}$, n=4 for *Klf5*$^{wt/\Delta}$ and n=4 for *Klf5*$^{\Delta/\Delta}$ mice. The p-value was obtained from t-tests conducted between *Klf5*$^{fl/fl}$ and *Klf5*$^{\Delta/\Delta}$ group using Graphpad Prism. *Significantly different between *Klf5*$^{fl/fl}$ and *Klf5*$^{\Delta/\Delta}$ mice ($P< 0.05$).

Previous work from our group has suggested that *Klf5* has a functional role during granulopoiesis [28], and *Klf5* has also been found to be down-regulated in AML patient samples compared to normal haemopoietic populations [28]. A previous study by *Humbert et al.* also suggested *Klf5* involvement during granulopoiesis [33]. Thus, we conducted further analyses on PB and BM using flow cytometry to quantitate different haemopoietic progenitor and mature cell populations. Interestingly, we observed a significant decrease of mature neutrophils in PB and BM of $Klf5^{\Delta/\Delta}$ mice at 3 and 9 months of age. In addition, BM data showed a decrease in neutrophils in $Klf5^{\Delta/\Delta}$ mice at 12 months age. Together, these results are consistent with the hypothesis that *Klf5* has a functional role in the granulocyte lineage.

From flow cytometry analysis, the $CD3e^{+}$ T-cell percentage was consistently increased in PB and BM of $Klf5^{\Delta/\Delta}$ mice compared to age-matched $Klf5^{fl/fl}$ mice suggesting that Klf5 may have a role in regulation of lymphocyte production. The $B220^{+}$ B-cell percentage determined by flow cytometry was found to be inconsistent in PB and BM possibly due to the low frequency and small group size. Interestingly, our lab has previously shown that *Klf5* expression is down-regulated in T-cells, B-cells and NK cells from mouse (refer Figure 1.4: Expression of KLF family members in mouse and human haemopoietic lineages). This is also observed in the HemaExplorer gene expression database where *KLF5* expression in T-cells is relatively low compared to myeloid and HSC (**Appendix I**) [327]. Consistent with this initial finding, a study conducted in cell lines and primary tissues showed that *Klf5* was expressed in pro-T-cells but not in the more mature T-cells [277]. It has also been suggested that Klf5 has a role in regulating T-cell receptor expression and that *Klf5* expression is high in RAG-2–deficient thymus and low in healthy thymus

and bone marrow [277]. In addition, a number of independent studies have shown the involvement of other Klf family members during mature lymphoid cell development [74, 86, 108, 164-168]. Thus Klf5 may cooperate with other Klf family members to control lymphocyte production.

We also performed flow cytometry analysis on the stem and progenitor cell compartments to assess if there were any changes at earlier stages of myeloid cell formation. The flow cytometry analysis of the BM myelo-erythroid progenitor compartment revealed no gross differences in progenitor populations consistent with Klf5 being functionally important at the later stages during myelopoiesis. Interestingly, we found that the HSPC fraction defined by c-Kit^{+}, Lin^{-}, IL7Rα^{-}, Sca-1^{+} was reduced in the BM of *Klf5*$^{\Delta/\Delta}$ mice compared to *Klf5*$^{fl/fl}$ mice. However, none of the primitive stem cell compartments including LT-HSC, ST-HSC and MPP revealed significant differences between genotypes possibly due to small sample sizes.

To further understand the role of *Klf5* in haemopoiesis, we conducted CFU and serial replating assays. We observed a significant decrease in replating potential for the *Klf5*$^{\Delta/\Delta}$ bone marrow compared to *Klf5*$^{fl/fl}$ controls, with a dramatic decrease in the third serial plating of 9 months old mice. This result suggests that progenitor cells from knockout mice have a reduced self-renewal capability. On the other hand, *Klf5*$^{\Delta/\Delta}$ mice have decreased CFU-M and CFU-G frequency in BM compared to age-matched *Klf5*$^{fl/fl}$ mice. This result is consistent with a role for Klf5 in committed myeloid progenitors. Interestingly, we did not see a lineage bias in the type of colonies formed which may have been predicted based on other finding of fewer neutrophils in PB and BM by flow cytometry. However, this may be reflective of the difference of cells that differentiate *in vivo* compared to an *in vitro* model system.

The CBC data obtained from 3 month old mice showed decreased RBC counts in *Klf5*$^{\Delta/\Delta}$ mice compared to control mice. At 3 months, the haematocrit and haemoglobin levels were also lower in the *Klf5*$^{\Delta/\Delta}$ mice compared to control mice. In addition, flow cytometry results revealed a decrease of the erythroid progenitor compartment in the *Klf5*$^{\Delta/\Delta}$ mice, compared to aged-matched control mice at 9 months. This finding has been confirmed with *in vitro* CFU assays which show that CFU-E and BFU-E are less frequent for *Klf5*$^{\Delta/\Delta}$ bone marrow compared to *Klf5*$^{fl/fl}$ controls. Initially, Erythroid Krüppel-like factor (EKLF/KLF1) was known to have a significant role in erythropoiesis by specifically binding to CAACC elements [170]. EKLF stimulates *β-globin* gene expression and facilitates the switch from the foetal γ-globin to the adult β-globin [171]. However, later studies have shown that, not only Klf1, but also Klf2, Klf3 and Klf4 were also important in regulating erythroid maturation [90, 173-175, 177-179]. KLF family members share three C2H2 zinc finger DNA binding domains. Although there is no direct evidence of *Klf5* involvement in regulating erythropoiesis, the sequence analysis has shown that *KLF5* can bind and transactivate the same CACCC promoter element which is known to regulate the *γ-globin* gene [180]. In addition, an independent study has shown that KLF5 has a similar domain to transactivation domain 2 of KLF1 (EKLFTAD2). In fact this region has been shown to interact with CBP/p300 [328]. Thus, Klf5 may contribute to erythropoiesis through a complementary function to Klf1. This may be particularly important in younger animals given that reduced red blood cell, haematocrit and haemoglobin was observed at 3 months for *Klf5*$^{\Delta/\Delta}$ animals.

Chapter 5: Extended analysis on the effect of knocking out the Klf5 gene in the haemopoietic system

5.1 Introduction

The studies described in the previous chapter demonstrate that Klf5 has important functions in haemopoiesis and are consistent with initial studies which showed that knockdown of *Klf5* gene expression reduces neutrophil differentiation in response to cytokine simulation [28]. This is strongly supported by another independent study done by *Humbert et al.* which showed a function for Klf5 in regulating neutrophil development [33]. In the previous chapter, we demonstrated that $Klf5^{\Delta/\Delta}$ mice have fewer neutrophils compared to wildtype controls establishing a role for *Klf5* as an inducer of granulocyte differentiation *in vivo*. Thus, in this chapter we aimed to extend the phenotypic analysis of the *Klf5*-KO model to look at other haemopoietic organs and to look specifically at eosinophils.

Haemopoietic stem cells (HSC) can be found at low levels in extramedullary tissues such as the spleen and liver throughout adult life [329], but during haemopoietic stress, HSC are mobilised to these tissues [330, 331]. *Ishikawa et. al.* reported that *Klf5* plays an important role in HSC retention and adhesion in the bone marrow [275], suggesting that changes to Klf5 levels may affect HSC mobilisation. Independent studies have shown that *Klf5* is a key regulator of cellular migration in non-haemopoietic tissue [210, 219, 332]. For example in primary esophageal epithelial cells, *Klf5* stimulates expression of the pro-migratory protein Integrin-linked kinase, ILK [219]. *Klf5* has also been implicated in the metastasis of prostate cancer cells to bone tissue by up-regulating the expression of cell-surface chemokine receptor CXCR4 [210]. In addition, *Klf5* also up-regulates expression of Matrix

metallopeptidase 9 resulting in degradation of extracellular matrix in skeletal muscle cells and enhancing migratory activity [333]. Together, these observations raise the question of whether loss of Klf5 in HSC will lead to HSC mobilisation to other haemopoietic organs, especially spleen. Previous studies conducted on *Klf5* in haemopoiesis did not look closely in spleen. In this chapter, we analysed changes in splenic haemopoiesis from *Klf5*$^{\Delta/\Delta}$ mice using flow cytometry and CFU assays to identify the differences compared to the control littermates.

Given the changes observed in the levels of neutrophils (as discussed in Chapter 4), we also extended our analysis of steady-state haemopoiesis to look at eosinophil production in our Klf5-KO model. Under normal conditions, numbers of eosinophils are very low but increase considerably during a parasitic infection or allergic reaction [334]. In this chapter we assessed eosinophil production using eosinophil-specific lineage markers in peripheral blood (PB) and bone marrow (BM), followed by measuring eosinophil infiltration in the lung tissue of Klf5-KO mice compared to wildtype controls.

5.2 Results

5.2.1 Analysis of the extramedullary haemopoietic organs

We first conducted necroscopy analysis on spleen and liver of *Klf5*$^{\Delta/\Delta}$ mice and littermate controls. From visual inspection, there were no obvious differences in the appearance of the liver (data not shown). Interestingly, we observed an enlarged spleen size for *Klf5*$^{\Delta/\Delta}$ mice compared to *Klf5*$^{fl/fl}$ mice (Figure 5.1-A). There was no difference in the spleen colour or appearance of knockout spleens compared to the wildtype controls (Figure 5.1-A). Interestingly, the spleen weight of *Klf5*$^{\Delta/\Delta}$ mice

was significantly higher compared to *Klf5*$^{fl/fl}$ mice ($p<0.01$) (Figure 5.1-B). The *Klf5*$^{wt/\Delta}$ spleens were also larger than spleens from *Klf5*$^{fl/fl}$ mice ($p<0.01$) (Figure 5.1-B). This was also consistent with the spleen weight at 9 and 12 months, where the *Klf5*$^{\Delta/\Delta}$ mice have larger spleens compared to *Klf5*$^{fl/fl}$ mice ($p<0.05$) (Figure 5.1-B). Interestingly, when the spleen weight is normalised to body weight, we found that the ratio of spleen size was significantly higher in the *Klf5*$^{\Delta/\Delta}$ and *Klf5*$^{wt/\Delta}$ mice compared to *Klf5*$^{fl/fl}$ mice at 9 and 12 months of age (Figure 5.1-**C**, also refer to Figure 3.11 for body weight comparison).

Spleen histopathology was then evaluated using Haematoxylin and Eosin (HE) and myeloperoxidase (MPO) staining (tissue dissection and staining procedures were performed by Jim Manavis and John Finnie, SA Pathology). These analyses revealed no gross abnormalities in the spleen of *Klf5*$^{\Delta/\Delta}$ mice when compared with *Klf5*$^{fl/fl}$ mice (Figure 5.2 and Figure 5.3). As observed in the MPO staining of spleen (Figure 5.2 and Figure 5.3), spleen granulopoiesis is more restricted and mainly observed around traberculae projecting from the capsule [335]. However, there was no gross difference observed in the MPO stained dissected spleens isolated from *Klf5*$^{\Delta/\Delta}$ mice compared with *Klf5*$^{fl/fl}$ mice (Figure 5.2 and Figure 5.3). More histopathology pictures are shown in the **Appendices J** and **K**.

5.2.2 Characterisation of the cellular spleen phenotype of *Klf5*$^{\Delta/\Delta}$ mice

5.2.2.1 Cell number and colony assay analysis on spleen

We next investigated whether any specific cell types were contributing to the observed splenomegaly in the *Klf5*$^{\Delta/\Delta}$ mice. Nucleated cell counts for each genotype

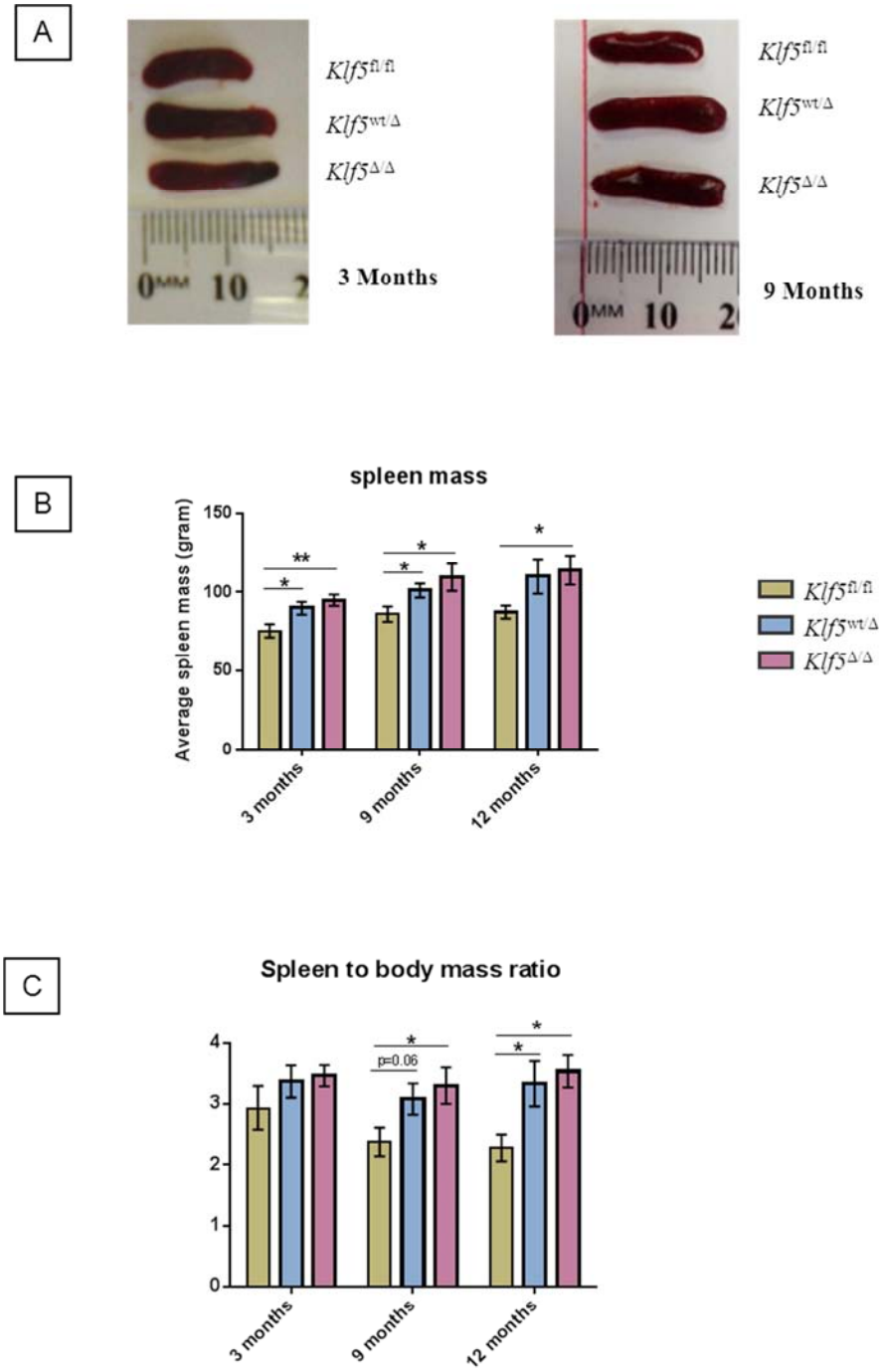

Figure 5.1: Analysis of spleen size from 3, 9 and 12 month old mice

(A) Representative spleens from 3 and 9 month old mice. **(B)** Average spleen weights from 3, 9 and 12 months old mice (mean ± SEM). **(C)** Average of spleen to body weight ratio from of 3, 9 and 12 months old mice (mean ± SEM). P-values were obtained from t-test conducted between $Klf5^{fl/fl}$ and $Klf5^{\Delta/\Delta}$ group using Graphpad Prism. Significantly different between $Klf5^{fl/fl}$ and $Klf5^{\Delta/\Delta}$ mice *($P< 0.05$) and **($P< 0.01$). Results obtained from n=5 for $Klf5^{fl/fl}$, n=4 for $Klf5^{wt/\Delta}$ and n= 7 for $Klf5^{\Delta/\Delta}$ mice at 3 months, n=7 for $Klf5^{fl/fl}$, n=7 for $Klf5^{wt/\Delta}$ and n=8 for $Klf5^{\Delta/\Delta}$ mice at 9 months and n=5 for $Klf5^{fl/fl}$, n=6 for $Klf5^{wt/\Delta}$ and n=7 for $Klf5^{\Delta/\Delta}$ mice at 12 months.

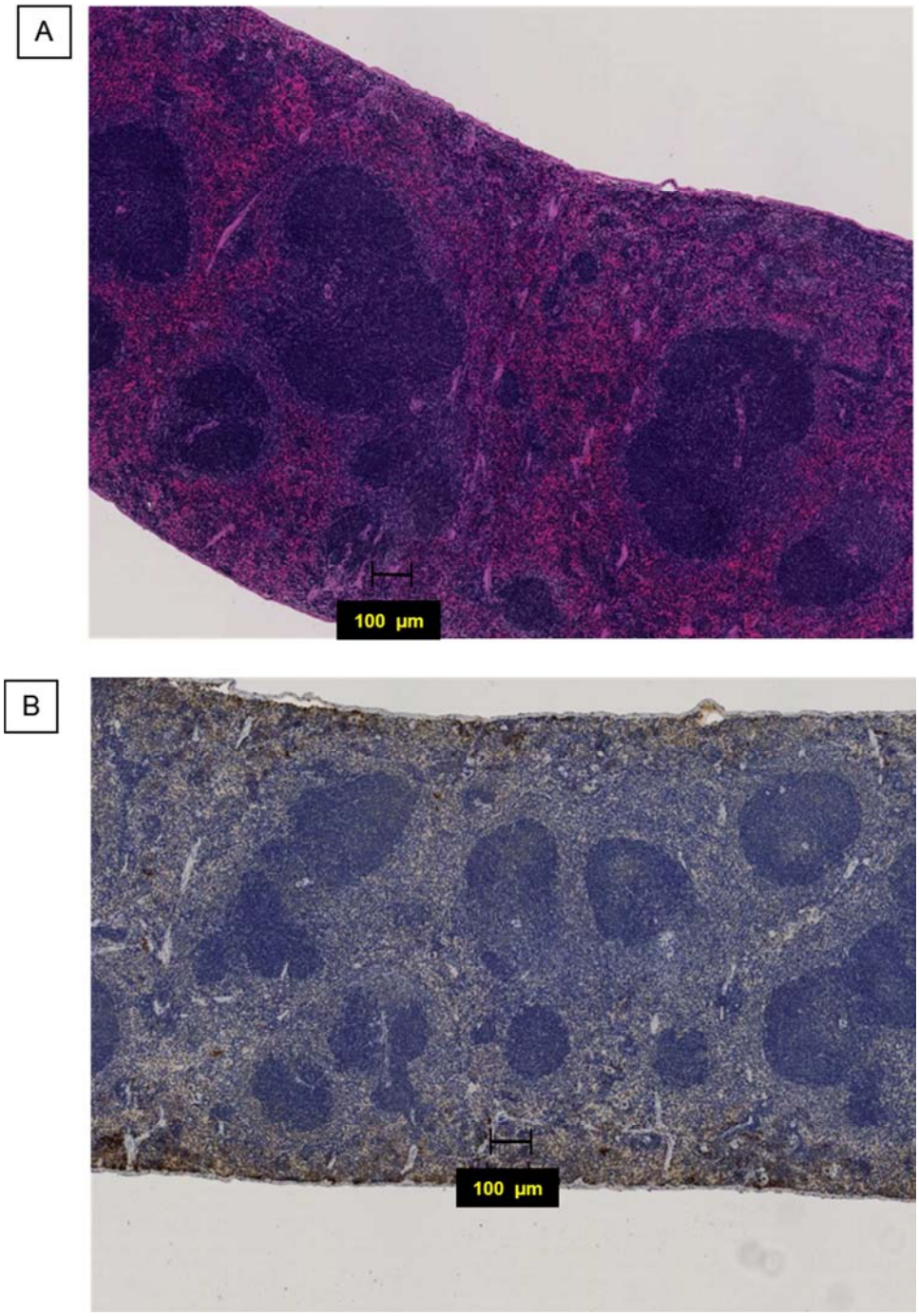

Figure 5.2(i): Representative spleen morphology of *Klf5*-flox mice at 3 months

Mouse spleens from an age-matched control littermates was sectioned and stained with **A)** H&E and **B)** anti-MPO antibody. Images captured at 5X using Nanozoomer DP.

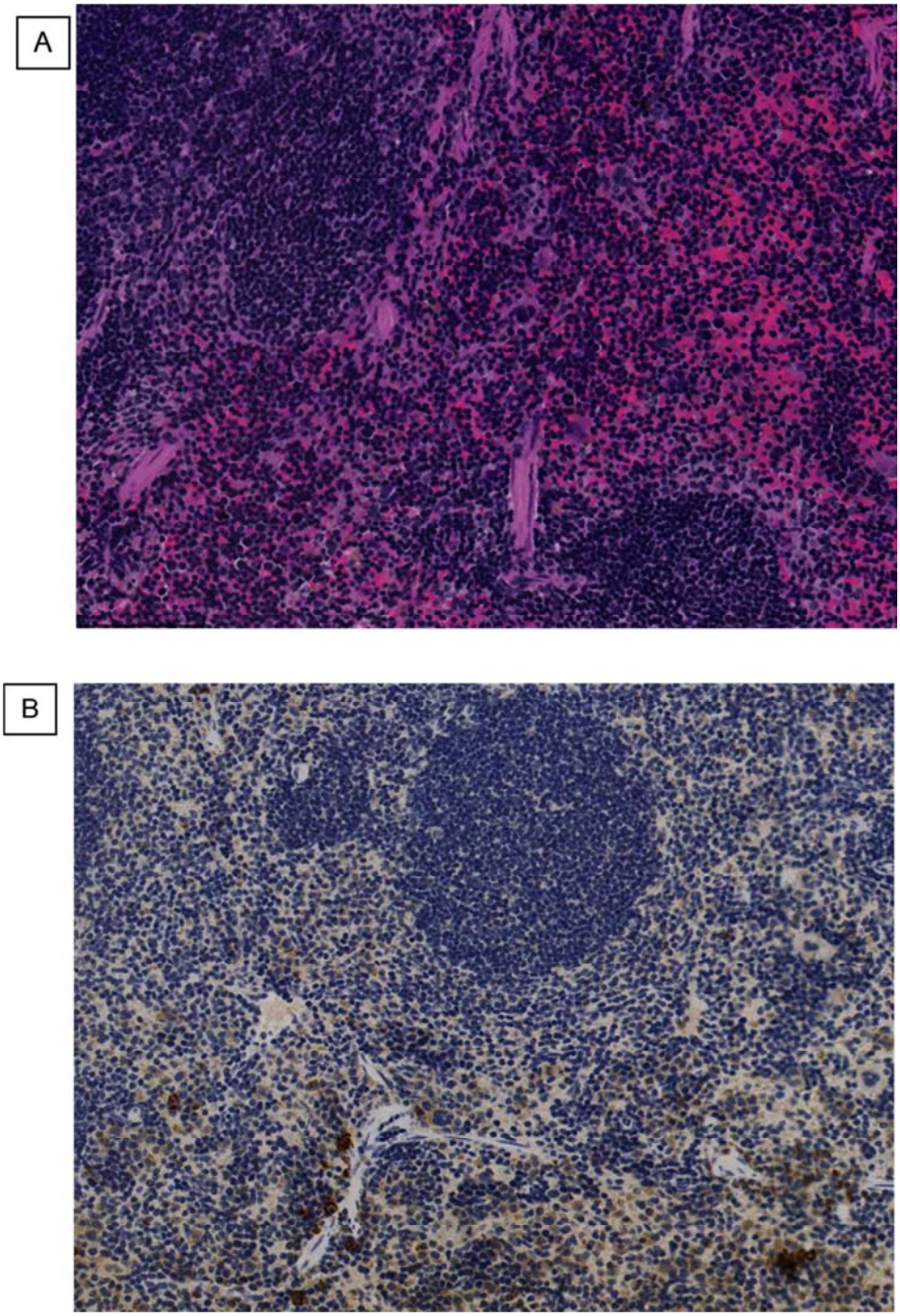

Figure 5.2(ii): Representative spleen morphology of *Klf5*-flox mice at 3 months

Mouse spleens from an aged matched control littermatse were sectioned and stained with **A)** H&E and **B)** anti-MPO antibody. Images captured at 20X using Nanozoomer DP.

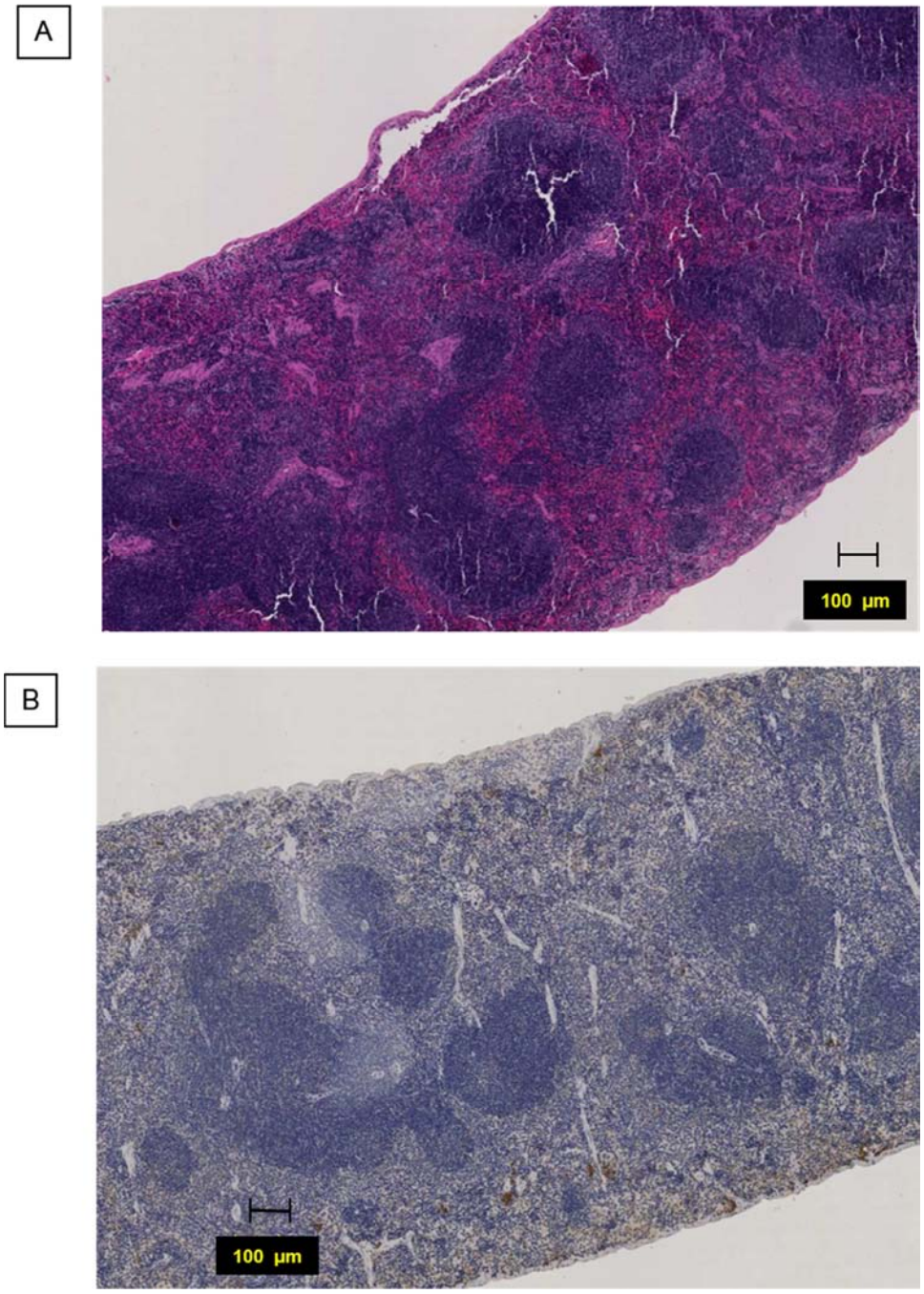

Figure 5.3(i): Representative spleen morphology of *Klf5*$^{\Delta/\Delta}$ mice at 3 months

Mouse spleens from an age-matched control littermates was sectioned and stained with **A)** H&E and **B)** anti-MPO antibody. Images captured at 5X using Nanozoomer DP.

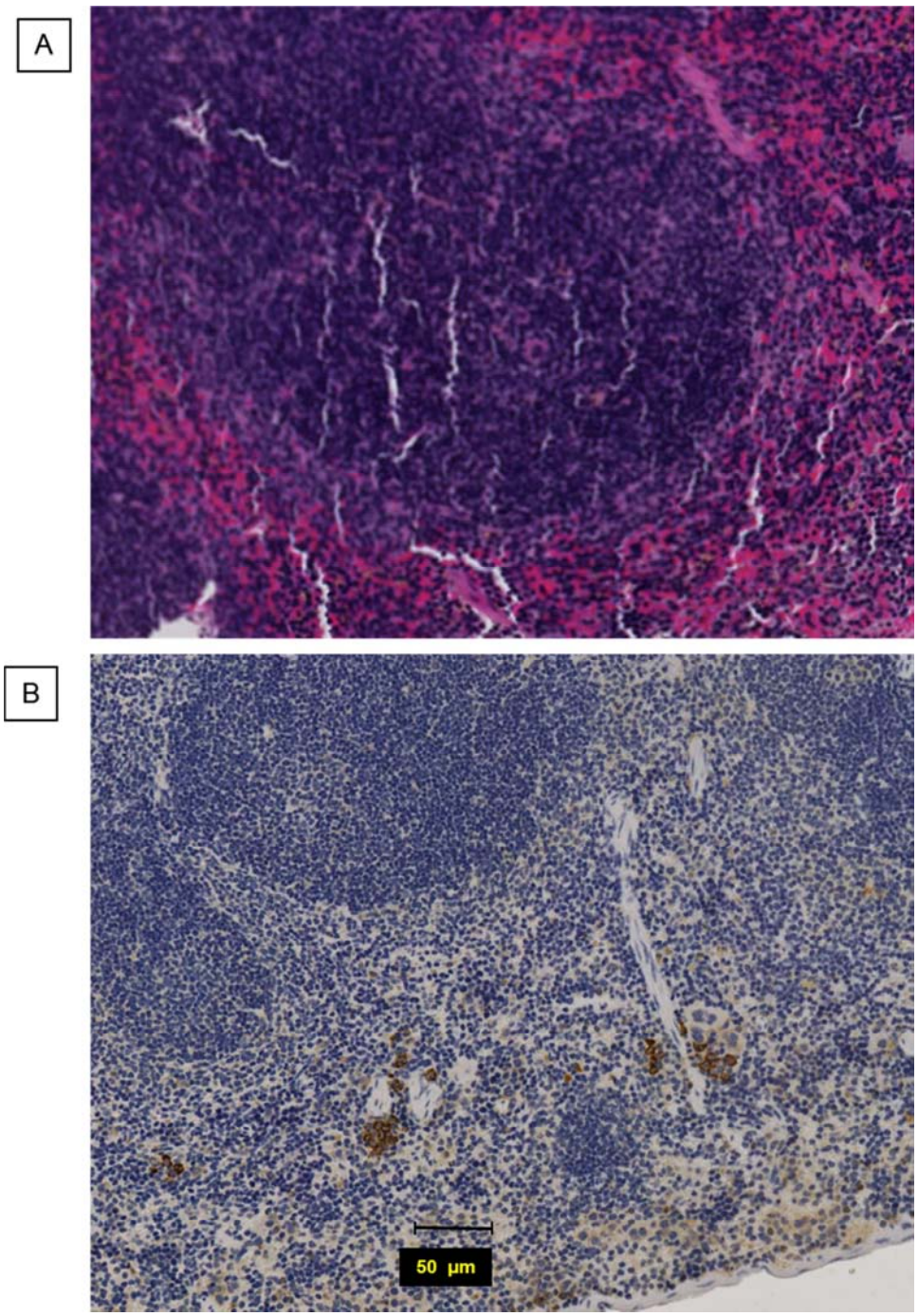

Figure 5.3(ii): Representative spleen morphology of *Klf5*$^{\Delta/\Delta}$ mice at 3 months

Mouse spleens from an age-matched control littermates was sectioned and stained with **A)** H&E and **B)** anti-MPO antibody. Images captured at 20X using Nanozoomer DP.

showed that the *Klf5*$^{\Delta/\Delta}$ mice displayed increased splenic cellularity compared to *Klf5*$^{fl/fl}$ mice (Figure 5.4) consistent with increased size. We then assayed myelo-erythroid progenitor cells using colony assays. We observed a significant increase in the frequencies of colonies scored from 9 and 12 month old *Klf5*$^{\Delta/\Delta}$ mice compared to *Klf5*$^{fl/fl}$ mice (Figure 5.5-A). In addition to the colonies scored, we were interested in determining the total CFU colony scored. Interestingly, there was a 2-fold increase in the *Klf5*$^{\Delta/\Delta}$ mice compared to *Klf5*$^{fl/fl}$ mice at 9 months and a 3- fold increase at 12 months ($p<0.05$ and $p<0.01$ respectively) (Figure 5.5-B). However this result was not due to any individual type of colony since all myeloid colony types (CFU-G, CFU-M and CFU-GM) were scored higher in *Klf5*$^{\Delta/\Delta}$ mice compared to *Klf5*$^{fl/fl}$ mice (Figure 5.6).

5.2.2.2 Flow cytometry analysis on spleen cells

To further characterise the haemopoietic cell types that may contribute to the increased spleen size in *Klf5*$^{\Delta/\Delta}$ mice, we used flow cytometry analysis to determine different cell populations present in the spleen of *Klf5*$^{\Delta/\Delta}$ mice and wildtype controls.

To evaluate the mature haemopoietic cell types, spleen cells were stained with TER119, CD45.2, GR-1, Mac-1, B220, CD3ε and Siglec-F antibodies. The gating strategies used are as described earlier in Chapter 4 and the representative gating plots for flow cytometry on mature cells type from spleen were showed in the **Appendix L**. As shown in Figure 5.7 and Figure 5.8, there were no significant differences observed in any of the specific mature lymphoid or myeloid cell types between the different genotypes.

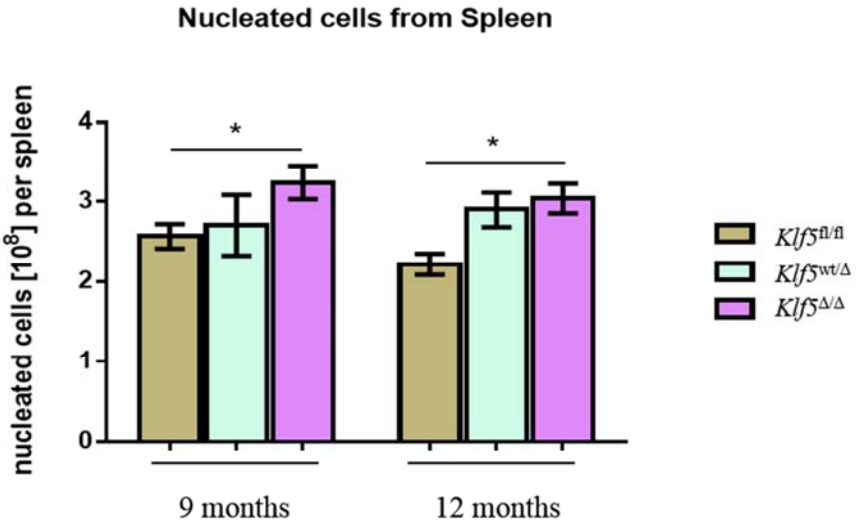

Figure 5.4: Average nucleated cell counts from spleens of 9 and 12 month old mice

Bar chart represent data by comparing nucleated cells count in between genotype at 9 and 12 months. Mean and SEM are shown. Spleens were mashed in the petri dish and passed through the cell strainer to obtain single-cell suspensions. P-value obtained from t-test conducted between genotype or age group using Graphpad Prism. Significantly different between age *($P< 0.05$) and **($P< 0.01$). Results obtained from n=7 for $Klf5^{fl/fl}$, n=7 for $Klf5^{wt/\Delta}$ and n=8 for $Klf5^{\Delta/\Delta}$ mice at 3 months, and n=5 for $Klf5^{fl/fl}$, n=6 for $Klf5^{wt/\Delta}$ and n=7 for $Klf5^{\Delta/\Delta}$ mice at 9 months.

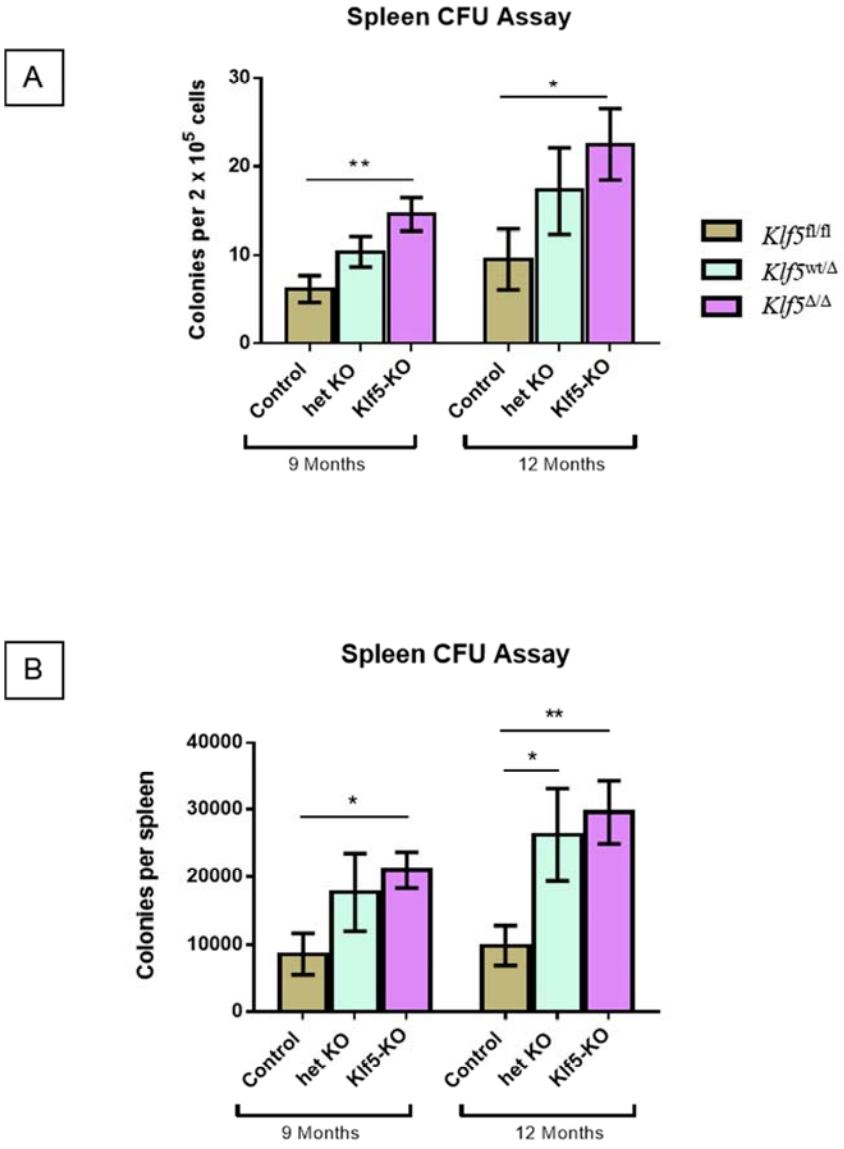

Figure 5.5: Enumeration of myelo-erythoroid colonies from spleen cells of *Klf5*-KO mice at 9 and 12 months old

A) The bar chart show the total colony numbers scored from both age groups. **B)** The bar chart shows the absolute numbers obtained from the CFU assay. Colonies were scored from independent triplicate after 8 days 2 x 10^5 of spleen cells were seeded in methylcellulose containing SCF, IL3, IL6, EPO and GM-CSF. P-values were obtained from t-tests conducted between each genotype group using Graphpad Prism. Significantly different between *Klf5*$^{fl/fl}$ and *Klf5*$^{\Delta/\Delta}$ mice *($P< 0.05$) and **($P< 0.01$). Results obtained from n=6 for *Klf5*$^{fl/fl}$, n=5 for *Klf5*$^{wt/\Delta}$ and n=7 for *Klf5*$^{\Delta/\Delta}$ mice at 3 months, and n=6 for *Klf5*$^{fl/fl}$, n=4 for *Klf5*$^{wt/\Delta}$ and n=6 for *Klf5*$^{\Delta/\Delta}$ mice at 9 months.

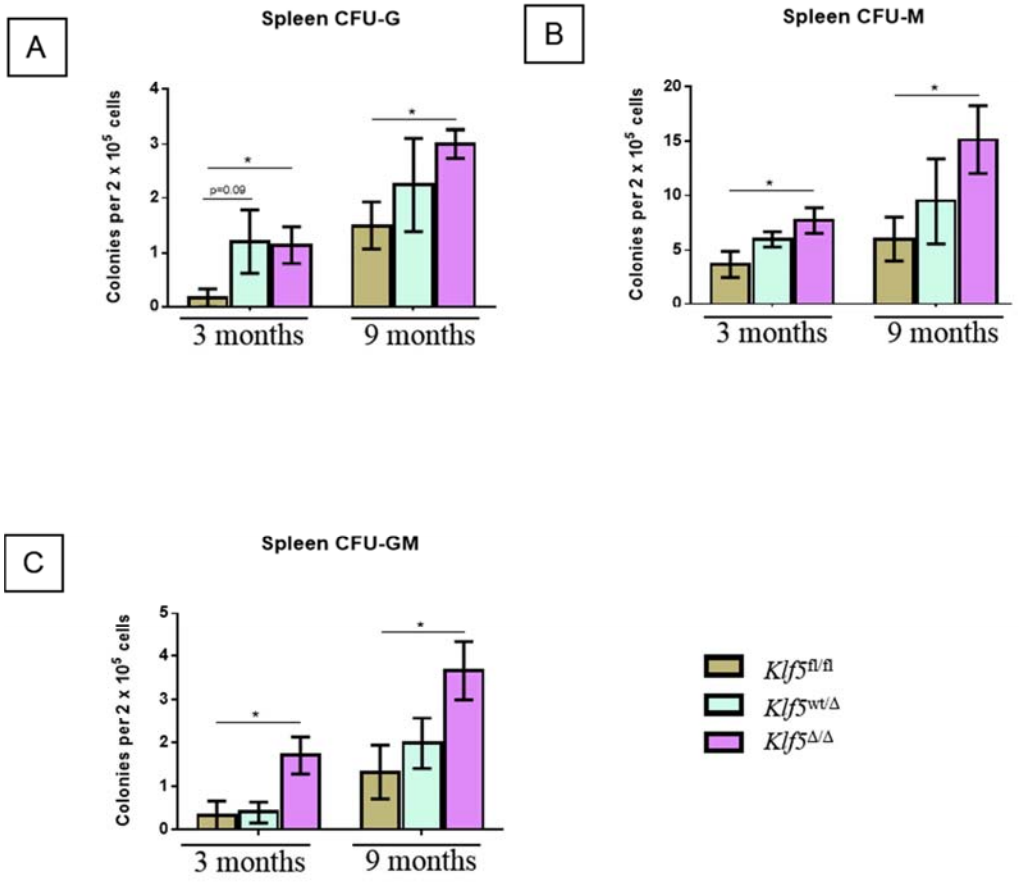

Figure 5.6: Individual types of colonies scored from spleen CFU assay at 3 and 9 months of age

A) The average of colony-forming unit-granulocyte (CFU-G) colonies. **(B)** The average of colony-forming unit-macrophage (CFU-M) colonies. **(C)** The average of colony-forming unit-granulocyte-macrophage (CFU-M) colonies. Colonies were scored from independent triplicate after 8 days 2 x 10^5 of spleen cells were seeded in methylcellulose containing SCF, IL3, IL6, EPO and GM-CSF. Mean and SEM are shown. P-values were obtained from t-test conducted between each genotype group using Graphpad Prism. Significantly different between *Klf5*$^{fl/fl}$ and *Klf5*$^{\Delta/\Delta}$ mice *($P<$ 0.05). Results obtained from n=6 for *Klf5*$^{fl/fl}$, n=5 for *Klf5*$^{wt/\Delta}$ and n=7 for *Klf5*$^{\Delta/\Delta}$ mice at 3 months, and n=6 for *Klf5*$^{fl/fl}$, n=4 for *Klf5*$^{wt/\Delta}$ and n=6 for *Klf5*$^{\Delta/\Delta}$ mice at 9 months.

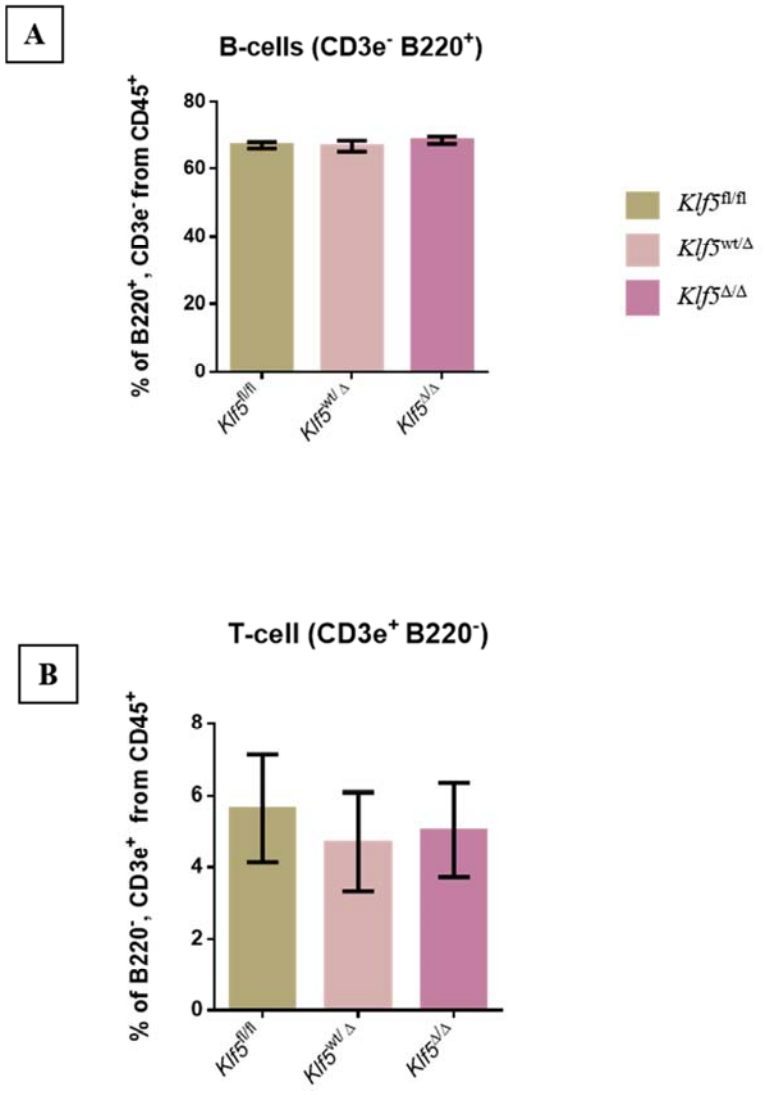

Figure 5.7: Characterisation of mature lymphoid cells in the spleen at 9 months using flow cytometry

Each graph represents the percentage of cell population determined by the specific cell surface marker from the spleen of 9 month old mice. Each bar shown is mean value plus or minus SEM of **(A)** percentage of B-cells ($B220^{+}CD3\varepsilon^{-}$ from $CD45^{+}$, $TER119^{-}$) and **(B)** percentage of T-cells ($B220^{-}CD3\varepsilon^{+}$ from $CD45^{+}$, $TER119^{-}$) respectively. n=6 for $Klf5^{fl/fl}$, n=6 for $Klf5^{wt/\Delta}$ and n=7 for $Klf5^{\Delta/\Delta}$ mice.

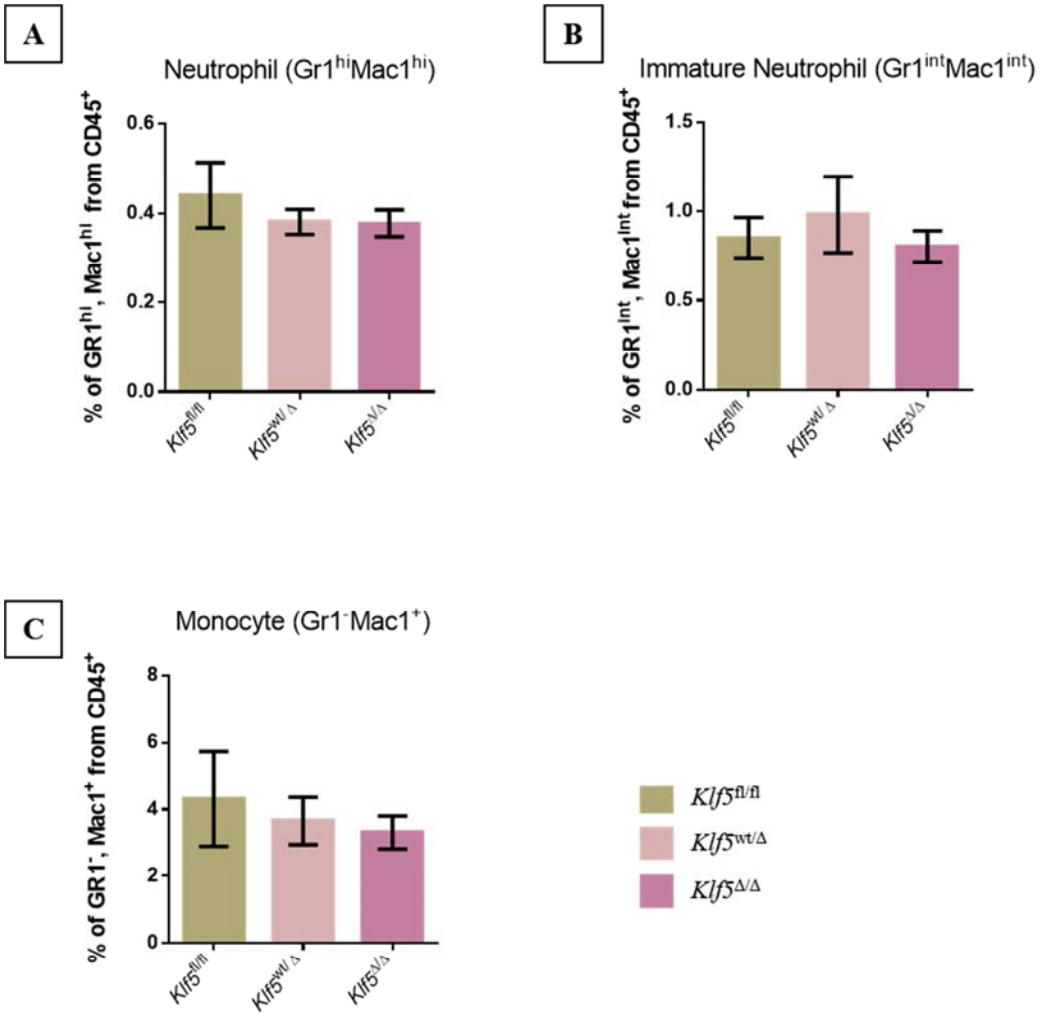

Figure 5.8: Characterisation of mature myeloid cells in the spleen at 9 months using flow cytometry

Each graph represents the percentage of specific cell types determined by cell surface markers from the spleen of 9 month old mice. Each bar shown is mean values plus or minus SEM for **(A)** neutrophils **(**$Gr1^{hi}Mac1^{hi}$ cells from $CD45^{+}$, $TER119^{-}$), **(B)** immature neutrophils ($Gr1^{int}Mac1^{int}$ cells from $CD45^{+}$, $TER119^{-}$) and **(C)** monocytes ($Gr1^{-}Mac1^{+}$cells from $CD45^{+}$, $TER119^{-}$). Data were generated from n=6 for $Klf5^{fl/fl}$, n=6 for $Klf5^{wt/\Delta}$ and n=7 for $Klf5^{\Delta/\Delta}$ mice.

To further assess the myeloid progenitor compartment in the spleen, spleen cells were also stained with multiple cell surface markers (CD41, CD105, CD150, c-Kit, Sca-1, FcγRII/III and lineage specific antibodies; Mac-1, Gr-1, B220, CD3ε and TER119). Similar gating strategies to those used in Chapter 4 for myeloid progenitor analysis were used for this analysis. A representative of the gating plot for myeloid progenitor analysis in the spleen is attached in the **Appendix M**. In this chapter, data is presented as the absolute cell numbers for each cell type per spleen. From the analysis, we found that the LSK compartment was significantly increased in spleens from the *Klf5*$^{\Delta/\Delta}$ mice compared to *Klf5*$^{fl/fl}$ mice (Figure 5.9). Interestingly, we did not observe any significant changes for the committed myeloid progenitor cell populations between knockout and control groups (Figure 5.10). To further characterise the haemopoietic stem cell subsets we analysed 12 month old mice and used multi-colour flow cytometry to focus on the more primitive cell compartment. The methods used for this analysis were the same as those detailed in Section 4.2.2.3 of chapter 4. Again, antibodies used for staining were anti- CD48, Flt3, CD150, c-Kit, Sca-1, IL7Rα and lineage specific antibodies; Mac-1, Gr-1, B220, CD3e and TER119. A representative plot and gating strategy used for this flow analysis is shown in the **Appendix N**. Interestingly, as shown in Figure 5.11, the number of HSPC, MPP and ST-HSC in the *Klf5*$^{\Delta/\Delta}$ mice were significantly higher than in *Klf5*$^{fl/fl}$ mice. Data for long-term HSC (LT-HSC) is not shown as frequency of detection was below 1% and is not reliable for analysis. Together, these results are consistent with the CFU assay results (Section 5.2.2.1) which showed an increase in the CFU frequency and number in spleens from *Klf5*$^{\Delta/\Delta}$ mice but without a bias in the output of more committed myeloid cell types.

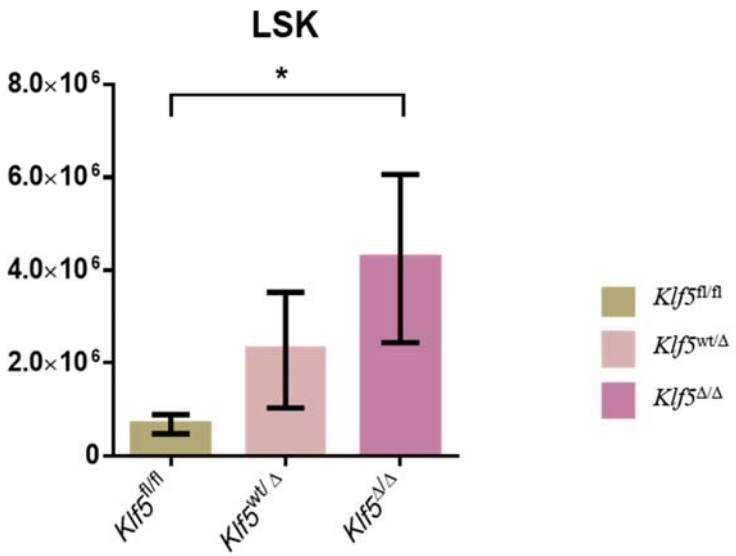

Figure 5.9: Characterisation of LSK in the spleen at 9 months using flow cytometry

LSK population was defined by c-Kit^{+}, Lin^{-}, Sca-1^{+} cell surface markers. P-value obtained from t-test conducted between each genotype group using Graphpad Prism. Significantly different between *Klf5*$^{fl/fl}$ and *Klf5*$^{\Delta/\Delta}$ mice *(P<0.05). The bar charts shown were mean values of cells per spleen plus or minus SEM percentage of n=6 for *Klf5*$^{fl/fl}$, n=6 for *Klf5*$^{wt/\Delta}$ and n=7 for *Klf5*$^{\Delta/\Delta}$ mice.

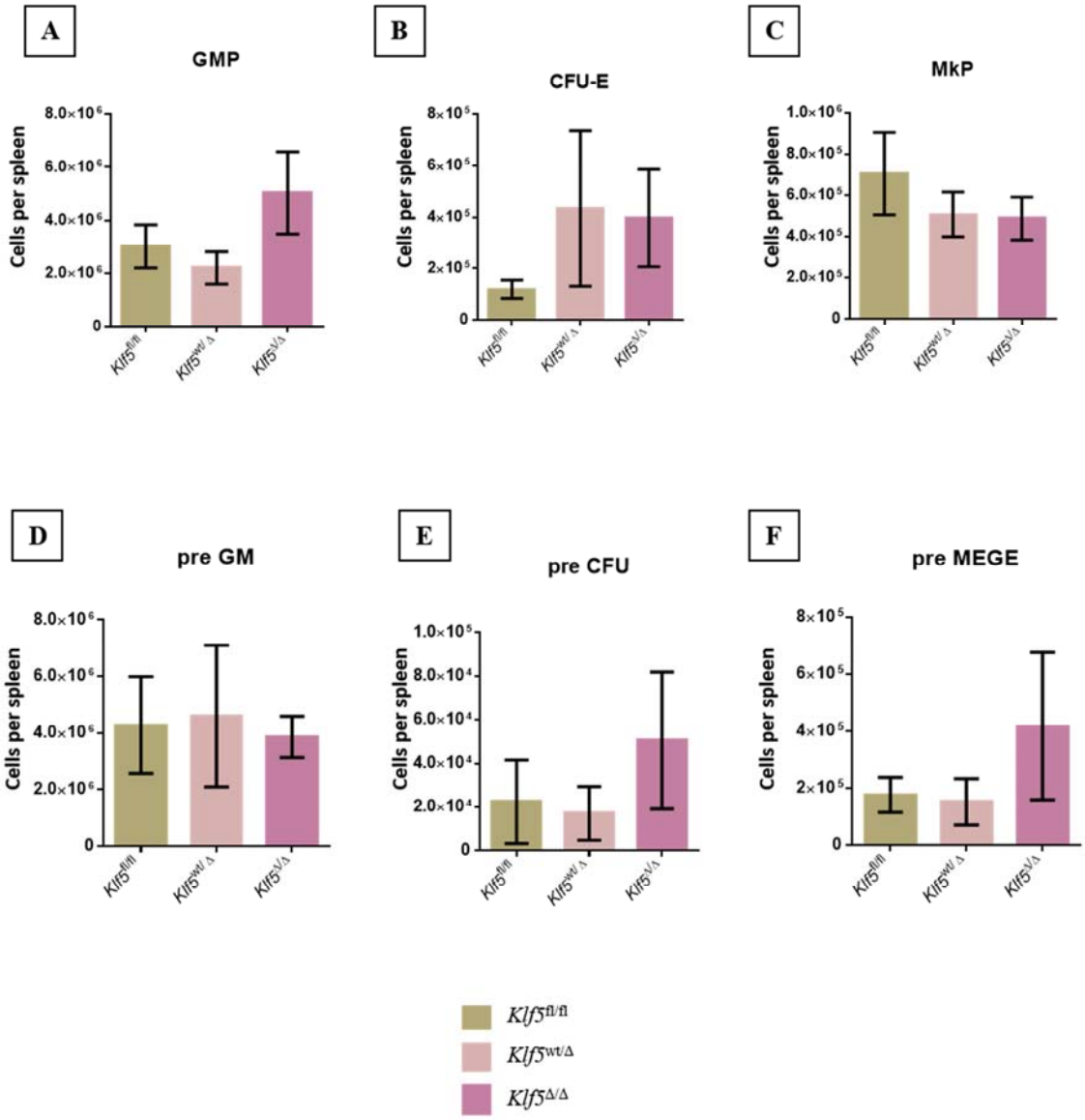

Figure 5.10: Characterisation of committed myeloid progenitors in spleen at 9 months using flow cytometry

The bar charts shown were cells per spleen plus or minus SEM from n=6 for *Klf5*$^{fl/fl}$, n=6 for *Klf5*$^{wt/\Delta}$ and n=7 for *Klf5*$^{\Delta/\Delta}$ mice for **(A)** granulocyte/macrophage progenitors (GMP), **(B)** erythroid progenitor (CFU-E), **(C)** megakaryocyte progenitors (MkP), **(D)** primitive granulocyte/macrophage progenitors (preGM), **(E)** early monopotent erythroid (preCFU-E), **(F)** the erythroid/megakaryocyte lineages progenitor (preMegE).

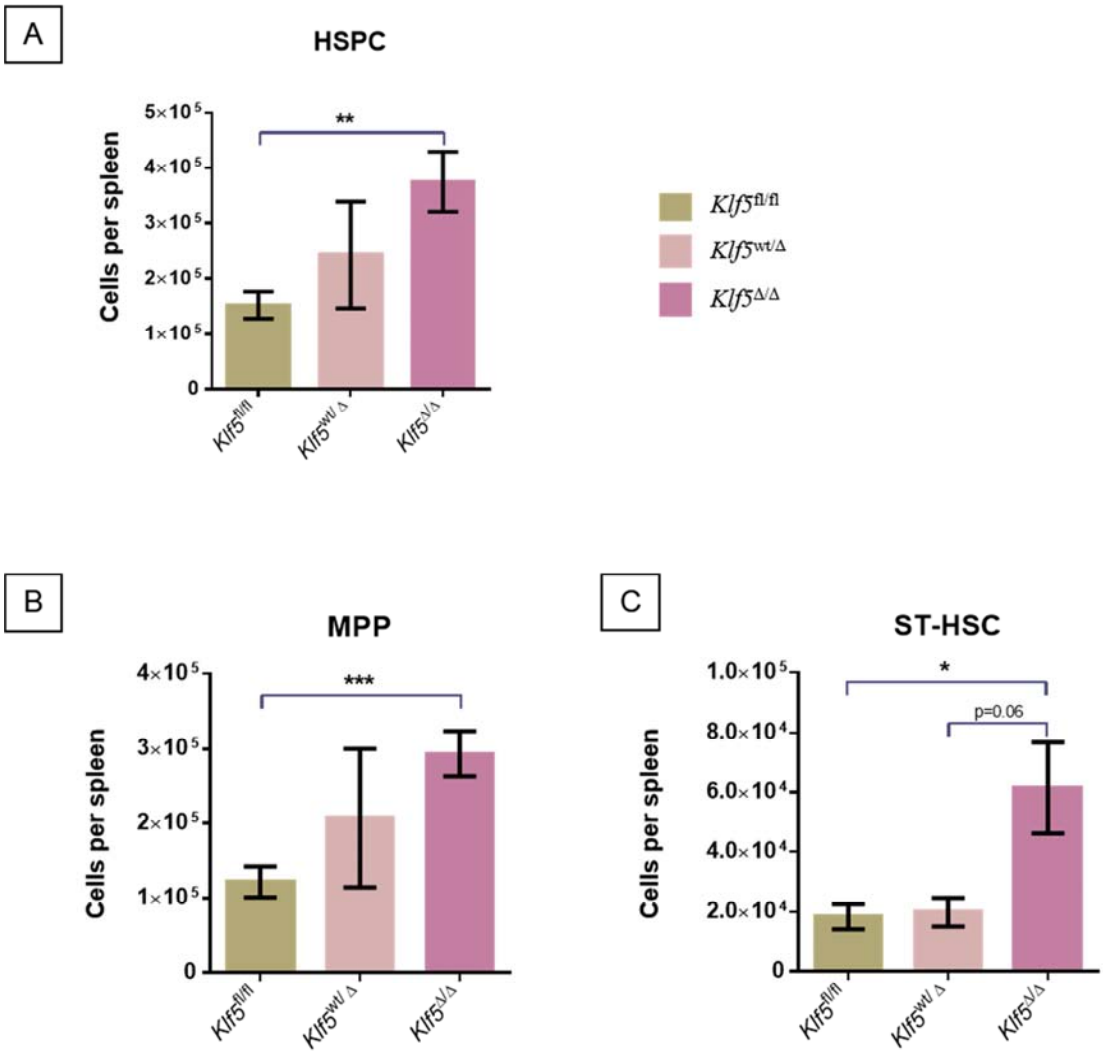

Figure 5.11: Characterisation of stem and progenitor cells in spleen at 12 months using flow cytometry

The bar charts shown were mean values plus or minus SEM of cells per spleen from n=7 for $Klf5^{fl/fl}$, n=5 for $Klf5^{wt/\Delta}$ and n=8 for $Klf5^{\Delta/\Delta}$ mice for the **(A)** HSPC population defined by c-Kit^{+}, Lin^{-}, IL7Rα^{-}, Sca-1^{+} cell surface markers, **(C)** multi-potent progenitor (MPP) and **(D)** short-term HSC (ST-HSC). P-values were obtained from t-tests conducted between different genotypes group using Graphpad Prism. Significantly different between $Klf5^{fl/fl}$ and $Klf5^{\Delta/\Delta}$ mice *(P<0.05), **(P<0.01) or ***(P<0.001).

5.2.3 Effect of *Klf5* knockout on the eosinophil compartment

5.2.3.1 Flow cytometry analysis to assess eosinophils in the peripheral blood and bone marrow of $Klf5^{\Delta/\Delta}$ mice.

We next used a flow cytometry based strategy to measure eosinophils in PB and BM. In this flow cytometry analysis, the antibodies used were TER119, CD45.2, Mac-1 and Siglec-F. Details of the methods used are described in Chapter 2, section 2.12.4. Mouse eosinophils in PB and BM are known to be positive for the Mac-1 and Siglec-F cell surface markers [336-338]. The specific detection protocol for eosinophils is summarised in Figure 5.12. Dead cells were first excluded based on the fluorogold positive stained population followed by selection based on the forward (FS) and side (SS) scatter. Next, we excluded the TER119-negative cells and a gate was set to capture the CD45-positive cell population. The percentage of Mac-1, Siglec-F double-positive cells was determined within this population. The Sig-F^+, Mac-1^+ double-positive gate was set to exclude the Sig-F^+, $Mac1^{hi}$ population which was identified as neutrophils based on the FS/SS character (shown in the **Appendix O**). From this analysis, we observed a small but a significant increase of the percentage of Sig-F^+, Mac-1^+ cells (eosinophils) in the $CD45^+$ gate in PB of 3 and 9 month old $Klf5^{\Delta/\Delta}$ mice compared to age-matched $Klf5^{fl/fl}$ mice ($p<0.05$) (Figure 5.13-A). Consistent results were also obtained from the analysis conducted on BM cells, where the Sig-F^+, Mac-1^+ cells (eosinophils) in the $CD45^+$ gate were also significantly increased in 3 and 9 months old $Klf5^{\Delta/\Delta}$ mice compared to age-matched $Klf5^{fl/fl}$ controls ($p<0.05$) (Figure 5.13-B).

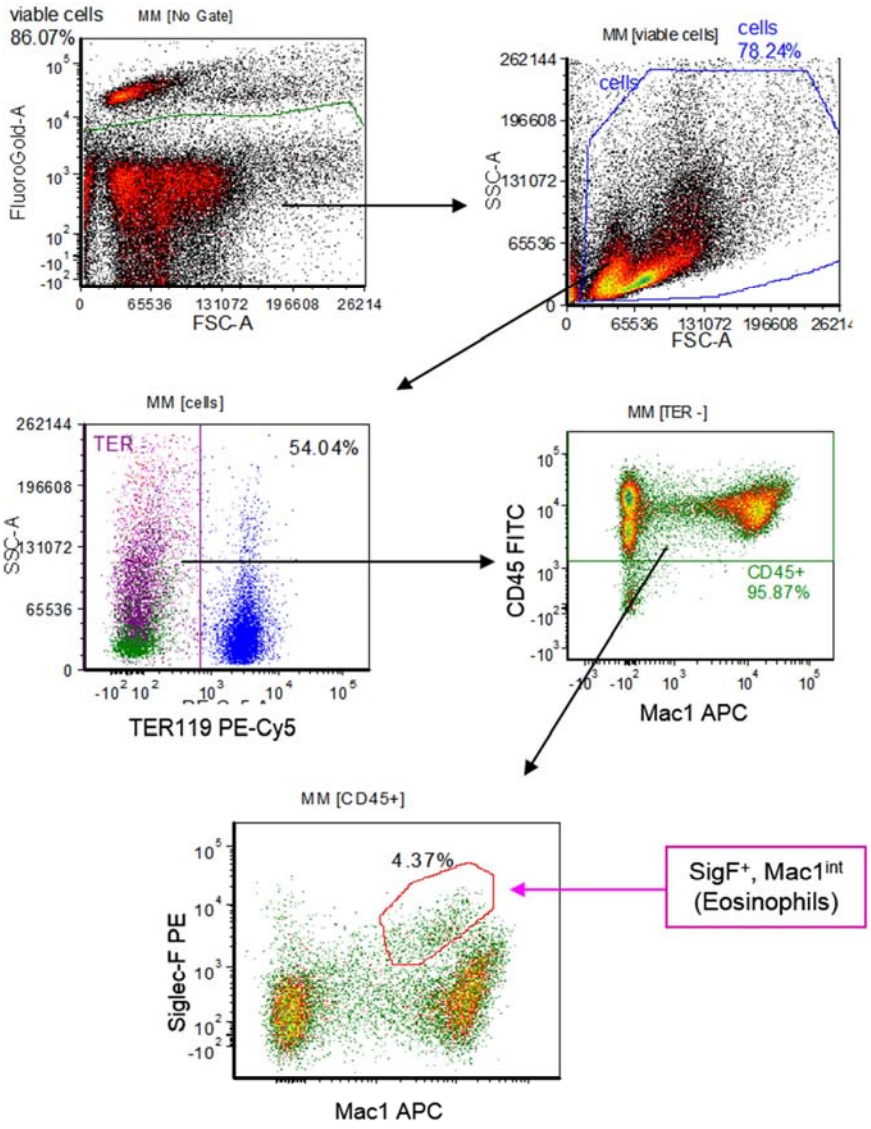

Figure 5.12: Schematic diagram to show the gating strategy used for flow cytometry analysis on cell surface markers of eosinophil cells in peripheral blood and bone marrow

A) Fluorogold negative (viable) cells were selected **(B)** debris was excluded on the forward and side scatter and **(C)** the following gate was set on $TER119^-$ cells to eliminate the $TER119^+$ cells (erythrocytes) from analysis. **D)** Selection of the $CD45^+$population **(E)** selection of $SigF^+$, $Mac1^{int}$ cells on the histogram.

5.2.3.2 Flow cytometry analysis to assess eosinophil cells in the lung of *Klf5*$^{\Delta/\Delta}$ mice.

As we observed an increase in the eosinophil population for both in PB and BM of *Klf5*$^{\Delta/\Delta}$ mice, we extended our analysis of eosinophils to the lungs of *Klf5*$^{\Delta/\Delta}$ mice. In normal lungs, eosinophils play a very minor role as antigen presenting cells, however in inflamed lungs, large percentages of eosinophils can be found [339]. In this study, flow cytometry analysis was conducted on lung cells from 12 months old mice. Details of procedures used for this analysis are described in Chapter 2, section 2.12.4. In this analysis, the antibodies used were CD45, Mac1 and Siglec-F for cell surface marker detection as above. The gating strategy used to identify eosinophils in lung is shown in the **Appendix P**. Eosinophils in lung are identified as CD45^{+}, Mac1^{int}, Sig-F^{+} [336, 340]. As lung macrophages also express the Siglec-F marker, the CD45^{+}, Mac1^{hi}, Sig-F^{+} cell population, is excluded from the analysis. Figure 5.14-**A** shows a representative plot for each genotype. From the results obtained, the mean percentage of eosinophils within the CD45^{+} leukocyte population in the lungs of *Klf5*$^{\Delta/\Delta}$ mice was significantly higher than *Klf5*$^{fl/fl}$ mice ($p<0.001$) (Figure 5.14-B). Interestingly, the mean percentage of eosinophils in the lung of *Klf5*$^{wt/\Delta}$ mice was significantly lower than the *Klf5*$^{\Delta/\Delta}$ mice ($p<0.01$) but also higher in trend when compared to *Klf5*$^{fl/fl}$ mice ($p=0.06$).

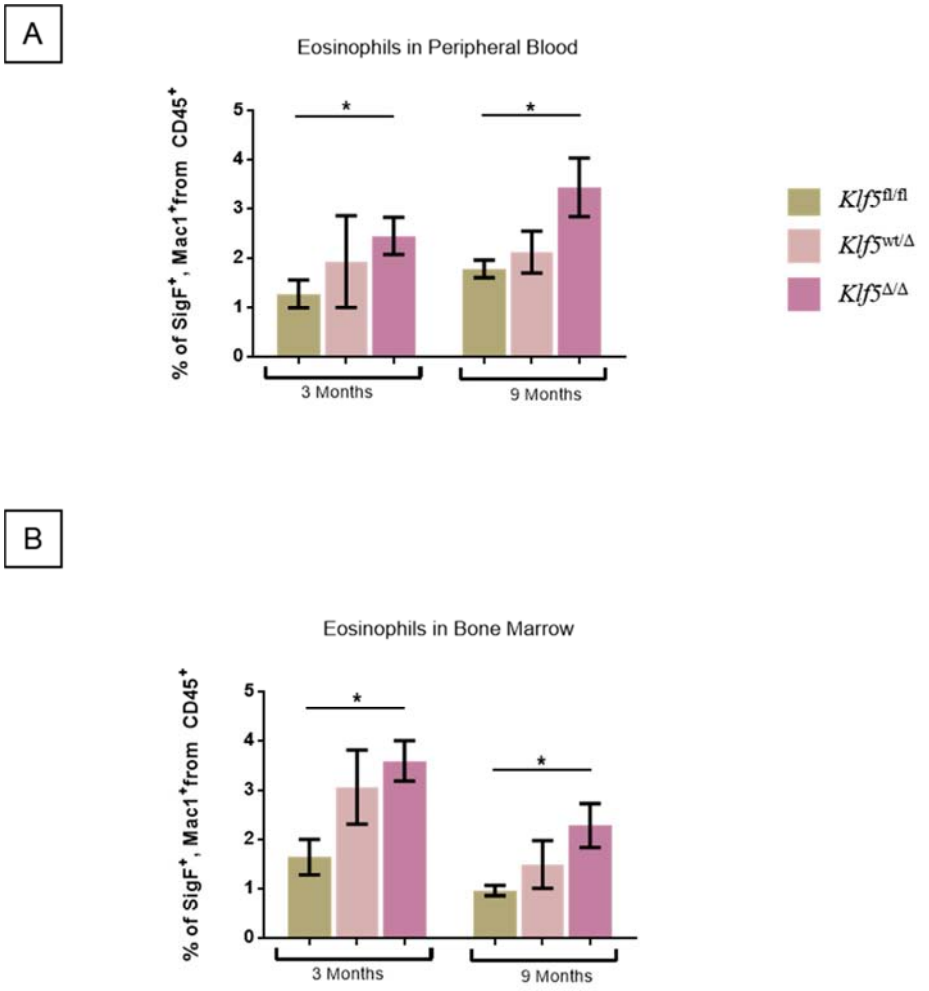

Figure 5.13: Identification of eosinophils in the peripheral blood and bone marrow using flow cytometry

Shown were mean values plus or minus of TER119^{-}, CD45^{+}, Mac1^{+}, SigF^{+} cell populations determined from **A)** peripheral blood drawn from each individual mouse at 3 and 9 months old and results obtained from n=10 for *Klf5*$^{fl/fl}$, n=6 for *Klf5*$^{wt/\Delta}$ and n=11 for *Klf5*$^{\Delta/\Delta}$ mice at 3 months, and n=8 for *Klf5*$^{fl/fl}$, n=8 for *Klf5*$^{wt/\Delta}$ and n=10 for *Klf5*$^{\Delta/\Delta}$ mice at 9 months. **B)** The bone marrow obtained from femurs and tibia of each mouse at 3 and 9 months old. Mean and SEM are shown. P-values obtained from t-tests conducted between each genotype groups using Graphpad Prism. *Significantly different between *Klf5*$^{fl/fl}$ and *Klf5*$^{\Delta/\Delta}$ mice (P<0.05). Results obtained from n=7 for *Klf5*$^{fl/fl}$, n=7 for *Klf5*$^{wt/\Delta}$ and n=8 for *Klf5*$^{\Delta/\Delta}$ mice at 3 months, and n=8 for *Klf5*$^{fl/fl}$, n=8 for *Klf5*$^{wt/\Delta}$ and n=9 for *Klf5*$^{\Delta/\Delta}$ mice at 9 months.

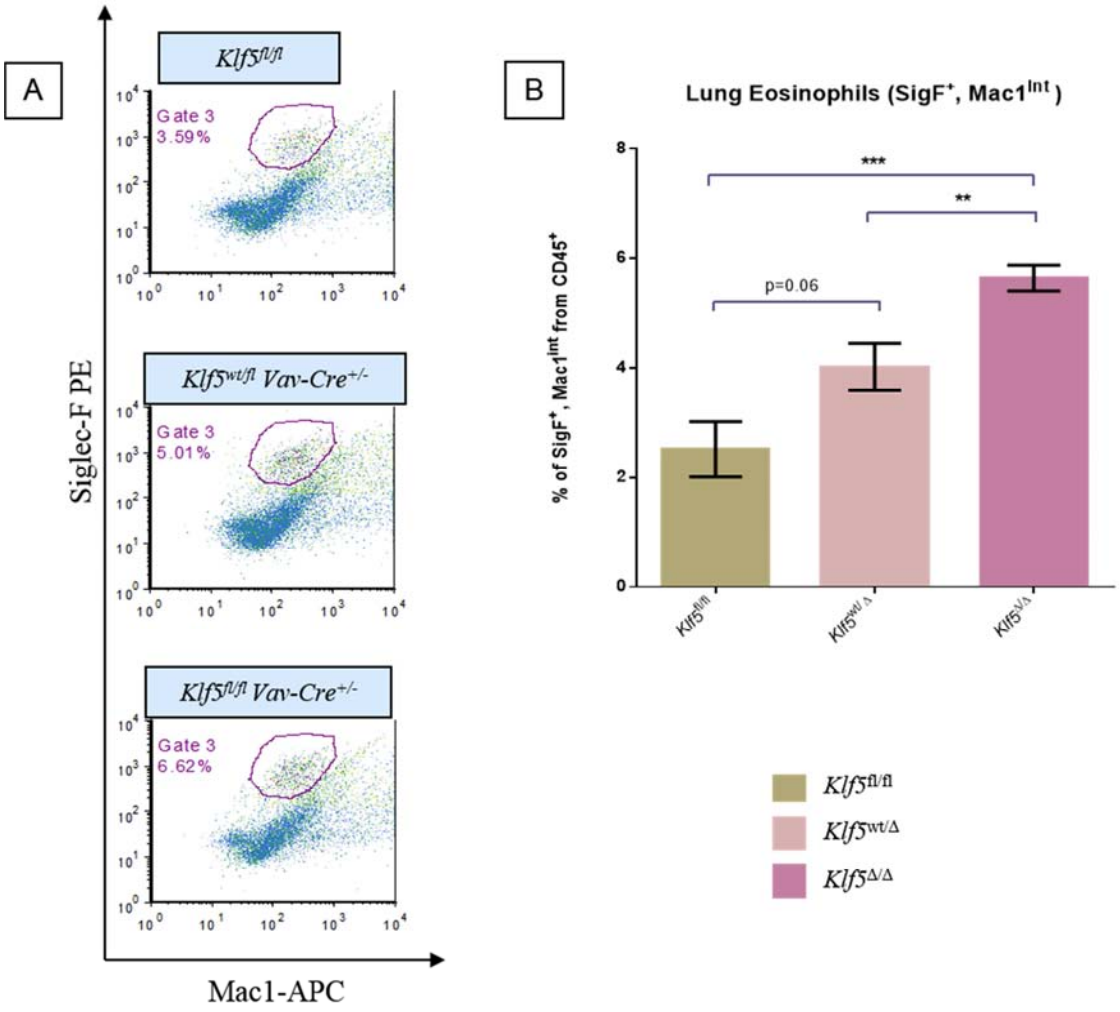

Figure 5.14: Flow cytometry detection of eosinophils from lung

(A) Plots shown were the representative gate used to select for the eosinophil cell population in the lung where CD45 positive cells were gated on $Mac1^{low}$ and $Siglec\text{-}F^{+}$ from all genotypes mice. **(B)** The bar chart shown were mean values plus or minus SEM percentage of $CD45^{+}$, $Mac1^{low}$, $SigF^{+}$ cells, from n=6 for $Klf5^{fl/fl}$, n=4 for $Klf5^{wt/\Delta}$ and n=6 for $Klf5^{\Delta/\Delta}$ mice. P-value obtained from t-test conducted between each genotype group using Graphpad Prism. Significantly different between $Klf5^{fl/fl}$ and $Klf5^{\Delta/\Delta}$ mice ***(P<0.001) and significantly different between $Klf5^{wt/\Delta}$ and $Klf5^{\Delta/\Delta}$ mice **(P<0.01).

5.3 Discussion

In this chapter we investigated changes in the extramedullary tissues in *Klf5*$^{\Delta/\Delta}$ mice. We observed enlarged spleen size in the *Klf5*$^{\Delta/\Delta}$ mice at every age examined. In general, when bone-marrow haemopoiesis is impaired by age, cancer or myeloablation, expanded numbers of HSCs can engage in extramedullary haemopoiesis in the spleen or other organs [341]. Interestingly, splenomegaly occurs for several blood diseases including myeloid leukaemia where extensive infiltration of myeloid cells is the documented feature [342-345]. However, in this study, the histopathology analysis did not show any morphological difference or myeloid cell infiltrates (as measured by MPO staining) in the dissected spleen sections of *Klf5*$^{\Delta/\Delta}$ mice. Hence, we further analysed spleens from *Klf5*$^{\Delta/\Delta}$ mice by conducting CFU assays and flow cytometry analysis. For mice at 9 and 12 months, the CFU frequency and numbers in the spleens of *Klf5*$^{\Delta/\Delta}$ mice were significantly higher than *Klf5*$^{fl/fl}$ controls, consistent with the extramedullary haemopoiesis in *Klf5*$^{\Delta/\Delta}$ mice. In addition, through flow cytometry analysis, we found that the stem cell compartments (ST-HSC and MPP) were significantly increased in the spleens of *Klf5*$^{\Delta/\Delta}$ mice compared to *Klf5*$^{fl/fl}$ mice. A recent study of Klf5 function in haemopoiesis has shown that *Klf5* is crucial for adhesion, homing, lodging and retention of haematopoietic stem cells and progenitors in the bone marrow [275]. However, in their study, they did not demonstrate extramedullary haemopoiesis in the spleen. We propose that reduced HSPC numbers in bone marrow (see Chapter 4) and an increase of equivalent populations in the spleen is consistent with impaired HSPC retention in the bone marrow [275] and increased migration of HSPC to spleen, resulting increased production of progenitor cells in spleen.

To assess eosinophil production in the *Klf5*$^{\Delta/\Delta}$ mice we investigated the effect of *Klf5* tissue-specific ablation on eosinophils in the BM, PB and lung. Eosinophils normally develop in the bone marrow with mature eosinophils typically released into the peripheral blood. In allergic conditions, newly released eosinophils circulate in the blood for a short period before homing preferentially to the lung, skin, and gut mucosa in response to eotaxin chemokine signals and the expressed adhesion marker MAdCAM-1 [346, 347]. Interestingly, in this study we observed a subtle increase in the percentage of eosinophils in the PB and BM of *Klf5*$^{\Delta/\Delta}$ mice when compared to *Klf5*$^{fl/fl}$ mice. We also found significantly increased eosinophils in the lung of *Klf5*$^{\Delta/\Delta}$ mice compared to *Klf5*$^{fl/fl}$ mice ($p<0.001$). Eosinophil production is controlled by a number of transcription factors (TFs) both in human and mouse which include GATA-1, GATA-2, C/EBP-α, PU.1 and FOG-1 (reviewed in *Kelly and Thomas* [348]). GATA-1 and C/EBP-α have been described as the key regulators of eosinophil development and knocking out these genes in mice results in impaired eosinophil production [349, 350]. As such, eosinophil origins during normal haemopoiesis have been described to have alternative pathways depending on the expression of the TFs for eosinophil maturation (reviewed in *Kelly and Thomas* [348]). These models have been proposed for eosinophils originating either from granulocyte-macrophage progenitors (GMP), common myeloid progenitors (CMP) or megakaryocyte-erythrocyte progenitors (MEP) [348]. In normal haemopoiesis, in the presence of moderate levels of GATA-1 and C/EBPα and the absence of FOG-1, eosinophils were derived from GMP or CMP. However, eosinophils originate from MEP via up-regulation of C/EBPα [348]. Interestingly, a recent study showed *KLF5* is a target gene of C/EBPα, which is a master regulator of eosinophil development [283]. This study reported that C/EBPα is a crucial positive regulator of *KLF5* during

granulocytic differentiation [283]. Since C/EBPα has been described as one of the key regulators of eosinophil development [349, 350] and *KLF5* is a target gene of C/EBPα [283], we suggest that Klf5 also has a functional role in eosinophil regulation downstream of C/EBPα. It is not clear whether the increased numbers of eosinophils in the lungs of $Klf5^{\Delta/\Delta}$ mice is simply a consequence of overproduction in the bone marrow. An alternative explanation could be that the eosinophils also have increased migration potential as is seen in $Klf5^{\Delta/\Delta}$ HSC [137, 138], an aspect that would require further investigation.

In summary, the experiments conducted in this chapter revealed two independent phenotypes in the *Klf5* conditional knockout mice. First, we showed that the stem cell compartment (predominantly ST-HSC and MPP) is significantly increased in the spleen of $Klf5^{\Delta/\Delta}$ mice compared to $Klf5^{fl/fl}$ mice, due to the establishment of extramedullary haemopoiesis in spleen. Finally, the experiments in this chapter revealed that *Klf5* ablation favors eosinophil production.

Chapter 6: Relevance and conclusions

6.1 Introduction

A potential functional role of KLF5 as a myeloid lineage-specific transcription factor was identified by the Acute Leukaemia Laboratory at the IMVS during a microarray study of GM-CSF induced granulocyte-macrophage differentiation of the FDB1 myeloid cell line [278]. It is known that *KLF5* is upregulated during granulocytic differentiation and this was confirmed by the analysis of microarray gene expression data from *in vitro* differentiation of $CD34^+$ cells [282]. Although the roles of KLF5 in various tissues has been increasingly studied (reviewed in *Diakiw et al.*) [199], the mechanisms that regulate KLF5 biologic activity in normal haemopoiesis and leukaemia are not fully understood.

A growing number of observations suggest that the functional role of KLF5 is not only tissue-specific but also changes with cell and developmental context [110, 190, 210, 215]. KLF5 function in specific tissues can be modified in several ways including, for example, post-translational modification on the KLF5 protein as observed in breast and prostate cancer studies [185, 187, 193]. In this study we focused on the role of Klf5 in haemopoiesis and described the development of a conditional haemopoietic *Klf5*-gene ablation model. Previous studies by us and others have provided *in vitro* data suggested that Klf5 plays a role in regulating myeloid growth and differentiation, particularly in the neutrophil granulocyte lineage [28, 33]. In addition, studies have shown that reduced expression of *KLF5* is observed in AML patients [28]. This reduced expression is associated with *KLF5* hypermethylation in intron 1 [52] indicating that KLF5 loss of function is associated with AML. Although, few studies have examined the role of Klf5 in the lymphoid

compartment, microarray gene expression data has shown that *Klf5* expression is down-regulated in natural killer cells, B-cells and T-cells relative to normal HSC from mouse [276]. This is consistent with data generated from the HemaExplorer gene expression database where *KLF5* expression in T-cells is relatively low compared to myeloid cells and HSC (**Appendix J**) [327]. In the haemopoietic stem cell compartment, Klf5 has been shown to regulate the homing and retention of the HSC in the bone marrow [275].

In the current study we sought to investigate in detail the functional role of Klf5 in haemopoiesis by removing exon 2 of the *Klf5* gene using the Cre/loxP recombination system in a mouse model. The conditional *Klf5* gene ablation model was generated by mating the $Klf5^{fl/fl}$ mouse line with the $VavCre^{+/+}$ mouse line. Using a mouse model system in which the *Klf5* gene is deleted in haemopoietic cells allowed us to assess the consequences of loss of Klf5 activity on haemopoiesis. Overall, myeloid and lymphoid lineages and the stem and progenitor compartment of *Klf5*-KO mice were assessed for any differences in comparison to *KLF5*-floxed and heterozygous *Klf5*-KO littermate.

In this chapter, we discuss the major findings from this project and how these relate to other studies conducted in haemopoiesis and for other Klf family members.

6.2 Generation of animals deficient for *Klf5* in the haemopoietic system

Klf5-KO ($Klf5^{-/-}$) mice are embryonic lethal at 8.5 days postcoitum (dpc) [79], necessitating the use of a conditional *Klf5*-gene knockout model to investigate the role of Klf5 in haemopoiesis. As stated earlier, the conditional *Klf5* gene KO model outlined in this work was generated using the Cre/*LoxP* recombination system

in combination with the *Vav* tissue-specific promoter driving the Cre recombinase (see Chapter 3, Section 3.2.1). Although *Vav* is primarily expressed in haemopoietic cells, we cannot exclude the possibility that *Klf5* deletion occurs in non-haemopoietic tissues (discussed in Section 6.6 of this chapter). *In vivo* studies have shown that *Vav* expression is not only restricted to haemopoietic tissues but also is observed in vascular endothelial tissues (endothelial cells lining all blood vessels) [295, 300]. *Ishikawa et al.*, have also generated a conditional *Klf5*-gene ablation model to study the functional role of Klf5 during haemopoiesis, however the strategy that they employed was different [275]. They generated *Mx1-Cre;Klf5*$^{flox/flox}$ mice by crossing *Klf5*$^{flox/flox}$ mice and *Mx1-Cre* transgenic mice [275]. In their model (*Mx1-Cre;Klf5*$^{flox/flox}$) exons 2 and 3 of the *Klf5* gene were deleted following Cre-induction with polyinositide:polycytidine (pI:pC) [275]. Cre-induction with (pI:pC) allows complete inactivation of the specific gene in liver and nearly complete deletion in lymphocytes within a few days, whereas partial deletion was obtained in other tissues [313]. In our model (referred to as *Klf5*$^{\Delta/\Delta}$ mice in this study) exon 2 of the *Klf5* gene was constitutively deleted in the haemopoietic system.

The *Klf5*$^{\Delta/\Delta}$ mice survived until adult age and all littermates were born at the expected Mendelian ratios for each genotype indicating that conditional *Klf5* ablation via Vav-cre was not interfering with embryonic development or embryo implantation (Table 3.1). This finding also suggests that Klf5 is not an essential factor for embryonic haemopoiesis. None of the *Klf5*$^{\Delta/\Delta}$ mice shows signs of stress or disease through to adulthood thus we conducted a comprehensive analysis of steady-state adult haemopoiesis.

6.3 The functional role of *Klf5* in the myeloid lineage

Given the previous studies showing that *Klf5*-knockdown leads to reduced granulocyte differentiation in the 32D cell line, we hypothesised that *Klf5* ablation in haemopoietic progenitors would lead to aberrant granulopoiesis in an *in vivo* model. Thus, a major focus of this study was to investigate whether the myeloid cell compartment and specifically granulocyte lineages were altered due to loss of *Klf5* expression. Although several studies have shown that *Klf5* loss of expression has an association with impaired neutrophil differentiation [28, 33, 52], analysis of an *in vivo* model was still warranted in order to better establish the role of KLF5 in granulocyte-macrophage lineage specification. As described in Chapter 1, although murine models for the *in vivo* deletion of *Klf5* have been reported in the literature, these have not been utilised for an extended analysis of the myeloid lineage and *Klf5*$^{-/-}$ mice are embryonic lethal prior to the onset of definitive haemopoiesis [285, 286]. Heterozygous *Klf5*$^{+/-}$ mice have a number of defects in adipogenesis, cardiovascular remodelling, and intestinal development [78, 200, 215] but no analysis of steady state haemopoiesis was reported. In parallel, it has been reported that the Mx1-*Cre;Klf5*$^{flox/flox}$ mice following pI:pC induction have defects in adult haemopoietic stem cells. *Ishikawa et al*. reported that Klf5 has a functional role in the retention, adhesion and homing of HSC in the bone marrow [275]. It was also reported that the numbers of circulating myeloid cells from peripheral blood were decreased in their *Klf5*-deficient mice [275]. Although, these studies reported defects in the myeloid lineage, the extended analysis in this thesis has revealed changes in the myeloid lineage both in the primitive and more differentiated myeloid compartments.

6.3.1 The functional role of *Klf5* in neutrophil production

In Chapter 4 of this thesis, we provided evidence using flow cytometry analysis that *Klf5*$^{\Delta/\Delta}$ mice have fewer neutrophils in the PB and BM compared to *Klf5*$^{fl/fl}$ mice, consistent with the hypothesis that KLF5 acts as a regulator in the granulocyte lineage (**Figure 4.5A** and **Figure 4.9A**). These findings are consistent with the expression profile of *Klf5* which increases during primary granulocyte differentiation, and with *Klf5*-knockdown experiments which revealed that expression of *Klf5* is a requirement for neutrophil differentiation of 32D cells in response to G-CSF [28]. To gain further insight into the Klf5 mediated regulation of the myeloid lineage, particularly in the early myeloid progenitor stages, we conducted flow cytometry analysis to assess the myeloid progenitor compartment. From this analysis, none of the cells within the myeloid progenitor compartment showed significant changes in the *Klf5*$^{\Delta/\Delta}$ mice compared to *Klf5*$^{fl/fl}$ mice (Figure 4.12 - Figure 4.15). A previous study by *Humbert et al.* also suggested *Klf5* involvement during myelopoiesis by demonstrating a role for this protein in neutrophil differentiation of acute promyelocytic leukemia cells in response to ATRA [33]. Relatively few studies have assessed the cooperative role of KLF5 with other key transcriptional regulators in the myeloid lineage. For instance, *Klf5* has been reported to be a direct target of C/EBPα in the APL cell line model, NB4. C/EBPα is a transcription factor known to be a critical regulator during the formation of granulocyte-monocyte progenitors and neutrophil differentiation [23, 283, 284]. It has been reported that higher levels of C/EBPα are required for granulocyte lineage and lower levels for monocyte lineage specification [284]. Interestingly, it has been reported that upregulation of *KLF5* during ATRA-induced neutrophil differentiation of APL cells is *CEBPA*-dependent [283]. *Klf5* expression was also shown to be

reduced following *Cebpα* knockdown in lineage-negative bone marrow cells [284]. Consistent with these findings, *Klf5* expression has been shown to be associated with *Cebpα* [284]. This relationship between *Cebpα* and *Klf5* is supportive of our finding of a role for Klf5 in regulating granulocyte development. Since our study revealed that loss of functional Klf5 did not affect the GMP population, this suggests that Klf5 is not required for GMP formation but acts at the level of the GMP to influence lineage specification (Figure 6.1).

Comparatively few studies have scrutinised the role of KLF family members in the myeloid lineage. KLF1 which was originally described as an erythroid-specific gene has been more recently described as a transcription factor in primary human macrophages by controlling IL-12 p40 transcription [351]. KLF3 has been suggested to modulate the proliferative and/or survival capacity of myeloid progenitor cells based on the observation that *Klf3* knock-out mice develop a chronic myeloproliferative disorder due to increased proliferative capacity of myeloid cells [352]. Interestingly, KLF6, which like KLF5 has a hydrophobic activation domain close to the zinc-finger motif (**Figure 1.2**) also has been shown to regulate granulocyte differentiation in APL cells [33]. The most detailed studies with regard to KLF family members in myelopoiesis have been undertaken with KLF4. Klf4 was identified as an essential regulator in monocyte formation [169]. *KLF4* expression is restricted to the monocyte lineage and is differentiation stage-specific [169]. Gene expression analysis conducted by *Diakiw et al.* has also shown that *KLF4* is upregulated in human monocytes when compared to $CD34^+$ cells (Figure 1.4). Enforced expression of *KLF4* in primary common myeloid progenitors (CMP) or HSC induced exclusive monocyte differentiation in clonogenic assays, whereas ablation of KLF4 in CMPs induced development of granulocyte colonies at the

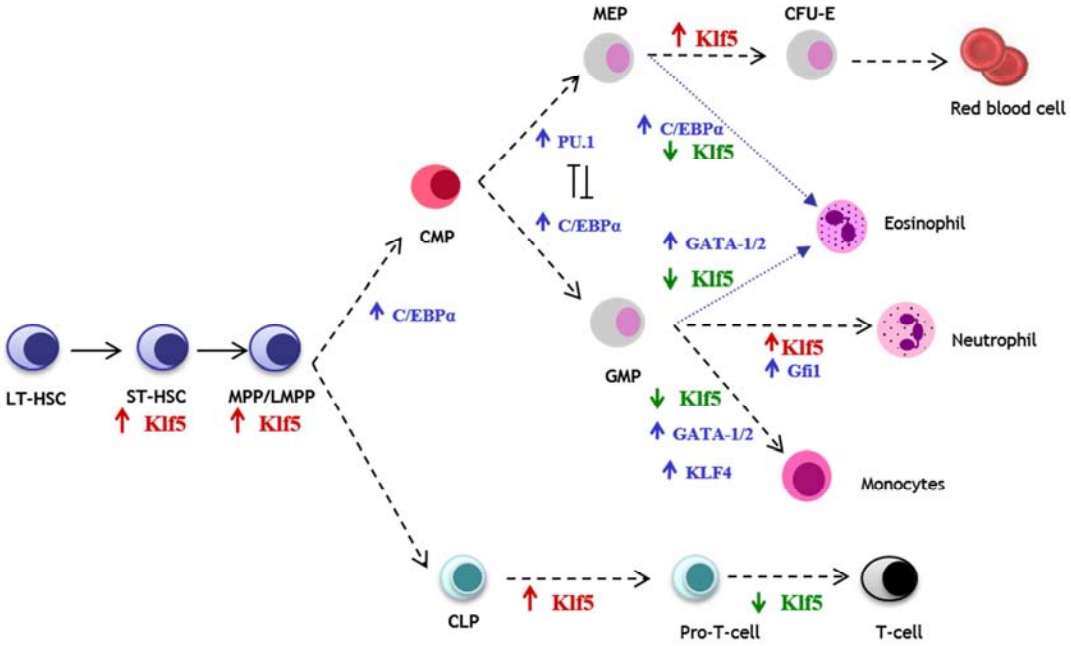

Figure 6.1: The functional role of *Klf5* in haemopoiesis

The schematic diagram summarises the findings from analysis of conditional $Klf5^{\Delta/\Delta}$ mice. We propose that Klf5 expression is necessary for maintaining the HSCP niche in the bone marrow. In the myeloid lineage, we propose that balance of *Klf5* expression is necessary for granulocyte development with up-regulation required in GMP for neutrophil with down-regulation of *Klf5* will lead to eosinophil formation from GMP. Eosinophils can also originate from MEP in the absence of *Klf5* (see Section 6.3.2). In lymphoid lineage, while *Klf5* expression was found to be important at the early stage of T-cells formation, down-regulation of *Klf5* is desired for T-cells maturation. HSC; haemopoietic stem cell, HSCP; haemopoietic stem cell progenitors, CMP; Common myeloid progenitor, CLP; common lymphoid progenitor, MEP; myelo-erythroid progenitor, GMP; granulocyte-macrophage progenitor and CFU-E; erythroid progenitor. Red arrows indicate up-regulation of *Klf5* expression and green arrows represent down-regulation of *Klf5* expression.

expense of macrophage colonies [169]. Consistent with a role in promoting monocyte differentiation, *Feinberg et al.* also demonstrated that *KLF4* is a target gene of the monocytic transcription factor PU.1 [169]. Interestingly, numerous studies have shown that KLF4 and KLF5 often function in a competitive manner [353]. *Dang et al.* reported that both Klf4 and Klf5 bind to GC-2, the *cis*-element in the *Klf4* promoter [55]. Interestingly, it was reported that Klf4 and Klf5 compete to regulate *Klf4* expression with Klf4 activating and Klf5 repressing the *Klf4* promoter [55]. Very recently, a study on the functional role of Klf4 and Klf5 in embryonic stem cell development has also revealed opposing roles of Klf4 and Klf5 in mesoderm and endoderm differentiation [91]. Through chromatin immunoprecipitation (ChIP) coupled with ultra-high-throughput DNA sequencing (ChIP-seq), this study has reported that Klf4 and Klf5 share many common targets [91]. However, Klf4 preferentially regulates the expression of genes associated with endoderm differentiation, whereas Klf5 preferentially regulates the expression of genes associated with mesoderm differentiation [91]. The observed reduction in neutrophils but preserved levels of monocytes in our studies (Figure 4.9) is consistent with the hypothesis of opposing roles of Klf5 and Klf4 in myeloid lineage, with Klf5 and Klf4 competing in the GMP to specify neutrophil versus monocyte differentiation respectively. This could be further tested by using gene expression profiling and ChIP coupled with Next-Generation Sequencing, analysis to identify Klf4/Klf5 target genes in myeloid cells, and whether the genes are targets of activation or repression.

6.3.2 The functional role of *Klf5* in eosinophil production and migration

6.3.2.1 Eosinophil lineage specification

Our studies have focused on defining the role of KLF5 in the granulocyte lineages, with an initial finding that loss of Klf5 affects neutrophil production. Since KLF5 has been shown to be regulated downstream of CEBPα and *Cebpα*-null mice lack the production of neutrophils and eosinophils [23, 284], this led us to directly examine the functional role of Klf5 in eosinophil production. Surprisingly, our study revealed that loss of *Klf5* in the haemopoietic system increased the eosinophil production. We observed that eosinophil production was increased in the peripheral blood, bone marrow and lung of the $Klf5^{\Delta/\Delta}$ mice suggesting that Klf5 is a negative regulator of eosinophil development (Figure 5.13 and Figure 5.14). A number of transcription factors have been identified to play key roles both in human and mouse eosinophil production. For example, GATA-1 and C/EBP-α functionally regulate eosinophils, as evidenced by their associated knockout mice phenotypes where a loss of neutrophils and eosinophils was observed [23, 354]. PU.1, which is a transcriptional regulator during monocyte development, also regulates eosinophil production [355-358]. Interestingly, FOG-1 which was originally identified as a regulator of erythrocytes and megakaryocyte development has also been identified to have functional roles both in human and mouse eosinophil productions [359]. FOG-1 was described as a repressor of the eosinophil lineage and constitutive expression of *FOG-1* in multipotent progenitors blocked activation of eosinophil-specific gene expression by C/EBPß [360]. Interestingly, *Oishi et al*., have shown that *Klf5* is both a target gene of C/EBPß and a co-factor of C/EBPß during adipocyte differentiation [78]. Having observed increased eosinophils in the absence of *Klf5* in haemopoietic cells suggests a repressive role for Klf5 in regulating eosinophil development and

further investigation could examine whether Klf5 potentially mediates these effects through interaction with C/EBPß.

As discussed in Chapter 5 of this study, eosinophils can originate from three different progenitors which are the granulocyte-macrophage progenitor (GMP), common myeloid progenitor (CMP) or megakaryocyte-erythrocyte progenitor (MEP) depending on the levels of particular TFs [348]. Eosinophils are derived from GMP or CMP in the absence of FOG-1 and the presence of moderate levels of GATA-1 and C/EBPα, whereas the MEP eosinophil pathway is activated via up-regulation of C/EBPα [348]. Interestingly, a recent study has reported that while human eosinophils originate directly from CMP, mouse eosinophils originate from CMP via GMP [347]. Since we observed upregulation of eosinophils in the absence of *Klf5*, we propose that upregulation of eosinophils observed in the $Klf5^{\Delta/\Delta}$ mice occurs in parallel to reduced neutrophil maturation in the myeloid lineage. In addition, as we observed a decrease of erythroid progenitors in $Klf5^{\Delta/\Delta}$ mice it is possible that loss of *Klf5* leads to excessive eosinophil production originating from MEP. Thus, we propose that in our $Klf5^{\Delta/\Delta}$ mice, increased eosinophil production occurs from two different progenitors (GMP and MEP) as shown in Figure 6.1.

6.3.2.2 The link between eosinophil migration and T-cell production

In Chapter 5 of this study we showed that eosinophil levels were not only increased in the PB and BM of $Klf5^{\Delta/\Delta}$ mice but also in the lung, demonstrating eosinophil migration from the peripheral blood into the inflammatory organs. In Chapter 4 of this study we showed that T-cell levels were higher in the PB and BM of $Klf5^{\Delta/\Delta}$ mice. Interestingly, other studies have reported that eosinophil migration is associated with T-cell production and migration in both mouse and humans [361-

363]. Thus, this presents another mechanism that may contribute to increased numbers of eosinophils in this *Klf5* knockout model.

In conclusion, evidence from the literature combined with data from our model suggests that Klf5 could influence eosinophil numbers through 1) a direct effect on the eosinophil progenitor, 2) regulation of eosinophil migration and 3) indirect regulation of T-cells and cytokine production.

6.4 The functional role of *Klf5* in regulating erythroid cells

Another interesting finding in this study was the changes in the erythroid lineage in the $Klf5^{\Delta/\Delta}$ mice. Initial data obtained from CBC of 3 month old mice showed a significant reduction of the RBC count in $Klf5^{\Delta/\Delta}$ mice compared to control mice (Figure 4.1-**A**). The counts for haematocrit and haemoglobin were also reduced in 3 month old $Klf5^{\Delta/\Delta}$ mice (Figure 4.1-**B** and Figure 4.1-**C**). Further analysis from CFU assays at 9 months revealed that erythroid progenitor cells in the $Klf5^{\Delta/\Delta}$ mice were reduced when compared to aged matched control mice from bone marrow (Figure 4.22). Interestingly, a gene expression study has shown that *KLF5* can directly bind and transactivate the γ-globin gene in K562 cells [180]. *KLF5* mRNA is expressed in both human and mouse erythroid cells [180]. This is also consistent with our gene expression studies where KLF5 is upregulated in the human and mouse erythroid lineage when compared to normal human $CD34^{+}$ and mouse HSC respectively (Figure 1.4). Although there was no previous direct functional evidence for the involvement of Klf5 in regulating erythropoiesis, an independent study had shown that KLF5 has a domain that is similar to the transactivation domain 2 of KLF1 (EKLFTAD2), a known regulator of erythropoiesis [328]. In fact this region

homologous to EKLFTAD2 was shown to interact with CBP/p300 [328]. KLF1, which is also known as *Erythroid Krüppel-like factor (EKLF)*, was identified as an important regulator during erythroid maturation and it was shown to specifically bind CAACC elements in the *β-globin* promoter [170]. KLF1 stimulates *β-globin* gene expression and helps enable the switch from the foetal *γ-globin* to the adult *β-globin* [171]. *Klf1*-null embryos die at embryonic day E14.5 from anaemia because definitive erythroid cells fail to produce *β-globin* transcripts *in vivo* hence leading to a profound β-thalassemia [71, 172]. However, later studies have shown the involvement of other KLF members in regulating erythroid maturation [90, 173-179, 364]. KLF4 also has been identified as a regulator of erythropoiesis. Over-expression of *KLF4* in K562 cells (a BCR-ABL positive leukaemic cell line capable of erythroid differentiation), resulted in increased expression of the endogenous *HBA* genes, and consistent results were obtained in *KLF4* shRNA knockdown experiments [178]. KLF4 also regulates the *HBG* gene (γ-globin) [179]. Genetic studies support a role for Klf4 in erythropoiesis where a study has reported that foetal liver cells from $Klf4^{-/-}$ mice cultured in methylcellulose medium with complete cytokine have more erythroid progenitor colonies compared to $Klf4^{+/+}$ mice [31].

With regard to KLF5, *Zhang, et al*. demonstrated that *KLF5* mRNA expression increases during erythroid differentiation of the K562 cell line where it binds to and activates transcription of the haemoglobin *HBG* gene [180]. In our present study, which examined adult erythropoiesis, we have shown that loss of *Klf5* is associated with reduced red blood cell counts at 3 months old (Figure 4.1), and reduced erythroid progenitor colonies from bone marrow at 9 months old scored in the methylcellulose assay (Figure 4.22). Since previous studies have shown that both KLF4 and KLF5 regulate foetal haemoglobin genes, further investigation in the

foetal liver of *Klf5*$^{\Delta/\Delta}$ mice will be important. As discussed earlier KLF4 and KLF5 often display similar tissue distribution patterns yet act in an opposing manner [353], and the functional BFU-E colony assays suggest this may also be the case in erythropoiesis. Thus it will be interesting to investigate the functional cooperation between KLF4 and KLF5 in erythropoiesis. For example, the conditional *Klf5*$^{\Delta/\Delta}$ mice could be used to generate a double-conditional Klf4/Klf5 knockout in haemopoiesis. Comparison to the single knockout would allow a detailed study of the genetic interaction between these two factors. This may be particularly important in younger animals given that reduced red blood cell, haematocrit and haemoglobin are observed at 3 months for *Klf5*$^{\Delta/\Delta}$ animals.

6.5 The functional role of *Klf5* in regulating the lymphoid lineage

In Chapter 4 of this thesis, we demonstrated a potential role for Klf5 as a regulator of lymphoid development. The results presented in Section 4.2.1.2 and 4.2.2.1 demonstrated that CD3ε^{+} T-cells were up-regulated in the peripheral blood and bone marrow of *Klf5*$^{\Delta/\Delta}$ mice (Figure 4.6-**A** and Figure 4.10-**A**). However, in Section 4.2.2.3, we observed a decrease in the average percentage of common lymphoid population (CLP) in the 9 month old *Klf5*$^{\Delta/\Delta}$ mice. Interestingly, it has been shown previously that *Klf5* expression is reduced in mature T-cell populations relative to murine haemopoietic stem cells (see Figure 1.4) and this concurs with a previous study that reported precursor T-cells as having high levels of *KLF5* mRNA with expression decreasing on maturation [277]. Since the level of *Klf5* expression has been described to vary depending on the stage of T-cell development, it is possible that *Klf5* expression is important at the early stage of lymphoid and T-cell development when it is expressed at the highest levels yet down-regulation of *Klf5*

expression is desired for T-cell maturation. Collectively, this study described a new role for Klf5 in the T-cell lineage. However, further investigations including an examination of measuring the T-cells in the thymus are still warranted.

6.6 The functional role of *Klf5* in regulating normal haemopoietic stem cell activity

In Chapter 4 of this study we demonstrated a reduction in colony numbers following secondary and tertiary platings in a serial replating assay from bone marrow of *Klf5*$^{\Delta/\Delta}$ mice (Figure 4.20). This was evident at 9 months but not 3 months suggesting that progenitors from knockout mice have an age-related loss in self-renewal capability. This finding is consistent with the recent published report that the repopulation ability of the long-term HSC compartment was impaired in *Klf5*-deficient mice [275]. Assays conducted using bone marrow from *Mx1-Cre;Klf5*$^{flox/flox}$ mice transplanted into lethally irradiated mice revealed that loss of *Klf5* in HSPC populations impaired their ability to contribute to repopulation *in vivo*. The impaired engraftment of *Klf5*-deficient HSC was not associated with a significant bias or skewing of multi-lineage repopulation, and this phenotype was confirmed in secondary recipient mice [275]. Consistent with this, we did not observe any differences in CFU-G, CFU-M or CFU-GM and taken together with the findings of *Ishikawa et al.* suggest that this effect is most likely at the stem cell level rather than a committed progenitor.

In Chapter 4 of this study, we also showed that the HSPC fraction from flow cytometry analysis was reduced in the bone marrow of *Klf5*$^{\Delta/\Delta}$ mice although none of the specific primitive stem cell compartments (LT-HSC, ST-HSC and MPP) revealed significant differences between genotypes (Figure 4.17). In contrast, in Chapter 5 of

this study, again based on flow cytometry analysis, we showed that the percentages of HSPC (predominantly the ST-HSC and MPP) were increased in the spleen of *Klf5*$^{\Delta/\Delta}$ mice (Figure 5.11). The numbers of committed progenitor as determined from colony assays were also higher in the spleen of *Klf5*$^{\Delta/\Delta}$ mice (Figure 5.5). Interestingly, *Ishikawa et al.* reported that loss of *Klf5* impaired HSC retention and adhesion in the bone marrow [275]. This study has reported that loss of Klf5 results in the loss of β1- and β2-integrins via Rab5 inactivation thus leading to decreased adhesion to the extracellular matrix and homing and lodging in the bone marrow endosteal space [275]. Therefore, one explanation for our finding of increased HSPC in the spleen and reduced HSPC in the BM of *Klf5*$^{\Delta/\Delta}$ mice is a defect in HSC retention and adhesion in the BM, hence enhancing the HSC migration into the spleen. Additionally KLF5 has been shown to regulate other molecules involved in adhesion and migration that could also be contributing to this effect [210, 219, 332, 333].

Although the HSC difference between bone marrow and spleen is most likely due to the effect of impaired HSC adhesion due to *Klf5*-gene ablation in haemopoietic cells, it is also necessary to consider the possible indirect effect from C*re* mediated *Klf5* ablation in endothelial cells. As discussed in Chapter 3, *Vav* is a proto-oncogene that has been reported to be expressed in the haemopoietic system as well as vascular endothelial tissues [299, 300]. Thus, endothelial cells of *Klf5*$^{\Delta/\Delta}$ mice may experience loss of functional Klf5 in the presence of this *Vav-Cre* transgene. Endothelial cells form the endothelium that lines the interior surface of blood vessels and lymphatic vessels [295]. *Klf5*$^{+/-}$ mice are reported to have abnormal thinning of the medial and adventitial layers of the aortic wall suggesting that Klf5 functions in regulating vascular endothelial cells in the aorta [54, 79]. Numerous

studies have reported that the endothelial cells in the bone marrow contribute to the creation of HSC niches and also regulate HSC function [365-368]. However, as a defect in HSC homing and adhesion was observed in transplanted wildtype recipients by *Ishikawa et al.*, this suggests that the alterations in HSC in between bone marrow and spleen are most likely cell autonomous in nature. To confirm this in our *Klf5* gene ablation model it would be necessary to transplant *Klf5*$^{\Delta/\Delta}$ HSC into wildtype recipients.

6.7 Conclusion

In summary, this study revealed multiple functional roles for Klf5 in haemopoiesis. In the myeloid lineage, KLF5 plays a role in myeloid differentiation, and previous studies have demonstrated that hypermethylation of the *KLF5* proximal promoter and intron 1 act as functional mechanisms for down-regulation in AML. Throughout this study, we showed that loss of *Klf5* impaired neutrophil development and promoted eosinophil production in the *Klf5*$^{\Delta/\Delta}$ mice. As the percentages of CMP and GMP were normal and we did not observe an accumulation of neutrophil precursors or abnormal neutrophils, we suggest that *Klf5* ablation alters lineage specification downstream of CMP and GMP. Our investigation of eosinophil levels suggests that loss of *Klf5* may bias myeloid differentiation towards eosinophil production and differentiation. Further studies are still warranted to determine the specific pathways which are involved in modulating eosinophil production in this system and it would be of interest to see if the production or function of eosinophils is altered following a parasitic challenge to the mice [369] as eosinophils are the major mediators of parasite response. Loss of Klf5 in haemopoiesis enhanced CD3ε^{+} T-cell production in the bone marrow and peripheral blood suggesting a previously unidentified role

for Klf5 outside the myeloid compartment. This could be examined more specifically by using a T-cell restricted Cre transgenic mouse [370]. As discussed earlier, Klf5 also has been reported to be a functional regulator of HSC homing in the bone marrow. In this study, we showed that some stem cell compartments (ST-HSC and MPP) were significantly increased in the spleen of $Klf5^{\Delta/\Delta}$ mice compared to $Klf5^{fl/fl}$ mice, suggesting migration of HSC may initiate extra-medullary splenic haemopoiesis. A future experiment to transplant $Klf5^{\Delta/\Delta}$ HSC into wildtype recipients is important to establish the cell-autonomous nature of the haemopoietic change in the $Klf5^{\Delta/\Delta}$ mice. As summarised in Figure 6.1, this study provides novel evidence for various functional roles of Klf5 in haemopoiesis, such that loss of *Klf5* in haemopoietic cells is associated with changes to primitive and more mature cell types, and extramedullary splenic haemopoiesis. As such, a future experiment to examine the changes in gene expression by microarray analysis will be beneficial. This could be designed to compare the $Klf5^{fl/fl}$ and $Klf5^{\Delta/\Delta}$ haemopoietic transcriptomes in HSC, eosinophils and neutrophils from bone marrow specifically from 9 and 12 months old mice. This would identify the changes in gene expression associated with HSC, eosinophils and neutrophils phenotype observed in the earlier study. Finally, the finding of *KLF5* silencing in human AML combined with our functional *in vivo* data here on the myeloid lineage suggests that the *Klf5* conditional knockout mice may provide a good model to combine with potential co-operating AML oncogenes to better understand the role of KLF5 in this devastating disease.

Chapter 7: References

1. Seke Etet, P.F., L. Vecchio, P. Bogne Kamga, E. Nchiwan Nukenine, M. Krampera, and A.H. Nwabo Kamdje, *Normal hematopoiesis and hematologic malignancies: role of canonical Wnt signaling pathway and stromal microenvironment.* Biochim Biophys Acta, 2013. 1835(1): p. 1-10.
2. Seita, J. and I.L. Weissman, *Hematopoietic stem cell: self-renewal versus differentiation.* Wiley Interdiscip Rev Syst Biol Med, 2010. 2(6): p. 640-53.
3. Ceredig, R., A.G. Rolink, and G. Brown, *Models of haematopoiesis: seeing the wood for the trees.* Nat Rev Immunol, 2009. 9(4): p. 293-300.
4. Nakamura-Ishizu, A. and T. Suda, *Hematopoietic stem cell niche: an interplay among a repertoire of multiple functional niches.* Biochim Biophys Acta, 2013. 1830(2): p. 2404-9.
5. Kiel, M.J. and S.J. Morrison, *Maintaining hematopoietic stem cells in the vascular niche.* Immunity, 2006. 25(6): p. 862-4.
6. Cross, M.A., C.M. Heyworth, A.M. Murrell, E.O. Bockamp, T.M. Dexter, and A.R. Green, *Expression of lineage restricted transcription factors precedes lineage specific differentiation in a multipotent haemopoietic progenitor cell line.* Oncogene, 1994. 9(10): p. 3013-6.
7. Alenzi, F.Q., B.Q. Alenazi, S.Y. Ahmad, M.L. Salem, A.A. Al-Jabri, and R.K. Wyse, *The haemopoietic stem cell: between apoptosis and self renewal.* Yale J Biol Med, 2009. 82(1): p. 7-18.
8. Weissman, I.L., *Translating stem and progenitor cell biology to the clinic: barriers and opportunities.* Science, 2000. 287(5457): p. 1442-6.
9. Zhu, J. and S.G. Emerson, *Hematopoietic cytokines, transcription factors and lineage commitment.* Oncogene, 2002. 21(21): p. 3295-313.
10. Ogawa, M., *Differentiation and proliferation of hematopoietic stem cells.* Blood, 1993. 81(11): p. 2844-53.
11. Pabo, C.O. and R.T. Sauer, *Transcription factors: structural families and principles of DNA recognition.* Annu Rev Biochem, 1992. 61: p. 1053-95.
12. Maston, G.A., S.K. Evans, and M.R. Green, *Transcriptional regulatory elements in the human genome.* Annu Rev Genomics Hum Genet, 2006. 7: p. 29-59.
13. Subramanian, L., M.D. Benson, and J.A. Iniguez-Lluhi, *A synergy control motif within the attenuator domain of CCAAT/enhancer-binding protein alpha inhibits transcriptional synergy through its PIASy-enhanced modification by SUMO-1 or SUMO-3.* J Biol Chem, 2003. 278(11): p. 9134-41.
14. Hollenhorst, P.C., K.J. Chandler, R.L. Poulsen, W.E. Johnson, N.A. Speck, and B.J. Graves, *DNA specificity determinants associate with distinct transcription factor functions.* PLoS Genet, 2009. 5(12): p. e1000778.
15. He, X., C.C. Chen, F. Hong, F. Fang, S. Sinha, H.H. Ng, and S. Zhong, *A biophysical model for analysis of transcription factor interaction and binding site arrangement from genome-wide binding data.* PLoS One, 2009. 4(12): p. e8155.
16. Kato, M., N. Hata, N. Banerjee, B. Futcher, and M.Q. Zhang, *Identifying combinatorial regulation of transcription factors and binding motifs.* Genome Biol, 2004. 5(8): p. R56.
17. Wang, Y., X.S. Zhang, and Y. Xia, *Predicting eukaryotic transcriptional cooperativity by Bayesian network integration of genome-wide data.* Nucleic Acids Res, 2009. 37(18): p. 5943-58.

18. Pape, U.J., H. Klein, and M. Vingron, *Statistical detection of cooperative transcription factors with similarity adjustment.* Bioinformatics, 2009. 25(16): p. 2103-9.
19. Attar, E.C. and D.T. Scadden, *Regulation of hematopoietic stem cell growth.* Leukemia, 2004. 18(11): p. 1760-8.
20. Giorgetti, L., T. Siggers, G. Tiana, G. Caprara, S. Notarbartolo, T. Corona, M. Pasparakis, P. Milani, M.L. Bulyk, and G. Natoli, *Noncooperative interactions between transcription factors and clustered DNA binding sites enable graded transcriptional responses to environmental inputs.* Mol Cell, 2010. 37(3): p. 418-28.
21. Back, J., D. Allman, S. Chan, and P. Kastner, *Visualizing PU.1 activity during hematopoiesis.* Exp Hematol, 2005. 33(4): p. 395-402.
22. Okuda, T., Z. Cai, S. Yang, N. Lenny, C.J. Lyu, J.M. van Deursen, H. Harada, and J.R. Downing, *Expression of a knocked-in AML1-ETO leukemia gene inhibits the establishment of normal definitive hematopoiesis and directly generates dysplastic hematopoietic progenitors.* Blood, 1998. 91(9): p. 3134-43.
23. Zhang, D.E., P. Zhang, N.D. Wang, C.J. Hetherington, G.J. Darlington, and D.G. Tenen, *Absence of granulocyte colony-stimulating factor signaling and neutrophil development in CCAAT enhancer binding protein alpha-deficient mice.* Proc Natl Acad Sci U S A, 1997. 94(2): p. 569-74.
24. Hock, H., M.J. Hamblen, H.M. Rooke, D. Traver, R.T. Bronson, S. Cameron, and S.H. Orkin, *Intrinsic requirement for zinc finger transcription factor Gfi-1 in neutrophil differentiation.* Immunity, 2003. 18(1): p. 109-20.
25. Keeshan, K., G. Santilli, F. Corradini, D. Perrotti, and B. Calabretta, *Transcription activation function of C/EBPalpha is required for induction of granulocytic differentiation.* Blood, 2003. 102(4): p. 1267-75.
26. Rosenbauer, F. and D.G. Tenen, *Transcription factors in myeloid development: balancing differentiation with transformation.* Nat Rev Immunol, 2007. 7(2): p. 105-17.
27. Tamura, T., T. Nagamura-Inoue, Z. Shmeltzer, T. Kuwata, and K. Ozato, *ICSBP directs bipotential myeloid progenitor cells to differentiate into mature macrophages.* Immunity, 2000. 13(2): p. 155-65.
28. Diakiw, S.M., C.H. Kok, L.B. To, I.D. Lewis, A.L. Brown, and R.J. D'Andrea, *The granulocyte-associated transcription factor Kruppel-like factor 5 is silenced by hypermethylation in acute myeloid leukemia.* Leuk Res, 2012. 36(1): p. 110-6.
29. Yamanaka, R., C. Barlow, J. Lekstrom-Himes, L.H. Castilla, P.P. Liu, M. Eckhaus, T. Decker, A. Wynshaw-Boris, and K.G. Xanthopoulos, *Impaired granulopoiesis, myelodysplasia, and early lethality in CCAAT/enhancer binding protein epsilon-deficient mice.* Proc Natl Acad Sci U S A, 1997. 94(24): p. 13187-92.
30. Okuda, T., J. van Deursen, S.W. Hiebert, G. Grosveld, and J.R. Downing, *AML1, the target of multiple chromosomal translocations in human leukemia, is essential for normal fetal liver hematopoiesis.* Cell, 1996. 84(2): p. 321-30.
31. Alder, J.K., R.W. Georgantas, 3rd, R.L. Hildreth, I.M. Kaplan, S. Morisot, X. Yu, M. McDevitt, and C.I. Civin, *Kruppel-like factor 4 is essential for inflammatory monocyte differentiation in vivo.* J Immunol, 2008. 180(8): p. 5645-52.
32. Shivdasani, R.A., E.L. Mayer, and S.H. Orkin, *Absence of blood formation in mice lacking the T-cell leukaemia oncoprotein tal-1/SCL.* Nature, 1995. 373(6513): p. 432-4.
33. Humbert, M., V. Halter, D. Shan, J. Laedrach, E.O. Leibundgut, G.M. Baerlocher, A. Tobler, M.F. Fey, and M.P. Tschan, *Deregulated expression of Kruppel-like factors in acute myeloid leukemia.* Leuk Res, 2011. 35(7): p. 909-13.
34. Barnes, M.R., *Genetic variation analysis for biomedical researchers: a primer.* Methods Mol Biol, 2010. 628: p. 1-20.
35. Van de Peer, Y., J.A. Fawcett, S. Proost, L. Sterck, and K. Vandepoele, *The flowering world: a tale of duplications.* Trends Plant Sci, 2009. 14(12): p. 680-8.

36. Hastings, P.J., J.R. Lupski, S.M. Rosenberg, and G. Ira, *Mechanisms of change in gene copy number.* Nat Rev Genet, 2009. 10(8): p. 551-64.
37. Irvine, R.A., I.G. Lin, and C.L. Hsieh, *DNA methylation has a local effect on transcription and histone acetylation.* Mol Cell Biol, 2002. 22(19): p. 6689-96.
38. Pabst, T., B.U. Mueller, P. Zhang, H.S. Radomska, S. Narravula, S. Schnittger, G. Behre, W. Hiddemann, and D.G. Tenen, *Dominant-negative mutations of CEBPA, encoding CCAAT/enhancer binding protein-alpha (C/EBPalpha), in acute myeloid leukemia.* Nat Genet, 2001. 27(3): p. 263-70.
39. Gombart, A.F., W.K. Hofmann, S. Kawano, S. Takeuchi, U. Krug, S.H. Kwok, R.J. Larsen, H. Asou, C.W. Miller, D. Hoelzer, and H.P. Koeffler, *Mutations in the gene encoding the transcription factor CCAAT/enhancer binding protein alpha in myelodysplastic syndromes and acute myeloid leukemias.* Blood, 2002. 99(4): p. 1332-40.
40. Kirstetter, P., M.B. Schuster, O. Bereshchenko, S. Moore, H. Dvinge, E. Kurz, K. Theilgaard-Monch, R. Mansson, T.A. Pedersen, T. Pabst, E. Schrock, B.T. Porse, S.E. Jacobsen, P. Bertone, D.G. Tenen, and C. Nerlov, *Modeling of C/EBPalpha mutant acute myeloid leukemia reveals a common expression signature of committed myeloid leukemia-initiating cells.* Cancer Cell, 2008. 13(4): p. 299-310.
41. Schuster, M.B., A.K. Frank, F.O. Bagger, N. Rapin, J. Vikesaa, and B.T. Porse, *Lack of the p42 form of C/EBPalpha leads to spontaneous immortalization and lineage infidelity of committed myeloid progenitors.* Exp Hematol, 2013. 41(10): p. 882-893 e16.
42. Zhang, P., J. Iwasaki-Arai, H. Iwasaki, M.L. Fenyus, T. Dayaram, B.M. Owens, H. Shigematsu, E. Levantini, C.S. Huettner, J.A. Lekstrom-Himes, K. Akashi, and D.G. Tenen, *Enhancement of Hematopoietic Stem Cell Repopulating Capacity and Self-Renewal in the Absence of the Transcription Factor C/EBP[alpha].* Immunity, 2004. 21(6): p. 853-863.
43. Zhang, H., M. Alberich-Jorda, G. Amabile, H. Yang, P.B. Staber, A. Diruscio, R.S. Welner, A. Ebralidze, J. Zhang, E. Levantini, V. Lefebvre, P.J. Valk, R. Delwel, M. Hoogenkamp, C. Nerlov, J. Cammenga, B. Saez, D.T. Scadden, C. Bonifer, M. Ye, and D.G. Tenen, *Sox4 is a key oncogenic target in C/EBPalpha mutant acute myeloid leukemia.* Cancer Cell, 2013. 24(5): p. 575-88.
44. Downing, J.R., *The AML1-ETO chimaeric transcription factor in acute myeloid leukaemia: biology and clinical significance.* Br J Haematol, 1999. 106(2): p. 296-308.
45. Cai, Z., M. de Bruijn, X. Ma, B. Dortland, T. Luteijn, J.R. Downing, and E. Dzierzak, *Haploinsufficiency of AML1 Affects the Temporal and Spatial Generation of Hematopoietic Stem Cells in the Mouse Embryo.* Immunity, 2000. 13(4): p. 423-431.
46. Podgornik, H., M. Debeljak, D. Zontar, P. Cernelc, V.V. Prestor, and J. Jazbec, *RUNX1 amplification in lineage conversion of childhood B-cell acute lymphoblastic leukemia to acute myelogenous leukemia.* Cancer Genet Cytogenet, 2007. 178(1): p. 77-81.
47. Gulten, T., T. Yakut, M. Karkucak, B. Baytan, and A.M. Gunes, *AML1 amplification and 17q25 deletion in a case of childhood acute lymphoblastic leukemia.* J Clin Lab Anal, 2009. 23(6): p. 368-71.
48. Chim, C.S., A.S. Wong, and Y.L. Kwong, *Infrequent hypermethylation of CEBPA promotor in acute myeloid leukaemia.* Br J Haematol, 2002. 119(4): p. 988-90.
49. Szankasi, P., A.K. Ho, D.W. Bahler, O. Efimova, and T.W. Kelley, *Combined testing for CCAAT/enhancer-binding protein alpha (CEBPA) mutations and promoter methylation in acute myeloid leukemia demonstrates shared phenotypic features.* Leuk Res, 2011. 35(2): p. 200-7.
50. Jost, E., O.N. do, S. Wilop, J.G. Herman, R. Osieka, and O. Galm, *Aberrant DNA methylation of the transcription factor C/EBPalpha in acute myelogenous leukemia.* Leuk Res, 2009. 33(3): p. 443-9.
51. Ko, Y.C., W.H. Fang, T.C. Lin, H.A. Hou, C.Y. Chen, H.F. Tien, and L.I. Lin, *MicroRNA let-7a-3 gene methylation is associated with karyotyping, CEBPA promoter methylation, and survival in acute myeloid leukemia.* Leuk Res, 2014. 38(5): p. 625-31.

52. Diakiw, S.M., M. Perugini, C.H. Kok, G.A. Engler, N. Cummings, L.B. To, A.H. Wei, I.D. Lewis, A.L. Brown, and R.J. D'Andrea, *Methylation of KLF5 contributes to reduced expression in acute myeloid leukaemia and is associated with poor overall survival.* Br J Haematol, 2013.
53. Pearson, R., J. Fleetwood, S. Eaton, M. Crossley, and S. Bao, *Kruppel-like transcription factors: a functional family.* Int J Biochem Cell Biol, 2008. 40(10): p. 1996-2001.
54. Nagai, R., T. Suzuki, K. Aizawa, T. Shindo, and I. Manabe, *Significance of the transcription factor KLF5 in cardiovascular remodeling.* J Thromb Haemost, 2005. 3(8): p. 1569-76.
55. Dang, D.T., J. Pevsner, and V.W. Yang, *The biology of the mammalian Krüppel-like family of transcription factors.* The International Journal of Biochemistry & Cell Biology, 2000. 32(11-12): p. 1103-1121.
56. Knoedler, J.R. and R.J. Denver, *Kruppel-like factors are effectors of nuclear receptor signaling.* Gen Comp Endocrinol, 2014. 203C: p. 49-59.
57. Turner, J. and M. Crossley, *Cloning and characterization of mCtBP2, a co-repressor that associates with basic Kruppel-like factor and other mammalian transcriptional regulators.* EMBO J, 1998. 17(17): p. 5129-40.
58. Zhang, J.S., M.C. Moncrieffe, J. Kaczynski, V. Ellenrieder, F.G. Prendergast, and R. Urrutia, *A conserved alpha-helical motif mediates the interaction of Sp1-like transcriptional repressors with the corepressor mSin3A.* Mol Cell Biol, 2001. 21(15): p. 5041-9.
59. Nandan, M.O. and V.W. Yang, *The role of Kruppel-like factors in the reprogramming of somatic cells to induced pluripotent stem cells.* Histol Histopathol, 2009. 24(10): p. 1343-55.
60. Black, A.R., J.D. Black, and J. Azizkhan-Clifford, *Sp1 and kruppel-like factor family of transcription factors in cell growth regulation and cancer.* J Cell Physiol, 2001. 188(2): p. 143-60.
61. Simmen, R.C., J.M. Pabona, M.C. Velarde, C. Simmons, O. Rahal, and F.A. Simmen, *The emerging role of Kruppel-like factors in endocrine-responsive cancers of female reproductive tissues.* J Endocrinol, 2010. 204(3): p. 223-31.
62. Suske, G., E. Bruford, and S. Philipsen, *Mammalian SP/KLF transcription factors: bring in the family.* Genomics, 2005. 85(5): p. 551-6.
63. Mayani, H., E. Flores-Figueroa, and A. Chavez-Gonzalez, *In vitro biology of human myeloid leukemia.* Leuk Res, 2008.
64. Frohling, S., R.F. Schlenk, I. Stolze, J. Bihlmayr, A. Benner, S. Kreitmeier, K. Tobis, H. Dohner, and K. Dohner, *CEBPA mutations in younger adults with acute myeloid leukemia and normal cytogenetics: prognostic relevance and analysis of cooperating mutations.* J Clin Oncol, 2004. 22(4): p. 624-33.
65. Steffen, B., C. Muller-Tidow, J. Schwable, W.E. Berdel, and H. Serve, *The molecular pathogenesis of acute myeloid leukemia.* Crit Rev Oncol Hematol, 2005. 56(2): p. 195-221.
66. Nakamura, Y., T. Migita, F. Hosoda, N. Okada, M. Gotoh, Y. Arai, M. Fukushima, M. Ohki, S. Miyata, K. Takeuchi, I. Imoto, H. Katai, T. Yamaguchi, J. Inazawa, S. Hirohashi, Y. Ishikawa, and T. Shibata, *Kruppel-like factor 12 plays a significant role in poorly differentiated gastric cancer progression.* Int J Cancer, 2009. 125(8): p. 1859-67.
67. Henson, B.J. and S.M. Gollin, *Overexpression of KLF13 and FGFR3 in oral cancer cells.* Cytogenet Genome Res, 2010. 128(4): p. 192-8.
68. Dang, D.T., W. Zhao, C.S. Mahatan, D.E. Geiman, and V.W. Yang, *Opposing effects of Kruppel-like factor 4 (gut-enriched Kruppel-like factor) and Kruppel-like factor 5 (intestinal-enriched Kruppel-like factor) on the promoter of the Kruppel-like factor 4 gene.* Nucleic Acids Res, 2002. 30(13): p. 2736-41.

69. Eaton, S.A., A.P. Funnell, N. Sue, H. Nicholas, R.C. Pearson, and M. Crossley, *A network of Kruppel-like Factors (Klfs). Klf8 is repressed by Klf3 and activated by Klf1 in vivo.* J Biol Chem, 2008. 283(40): p. 26937-47.
70. Shi, H., Z. Zhang, X. Wang, S. Liu, and C.T. Teng, *Isolation and characterization of a gene encoding human Kruppel-like factor 5 (IKLF): binding to the CAAT/GT box of the mouse lactoferrin gene promoter.* Nucleic Acids Res, 1999. 27(24): p. 4807-15.
71. Perkins, A.C., A.H. Sharpe, and S.H. Orkin, *Lethal beta-thalassaemia in mice lacking the erythroid CACCC-transcription factor EKLF.* Nature, 1995. 375(6529): p. 318-22.
72. Kuo, C.T., M.L. Veselits, K.P. Barton, M.M. Lu, C. Clendenin, and J.M. Leiden, *The LKLF transcription factor is required for normal tunica media formation and blood vessel stabilization during murine embryogenesis.* Genes Dev, 1997. 11(22): p. 2996-3006.
73. Wani, M.A., R.T. Means, Jr., and J.B. Lingrel, *Loss of LKLF function results in embryonic lethality in mice.* Transgenic Res, 1998. 7(4): p. 229-38.
74. Vu, T.T., D. Gatto, V. Turner, A.P. Funnell, K.S. Mak, L.J. Norton, W. Kaplan, M.J. Cowley, F. Agenes, J. Kirberg, R. Brink, R.C. Pearson, and M. Crossley, *Impaired B cell development in the absence of Kruppel-like factor 3.* J Immunol, 2011. 187(10): p. 5032-42.
75. Sue, N., B.H. Jack, S.A. Eaton, R.C. Pearson, A.P. Funnell, J. Turner, R. Czolij, G. Denyer, S. Bao, J.C. Molero-Navajas, A. Perkins, Y. Fujiwara, S.H. Orkin, K. Bell-Anderson, and M. Crossley, *Targeted disruption of the basic Kruppel-like factor gene (Klf3) reveals a role in adipogenesis.* Mol Cell Biol, 2008. 28(12): p. 3967-78.
76. Segre, J.A., C. Bauer, and E. Fuchs, *Klf4 is a transcription factor required for establishing the barrier function of the skin.* Nat Genet, 1999. 22(4): p. 356-60.
77. Katz, J.P., N. Perreault, B.G. Goldstein, C.S. Lee, P.A. Labosky, V.W. Yang, and K.H. Kaestner, *The zinc-finger transcription factor Klf4 is required for terminal differentiation of goblet cells in the colon.* Development, 2002. 129(11): p. 2619-28.
78. Oishi, Y., I. Manabe, K. Tobe, K. Tsushima, T. Shindo, K. Fujiu, G. Nishimura, K. Maemura, T. Yamauchi, N. Kubota, R. Suzuki, T. Kitamura, S. Akira, T. Kadowaki, and R. Nagai, *Kruppel-like transcription factor KLF5 is a key regulator of adipocyte differentiation.* Cell Metab, 2005. 1(1): p. 27-39.
79. Shindo, T., I. Manabe, Y. Fukushima, K. Tobe, K. Aizawa, S. Miyamoto, K. Kawai-Kowase, N. Moriyama, Y. Imai, H. Kawakami, H. Nishimatsu, T. Ishikawa, T. Suzuki, H. Morita, K. Maemura, M. Sata, Y. Hirata, M. Komukai, H. Kagechika, T. Kadowaki, M. Kurabayashi, and R. Nagai, *Kruppel-like zinc-finger transcription factor KLF5/BTEB2 is a target for angiotensin II signaling and an essential regulator of cardiovascular remodeling.* Nat Med, 2002. 8(8): p. 856-63.
80. Matsumoto, N., A. Kubo, H. Liu, K. Akita, F. Laub, F. Ramirez, G. Keller, and S.L. Friedman, *Developmental regulation of yolk sac hematopoiesis by Kruppel-like factor 6.* Blood, 2006. 107(4): p. 1357-65.
81. Laub, F., L. Lei, H. Sumiyoshi, D. Kajimura, C. Dragomir, S. Smaldone, A.C. Puche, T.J. Petros, C. Mason, L.F. Parada, and F. Ramirez, *Transcription factor KLF7 is important for neuronal morphogenesis in selected regions of the nervous system.* Mol Cell Biol, 2005. 25(13): p. 5699-711.
82. Morita, M., A. Kobayashi, T. Yamashita, T. Shimanuki, O. Nakajima, S. Takahashi, S. Ikegami, K. Inokuchi, K. Yamashita, M. Yamamoto, and Y. Fujii-Kuriyama, *Functional analysis of basic transcription element binding protein by gene targeting technology.* Mol Cell Biol, 2003. 23(7): p. 2489-500.
83. Simmen, R.C., R.R. Eason, J.R. McQuown, A.L. Linz, T.J. Kang, L. Chatman, Jr., S.R. Till, Y. Fujii-Kuriyama, F.A. Simmen, and S.P. Oh, *Subfertility, uterine hypoplasia, and partial progesterone resistance in mice lacking the Kruppel-like factor 9/basic transcription element-binding protein-1 (Bteb1) gene.* J Biol Chem, 2004. 279(28): p. 29286-94.
84. Subramaniam, M., G. Gorny, S.A. Johnsen, D.G. Monroe, G.L. Evans, D.G. Fraser, D.J. Rickard, K. Rasmussen, J.M. van Deursen, R.T. Turner, M.J. Oursler, and T.C. Spelsberg,

TIEG1 null mouse-derived osteoblasts are defective in mineralization and in support of osteoclast differentiation in vitro. Mol Cell Biol, 2005. 25(3): p. 1191-9.
85. Song, C.Z., G. Gavriilidis, H. Asano, and G. Stamatoyannopoulos, *Functional study of transcription factor KLF11 by targeted gene inactivation.* Blood Cells Mol Dis, 2005. 34(1): p. 53-9.
86. Zhou, M., L. McPherson, D. Feng, A. Song, C. Dong, S.C. Lyu, L. Zhou, X. Shi, Y.T. Ahn, D. Wang, C. Clayberger, and A.M. Krensky, *Kruppel-like transcription factor 13 regulates T lymphocyte survival in vivo.* J Immunol, 2007. 178(9): p. 5496-504.
87. Fisch, S., S. Gray, S. Heymans, S.M. Haldar, B. Wang, O. Pfister, L. Cui, A. Kumar, Z. Lin, S. Sen-Banerjee, H. Das, C.A. Petersen, U. Mende, B.A. Burleigh, Y. Zhu, Y.M. Pinto, R. Liao, and M.K. Jain, *Kruppel-like factor 15 is a regulator of cardiomyocyte hypertrophy.* Proc Natl Acad Sci U S A, 2007. 104(17): p. 7074-9.
88. Rosenzweig, J.M., J.D. Glenn, P.A. Calabresi, and K.A. Whartenby, *KLF4 modulates expression of IL-6 in dendritic cells via both promoter activation and epigenetic modification.* J Biol Chem, 2013. 288(33): p. 23868-74.
89. Basu, P., T.G. Sargent, L.C. Redmond, J.C. Aisenberg, E.P. Kransdorf, S.Z. Wang, G.D. Ginder, and J.A. Lloyd, *Evolutionary conservation of KLF transcription factors and functional conservation of human [gamma]-globin gene regulation in chicken.* Genomics, 2004. 84(2): p. 311-319.
90. Funnell, A.P., L.J. Norton, K.S. Mak, J. Burdach, C.M. Artuz, N.A. Twine, M.R. Wilkins, C.A. Power, T.T. Hung, J. Perdomo, P. Koh, K.S. Bell-Anderson, S.H. Orkin, S.T. Fraser, A.C. Perkins, R.C. Pearson, and M. Crossley, *The CACCC-binding protein KLF3/BKLF represses a subset of KLF1/EKLF target genes and is required for proper erythroid maturation in vivo.* Mol Cell Biol, 2012. 32(16): p. 3281-92.
91. Aksoy, I., V. Giudice, E. Delahaye, F. Wianny, M. Aubry, M. Mure, J. Chen, R. Jauch, G.K. Bogu, T. Nolden, H. Himmelbauer, M. Xavier Doss, A. Sachinidis, H. Schulz, O. Hummel, P. Martinelli, N. Hubner, L.W. Stanton, F.X. Real, P.Y. Bourillot, and P. Savatier, *Klf4 and Klf5 differentially inhibit mesoderm and endoderm differentiation in embryonic stem cells.* Nat Commun, 2014. 5: p. 3719.
92. Tetreault, M.P., Y. Yang, and J.P. Katz, *Kruppel-like factors in cancer.* Nat Rev Cancer, 2013. 13(10): p. 701-13.
93. Limame, R., K. Op de Beeck, F. Lardon, O. De Wever, and P. Pauwels, *Kruppel-like factors in cancer progression: three fingers on the steering wheel.* Oncotarget, 2014. 5(1): p. 29-48.
94. Chen, Z.Y., J. Shie, and C. Tseng, *Up-regulation of gut-enriched kruppel-like factor by interferon-gamma in human colon carcinoma cells.* FEBS Lett, 2000. 477(1-2): p. 67-72.
95. Wang, X. and J. Zhao, *KLF8 transcription factor participates in oncogenic transformation.* Oncogene, 2007. 26(3): p. 456-61.
96. Wang, X., A.M. Urvalek, J. Liu, and J. Zhao, *Activation of KLF8 transcription by focal adhesion kinase in human ovarian epithelial and cancer cells.* J Biol Chem, 2008. 283(20): p. 13934-42.
97. Li, J.C., X.R. Yang, H.X. Sun, Y. Xu, J. Zhou, S.J. Qiu, A.W. Ke, Y.H. Cui, Z.J. Wang, W.M. Wang, K.D. Liu, and J. Fan, *Up-regulation of Kruppel-like factor 8 promotes tumor invasion and indicates poor prognosis for hepatocellular carcinoma.* Gastroenterology, 2010. 139(6): p. 2146-2157 e12.
98. Wang, X., H. Lu, A.M. Urvalek, T. Li, L. Yu, J. Lamar, C.M. DiPersio, P.J. Feustel, and J. Zhao, *KLF8 promotes human breast cancer cell invasion and metastasis by transcriptional activation of MMP9.* Oncogene, 2011. 30(16): p. 1901-11.
99. Wang, X., H. Lu, T. Li, L. Yu, G. Liu, X. Peng, and J. Zhao, *Kruppel-like factor 8 promotes tumorigenic mammary stem cell induction by targeting miR-146a.* Am J Cancer Res, 2013. 3(4): p. 356-73.

100. Lin, F., Z. Shen, L.N. Tang, S.E. Zheng, Y.J. Sun, D.L. Min, and Y. Yao, *KLF8 knockdown suppresses proliferation and invasion in human osteosarcoma cells.* Mol Med Rep, 2014. 9(5): p. 1613-7.
101. Lu, H., X. Wang, A.M. Urvalek, T. Li, H. Xie, L. Yu, and J. Zhao, *Transformation of human ovarian surface epithelial cells by Kruppel-like factor 8.* Oncogene, 2014. 33(1): p. 10-8.
102. Choi, B.J., Y.G. Cho, J.W. Song, C.J. Kim, S.Y. Kim, S.W. Nam, N.J. Yoo, J.Y. Lee, and W.S. Park, *Altered expression of the KLF4 in colorectal cancers.* Pathol Res Pract, 2006. 202(8): p. 585-9.
103. Kanai, M., D. Wei, Q. Li, Z. Jia, J. Ajani, X. Le, J. Yao, and K. Xie, *Loss of Kruppel-like factor 4 expression contributes to Sp1 overexpression and human gastric cancer development and progression.* Clin Cancer Res, 2006. 12(21): p. 6395-402.
104. Yu, F., J. Li, H. Chen, J. Fu, S. Ray, S. Huang, H. Zheng, and W. Ai, *Kruppel-like factor 4 (KLF4) is required for maintenance of breast cancer stem cells and for cell migration and invasion.* Oncogene, 2011. 30(18): p. 2161-72.
105. Wang, N., Z.H. Liu, F. Ding, X.Q. Wang, C.N. Zhou, and M. Wu, *Down-regulation of gut-enriched Kruppel-like factor expression in esophageal cancer.* World J Gastroenterol, 2002. 8(6): p. 966-70.
106. Bloethner, S., K. Hemminki, R.K. Thirumaran, B. Chen, J. Mueller-Berghaus, S. Ugurel, D. Schadendorf, and R. Kumar, *Differences in global gene expression in melanoma cell lines with and without homozygous deletion of the CDKN2A locus genes.* Melanoma Res, 2006. 16(4): p. 297-307.
107. Kharas, M.G., I. Yusuf, V.M. Scarfone, V.W. Yang, J.A. Segre, C.S. Huettner, and D.A. Fruman, *KLF4 suppresses transformation of pre-B cells by ABL oncogenes.* Blood, 2007. 109(2): p. 747-55.
108. Yasunaga, J., Y. Taniguchi, K. Nosaka, M. Yoshida, Y. Satou, T. Sakai, H. Mitsuya, and M. Matsuoka, *Identification of aberrantly methylated genes in association with adult T-cell leukemia.* Cancer Res, 2004. 64(17): p. 6002-9.
109. Nandan, M.O., B.B. McConnell, A.M. Ghaleb, A.B. Bialkowska, H. Sheng, J. Shao, B.A. Babbin, S. Robine, and V.W. Yang, *Kruppel-like factor 5 mediates cellular transformation during oncogenic KRAS-induced intestinal tumorigenesis.* Gastroenterology, 2008. 134(1): p. 120-30.
110. Zhang, H., A. Bialkowska, R. Rusovici, S. Chanchevalap, H. Shim, J.P. Katz, V.W. Yang, and C.C. Yun, *Lysophosphatidic acid facilitates proliferation of colon cancer cells via induction of Kruppel-like factor 5.* J Biol Chem, 2007. 282(21): p. 15541-9.
111. Zhao, Y., M.S. Hamza, H.S. Leong, C.B. Lim, Y.F. Pan, E. Cheung, K.C. Soo, and N.G. Iyer, *Kruppel-like factor 5 modulates p53-independent apoptosis through Pim1 survival kinase in cancer cells.* Oncogene, 2008. 27(1): p. 1-8.
112. Poulogiannis, G., F. Luo, and M.J. Arends, *RAS signalling in the colorectum in health and disease.* Cell Commun Adhes, 2012. 19(1): p. 1-9.
113. Kwak, M.K., H.J. Lee, K. Hur, J. Park do, H.S. Lee, W.H. Kim, K.U. Lee, K.J. Choe, P. Guilford, and H.K. Yang, *Expression of Kruppel-like factor 5 in human gastric carcinomas.* J Cancer Res Clin Oncol, 2008. 134(2): p. 163-7.
114. Chen, C., M.S. Benjamin, X. Sun, K.B. Otto, P. Guo, X.Y. Dong, Y. Bao, Z. Zhou, X. Cheng, J.W. Simons, and J.T. Dong, *KLF5 promotes cell proliferation and tumorigenesis through gene regulation and the TSU-Pr1 human bladder cancer cell line.* Int J Cancer, 2006. 118(6): p. 1346-55.
115. Chen, C., H.V. Bhalala, H. Qiao, and J.T. Dong, *A possible tumor suppressor role of the KLF5 transcription factor in human breast cancer.* Oncogene, 2002. 21(43): p. 6567-72.
116. Zheng, H.Q., Z. Zhou, J. Huang, L. Chaudhury, J.T. Dong, and C. Chen, *Kruppel-like factor 5 promotes breast cell proliferation partially through upregulating the transcription of fibroblast growth factor binding protein 1.* Oncogene, 2009. 28(42): p. 3702-13.

117. Bloethner, S., B. Chen, K. Hemminki, J. Muller-Berghaus, S. Ugurel, D. Schadendorf, and R. Kumar, *Effect of common B-RAF and N-RAS mutations on global gene expression in melanoma cell lines.* Carcinogenesis, 2005. 26(7): p. 1224-32.
118. Sur, I., A.B. Unden, and R. Toftgard, *Human Kruppel-like factor5/KLF5: synergy with NF-kappaB/Rel factors and expression in human skin and hair follicles.* Eur J Cell Biol, 2002. 81(6): p. 323-34.
119. Li, Q., Z. Dong, F. Zhou, X. Cai, Y. Gao, and L.W. Wang, *Kruppel-Like Factor 5 Promotes Lung Tumorigenesis through Upregulation of Sox4.* Cell Physiol Biochem, 2014. 33(1): p. 1-10.
120. Zhu, N., L. Gu, H.W. Findley, C. Chen, J.T. Dong, L. Yang, and M. Zhou, *KLF5 Interacts with p53 in regulating survivin expression in acute lymphoblastic leukemia.* J Biol Chem, 2006. 281(21): p. 14711-8.
121. Reeves, H.L., G. Narla, O. Ogunbiyi, A.I. Haq, A. Katz, S. Benzeno, E. Hod, N. Harpaz, S. Goldberg, S. Tal-Kremer, F.J. Eng, M.J. Arthur, J.A. Martignetti, and S.L. Friedman, *Kruppel-like factor 6 (KLF6) is a tumor-suppressor gene frequently inactivated in colorectal cancer.* Gastroenterology, 2004. 126(4): p. 1090-103.
122. Sangodkar, J., J. Shi, A. DiFeo, R. Schwartz, R. Bromberg, A. Choudhri, K. McClinch, R. Hatami, E. Scheer, S. Kremer-Tal, J.A. Martignetti, A. Hui, W.K. Leung, S.L. Friedman, and G. Narla, *Functional role of the KLF6 tumour suppressor gene in gastric cancer.* Eur J Cancer, 2009. 45(4): p. 666-76.
123. Narla, G., K.E. Heath, H.L. Reeves, D. Li, L.E. Giono, A.C. Kimmelman, M.J. Glucksman, J. Narla, F.J. Eng, A.M. Chan, A.C. Ferrari, J.A. Martignetti, and S.L. Friedman, *KLF6, a candidate tumor suppressor gene mutated in prostate cancer.* Science, 2001. 294(5551): p. 2563-6.
124. Narla, G., A. DiFeo, S. Yao, A. Banno, E. Hod, H.L. Reeves, R.F. Qiao, O. Camacho-Vanegas, A. Levine, A. Kirschenbaum, A.M. Chan, S.L. Friedman, and J.A. Martignetti, *Targeted inhibition of the KLF6 splice variant, KLF6 SV1, suppresses prostate cancer cell growth and spread.* Cancer Res, 2005. 65(13): p. 5761-8.
125. Hartel, M., G. Narla, M.N. Wente, N.A. Giese, M.E. Martignoni, J.A. Martignetti, H. Friess, and S.L. Friedman, *Increased alternative splicing of the KLF6 tumour suppressor gene correlates with prognosis and tumour grade in patients with pancreatic cancer.* Eur J Cancer, 2008. 44(13): p. 1895-903.
126. Ito, G., M. Uchiyama, M. Kondo, S. Mori, N. Usami, O. Maeda, T. Kawabe, Y. Hasegawa, K. Shimokata, and Y. Sekido, *Kruppel-like factor 6 is frequently down-regulated and induces apoptosis in non-small cell lung cancer cells.* Cancer Res, 2004. 64(11): p. 3838-43.
127. Camacho-Vanegas, O., G. Narla, M.S. Teixeira, A. DiFeo, A. Misra, G. Singh, A.M. Chan, S.L. Friedman, B.G. Feuerstein, and J.A. Martignetti, *Functional inactivation of the KLF6 tumor suppressor gene by loss of heterozygosity and increased alternative splicing in glioblastoma.* Int J Cancer, 2007. 121(6): p. 1390-5.
128. Guo, H., Y. Lin, H. Zhang, J. Liu, N. Zhang, Y. Li, D. Kong, Q. Tang, and D. Ma, *Tissue factor pathway inhibitor-2 was repressed by CpG hypermethylation through inhibition of KLF6 binding in highly invasive breast cancer cells.* BMC Mol Biol, 2007. 8(110): p. 110.
129. DiFeo, A., G. Narla, J. Hirshfeld, O. Camacho-Vanegas, J. Narla, S.L. Rose, T. Kalir, S. Yao, A. Levine, M.J. Birrer, T. Bonome, S.L. Friedman, R.E. Buller, and J.A. Martignetti, *Roles of KLF6 and KLF6-SV1 in ovarian cancer progression and intraperitoneal dissemination.* Clin Cancer Res, 2006. 12(12): p. 3730-9.
130. Yang, M., H.S. Kim, and M.Y. Cho, *Different methylation profiles between intestinal and diffuse sporadic gastric carcinogenesis.* Clin Res Hepatol Gastroenterol, 2014. 38(5): p. 613-20.
131. Kang, L., B. Lu, J. Xu, H. Hu, and M. Lai, *Downregulation of Kruppel-like factor 9 in human colorectal cancer.* Pathol Int, 2008. 58(6): p. 334-8.

132. Song, K.D., D.J. Kim, J.E. Lee, C.H. Yun, and W.K. Lee, *KLF10, transforming growth factor-beta-inducible early gene 1, acts as a tumor suppressor.* Biochem Biophys Res Commun, 2012. 419(2): p. 388-94.
133. Hwang, Y.C., C.H. Yang, C.H. Lin, H.J. Ch'ang, V.H. Chang, and W.C. Yu, *Destabilization of KLF10, a tumor suppressor, relies on thr93 phosphorylation and isomerase association.* Biochim Biophys Acta, 2013. 1833(12): p. 3035-45.
134. Chang, V.H., P.Y. Chu, S.L. Peng, T.L. Mao, Y.S. Shan, C.F. Hsu, C.Y. Lin, K.K. Tsai, W.C. Yu, and H.J. Ch'ang, *Kruppel-like factor 10 expression as a prognostic indicator for pancreatic adenocarcinoma.* Am J Pathol, 2012. 181(2): p. 423-30.
135. Buck, A., M. Buchholz, M. Wagner, G. Adler, T. Gress, and V. Ellenrieder, *The tumor suppressor KLF11 mediates a novel mechanism in transforming growth factor beta-induced growth inhibition that is inactivated in pancreatic cancer.* Mol Cancer Res, 2006. 4(11): p. 861-72.
136. Yin, P., Z. Lin, S. Reierstad, J. Wu, H. Ishikawa, E.E. Marsh, J. Innes, Y. Cheng, K. Pearson, J.S.t. Coon, J.J. Kim, D. Chakravarti, and S.E. Bulun, *Transcription factor KLF11 integrates progesterone receptor signaling and proliferation in uterine leiomyoma cells.* Cancer Res, 2010. 70(4): p. 1722-30.
137. Peng, J.J., B. Wu, X.B. Xiao, Y.S. Shao, Y. Feng, and M.X. Yin, *Reduced Kruppel-like factor 17 (KLF17) expression correlates with poor survival in patients with gastric cancer.* Arch Med Res, 2014. 45(5): p. 394-9.
138. Ali, A., A.S. Shah, and A. Ahmad, *Gain-of-function of mutant p53: mutant p53 enhances cancer progression by inhibiting KLF17 expression in invasive breast carcinoma cells.* Cancer Lett, 2014. 354(1): p. 87-96.
139. Ismail, I.A., H.S. Kang, H.J. Lee, J.K. Kim, and S.H. Hong, *DJ-1 upregulates breast cancer cell invasion by repressing KLF17 expression.* Br J Cancer, 2014. 110(5): p. 1298-306.
140. Sun, Z., Q. Han, N. Zhou, S. Wang, S. Lu, C. Bai, and R.C. Zhao, *MicroRNA-9 enhances migration and invasion through KLF17 in hepatocellular carcinoma.* Mol Oncol, 2013. 7(5): p. 884-94.
141. Liu, F.Y., Y.L. Deng, Y. Li, D. Zeng, Z.Z. Zhou, D.A. Tian, and M. Liu, *Down-regulated KLF17 expression is associated with tumor invasion and poor prognosis in hepatocellular carcinoma.* Med Oncol, 2013. 30(1): p. 425.
142. Cai, X.D., Y.B. Zhou, L.X. Huang, Q.L. Zeng, L.J. Zhang, Q.Q. Wang, S.L. Li, J.Q. Feng, and A.J. Han, *Reduced expression of Kruppel-like factor 17 is related to tumor growth and poor prognosis in lung adenocarcinoma.* Biochem Biophys Res Commun, 2012. 418(1): p. 67-73.
143. Wang, W.F., J. Li, L.T. Du, L.L. Wang, Y.M. Yang, Y.M. Liu, H. Liu, X. Zhang, Z.G. Dong, G.X. Zheng, and C.X. Wang, *Kruppel-like factor 8 overexpression is correlated with angiogenesis and poor prognosis in gastric cancer.* World J Gastroenterol, 2013. 19(27): p. 4309-15.
144. Wei, Y., G. Chen, L. You, and Y. Zhao, *Krupel-like factor 8 is a potential prognostic factor for pancreatic cancer.* Chin Med J (Engl), 2014. 127(5): p. 856-9.
145. Hsu, L.S., P.R. Wu, K.T. Yeh, C.M. Yeh, K.H. Shen, C.J. Chen, and M.S. Soon, *Positive nuclear expression of KLF8 might be correlated with shorter survival in gastric adenocarcinoma.* Ann Diagn Pathol, 2014. 18(2): p. 74-7.
146. Foster, K.W., A.R. Frost, P. McKie-Bell, C.Y. Lin, J.A. Engler, W.E. Grizzle, and J.M. Ruppert, *Increase of GKLF messenger RNA and protein expression during progression of breast cancer.* Cancer Res, 2000. 60(22): p. 6488-95.
147. Leng, Z., K. Tao, Q. Xia, J. Tan, Z. Yue, J. Chen, H. Xi, J. Li, and H. Zheng, *Kruppel-like factor 4 acts as an oncogene in colon cancer stem cell-enriched spheroid cells.* PLoS One, 2013. 8(2): p. e56082.
148. Pandya, A.Y., L.I. Talley, A.R. Frost, T.J. Fitzgerald, V. Trivedi, M. Chakravarthy, D.C. Chhieng, W.E. Grizzle, J.A. Engler, H. Krontiras, K.I. Bland, A.F. LoBuglio, S.M. Lobo-Ruppert,

and J.M. Ruppert, *Nuclear localization of KLF4 is associated with an aggressive phenotype in early-stage breast cancer.* Clin Cancer Res, 2004. 10(8): p. 2709-19.
149. Wei, D., W. Gong, M. Kanai, C. Schlunk, L. Wang, J.C. Yao, T.T. Wu, S. Huang, and K. Xie, *Drastic down-regulation of Kruppel-like factor 4 expression is critical in human gastric cancer development and progression.* Cancer Res, 2005. 65(7): p. 2746-54.
150. Katz, J.P., N. Perreault, B.G. Goldstein, L. Actman, S.R. McNally, D.G. Silberg, E.E. Furth, and K.H. Kaestner, *Loss of Klf4 in mice causes altered proliferation and differentiation and precancerous changes in the adult stomach.* Gastroenterology, 2005. 128(4): p. 935-45.
151. Cheng, X.F., D. Li, M. Zhuang, Z.Y. Chen, D.X. Lu, and T. Hattori, *Growth inhibitory effect of Kruppel-like factor 6 on human prostatic carcinoma and renal carcinoma cell lines.* Tohoku J Exp Med, 2008. 216(1): p. 35-45.
152. Huang, X., X. Li, and B. Guo, *KLF6 induces apoptosis in prostate cancer cells through up-regulation of ATF3.* J Biol Chem, 2008. 283(44): p. 29795-801.
153. Mukai, S., T. Hiyama, S. Tanaka, M. Yoshihara, K. Arihiro, and K. Chayama, *Involvement of Kruppel-like factor 6 (KLF6) mutation in the development of nonpolypoid colorectal carcinoma.* World J Gastroenterol, 2007. 13(29): p. 3932-8.
154. Miyaki, M., T. Yamaguchi, T. Iijima, N. Funata, and T. Mori, *Difference in the role of loss of heterozygosity at 10p15 (KLF6 locus) in colorectal carcinogenesis between sporadic and familial adenomatous polyposis and hereditary nonpolyposis colorectal cancer patients.* Oncology, 2006. 71(1-2): p. 131-5.
155. Cho, Y.G., C.J. Kim, C.H. Park, Y.M. Yang, S.Y. Kim, S.W. Nam, S.H. Lee, N.J. Yoo, J.Y. Lee, and W.S. Park, *Genetic alterations of the KLF6 gene in gastric cancer.* Oncogene, 2005. 24(28): p. 4588-90.
156. Tahara, E., H. Kadara, L. Lacroix, D. Lotan, and R. Lotan, *Activation of protein kinase C by phorbol 12-myristate 13-acetate suppresses the growth of lung cancer cells through KLF6 induction.* Cancer Biol Ther, 2009. 8(9): p. 801-7.
157. Simmen, F.A., Y. Su, R. Xiao, Z. Zeng, and R.C. Simmen, *The Kruppel-like factor 9 (KLF9) network in HEC-1-A endometrial carcinoma cells suggests the carcinogenic potential of dys-regulated KLF9 expression.* Reprod Biol Endocrinol, 2008. 6: p. 41.
158. Korani, M., S. Fallah, A. Tehranian, M. Nourbakhsh, A. Samadikuchaksaraei, M.S. Pour, and J. Maleki, *The evaluation of the FOXO1, KLF9 and YT521 genes expression in human endometrial cancer.* Clin Lab, 2013. 59(5-6): p. 483-9.
159. Shen, P., J. Sun, G. Xu, L. Zhang, Z. Yang, S. Xia, Y. Wang, Y. Liu, and G. Shi, *KLF9, a transcription factor induced in flutamide-caused cell apoptosis, inhibits AKT activation and suppresses tumor growth of prostate cancer cells.* Prostate, 2014. 74(9): p. 946-58.
160. Zhang, X.L., D. Zhang, F.J. Michel, J.L. Blum, F.A. Simmen, and R.C. Simmen, *Selective interactions of Kruppel-like factor 9/basic transcription element-binding protein with progesterone receptor isoforms A and B determine transcriptional activity of progesterone-responsive genes in endometrial epithelial cells.* J Biol Chem, 2003. 278(24): p. 21474-82.
161. Zeng, Z., M.C. Velarde, F.A. Simmen, and R.C. Simmen, *Delayed parturition and altered myometrial progesterone receptor isoform A expression in mice null for Kruppel-like factor 9.* Biol Reprod, 2008. 78(6): p. 1029-37.
162. Ellenrieder, V., A. Buck, A. Harth, K. Jungert, M. Buchholz, G. Adler, R. Urrutia, and T.M. Gress, *KLF11 mediates a critical mechanism in TGF-beta signaling that is inactivated by Erk-MAPK in pancreatic cancer cells.* Gastroenterology, 2004. 127(2): p. 607-20.
163. Navarro, A., P. Yin, D. Monsivais, S.M. Lin, P. Du, J.J. Wei, and S.E. Bulun, *Genome-wide DNA methylation indicates silencing of tumor suppressor genes in uterine leiomyoma.* PLoS One, 2012. 7(3): p. e33284.
164. Wu, J. and J.B. Lingrel, *Kruppel-like factor 2, a novel immediate-early transcriptional factor, regulates IL-2 expression in T lymphocyte activation.* J Immunol, 2005. 175(5): p. 3060-6.

165. Carlson, C.M., B.T. Endrizzi, J. Wu, X. Ding, M.A. Weinreich, E.R. Walsh, M.A. Wani, J.B. Lingrel, K.A. Hogquist, and S.C. Jameson, *Kruppel-like factor 2 regulates thymocyte and T-cell migration.* Nature, 2006. 442(7100): p. 299-302.
166. Cao, Z., A.K. Wara, B. Icli, X. Sun, R.R. Packard, F. Esen, C.J. Stapleton, M. Subramaniam, K. Kretschmer, I. Apostolou, H. von Boehmer, G.K. Hansson, T.C. Spelsberg, P. Libby, and M.W. Feinberg, *Kruppel-like factor KLF10 targets transforming growth factor-beta1 to regulate CD4(+)CD25(-) T cells and T regulatory cells.* J Biol Chem, 2009. 284(37): p. 24914-24.
167. Hart, G.T., S.L. Peery, S.E. Hamilton, and S.C. Jameson, *Cutting edge: Kruppel-like factor 2 is required for phenotypic maintenance but not development of B1 B cells.* J Immunol, 2012. 189(7): p. 3293-7.
168. Good, K.L. and S.G. Tangye, *Decreased expression of Kruppel-like factors in memory B cells induces the rapid response typical of secondary antibody responses.* Proc Natl Acad Sci U S A, 2007. 104(33): p. 13420-5.
169. Feinberg, M.W., A.K. Wara, Z. Cao, M.A. Lebedeva, F. Rosenbauer, H. Iwasaki, H. Hirai, J.P. Katz, R.L. Haspel, S. Gray, K. Akashi, J. Segre, K.H. Kaestner, D.G. Tenen, and M.K. Jain, *The Kruppel-like factor KLF4 is a critical regulator of monocyte differentiation.* EMBO J, 2007. 26(18): p. 4138-48.
170. Funnell, A.P., C.A. Maloney, L.J. Thompson, J. Keys, M. Tallack, A.C. Perkins, and M. Crossley, *Erythroid Kruppel-like factor directly activates the basic Kruppel-like factor gene in erythroid cells.* Mol Cell Biol, 2007. 27(7): p. 2777-90.
171. Miller, I.J. and J.J. Bieker, *A novel, erythroid cell-specific murine transcription factor that binds to the CACCC element and is related to the Kruppel family of nuclear proteins.* Mol Cell Biol, 1993. 13(5): p. 2776-86.
172. Nuez, B., D. Michalovich, A. Bygrave, R. Ploemacher, and F. Grosveld, *Defective haematopoiesis in fetal liver resulting from inactivation of the EKLF gene.* Nature, 1995. 375(6529): p. 316-8.
173. Pang, C.J., W. Lemsaddek, Y.N. Alhashem, C. Bondzi, L.C. Redmond, N. Ah-Son, C.I. Dumur, K.J. Archer, J.L. Haar, J.A. Lloyd, and M. Trudel, *Kruppel-like factor 1 (KLF1), KLF2, and Myc control a regulatory network essential for embryonic erythropoiesis.* Mol Cell Biol, 2012. 32(13): p. 2628-44.
174. Alhashem, Y.N., D.S. Vinjamur, M. Basu, U. Klingmuller, K.M. Gaensler, and J.A. Lloyd, *Transcription factors KLF1 and KLF2 positively regulate embryonic and fetal beta-globin genes through direct promoter binding.* J Biol Chem, 2011. 286(28): p. 24819-27.
175. Redmond, L.C., C.I. Dumur, K.J. Archer, D.R. Grayson, J.L. Haar, and J.A. Lloyd, *Kruppel-like factor 2 regulated gene expression in mouse embryonic yolk sac erythroid cells.* Blood Cells Mol Dis, 2011. 47(1): p. 1-11.
176. Funnell, A.P., K.S. Mak, N.A. Twine, G.J. Pelka, L.J. Norton, T. Radziewic, M. Power, M.R. Wilkins, K.S. Bell-Anderson, S.T. Fraser, A.C. Perkins, P.P. Tam, R.C. Pearson, and M. Crossley, *Generation of mice deficient in both KLF3/BKLF and KLF8 reveals a genetic interaction and a role for these factors in embryonic globin gene silencing.* Mol Cell Biol, 2013. 33(15): p. 2976-87.
177. Gardiner, M.R., M.M. Gongora, S.M. Grimmond, and A.C. Perkins, *A global role for zebrafish klf4 in embryonic erythropoiesis.* Mech Dev, 2007. 124(9-10): p. 762-74.
178. Marini, M.G., L. Porcu, I. Asunis, M.G. Loi, M.S. Ristaldi, S. Porcu, T. Ikuta, A. Cao, and P. Moi, *Regulation of the human HBA genes by KLF4 in erythroid cell lines.* Br J Haematol, 2010. 149(5): p. 748-58.
179. Kalra, I.S., M.M. Alam, P.K. Choudhary, and B.S. Pace, *Kruppel-like Factor 4 activates HBG gene expression in primary erythroid cells.* Br J Haematol, 2011. 154(2): p. 248-59.
180. Zhang, P., P. Basu, L.C. Redmond, P.E. Morris, J.W. Rupon, G.D. Ginder, and J.A. Lloyd, *A functional screen for Kruppel-like factors that regulate the human gamma-globin gene through the CACCC promoter element.* Blood Cells Mol Dis, 2005. 35(2): p. 227-35.

181. Sogawa, K., H. Imataka, Y. Yamasaki, H. Kusume, H. Abe, and Y. Fujii-Kuriyama, *cDNA cloning and transcriptional properties of a novel GC box-binding protein, BTEB2.* Nucleic Acids Res, 1993. 21(7): p. 1527-32.
182. Conkright, M.D., M.A. Wani, K.P. Anderson, and J.B. Lingrel, *A gene encoding an intestinal-enriched member of the Kruppel-like factor family expressed in intestinal epithelial cells.* Nucleic Acids Res, 1999. 27(5): p. 1263-70.
183. Du, J.X., A.B. Bialkowska, B.B. McConnell, and V.W. Yang, *SUMOylation regulates nuclear localization of Kruppel-like factor 5.* J Biol Chem, 2008. 283(46): p. 31991-2002.
184. Guo, P., X.Y. Dong, X. Zhang, K.W. Zhao, X. Sun, Q. Li, and J.T. Dong, *Pro-proliferative factor KLF5 becomes anti-proliferative in epithelial homeostasis upon signaling-mediated modification.* J Biol Chem, 2008.
185. Miyamoto, S., T. Suzuki, S. Muto, K. Aizawa, A. Kimura, Y. Mizuno, T. Nagino, Y. Imai, N. Adachi, M. Horikoshi, and R. Nagai, *Positive and negative regulation of the cardiovascular transcription factor KLF5 by p300 and the oncogenic regulator SET through interaction and acetylation on the DNA-binding domain.* Mol Cell Biol, 2003. 23(23): p. 8528-41.
186. Guo, P., K.W. Zhao, X.Y. Dong, X. Sun, and J.T. Dong, *Acetylation of KLF5 alters the assembly of p15 transcription factors in transforming growth factor-beta-mediated induction in epithelial cells.* J Biol Chem, 2009. 284(27): p. 18184-93.
187. Zhang, Z. and C.T. Teng, *Phosphorylation of Kruppel-like factor 5 (KLF5/IKLF) at the CBP interaction region enhances its transactivation function.* Nucleic Acids Res, 2003. 31(8): p. 2196-208.
188. He, M., M. Han, B. Zheng, Y.N. Shu, and J.K. Wen, *Angiotensin II stimulates KLF5 phosphorylation and its interaction with c-Jun leading to suppression of p21 expression in vascular smooth muscle cells.* J Biochem, 2009. 146(5): p. 683-91.
189. Matsumura, T., T. Suzuki, K. Aizawa, Y. Munemasa, S. Muto, M. Horikoshi, and R. Nagai, *The deacetylase HDAC1 negatively regulates the cardiovascular transcription factor Kruppel-like factor 5 through direct interaction.* J Biol Chem, 2005. 280(13): p. 12123-9.
190. Xing, C., X. Fu, X. Sun, P. Guo, M. Li, and J.T. Dong, *Different expression patterns and functions of acetylated and unacetylated Klf5 in the proliferation and differentiation of prostatic epithelial cells.* PLoS One, 2013. 8(6): p. e65538.
191. Dong, J.T. and C. Chen, *Essential role of KLF5 transcription factor in cell proliferation and differentiation and its implications for human diseases.* Cell Mol Life Sci, 2009. 66(16): p. 2691-706.
192. Li, X., B. Zhang, Q. Wu, X. Ci, R. Zhao, Z. Zhang, S. Xia, D. Su, J. Chen, G. Ma, L. Fu, and J.T. Dong, *Interruption of KLF5 acetylation converts its function from tumor suppressor to tumor promoter in prostate cancer cells.* Int J Cancer, 2014.
193. Oishi, Y., I. Manabe, K. Tobe, M. Ohsugi, T. Kubota, K. Fujiu, K. Maemura, N. Kubota, T. Kadowaki, and R. Nagai, *SUMOylation of Kruppel-like transcription factor 5 acts as a molecular switch in transcriptional programs of lipid metabolism involving PPAR-delta.* Nat Med, 2008. 14(6): p. 656-66.
194. Wood, L.D., B.J. Irvin, G. Nucifora, K.S. Luce, and S.W. Hiebert, *Small ubiquitin-like modifier conjugation regulates nuclear export of TEL, a putative tumor suppressor.* Proc Natl Acad Sci U S A, 2003. 100(6): p. 3257-62.
195. Zhu, J., J. Zhou, L. Peres, F. Riaucoux, N. Honore, S. Kogan, and H. de The, *A sumoylation site in PML/RARA is essential for leukemic transformation.* Cancer Cell, 2005. 7(2): p. 143-53.
196. Chen, C., X. Sun, Q. Ran, K.D. Wilkinson, T.J. Murphy, J.W. Simons, and J.T. Dong, *Ubiquitin-proteasome degradation of KLF5 transcription factor in cancer and untransformed epithelial cells.* Oncogene, 2005. 24(20): p. 3319-27.

197. Zhao, D., H.Q. Zheng, Z. Zhou, and C. Chen, *The Fbw7 tumor suppressor targets KLF5 for ubiquitin-mediated degradation and suppresses breast cell proliferation.* Cancer Res, 2010. 70(11): p. 4728-38.
198. Zhao, D., X. Zhi, Z. Zhou, and C. Chen, *TAZ antagonizes the WWP1-mediated KLF5 degradation and promotes breast cell proliferation and tumorigenesis.* Carcinogenesis, 2012. 33(1): p. 59-67.
199. Diakiw, S.M., R.J. D'Andrea, and A.L. Brown, *The double life of KLF5: Opposing roles in regulation of gene-expression, cellular function, and transformation.* IUBMB Life, 2013. 65(12): p. 999-1011.
200. Nagai, R., T. Shindo, I. Manabe, T. Suzuki, and M. Kurabayashi, *KLF5/BTEB2, a Kruppel-like zinc-finger type transcription factor, mediates both smooth muscle cell activation and cardiac hypertrophy.* Adv Exp Med Biol, 2003. 538: p. 57-65; discussion 66.
201. Taneyhill, L. and D. Pennica, *Identification of Wnt responsive genes using a murine mammary epithelial cell line model system.* BMC Dev Biol, 2004. 4: p. 6.
202. Ziemer, L.T., D. Pennica, and A.J. Levine, *Identification of a mouse homolog of the human BTEB2 transcription factor as a beta-catenin-independent Wnt-1-responsive gene.* Mol Cell Biol, 2001. 21(2): p. 562-74.
203. Nandan, M.O., S. Chanchevalap, W.B. Dalton, and V.W. Yang, *Kruppel-like factor 5 promotes mitosis by activating the cyclin B1/Cdc2 complex during oncogenic Ras-mediated transformation.* FEBS Lett, 2005. 579(21): p. 4757-62.
204. Kawai-Kowase, K., M. Kurabayashi, Y. Hoshino, Y. Ohyama, and R. Nagai, *Transcriptional activation of the zinc finger transcription factor BTEB2 gene by Egr-1 through mitogen-activated protein kinase pathways in vascular smooth muscle cells.* Circ Res, 1999. 85(9): p. 787-95.
205. Yang, Y., B.G. Goldstein, H. Nakagawa, and J.P. Katz, *Kruppel-like factor 5 activates MEK/ERK signaling via EGFR in primary squamous epithelial cells.* Faseb J, 2007. 21(2): p. 543-50.
206. Chen, C., Y. Zhou, Z. Zhou, X. Sun, K.B. Otto, R.M. Uht, and J.T. Dong, *Regulation of KLF5 involves the Sp1 transcription factor in human epithelial cells.* Gene, 2004. 330: p. 133-42.
207. Mori, D., N. Okuro, Y. Fujii-Kuriyama, and K. Sogawa, *Gene structure and promoter analysis of the rat BTEB2 gene.* Gene, 2003. 304: p. 163-70.
208. Du, J.X., C.C. Yun, A. Bialkowska, and V.W. Yang, *Protein inhibitor of activated STAT1 interacts with and up-regulates activities of the pro-proliferative transcription factor Kruppel-like factor 5.* J Biol Chem, 2007. 282(7): p. 4782-93.
209. Suzuki, T., D. Sawaki, K. Aizawa, Y. Munemasa, T. Matsumura, J. Ishida, and R. Nagai, *Kruppel-like factor 5 shows proliferation-specific roles in vascular remodeling, direct stimulation of cell growth, and inhibition of apoptosis.* J Biol Chem, 2009. 284(14): p. 9549-57.
210. Frigo, D.E., A.B. Sherk, B.M. Wittmann, J.D. Norris, Q. Wang, J.D. Joseph, A.P. Toner, M. Brown, and D.P. McDonnell, *Induction of Kruppel-like factor 5 expression by androgens results in increased CXCR4-dependent migration of prostate cancer cells in vitro.* Mol Endocrinol, 2009. 23(9): p. 1385-96.
211. Nandan, M.O., A.M. Ghaleb, B.B. McConnell, N.V. Patel, S. Robine, and V.W. Yang, *Kruppel-like factor 5 is a crucial mediator of intestinal tumorigenesis in mice harboring combined ApcMin and KRASV12 mutations.* Mol Cancer, 2010. 9(1): p. 63.
212. Soon, M.S., L.S. Hsu, C.J. Chen, P.Y. Chu, J.H. Liou, S.H. Lin, J.D. Hsu, and K.T. Yeh, *Expression of Kruppel-like factor 5 in gastric cancer and its clinical correlation in Taiwan.* Virchows Arch, 2011. 459(2): p. 161-6.
213. Goldstein, B.G., H.H. Chao, Y. Yang, Y.A. Yermolina, J.W. Tobias, and J.P. Katz, *Overexpression of Kruppel-like factor 5 in esophageal epithelia in vivo leads to increased*

proliferation in basal but not suprabasal cells. Am J Physiol Gastrointest Liver Physiol, 2007. 292(6): p. G1784-92.
214. Nandan, M.O., H.S. Yoon, W. Zhao, L.A. Ouko, S. Chanchevalap, and V.W. Yang, *Kruppel-like factor 5 mediates the transforming activity of oncogenic H-Ras.* Oncogene, 2004. 23(19): p. 3404-13.
215. Bateman, N.W., D. Tan, R.G. Pestell, J.D. Black, and A.R. Black, *Intestinal tumor progression is associated with altered function of KLF5.* J Biol Chem, 2004. 279(13): p. 12093-101.
216. Nagai, R., K. Kowase, and M. Kurabayashi, *Transcriptional regulation of smooth muscle phenotypic modulation.* Ann N Y Acad Sci, 2000. 902: p. 214-22; discussion 222-3.
217. Liu, R., H.Q. Zheng, Z. Zhou, J.T. Dong, and C. Chen, *KLF5 promotes breast cell survival partially through fibroblast growth factor-binding protein 1-pERK-mediated dual specificity MKP-1 protein phosphorylation and stabilization.* J Biol Chem, 2009. 284(25): p. 16791-8.
218. Takeda, N., I. Manabe, Y. Uchino, K. Eguchi, S. Matsumoto, S. Nishimura, T. Shindo, M. Sano, K. Otsu, P. Snider, S.J. Conway, and R. Nagai, *Cardiac fibroblasts are essential for the adaptive response of the murine heart to pressure overload.* J Clin Invest, 2010. 120(1): p. 254-65.
219. Yang, Y., M.P. Tetreault, Y.A. Yermolina, B.G. Goldstein, and J.P. Katz, *Kruppel-like factor 5 controls keratinocyte migration via the integrin-linked kinase.* J Biol Chem, 2008. 283(27): p. 18812-20.
220. Martinez-Ceballos, E., P. Chambon, and L.J. Gudas, *Differences in gene expression between wild type and Hoxa1 knockout embryonic stem cells after retinoic acid treatment or leukemia inhibitory factor (LIF) removal.* J Biol Chem, 2005. 280(16): p. 16484-98.
221. Liu, Y., J.K. Wen, L.H. Dong, B. Zheng, and M. Han, *Kruppel-like factor (KLF) 5 mediates cyclin D1 expression and cell proliferation via interaction with c-Jun in Ang II-induced VSMCs.* Acta Pharmacol Sin, 2010. 31(1): p. 10-8.
222. Shao, J., V.W. Yang, and H. Sheng, *Prostaglandin E2 and Kruppel-like transcription factors synergistically induce the expression of decay-accelerating factor in intestinal epithelial cells.* Immunology, 2008. 125(3): p. 397-407.
223. Shinoda, Y., N. Ogata, A. Higashikawa, I. Manabe, T. Shindo, T. Yamada, F. Kugimiya, T. Ikeda, N. Kawamura, Y. Kawasaki, K. Tsushima, N. Takeda, R. Nagai, K. Hoshi, K. Nakamura, U.I. Chung, and H. Kawaguchi, *Kruppel-like factor 5 causes cartilage degradation through transactivation of matrix metalloproteinase 9.* J Biol Chem, 2008. 283(36): p. 24682-9.
224. Guo, P., X.Y. Dong, K. Zhao, X. Sun, Q. Li, and J.T. Dong, *Opposing effects of KLF5 on the transcription of MYC in epithelial proliferation in the context of transforming growth factor beta.* J Biol Chem, 2009. 284(41): p. 28243-52.
225. Jiang, J., Y.S. Chan, Y.H. Loh, J. Cai, G.Q. Tong, C.A. Lim, P. Robson, S. Zhong, and H.H. Ng, *A core Klf circuitry regulates self-renewal of embryonic stem cells.* Nat Cell Biol, 2008. 10(3): p. 353-60.
226. Sun, S.G., B. Zheng, M. Han, X.M. Fang, H.X. Li, S.B. Miao, M. Su, Y. Han, H.J. Shi, and J.K. Wen, *miR-146a and Kruppel-like factor 4 form a feedback loop to participate in vascular smooth muscle cell proliferation.* EMBO Rep, 2011. 12(1): p. 56-62.
227. Nagai, R., T. Suzuki, K. Aizawa, S. Miyamoto, T. Amaki, K. Kawai-Kowase, K.I. Sekiguchi, and M. Kurabayashi, *Phenotypic modulation of vascular smooth muscle cells: dissection of transcriptional regulatory mechanisms.* Ann N Y Acad Sci, 2001. 947: p. 56-66; discussion 66-7.
228. Aizawa, K., T. Suzuki, N. Kada, A. Ishihara, K. Kawai-Kowase, T. Matsumura, K. Sasaki, Y. Munemasa, I. Manabe, M. Kurabayashi, T. Collins, and R. Nagai, *Regulation of platelet-derived growth factor-A chain by Kruppel-like factor 5: new pathway of cooperative activation with nuclear factor-kappaB.* J Biol Chem, 2004. 279(1): p. 70-6.

229. Usui, S., N. Sugimoto, N. Takuwa, S. Sakagami, S. Takata, S. Kaneko, and Y. Takuwa, *Blood lipid mediator sphingosine 1-phosphate potently stimulates platelet-derived growth factor-A and -B chain expression through S1P1-Gi-Ras-MAPK-dependent induction of Kruppel-like factor 5.* J Biol Chem, 2004. 279(13): p. 12300-11.
230. Adam, P.J., C.P. Regan, M.B. Hautmann, and G.K. Owens, *Positive- and negative-acting Kruppel-like transcription factors bind a transforming growth factor beta control element required for expression of the smooth muscle cell differentiation marker SM22alpha in vivo.* J Biol Chem, 2000. 275(48): p. 37798-806.
231. Meyer, S.E., J.R. Hasenstein, A. Baktula, C.S. Velu, Y. Xu, H. Wan, J.A. Whitsett, C.B. Gilks, and H.L. Grimes, *Kruppel-like factor 5 is not required for K-RasG12D lung tumorigenesis, but represses ABCG2 expression and is associated with better disease-specific survival.* Am J Pathol, 2010. 177(3): p. 1503-13.
232. Wong, W.K., K. Chen, and J.C. Shih, *Regulation of human monoamine oxidase B gene by Sp1 and Sp3.* Mol Pharmacol, 2001. 59(4): p. 852-9.
233. Lee, M.Y., J.S. Moon, S.W. Park, Y.K. Koh, Y.H. Ahn, and K.S. Kim, *KLF5 enhances SREBP-1 action in androgen-dependent induction of fatty acid synthase in prostate cancer cells.* Biochem J, 2009. 417(1): p. 313-22.
234. McConnell, B.B., A.B. Bialkowska, M.O. Nandan, A.M. Ghaleb, F.J. Gordon, and V.W. Yang, *Haploinsufficiency of Kruppel-like factor 5 rescues the tumor-initiating effect of the Apc(Min) mutation in the intestine.* Cancer Res, 2009. 69(10): p. 4125-33.
235. Guo, P., X.Y. Dong, K.W. Zhao, X. Sun, Q. Li, and J.T. Dong, *Estrogen-induced interaction between KLF5 and estrogen receptor (ER) suppresses the function of ER in ER-positive breast cancer cells.* Int J Cancer, 2010. 126(1): p. 81-9.
236. Mori, A., C. Moser, S.A. Lang, C. Hackl, E. Gottfried, M. Kreutz, H.J. Schlitt, E.K. Geissler, and O. Stoeltzing, *Up-regulation of Kruppel-like factor 5 in pancreatic cancer is promoted by interleukin-1beta signaling and hypoxia-inducible factor-1alpha.* Mol Cancer Res, 2009. 7(8): p. 1390-8.
237. Kojima, S., A. Kobayashi, O. Gotoh, Y. Ohkuma, Y. Fujii-Kuriyama, and K. Sogawa, *Transcriptional activation domain of human BTEB2, a GC box-binding factor.* J Biochem, 1997. 121(2): p. 389-96.
238. Suzuki, T., T. Nishi, T. Nagino, K. Sasaki, K. Aizawa, N. Kada, D. Sawaki, Y. Munemasa, T. Matsumura, S. Muto, M. Sata, K. Miyagawa, M. Horikoshi, and R. Nagai, *Functional interaction between the transcription factor Kruppel-like factor 5 and poly(ADP-ribose) polymerase-1 in cardiovascular apoptosis.* J Biol Chem, 2007. 282(13): p. 9895-901.
239. Chen, C., H.V. Bhalala, R.L. Vessella, and J.T. Dong, *KLF5 is frequently deleted and down-regulated but rarely mutated in prostate cancer.* Prostate, 2003. 55(2): p. 81-8.
240. Johnston, S.R. and M. Dowsett, *Aromatase inhibitors for breast cancer: lessons from the laboratory.* Nat Rev Cancer, 2003. 3(11): p. 821-31.
241. Tong, D., K. Czerwenka, G. Heinze, M. Ryffel, E. Schuster, A. Witt, S. Leodolter, and R. Zeillinger, *Expression of KLF5 is a prognostic factor for disease-free survival and overall survival in patients with breast cancer.* Clin Cancer Res, 2006. 12(8): p. 2442-8.
242. Ben-Porath, I., M.W. Thomson, V.J. Carey, R. Ge, G.W. Bell, A. Regev, and R.A. Weinberg, *An embryonic stem cell-like gene expression signature in poorly differentiated aggressive human tumors.* Nat Genet, 2008. 40(5): p. 499-507.
243. Liu, R., Z. Zhou, D. Zhao, and C. Chen, *The induction of KLF5 transcription factor by progesterone contributes to progesterone-induced breast cancer cell proliferation and dedifferentiation.* Mol Endocrinol, 2011. 25(7): p. 1137-44.
244. Zhi, X., D. Zhao, Z. Zhou, R. Liu, and C. Chen, *YAP promotes breast cell proliferation and survival partially through stabilizing the KLF5 transcription factor.* Am J Pathol, 2012. 180(6): p. 2452-61.

245. Takagi, K., Y. Miki, Y. Onodera, Y. Nakamura, T. Ishida, M. Watanabe, S. Inoue, H. Sasano, and T. Suzuki, *Kruppel-like factor 5 in human breast carcinoma: a potent prognostic factor induced by androgens.* Endocr Relat Cancer, 2012. 19(6): p. 741-50.
246. Xia, H., C. Wang, W. Chen, H. Zhang, L. Chaudhury, Z. Zhou, R. Liu, and C. Chen, *Kruppel-like factor 5 transcription factor promotes microsomal prostaglandin E2 synthase 1 gene transcription in breast cancer.* J Biol Chem, 2013. 288(37): p. 26731-40.
247. Dong, J.T., C. Chen, B.G. Stultz, J.T. Isaacs, and H.F. Frierson, Jr., *Deletion at 13q21 is associated with aggressive prostate cancers.* Cancer Res, 2000. 60(14): p. 3880-3.
248. Nakajima, Y., K. Akaogi, T. Suzuki, A. Osakabe, C. Yamaguchi, N. Sunahara, J. Ishida, K. Kako, S. Ogawa, T. Fujimura, Y. Homma, A. Fukamizu, A. Murayama, K. Kimura, S. Inoue, and J. Yanagisawa, *Estrogen regulates tumor growth through a nonclassical pathway that includes the transcription factors ERbeta and KLF5.* Sci Signal, 2011. 4(168): p. ra22.
249. Duhagon, M.A., E.M. Hurt, J.R. Sotelo-Silveira, X. Zhang, and W.L. Farrar, *Genomic profiling of tumor initiating prostatospheres.* BMC Genomics, 2010. 11: p. 324.
250. Ohnishi, S., S. Ohnami, F. Laub, K. Aoki, K. Suzuki, Y. Kanai, K. Haga, M. Asaka, F. Ramirez, and T. Yoshida, *Downregulation and growth inhibitory effect of epithelial-type Kruppel-like transcription factor KLF4, but not KLF5, in bladder cancer.* Biochem Biophys Res Commun, 2003. 308(2): p. 251-6.
251. Gao, Y., Q. Shi, S. Xu, C. Du, L. Liang, K. Wu, K. Wang, X. Wang, L.S. Chang, D. He, and P. Guo, *Curcumin Promotes KLF5 Proteasome Degradation through Downregulating YAP/TAZ in Bladder Cancer Cells.* Int J Mol Sci, 2014. 15(9): p. 15173-15187.
252. Ohnishi, S., F. Laub, N. Matsumoto, M. Asaka, F. Ramirez, T. Yoshida, and M. Terada, *Developmental expression of the mouse gene coding for the Kruppel-like transcription factor KLF5.* Dev Dyn, 2000. 217(4): p. 421-9.
253. Nandan, M.O., A.M. Ghaleb, Y. Liu, A.B. Bialkowska, B.B. McConnell, K.R. Shroyer, S. Robine, and V.W. Yang, *Inducible intestine-specific deletion of Kruppel-like factor 5 is characterized by a regenerative response in adult mouse colon.* Dev Biol, 2014. 387(2): p. 191-202.
254. Wu, F., T. Dassopoulos, L. Cope, A. Maitra, S.R. Brant, M.L. Harris, T.M. Bayless, G. Parmigiani, and S. Chakravarti, *Genome-wide gene expression differences in Crohn's disease and ulcerative colitis from endoscopic pinch biopsies: insights into distinctive pathogenesis.* Inflamm Bowel Dis, 2007. 13(7): p. 807-21.
255. Tetreault, M.P., R. Alrabaa, M. McGeehan, and J.P. Katz, *Kruppel-like factor 5 protects against murine colitis and activates JAK-STAT signaling in vivo.* PLoS One, 2012. 7(5): p. e38338.
256. Sjoblom, T., S. Jones, L.D. Wood, D.W. Parsons, J. Lin, T.D. Barber, D. Mandelker, R.J. Leary, J. Ptak, N. Silliman, S. Szabo, P. Buckhaults, C. Farrell, P. Meeh, S.D. Markowitz, J. Willis, D. Dawson, J.K. Willson, A.F. Gazdar, J. Hartigan, L. Wu, C. Liu, G. Parmigiani, B.H. Park, K.E. Bachman, N. Papadopoulos, B. Vogelstein, K.W. Kinzler, and V.E. Velculescu, *The consensus coding sequences of human breast and colorectal cancers.* Science, 2006. 314(5797): p. 268-74.
257. Bialkowska, A.B., Y. Liu, M.O. Nandan, and V.W. Yang, *A colon cancer-derived mutant of Kruppel-like factor 5 (KLF5) is resistant to degradation by glycogen synthase kinase 3beta (GSK3beta) and the E3 ubiquitin ligase F-box and WD repeat domain-containing 7alpha (FBW7alpha).* J Biol Chem, 2014. 289(9): p. 5997-6005.
258. Yang, Y., B.G. Goldstein, H.H. Chao, and J.P. Katz, *KLF4 and KLF5 regulate proliferation, apoptosis and invasion in esophageal cancer cells.* Cancer Biol Ther, 2005. 4(11): p. 1216-21.
259. Yang, Y., H. Nakagawa, M.P. Tetreault, J. Billig, N. Victor, A. Goyal, A.R. Sepulveda, and J.P. Katz, *Loss of transcription factor KLF5 in the context of p53 ablation drives invasive progression of human squamous cell cancer.* Cancer Res, 2011. 71(20): p. 6475-84.

260. Yang, Y., R.S. Tarapore, M.H. Jarmel, M.P. Tetreault, and J.P. Katz, *p53 mutation alters the effect of the esophageal tumor suppressor KLF5 on keratinocyte proliferation.* Cell Cycle, 2012. 11(21): p. 4033-9.
261. Tarapore, R.S., Y. Yang, and J.P. Katz, *Restoring KLF5 in esophageal squamous cell cancer cells activates the JNK pathway leading to apoptosis and reduced cell survival.* Neoplasia, 2013. 15(5): p. 472-80.
262. Fujii, Y., K. Yoshihashi, H. Suzuki, S. Tsutsumi, H. Mutoh, S. Maeda, Y. Yamagata, Y. Seto, H. Aburatani, and M. Hatakeyama, *CDX1 confers intestinal phenotype on gastric epithelial cells via induction of stemness-associated reprogramming factors SALL4 and KLF5.* Proc Natl Acad Sci U S A, 2012. 109(50): p. 20584-9.
263. Chia, N.Y., N. Deng, K. Das, D. Huang, L. Hu, Y. Zhu, K.H. Lim, M.H. Lee, J. Wu, X.X. Sam, G.S. Tan, W.K. Wan, W. Yu, A. Gan, A.L. Tan, S.T. Tay, K.C. Soo, W.K. Wong, L.T. Dominguez, H.H. Ng, S. Rozen, L.K. Goh, B.T. Teh, and P. Tan, *Regulatory crosstalk between lineage-survival oncogenes KLF5, GATA4 and GATA6 cooperatively promotes gastric cancer development.* Gut, 2014.
264. Wan, H., F. Luo, S.E. Wert, L. Zhang, Y. Xu, M. Ikegami, Y. Maeda, S.M. Bell, and J.A. Whitsett, *Kruppel-like factor 5 is required for perinatal lung morphogenesis and function.* Development, 2008. 135(15): p. 2563-72.
265. Li, X., X. Liu, Y. Xu, J. Liu, M. Xie, W. Ni, and S. Chen, *KLF5 promotes hypoxia-induced survival and inhibits apoptosis in non-small cell lung cancer cells via HIF-1alpha.* Int J Oncol, 2014.
266. Sur, I., B. Rozell, V. Jaks, A. Bergstrom, and R. Toftgard, *Epidermal and craniofacial defects in mice overexpressing Klf5 in the basal layer of the epidermis.* J Cell Sci, 2006. 119(Pt 17): p. 3593-601.
267. McConnell, B.B., A.M. Ghaleb, M.O. Nandan, and V.W. Yang, *The diverse functions of Kruppel-like factors 4 and 5 in epithelial biology and pathobiology.* Bioessays, 2007. 29(6): p. 549-57.
268. Sun, R., X. Chen, and V.W. Yang, *Intestinal-enriched Kruppel-like factor (Kruppel-like factor 5) is a positive regulator of cellular proliferation.* J Biol Chem, 2001. 276(10): p. 6897-900.
269. Sun, X., L. Zhang, H. Xie, H. Wan, B. Magella, J.A. Whitsett, and S.K. Dey, *Kruppel-like factor 5 (KLF5) is critical for conferring uterine receptivity to implantation.* Proc Natl Acad Sci U S A, 2012. 109(4): p. 1145-50.
270. Dong, Z., L. Yang, and D. Lai, *KLF5 strengthens drug resistance of ovarian cancer stem-like cells by regulating survivin expression.* Cell Prolif, 2013. 46(4): p. 425-35.
271. Marrero-Rodriguez, D., K. Taniguchi-Ponciano, F. Jimenez-Vega, P. Romero-Morelos, M. Mendoza-Rodriguez, A. Mantilla, M. Rodriguez-Esquivel, D. Hernandez, A. Hernandez, G. Gomez-Gutierrez, N. Munoz-Hernandez, H.A. la Cruz, C. Vargas-Requena, C. Diaz-Hernandez, L. Serna-Reyna, M. Meraz-Rios, C. Bandala, J. Ortiz-Leon, and M. Salcedo, *Kruppel-like factor 5 as potential molecular marker in cervical cancer and the KLF family profile expression.* Tumour Biol, 2014.
272. Cheng, Y., X. Liu, J. Yang, Y. Lin, D.Z. Xu, Q. Lu, E.A. Deitch, Y. Huo, E.S. Delphin, and C. Zhang, *MicroRNA-145, a novel smooth muscle cell phenotypic marker and modulator, controls vascular neointimal lesion formation.* Circ Res, 2009. 105(2): p. 158-66.
273. Hoshino, Y., M. Kurabayashi, T. Kanda, A. Hasegawa, H. Sakamoto, E. Okamoto, K. Kowase, N. Watanabe, I. Manabe, T. Suzuki, A. Nakano, S. Takase, J.N. Wilcox, and R. Nagai, *Regulated expression of the BTEB2 transcription factor in vascular smooth muscle cells: analysis of developmental and pathological expression profiles shows implications as a predictive factor for restenosis.* Circulation, 2000. 102(20): p. 2528-34.
274. Courboulin, A., V.L. Tremblay, M. Barrier, J. Meloche, M.H. Jacob, M. Chapolard, M. Bisserier, R. Paulin, C. Lambert, S. Provencher, and S. Bonnet, *Kruppel-like factor 5*

contributes to pulmonary artery smooth muscle proliferation and resistance to apoptosis in human pulmonary arterial hypertension. Respir Res, 2011. 12: p. 128.
275. Taniguchi Ishikawa, E., K.H. Chang, R. Nayak, H.A. Olsson, A.M. Ficker, S.K. Dunn, M.N. Madhu, A. Sengupta, J.A. Whitsett, H.L. Grimes, and J.A. Cancelas, *Klf5 controls bone marrow homing of stem cells and progenitors through Rab5-mediated beta1/beta2-integrin trafficking.* Nat Commun, 2013. 4: p. 1660.
276. Diakiw, S.M., *Characterisation of the Role of KLF5 in Normal Haemopoiesis and Acute Myeloid Leukaemia.* PhD Thesis, 2011.
277. Yang, X.O., R.T. Doty, J.S. Hicks, and D.M. Willerford, *Regulation of T-cell receptor D beta 1 promoter by KLF5 through reiterated GC-rich motifs.* Blood, 2003. 101(11): p. 4492-9.
278. Brown, A.L., C.R. Wilkinson, S.R. Waterman, C.H. Kok, D.G. Salerno, S.M. Diakiw, B. Reynolds, H.S. Scott, A. Tsykin, G.F. Glonek, G.J. Goodall, P.J. Solomon, T.J. Gonda, and R.J. D'Andrea, *Genetic regulators of myelopoiesis and leukemic signaling identified by gene profiling and linear modeling.* J Leukoc Biol, 2006. 80(2): p. 433-47.
279. Brown, A.L., M. Peters, R.J. D'Andrea, and T.J. Gonda, *Constitutive mutants of the GM-CSF receptor reveal multiple pathways leading to myeloid cell survival, proliferation, and granulocyte-macrophage differentiation.* Blood, 2004. 103(2): p. 507-516.
280. McCormack, M.P. and T.J. Gonda, *Novel murine myeloid cell lines which exhibit a differentiation switch in response to IL-3 or GM-CSF, or to different constitutively active mutants of the GM-CSF receptor á subunit.* Blood, 2000. 95: p. 120-127.
281. Chambers, S.M., N.C. Boles, K.Y. Lin, M.P. Tierney, T.V. Bowman, S.B. Bradfute, A.J. Chen, A.A. Merchant, O. Sirin, D.C. Weksberg, M.G. Merchant, C.J. Fisk, C.A. Shaw, and M.A. Goodell, *Hematopoietic fingerprints: an expression database of stem cells and their progeny.* Cell Stem Cell, 2007. 1(5): p. 578-91.
282. Tonks, A., L. Pearn, M. Musson, A. Gilkes, K.I. Mills, A.K. Burnett, and R.L. Darley, *Transcriptional dysregulation mediated by RUNX1-RUNX1T1 in normal human progenitor cells and in acute myeloid leukaemia.* Leukemia, 2007. 21(12): p. 2495-505.
283. Federzoni, E.A., M. Humbert, B.E. Torbett, G. Behre, M.F. Fey, and M.P. Tschan, *CEBPA-dependent HK3 and KLF5 expression in primary AML and during AML differentiation.* Sci Rep, 2014. 4: p. 4261.
284. Ma, O., S. Hong, H. Guo, G. Ghiaur, and A.D. Friedman, *Granulopoiesis requires increased C/EBPalpha compared to monopoiesis, correlated with elevated Cebpa in immature G-CSF receptor versus M-CSF receptor expressing cells.* PLoS One, 2014. 9(4): p. e95784.
285. Ema, M., D. Mori, H. Niwa, Y. Hasegawa, Y. Yamanaka, S. Hitoshi, J. Mimura, Y. Kawabe, T. Hosoya, M. Morita, D. Shimosato, K. Uchida, N. Suzuki, J. Yanagisawa, K. Sogawa, J. Rossant, M. Yamamoto, S. Takahashi, and Y. Fujii-Kuriyama, *Kruppel-like factor 5 is essential for blastocyst development and the normal self-renewal of mouse ESCs.* Cell Stem Cell, 2008. 3(5): p. 555-67.
286. Parisi, S., F. Passaro, L. Aloia, I. Manabe, R. Nagai, L. Pastore, and T. Russo, *Klf5 is involved in self-renewal of mouse embryonic stem cells.* J Cell Sci, 2008. 121(Pt 16): p. 2629-34.
287. Lin, S.C., M.A. Wani, J.A. Whitsett, and J.M. Wells, *Klf5 regulates lineage formation in the pre-implantation mouse embryo.* Development, 2010. 137(23): p. 3953-63.
288. Orban, P.C., D. Chui, and J.D. Marth, *Tissue- and site-specific DNA recombination in transgenic mice.* Proc Natl Acad Sci U S A, 1992. 89(15): p. 6861-5.
289. Rickert, R.C., J. Roes, and K. Rajewsky, *B lymphocyte-specific, Cre-mediated mutagenesis in mice.* Nucleic Acids Res, 1997. 25(6): p. 1317-8.
290. Hamilton, D.L. and K. Abremski, *Site-specific recombination by the bacteriophage P1 lox-Cre system. Cre-mediated synapsis of two lox sites.* J Mol Biol, 1984. 178(2): p. 481-6.

291. Fau, A.K., Hoess R Fau, and N. Sternberg, *Studies on the properties of P1 site-specific recombination: evidence for topologically unlinked products following recombination.* 1983(0092-8674 (Print)).
292. Voziyanov, Y., S. Pathania, and M. Jayaram, *A general model for site-specific recombination by the integrase family recombinases.* Nucleic Acids Res, 1999. 27(4): p. 930-41.
293. Zhao, C., J. Blum, A. Chen, H.Y. Kwon, S.H. Jung, J.M. Cook, A. Lagoo, and T. Reya, *Loss of beta-catenin impairs the renewal of normal and CML stem cells in vivo.* Cancer Cell, 2007. 12(6): p. 528-41.
294. Daria, D., M.D. Filippi, E.S. Knudsen, R. Faccio, Z. Li, T. Kalfa, and H. Geiger, *The retinoblastoma tumor suppressor is a critical intrinsic regulator for hematopoietic stem and progenitor cells under stress.* Blood, 2008. 111(4): p. 1894-902.
295. Georgiades, P., S. Ogilvy, H. Duval, D.R. Licence, D.S. Charnock-Jones, S.K. Smith, and C.G. Print, *VavCre transgenic mice: a tool for mutagenesis in hematopoietic and endothelial lineages.* Genesis, 2002. 34(4): p. 251-6.
296. Uemura, M., Y. Niwa, N. Kakazu, N. Adachi, and K. Kinoshita, *Chromosomal manipulation by site-specific recombinases and fluorescent protein-based vectors.* PLoS One, 2010. 5(3): p. e9846.
297. Cano, F., L.F. Drynan, R. Pannell, and T.H. Rabbitts, *Leukaemia lineage specification caused by cell-specific Mll-Enl translocations.* Oncogene, 2008. 27(13): p. 1945-50.
298. Ogilvy, S., D. Metcalf, L. Gibson, M.L. Bath, A.W. Harris, and J.M. Adams, *Promoter elements of vav drive transgene expression in vivo throughout the hematopoietic compartment.* Blood, 1999. 94(6): p. 1855-63.
299. Katzav, S., D. Martin-Zanca, and M. Barbacid, *vav, a novel human oncogene derived from a locus ubiquitously expressed in hematopoietic cells.* Embo J, 1989. 8(8): p. 2283-90.
300. Bustelo, X.R., S.D. Rubin, K.L. Suen, D. Carrasco, and M. Barbacid, *Developmental expression of the vav protooncogene.* Cell Growth Differ, 1993. 4(4): p. 297-308.
301. de Boer, J., A. Williams, G. Skavdis, N. Harker, M. Coles, M. Tolaini, T. Norton, K. Williams, K. Roderick, A.J. Potocnik, and D. Kioussis, *Transgenic mice with hematopoietic and lymphoid specific expression of Cre.* Eur J Immunol, 2003. 33(2): p. 314-25.
302. Mortensen, M., D.J.P. Ferguson, M. Edelmann, B. Kessler, K.J. Morten, M. Komatsu, and A.K. Simon, *Loss of autophagy in erythroid cells leads to defective removal of mitochondria and severe anemia in vivo.* Proceedings of the National Academy of Sciences, 2010. 107(2): p. 832-837.
303. Croker, B.A., D. Metcalf, L. Robb, W. Wei, S. Mifsud, L. DiRago, L.A. Cluse, K.D. Sutherland, L. Hartley, E. Williams, J.G. Zhang, D.J. Hilton, N.A. Nicola, W.S. Alexander, and A.W. Roberts, *SOCS3 is a critical physiological negative regulator of G-CSF signaling and emergency granulopoiesis.* Immunity, 2004. 20(2): p. 153-65.
304. D'Andrea, R.J., D. Harrison-Findik, C.M. Butcher, J. Finnie, P. Blumbergs, P. Bartley, M. McCormack, K. Jones, R. Rowland, T.J. Gonda, and M.A. Vadas, *Dysregulated hematopoiesis and a progressive neurological disorder induced by expression of an activated form of the human common beta chain in transgenic mice.* J Clin Invest, 1998. 102(11): p. 1951-60.
305. Metcalf, D., *Clonal culture of hemopoietic cells: techniques and applications*. 1984, Amsterdam: Elsevier.
306. Rodriguez, C.I., F. Buchholz, J. Galloway, R. Sequerra, J. Kasper, R. Ayala, A.F. Stewart, and S.M. Dymecki, *High-efficiency deleter mice show that FLPe is an alternative to Cre-loxP.* Nat Genet, 2000. 25(2): p. 139-40.
307. Shionyu, M., K. Takahashi, and M. Go, *AS-EAST: a functional annotation tool for putative proteins encoded by alternatively spliced transcripts.* Bioinformatics, 2012. 28(15): p. 2076-7.

308. Sayers, E.W., T. Barrett, D.A. Benson, S.H. Bryant, K. Canese, V. Chetvernin, D.M. Church, M. DiCuccio, R. Edgar, S. Federhen, M. Feolo, L.Y. Geer, W. Helmberg, Y. Kapustin, D. Landsman, D.J. Lipman, T.L. Madden, D.R. Maglott, V. Miller, I. Mizrachi, J. Ostell, K.D. Pruitt, G.D. Schuler, E. Sequeira, S.T. Sherry, M. Shumway, K. Sirotkin, A. Souvorov, G. Starchenko, T.A. Tatusova, L. Wagner, E. Yaschenko, and J. Ye, *Database resources of the National Center for Biotechnology Information.* Nucleic Acids Res, 2009. 37(Database issue): p. D5-15.
309. Benson, D.A., I. Karsch-Mizrachi, D.J. Lipman, J. Ostell, and E.W. Sayers, *GenBank.* Nucleic Acids Res, 2009. 37(Database issue): p. D26-31.
310. McConnell, B.B., S.S. Kim, K. Yu, A.M. Ghaleb, N. Takeda, I. Manabe, A. Nusrat, R. Nagai, and V.W. Yang, *Kruppel-like factor 5 is important for maintenance of crypt architecture and barrier function in mouse intestine.* Gastroenterology, 2011. 141(4): p. 1302-13, 1313 e1-6.
311. Kenchegowda, D., S. Swamynathan, D. Gupta, H. Wan, J. Whitsett, and S.K. Swamynathan, *Conditional disruption of mouse Klf5 results in defective eyelids with malformed meibomian glands, abnormal cornea and loss of conjunctival goblet cells.* Dev Biol, 2011. 356(1): p. 5-18.
312. Xing, C., X. Ci, X. Sun, X. Fu, Z. Zhang, E.N. Dong, Z.Z. Hao, and J.T. Dong, *Klf5 deletion promotes Pten deletion-initiated luminal-type mouse prostate tumors through multiple oncogenic signaling pathways.* Neoplasia, 2014. 16(11): p. 883-99.
313. Kuhn, R., F. Schwenk, M. Aguet, and K. Rajewsky, *Inducible gene targeting in mice.* Science, 1995. 269(5229): p. 1427-9.
314. Dumortier, A., P. Kirstetter, P. Kastner, and S. Chan, *Ikaros regulates neutrophil differentiation.* Blood, 2003. 101(6): p. 2219-26.
315. Henderson, R.B., J.A. Hobbs, M. Mathies, and N. Hogg, *Rapid recruitment of inflammatory monocytes is independent of neutrophil migration.* Blood, 2003. 102(1): p. 328-35.
316. Zhu, B., Y. Bando, S. Xiao, K. Yang, A.C. Anderson, V.K. Kuchroo, and S.J. Khoury, *CD11b+Ly-6C(hi) suppressive monocytes in experimental autoimmune encephalomyelitis.* J Immunol, 2007. 179(8): p. 5228-37.
317. Yang, L., L. Wang, T.A. Kalfa, J.A. Cancelas, X. Shang, S. Pushkaran, J. Mo, D.A. Williams, and Y. Zheng, *Cdc42 critically regulates the balance between myelopoiesis and erythropoiesis.* Blood, 2007. 110(12): p. 3853-61.
318. Dunay, I.R., A. Fuchs, and L.D. Sibley, *Inflammatory monocytes but not neutrophils are necessary to control infection with Toxoplasma gondii in mice.* Infect Immun, 2010. 78(4): p. 1564-70.
319. Obregon-Henao, A., M. Henao-Tamayo, I.M. Orme, and D.J. Ordway, *Gr1(int)CD11b+ myeloid-derived suppressor cells in Mycobacterium tuberculosis infection.* PLoS One, 2013. 8(11): p. e80669.
320. Pronk, C.J. and D. Bryder, *Flow cytometry-based identification of immature myeloerythroid development.* Methods Mol Biol, 2011. 699: p. 275-93.
321. Pronk, C.J., D.J. Rossi, R. Mansson, J.L. Attema, G.L. Norddahl, C.K. Chan, M. Sigvardsson, I.L. Weissman, and D. Bryder, *Elucidation of the phenotypic, functional, and molecular topography of a myeloerythroid progenitor cell hierarchy.* Cell Stem Cell, 2007. 1(4): p. 428-42.
322. Yilmaz, O.H., M.J. Kiel, and S.J. Morrison, *SLAM family markers are conserved among hematopoietic stem cells from old and reconstituted mice and markedly increase their purity.* Blood, 2006. 107(3): p. 924-30.
323. Adolfsson, J., R. Mansson, N. Buza-Vidas, A. Hultquist, K. Liuba, C.T. Jensen, D. Bryder, L. Yang, O.J. Borge, L.A. Thoren, K. Anderson, E. Sitnicka, Y. Sasaki, M. Sigvardsson, and S.E. Jacobsen, *Identification of Flt3+ lympho-myeloid stem cells lacking erythro-*

megakaryocytic potential a revised road map for adult blood lineage commitment. Cell, 2005. 121(2): p. 295-306.
324. Karsunky, H., M.A. Inlay, T. Serwold, D. Bhattacharya, and I.L. Weissman, *Flk2+ common lymphoid progenitors possess equivalent differentiation potential for the B and T lineages.* Blood, 2008. 111(12): p. 5562-70.
325. Bradley, T.R. and D. Metcalf, *The growth of mouse bone marrow cells in vitro.* Aust J Exp Biol Med Sci, 1966. 44(3): p. 287-99.
326. Buick, R.N., M.D. Minden, and E.A. McCulloch, *Self-renewal in culture of proliferative blast progenitor cells in acute myeloblastic leukemia.* Blood, 1979. 54(1): p. 95-104.
327. Bagger, F.O., N. Rapin, K. Theilgaard-Monch, B. Kaczkowski, L.A. Thoren, J. Jendholm, O. Winther, and B.T. Porse, *HemaExplorer: a database of mRNA expression profiles in normal and malignant haematopoiesis.* Nucleic Acids Res, 2013. 41(Database issue): p. D1034-9.
328. Mas, C., M. Lussier-Price, S. Soni, T. Morse, G. Arseneault, P. Di Lello, J. Lafrance-Vanasse, J.J. Bieker, and J.G. Omichinski, *Structural and functional characterization of an atypical activation domain in erythroid Kruppel-like factor (EKLF).* Proc Natl Acad Sci U S A, 2011. 108(26): p. 10484-9.
329. Taniguchi, H., T. Toyoshima, K. Fukao, and H. Nakauchi, *Presence of hematopoietic stem cells in the adult liver.* Nat Med, 1996. 2(2): p. 198-203.
330. Johnson, R.S., B.M. Spiegelman, and V. Papaioannou, *Pleiotropic effects of a null mutation in the c-fos proto-oncogene.* Cell, 1992. 71(4): p. 577-86.
331. Yang, B., S. Kirby, J. Lewis, P.J. Detloff, N. Maeda, and O. Smithies, *A mouse model for beta 0-thalassemia.* Proc Natl Acad Sci U S A, 1995. 92(25): p. 11608-12.
332. Kuo, P.L., Y.L. Hsu, M.S. Huang, S.L. Chiang, and Y.C. Ko, *Bronchial epithelium-derived IL-8 and RANTES increased bronchial smooth muscle cell migration and proliferation by Kruppel-like factor 5 in areca nut-mediated airway remodeling.* Toxicol Sci, 2011. 121(1): p. 177-90.
333. Li, H., S.B. Miao, L.H. Dong, Y.N. Shu, D.C. Shao, B.C. Chen, M. Han, and Y. Zhang, *Clinicopathological correlation of Kruppel-like factor 5 and matrix metalloproteinase-9 expression and cartilage degeneration in human osteoarthritis.* Pathol Res Pract, 2012. 208(1): p. 9-14.
334. Voehringer, D., N. van Rooijen, and R.M. Locksley, *Eosinophils develop in distinct stages and are recruited to peripheral sites by alternatively activated macrophages.* J Leukoc Biol, 2007. 81(6): p. 1434-44.
335. W., F.T.N.a.H.A., *ATLAS OF Mouse Hematopathology.* 2000.
336. Dyer, K.D., K.E. Garcia-Crespo, K.E. Killoran, and H.F. Rosenberg, *Antigen profiles for the quantitative assessment of eosinophils in mouse tissues by flow cytometry.* J Immunol Methods, 2011. 369(1-2): p. 91-7.
337. Bolles, M., D. Deming, K. Long, S. Agnihothram, A. Whitmore, M. Ferris, W. Funkhouser, L. Gralinski, A. Totura, M. Heise, and R.S. Baric, *A double-inactivated severe acute respiratory syndrome coronavirus vaccine provides incomplete protection in mice and induces increased eosinophilic proinflammatory pulmonary response upon challenge.* J Virol, 2011. 85(23): p. 12201-15.
338. Kim, H.J., E.S. Alonzo, G. Dorothee, J.W. Pollard, and D.B. Sant'Angelo, *Selective depletion of eosinophils or neutrophils in mice impacts the efficiency of apoptotic cell clearance in the thymus.* PLoS One, 2010. 5(7): p. e11439.
339. Rose, C.E., Jr., J.A. Lannigan, P. Kim, J.J. Lee, S.M. Fu, and S.S. Sung, *Murine lung eosinophil activation and chemokine production in allergic airway inflammation.* Cell Mol Immunol, 2010. 7(5): p. 361-74.

340. Stevens, W.W., T.S. Kim, L.M. Pujanauski, X. Hao, and T.J. Braciale, *Detection and quantitation of eosinophils in the murine respiratory tract by flow cytometry.* J Immunol Methods, 2007. 327(1-2): p. 63-74.
341. Kiel, M.J. and S.J. Morrison, *Uncertainty in the niches that maintain haematopoietic stem cells.* Nat Rev Immunol, 2008. 8(4): p. 290-301.
342. Lamothe, B., Y. Lai, L. Hur, N.M. Orozco, J. Wang, A.D. Campos, M. Xie, M.D. Schneider, C.R. Lockworth, J. Jakacky, D. Tran, M. Ho, S. Dawud, C. Dong, H.K. Lin, P. Hu, Z. Estrov, C.E. Bueso-Ramos, and B.G. Darnay, *Deletion of TAK1 in the myeloid lineage results in the spontaneous development of myelomonocytic leukemia in mice.* PLoS One, 2012. 7(12): p. e51228.
343. Ren, M., J.A. Tidwell, S. Sharma, and J.K. Cowell, *Acute progression of BCR-FGFR1 induced murine B-lympho/myeloproliferative disorder suggests involvement of lineages at the pro-B cell stage.* PLoS One, 2012. 7(6): p. e38265.
344. Ohkubo, N., Y. Suzuki, M. Aoto, J. Yamanouchi, S. Hirakawa, M. Yasukawa, and N. Mitsuda, *Accelerated destruction of erythrocytes in Tie2 promoter-driven STAT3 conditional knockout mice.* Life Sci, 2013. 93(9-11): p. 380-7.
345. Wang, H., W. Luo, J. Wang, C. Guo, S.L. Wolffe, J. Wang, E.B. Sun, K.N. Bradley, A.D. Campbell, and D.T. Eitzman, *Paradoxical protection from atherosclerosis and thrombosis in a mouse model of sickle cell disease.* Br J Haematol, 2013. 162(1): p. 120-9.
346. Walsh, G.M., *Advances in the immunobiology of eosinophils and their role in disease.* Crit Rev Clin Lab Sci, 1999. 36(5): p. 453-96.
347. Uhm, T.G., B.S. Kim, and I.Y. Chung, *Eosinophil development, regulation of eosinophil-specific genes, and role of eosinophils in the pathogenesis of asthma.* Allergy Asthma Immunol Res, 2012. 4(2): p. 68-79.
348. McNagny, K. and T. Graf, *Making eosinophils through subtle shifts in transcription factor expression.* J Exp Med, 2002. 195(11): p. F43-7.
349. Iwasaki, H., S. Mizuno, R. Mayfield, H. Shigematsu, Y. Arinobu, B. Seed, M.F. Gurish, K. Takatsu, and K. Akashi, *Identification of eosinophil lineage-committed progenitors in the murine bone marrow.* J Exp Med, 2005. 201(12): p. 1891-7.
350. Mori, Y., H. Iwasaki, K. Kohno, G. Yoshimoto, Y. Kikushige, A. Okeda, N. Uike, H. Niiro, K. Takenaka, K. Nagafuji, T. Miyamoto, M. Harada, K. Takatsu, and K. Akashi, *Identification of the human eosinophil lineage-committed progenitor: revision of phenotypic definition of the human common myeloid progenitor.* J Exp Med, 2009. 206(1): p. 183-93.
351. Luo, Q., X. Ma, S.M. Wahl, J.J. Bieker, M. Crossley, and L.J. Montaner, *Activation and repression of interleukin-12 p40 transcription by erythroid Kruppel-like factor in macrophages.* J Biol Chem, 2004. 279(18): p. 18451-6.
352. Kirberg, J., C. Gschwendner, J.P. Dangy, F. Ruckerl, F. Frommer, and J. Bachl, *Proviral integration of an Abelson-murine leukemia virus deregulates BKLF-expression in the hypermutating pre-B cell line 18-81.* Mol Immunol, 2005. 42(10): p. 1235-42.
353. Ghaleb, A.M., M.O. Nandan, S. Chanchevalap, W.B. Dalton, I.M. Hisamuddin, and V.W. Yang, *Kruppel-like factors 4 and 5: the yin and yang regulators of cellular proliferation.* Cell Res, 2005. 15(2): p. 92-6.
354. Hirasawa, R., R. Shimizu, S. Takahashi, M. Osawa, S. Takayanagi, Y. Kato, M. Onodera, N. Minegishi, M. Yamamoto, K. Fukao, H. Taniguchi, H. Nakauchi, and A. Iwama, *Essential and instructive roles of GATA factors in eosinophil development.* J Exp Med, 2002. 195(11): p. 1379-86.
355. Zhu, X.J., Z.F. Yang, Y. Chen, J. Wang, and A.G. Rosmarin, *PU.1 is essential for CD11c expression in CD8(+)/CD8(-) lymphoid and monocyte-derived dendritic cells during GM-CSF or FLT3L-induced differentiation.* PLoS One, 2012. 7(12): p. e52141.
356. Islam, R., W.J. Yoon, K.M. Woo, J.H. Baek, and H.M. Ryoo, *Pin1-mediated prolyl isomerization of Runx1 affects PU.1 expression in pre-monocytes.* J Cell Physiol, 2014. 229(4): p. 443-52.

357. Du, J., M.J. Stankiewicz, Y. Liu, Q. Xi, J.E. Schmitz, J.A. Lekstrom-Himes, and S.J. Ackerman, *Novel combinatorial interactions of GATA-1, PU.1, and C/EBPepsilon isoforms regulate transcription of the gene encoding eosinophil granule major basic protein.* J Biol Chem, 2002. 277(45): p. 43481-94.
358. Gombart, A.F., S.H. Kwok, K.L. Anderson, Y. Yamaguchi, B.E. Torbett, and H.P. Koeffler, *Regulation of neutrophil and eosinophil secondary granule gene expression by transcription factors C/EBP epsilon and PU.1.* Blood, 2003. 101(8): p. 3265-73.
359. Tsang, A.P., Y. Fujiwara, D.B. Hom, and S.H. Orkin, *Failure of megakaryopoiesis and arrested erythropoiesis in mice lacking the GATA-1 transcriptional cofactor FOG.* Genes Dev, 1998. 12(8): p. 1176-88.
360. Querfurth, E., M. Schuster, H. Kulessa, J.D. Crispino, G. Doderlein, S.H. Orkin, T. Graf, and C. Nerlov, *Antagonism between C/EBPbeta and FOG in eosinophil lineage commitment of multipotent hematopoietic progenitors.* Genes Dev, 2000. 14(19): p. 2515-25.
361. Ferraris, F.K., R. Rodrigues, V.P. da Silva, R. Figueiredo, C. Penido, and M. Henriques, *Modulation of T lymphocyte and eosinophil functions in vitro by natural tetranortriterpenoids isolated from Carapa guianensis Aublet.* Int Immunopharmacol, 2011. 11(1): p. 1-11.
362. Chensue, S.W., N.W. Lukacs, T.Y. Yang, X. Shang, K.A. Frait, S.L. Kunkel, T. Kung, M.T. Wiekowski, J.A. Hedrick, D.N. Cook, A. Zingoni, S.K. Narula, A. Zlotnik, F.J. Barrat, A. O'Garra, M. Napolitano, and S.A. Lira, *Aberrant in vivo T helper type 2 cell response and impaired eosinophil recruitment in CC chemokine receptor 8 knockout mice.* J Exp Med, 2001. 193(5): p. 573-84.
363. Hori, K., M. Hirashima, M. Ueno, M. Matsuda, S. Waga, S. Tsurufuji, and J. Yodoi, *Regulation of eosinophil migration by adult T cell leukemia-derived factor.* J Immunol, 1993. 151(10): p. 5624-30.
364. Vinjamur, D.S., K.J. Wade, S.F. Mohamad, J.L. Haar, S.T. Sawyer, and J.A. Lloyd, *Kruppel-like transcription factors KLF1 and KLF2 have unique and coordinate roles in regulating embryonic erythroid precursor maturation.* Haematologica, 2014. 99(10): p. 1565-73.
365. Kiel, M.J., O.H. Yilmaz, T. Iwashita, O.H. Yilmaz, C. Terhorst, and S.J. Morrison, *SLAM family receptors distinguish hematopoietic stem and progenitor cells and reveal endothelial niches for stem cells.* Cell, 2005. 121(7): p. 1109-21.
366. Butler, J.M., D.J. Nolan, E.L. Vertes, B. Varnum-Finney, H. Kobayashi, A.T. Hooper, M. Seandel, K. Shido, I.A. White, M. Kobayashi, L. Witte, C. May, C. Shawber, Y. Kimura, J. Kitajewski, Z. Rosenwaks, I.D. Bernstein, and S. Rafii, *Endothelial cells are essential for the self-renewal and repopulation of Notch-dependent hematopoietic stem cells.* Cell Stem Cell, 2010. 6(3): p. 251-64.
367. Ding, L., T.L. Saunders, G. Enikolopov, and S.J. Morrison, *Endothelial and perivascular cells maintain haematopoietic stem cells.* Nature, 2012. 481(7382): p. 457-62.
368. Doan, P.L., J.L. Russell, H.A. Himburg, K. Helms, J.R. Harris, J. Lucas, K.C. Holshausen, S.K. Meadows, P. Daher, L.B. Jeffords, N.J. Chao, D.G. Kirsch, and J.P. Chute, *Tie2(+) bone marrow endothelial cells regulate hematopoietic stem cell regeneration following radiation injury.* Stem Cells, 2013. 31(2): p. 327-37.
369. Cadman, E.T., K.A. Thysse, S. Bearder, A.Y. Cheung, A.C. Johnston, J.J. Lee, and R.A. Lawrence, *Eosinophils are important for protection, immunoregulation and pathology during infection with nematode microfilariae.* PLoS Pathog, 2014. 10(3): p. e1003988.
370. Roers, A., L. Siewe, E. Strittmatter, M. Deckert, D. Schluter, W. Stenzel, A.D. Gruber, T. Krieg, K. Rajewsky, and W. Muller, *T cell-specific inactivation of the interleukin 10 gene in mice results in enhanced T cell responses but normal innate responses to lipopolysaccharide or skin irritation.* J Exp Med, 2004. 200(10): p. 1289-97.

371. Dolence, J.J., K.A. Gwin, M.B. Shapiro, and K.L. Medina, *Flt3 signaling regulates the proliferation, survival, and maintenance of multipotent hematopoietic progenitors that generate B cell precursors.* Exp Hematol, 2014. 42(5): p. 380-393 e3.
372. Kunimoto, H., Y. Fukuchi, M. Sakurai, K. Sadahira, Y. Ikeda, S. Okamoto, and H. Nakajima, *Tet2 disruption leads to enhanced self-renewal and altered differentiation of fetal liver hematopoietic stem cells.* Sci Rep, 2012. 2: p. 273.

Appendix A: Final cloning and targeting of the *Klf5* allele.

This final cloning and targeting report was generated by the QIMR transgenic facility.

The construct pKlf5-FTC [Final Targeting Construct] is a 10754 bp conditional knockout targeting vector (Appendix A1). It contains exon 2 of Klf5 flanked by unidirectional loxP sites to perform Cre-mediated deletion. For antibiotic selection of targeted clones and subsequent removal of the cassette it harbours a FRT flanked neo selection cassette that lies upstream of the most 5' loxP site (see attached plasmid map) (Appendix A1). The construct was assembled using three basic plasmids- pKlf5A, B and C. The details of each plasmid are as follows.

pKlf5A:

This contains the 5' homology arm of the targeting construct encompassing from 12626-14400 [all numbering in this document corresponds to the attached Klf5 genomic sequence].

Using the 12446F2 X 14400R primer combinations an approximately 2kb PCR product was amplified from purified 24P5 BAC DNA. The PCR product was digested with HindIII [which cuts at the site beginning at position 12626] and EcoRI [the 14400R primer contains this site at its 5' end- in other words it's at the 3' termini of the fragment] and the approximately 1.4kb fragment was subcloned into the pL451 plasmid. This puts the 5' homology arm of the targeting vector upstream of the FRT flanked neo cassette, with a single loxP site being present downstream from the selection cassette. Sequence was confirmed in final construct.

pKlf5B:

This plasmid contains the middle homology [exon 2] and sequences from 14401-16409.

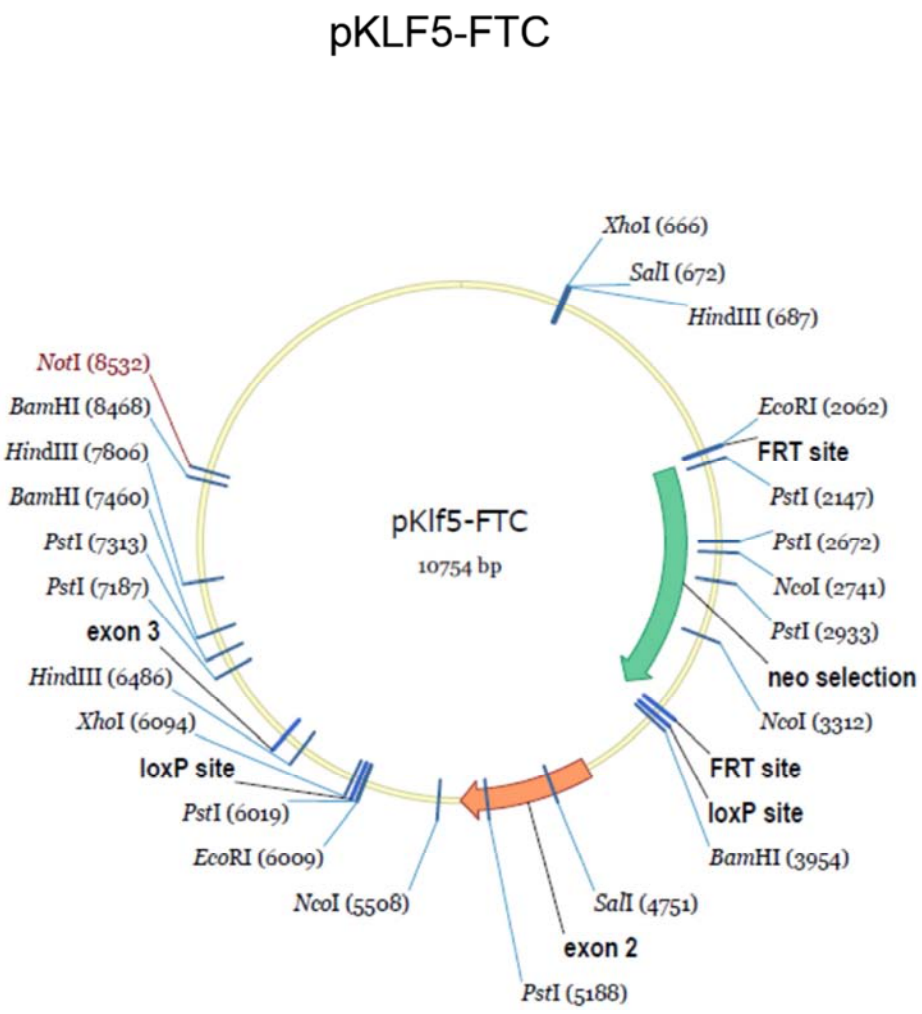

Appendix A1

The final targeting construct, pKlf5-FTC with 10754 bp conditional knockout targeting vector. It contains exon 2 of *Klf5* flanked by unidirectional loxP sites to perform Cre-mediated deletion. For antibiotic selection of targeted clones and subsequent removal of the cassette it harbours a FRT flanked neo selection cassette that lies upstream of the most 5' loxP site. This figure has been generated by the QIMR transgenic facility.

Position 14401-16409 was amplified using the 14001F X 16409R primer combination. The 2.4kb PCR product was cut with BamHI [found at the termini of the 14001F primer] and EcoRI [found at the termini of the 16409R primer] and subcloned into BamHI/EcoRI digested pSL1180. Sequence verified (P84)- clone#2 matches the consensus for Klf5 genome. Also sequence verified in the final construct as well.

pKlf5C:

This plasmid contains the 3' homology [including exon 3] and encompasses genomic sequences from 16410-18474.

An approximately 2kb fragment was amplified from 24P5 BAC DNA using 16410F+ X 18474R+ and this was digested with BclI [at the termini of the 16410F+ primer] and NotI [termini of the 18474R+ primer] and was subcloned into BamHI/NotI pL452. This places the loxP flanked neo cassette upstream of the homology. Plasmid from clone 1 was sequence verified [P80] and pKlf5C[1] was subsequently passaged through BS591 "Cre coli" and the Cre-mediated loss of the loxP flanked neo cassette was confirmed.

pKlf5-FTC:

The BamHI/EcoRI pKlf5B[2] and EcoRI/NotI pKlf5D inserts were subcloned into BamHI/NotI digested pKlf5A to yield pKlf5-FTC. Culture#1 was taken and the plasmid was purified, sequenced and linearised with NotI for targeting.

Primer sequences:

12446F2: AAAGAATTCCCGCTCCAGACTGGGACGCG

14400R: GGGGGGATCCTTTGAATTCGTGGAGCAGAAGCCTGTATTG

14401F: GGGGGATCCAGGTTCAAGTTTCTATTC

16409R: GGGGGAATTCGCTTATGCCTGCAACTTGG

16410F+: GGGGTGATCAAAGTTTATGATTAATGCAGGGC

18474R+: GGGGGCGGCCGCGTGGGCATTGTTCAGAC

Southern blot strategy to detect targeted clones.

EcoRI cuts 7921-25571

Probe: Use a 531bp PCR product generated from the following primers

CTTGTGACGGTACACTTTAC [denoted as 7860F in ordering but corresponds to approx 19701- 1227bp 3' to the downstream homology]

CATTTGTACACAGGATGCAG [denoted as 8391R].

The targeting construct has two EcoRI sites inserted. At approximately position 14000 and 16410. This would yield. A 9.2kb fragment for the lone loxP site located at position 16410 and a 13kb frag [11171bp plus the approx 2kb neo cassette, which must be included].

So southern blot will yield:

17650 [wild type] plus 9.2kb [for lone loxP site]

17650 [wild type] plus 13kb [for upstream lox P site].

Targeting.

$2X10^7$ C1368 [129/SV] P12 ES cells were electroporated with 50µg of NotI linearised pKl5-FTC and 10X96-well plates were picked and grown out to finally yield 2 DNA analysis plates and two plates that contained feeders and were subsequently frozen down. DNA plates were analysed by Southern blot (Appendix A 2). Obtained 8 clones [plus one

possible]. Of these, clone 2/E2 [plate#2 well E2] and 9/H8 gave the correct recombination products (Appendix A 2). The remaining clones carried the selection cassette but not the remote loxP site integrated homologously. Approximately .21% targeting frequency. These were cultured for blastocyst injection.

Klf5 targeting- Transmission report

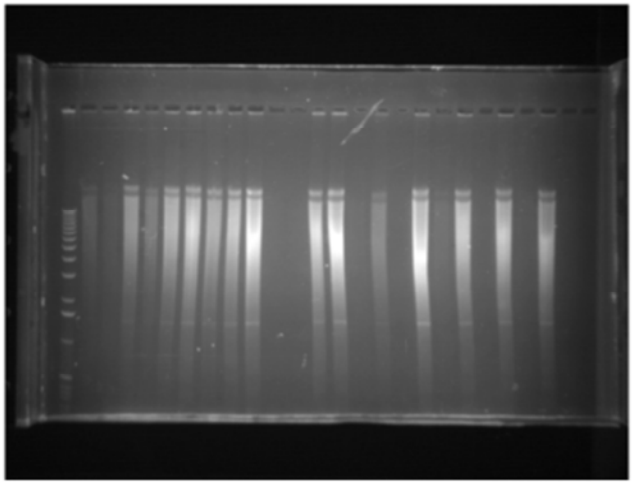

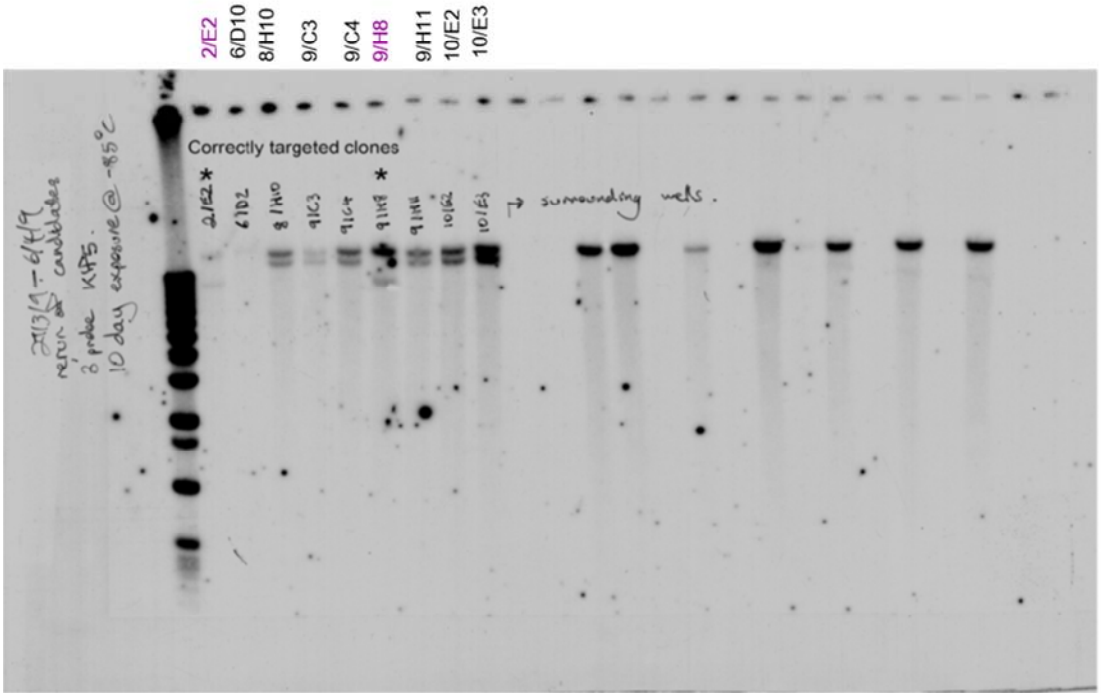

Appendix A 2

Southern blot analysis showing the nine possible targeted ES clones (ie 2/E2, 6/D2, 8/H10, 9/C3, 9/C4, 9/H8, 9/H11, 10/E2 and 10/E3). Clone #2/E2 and #9/H8 gave the correct recombination products by Southern blot indicating that both the selection cassette and remote loxP site had integrated homologously. The remaining clones carried the selection cassette but not the remote loxP site integrated homologously.

Appendix B: Klf5 targeting- Transmission report

This Klf5 targeting transmission report has been generated by the QIMR transgenic facility. Initial PCR analysis of agouti offspring obtained from crossing chimaeras with BL6 mice

Primer set#1: all primers are numbered according to the genomic sequence file.

Klf5-16031F CCAAgTTgCAggCATAAgC

Klf5-16629R CCCgTATgAgTCCTCAggTg

These primers anneal to regions flanking the lone 3' loxP site and they will amplify a 598bp wild type product and 694bp product for the floxed allele.

Caution must be exercised in using this set of primers- in fact I would avoid them altogether and use the second set that will be described (the second set could not be used for primary detection as they only detect a floxed allele that has undergone flp-e mediated recombination). The use of standard PCR conditions [i.e 2mM $MgCl_2$] will amplify 90%:10%::wild type:floxed allele (shown in the gel below). In some cases, the ratio was lower and the floxed allele was barely detectable in some tails that were later easily identified as being positive, once unusual PCR conditions were employed. This is not unheard of as I have experienced similar problems with other targetings, such as p130.

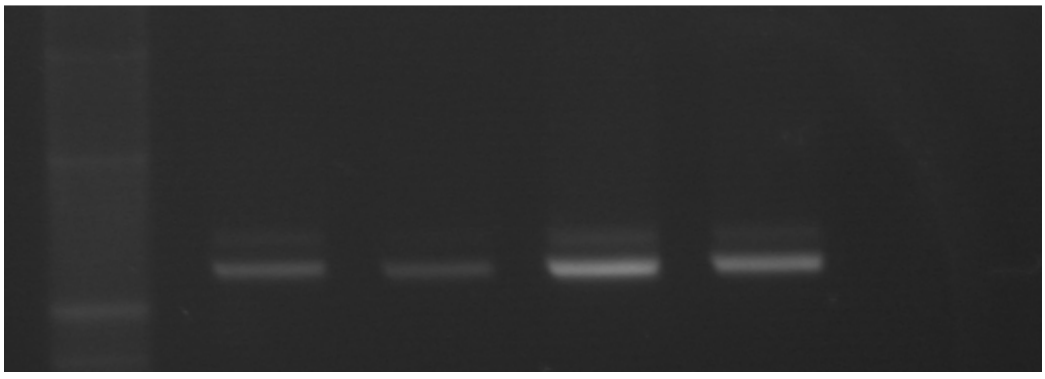

PCR of the DNA from 2/E2 and 9/H8 wells of targeting plates- 30ul 0.1XTE added to the 96-well plate and DNA allowed to resuspend briefly prior to PCR:

L→R 1kb ladder (500bp and 1kb markers shown), 2/E2 (1:10 dilution), 9/H8 (1:10 dilution), 2/E2 (undiluted), 9/H8 (undiluted)

It was established that at least 4mM $MgCl_2$ is required to give product yields that reflect the correct balance between wild type and floxed allele as 6mM $MgCl_2$ preferentially amplified the floxed allele (see below gel).

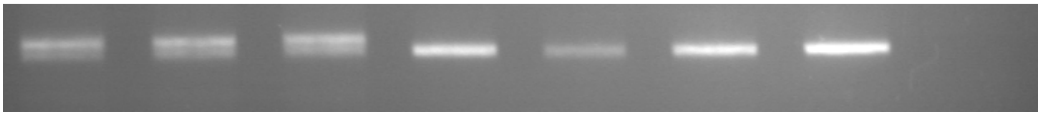

This gels shows L→R PCR of three suspected floxed tails 2/E2[1]→[3], control tails (X4), -ve – all amplified using 6mM $MgCl_2$

Consequently, 4mM $MgCl_2$ was used in all subsequent amplifications for primer set#1. This unusual result may be a reflection of the machine used, but is not attributable to the nature of the polymerase, as this same complication was observed using ampliTaq gold, NEB Taq polymerase and Finnzyme Phusion.

Once the conditions for Primer set#1 were optimised on DNA from the cell line and candidate tails and we were able to clearly amplify the lone (3') loxP site it was tested against at least 48 different agouti pups resulting from the mating of chimaeras

generated from the two different cell lines with C57BL6 mice. These PCR results were also supported by Southern blot analysis that was conducted at the same time.

This analysis has shown that only one of the initial 2/E2 chimaeras appears to have transmitted the floxed allele- with 4/5 progeny from one chimaera having transmitted (these progeny were 2/E2[1], [2], [3] and [5]). In contrast, none of the 9/H8 chimaeras transmitted the floxed allele. Southern blot analysis and PCR have definitely confirmed that these wells contained targeted cells and, at thawing for culture, the identity of the wells from which cells were taken/grown was confirmed by both Graham and Dianne.

The initial southern blot analysis of the 9/H8 clone showed that there was a disproportional level of wild type vs floxed product in the digested genomic DNA. Whilst this usually is attributable to a slight excess of growth-inactivated feeder cells that have carried through during the initial 1:4 split of the plates, it is feasible that, in this case, it was because a second ES cell line was present within that well. This situation arises when two different lines are growing on top of one another and they are not able to be seen properly or fully separated during selection. Our data from earlier targeting (such as Crim1) show that these lines generally only contain the selection cassette and no flanking homologies (hence using neo PCRs to detect the right cell lines is not always informative- and can give false positives). In contrast, the other line in 9/H8 is properly targeted. This only becomes problematic if the line possessing the random integration event outgrows the targeted line during either culture or colonisation of the embryo or has an advantage in transmission. The experience with the 2/E2 line has indicated that the modification to the Klf5 allele

may yield a slightly slower growing line so this could be an explanation for why no transmission is observed.

To check that the floxed cells were present in the 9/H8 cultures used for injections the cells were grown up and subject to PCR analysis:

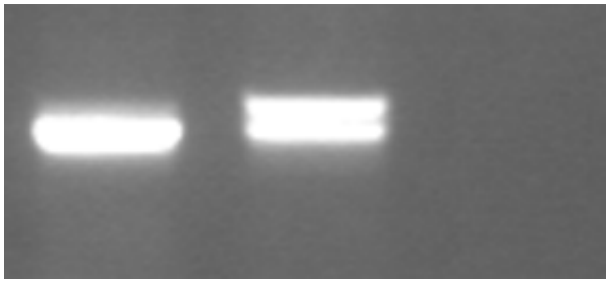

This gel shows: L→R P4 9/H8, P4 2/E2, -ve

Whilst the floxed allele is present in the P4 9/H8 line it is obvious that it is at much lower levels proportionally than for 2/E2 and this tends to confirm the suspicion that the original colony was probably a mix of two distinct lines. Please note though that this PCR was done on P4 cells (I was unwilling to thaw and waste early passage cells) so it is likely that the percentage of floxed cells is higher in earlier passages that were used for microinjection. It seems most likely that the random integrant had an overall advantage in embryo colonisation- it could be feasible to reclone 9/H8 but since 2/E2 has transmitted that should not be necessary.

Identification of flp-e mediated recombination in progeny of flp-e X 2/E2 matings

We bred the 2/E2[1],[2],[3] and [5] mice to flp-e mice. The progeny have been checked with primer set#1 and with primer set#2

Analysis with primer set#2

Klf5-13919F (called 1979F in my notes) CTggTTCAAgTgAACATTTgg

Klf5-14096R (called 2260R in my notes) CAAAgggCTTTTgTgTgTggAC

These primers anneal to regions that flank the 5'loxP and FRT sites. They will only amplify a product from the targeted allele after flp-e-mediated recombination. In this case the 385 bp product corresponding to the flp-recombined floxed allele will be 104 bp bigger than the wild type product (281 bp).

Primer set#2 was used on these tail tip DNAs

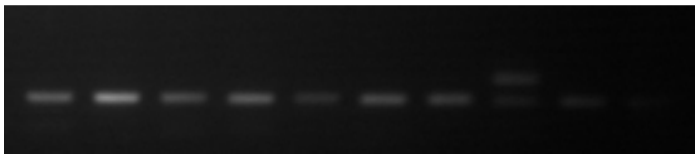

L→R 10.1a→g,11.1a-c

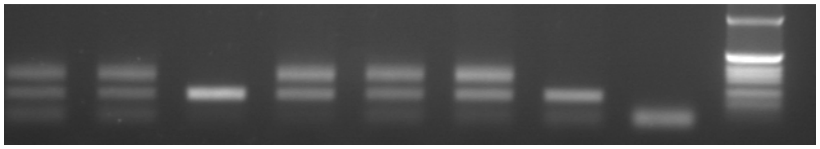

L→R 12.1c,d,13.1a,c,d,e,g,-ve,1kb ladder

11.1a, 12.1c,12.1d, 13.1a,13.1c and 13.1d all have the floxed allele and have experienced flpe-mediated recombination.

12.1c, 12.1d, 13.1c and 13.1d were selected and shipped to us.

Appendix C: Sequencing Results

KLF5-WT

Forward Primer (F)

Part of intron 2

GGTGCAANNGTTTTGTATCAGTGGATACAATACAGGCTTCTGCTCCACAGGTTCAAGTTTCTATTCAAA

AAGTATTGAAATGGCCAGAGAACATTTTATATTAGGCCTGATAAAATAACCTAGTCCACACACAAAAGC

Reverse Primer (R1)

CCTTTGGAATAATTATTTTTAAGATTTGCACAGGTTTTAGTTTTCAAG

KLF5-FLOX

Forward Primer (F)

Part of intron 2

EcoR1

FRT site

GGTGCAATTGTTTTGTATCAGTGGATACAATACAGGCTTCTGCTCCACGAATTCCGAAGTTCCTATTCT

FRT spacer

LoxP spacer

LoxP site

CTAGAAAGTATAGGAACTTCATCAGTCAGGTACATAATATAACTTCGTATAATGTATGCTATACGAAGT

TATTAGGTGGATCCAGGTTCAAGTTTCTATTCAAAAAGTATTGAAATGGCCAGAGAACATTTTATATTA

Reverse Primer (R1)

GGCCTGATAAAATAACCTAGTCCACACACAAAAGCCCTTTGGAATAATTATTTTTAAGATTTGCACAGG

TTTTAGTTTTCAAG

KLF5-deleted

Forward Primer (F)

Part of intron 2

EcoR1

GGTGCAATTGTTTTGTATCAGTGGATACAATACAGGCTTCTGCTCCACGAATTCCGAAGTTCCTATTCT

FRT spacer

LoxP spacer

LoxP site

CTAGAAAGTATAGGAACTTCATCAGTCAGGTACATAATATAACTTCGTATAATGTATGCTATACGAAGT

LoxP spacer

XhoI

Part of intron 3

TATTAGGTCCCTCGAGGGGATCAAAGTTTATGATTAATGCAGGGCATAATTTATTGACTGCACGATGTG

GCATGACATGCTAAATGAGAAAAACAAAGTAGGATTATAGAAAATGATAGTCATCTCCGATAATGACTT

AACACTGTTAGTTCTGCATCCATTACATTAAATATACATACATATATACATACATAACACACACACACA

Reverse Primer (R2)

CACACACACACGCACACACNCGTCCCACGATTGCTCTCCATTTAC

Appendix D

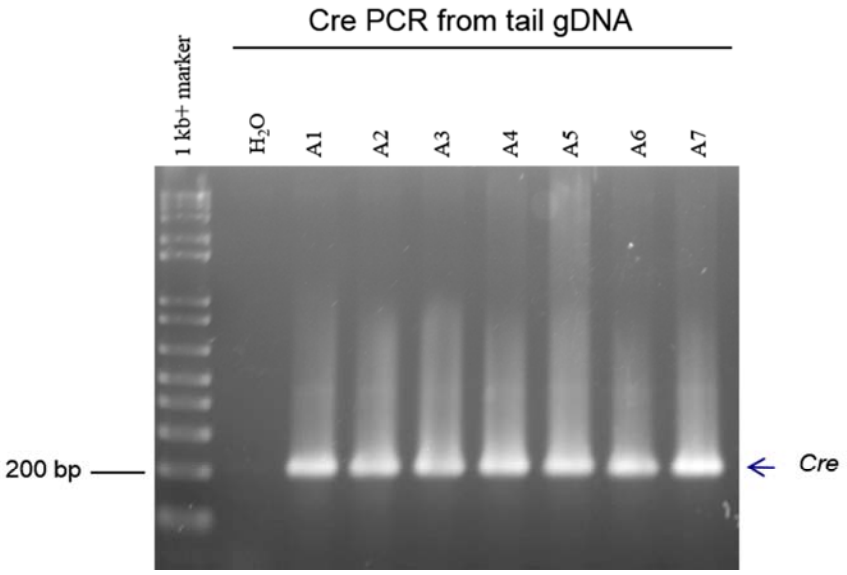

Appendix D 1

Gel electrophoresis diagrams of Cre PCR products from gDNA obtained from individual mice. Lane 3 to 9 represents mice with positive Cre allele with band at 210 bp. Lane 2 shows the negative control with no template. The marker used on lane 1 was 1 kb+ marker.

Appendix E

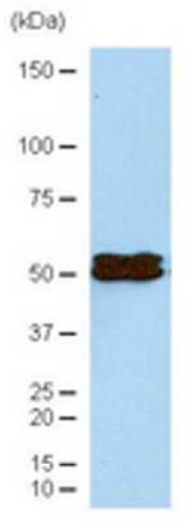

Biological Information	
Immunogen species	The immunogen was a KLH-conjugated synthetic peptide corresponding to amino acids 95-111 of mouse/rat KLF5.
Host	Rabbit
Specificity	This antibody recognizes human KLF5. A strong unidentified band at ~18 kDa is also detected in some cell lysates.
Species Reactivity	Mouse Human Rat
Species Reactivity Note	Human and rat. Expected to react with mouse, as immunogen sequence is identical in mouse and rat.
Antibody Type	Polyclonal Antibody

Appendix E 1

This higher molecular isoform of KLF5 was also observed in the data product sheets obtained from the commercial provider of the KLF5 antibody used for this study. #07-1580; Anti-KLF5 (Krüppel-like factor 5) Antibody from Millipore.

Appendix F

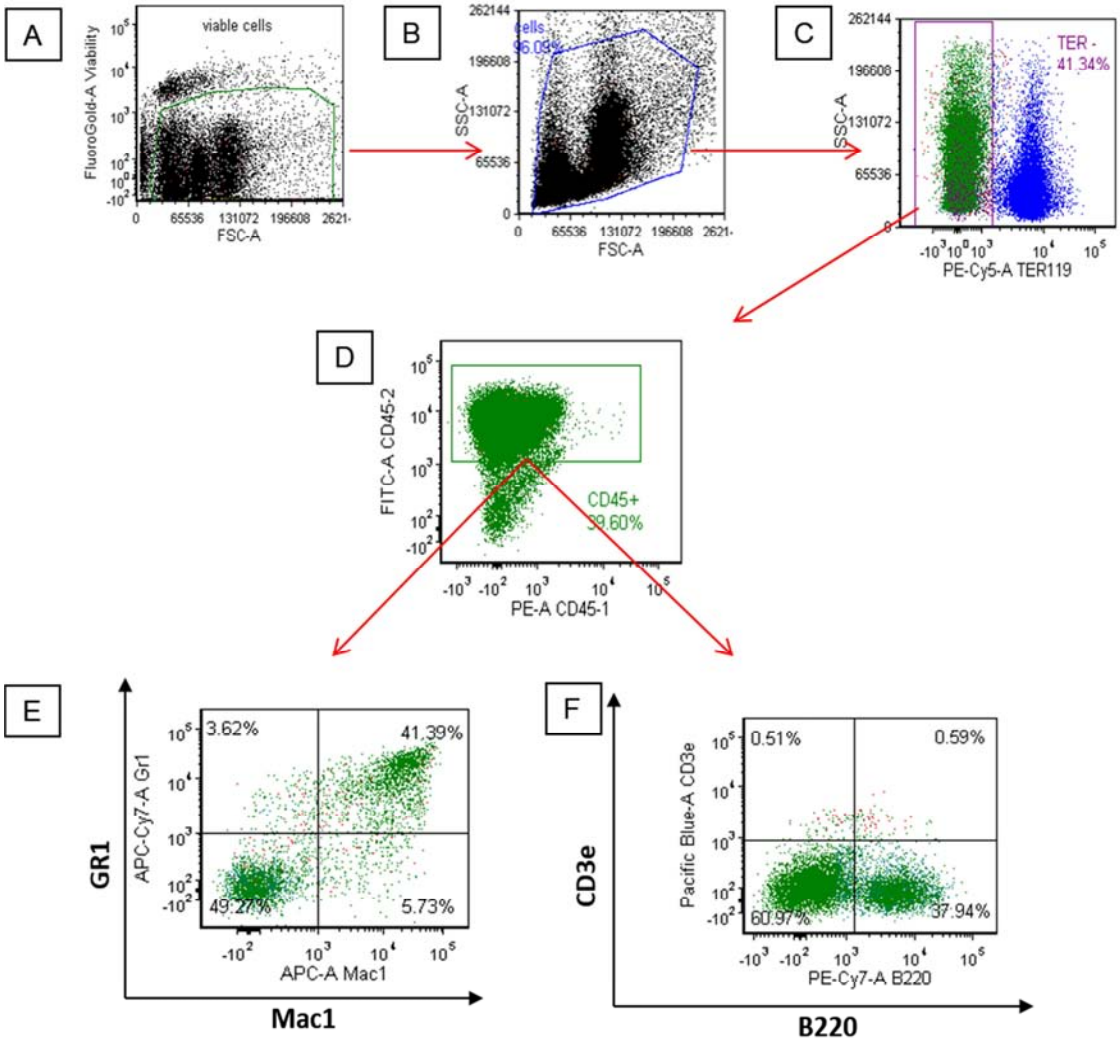

Appendix F 1

Schematic diagram of the gating strategy for cell surface marker flow cytometry analysis of mature myeloid and lymphoid cell types from bone marrow (A) Fluorogold negative cells were first gated as live cells (B) followed by excluding debris based on the forward and side scatter. (C) Next, is the selection of TER119 negative cells (removal of red blood cells). (D) Selection of CD45 positive cells (leukocytes). (E) Gr1 and Mac1 for selection of mature myeloid cells population and (F) and CD3e and B220 marker for selection of mature lymphoid cells type.

Appendix G

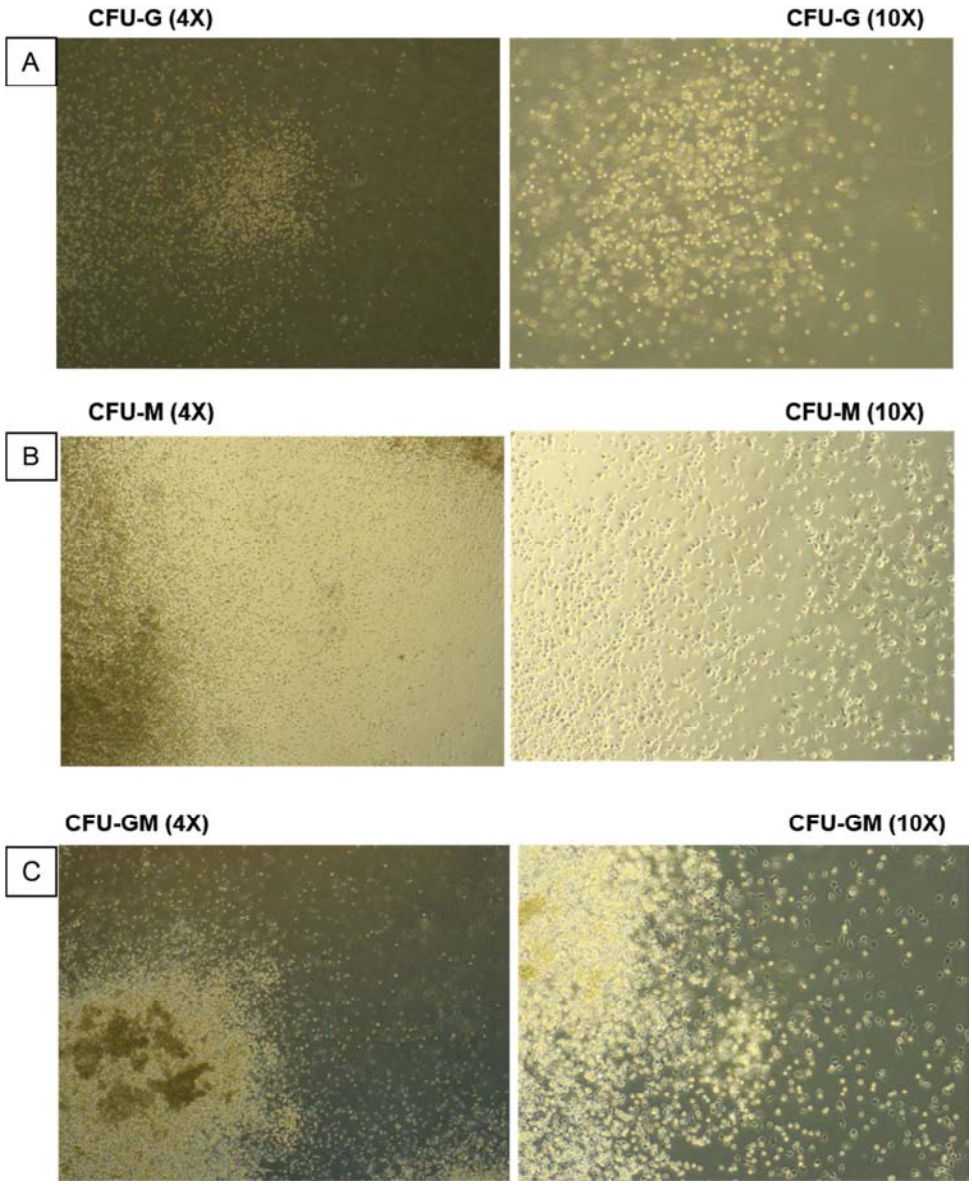

Appendix G 1

Examples of CFU-G, CFU-M and CFU-GM colonies enumerated during colony forming assays from bone marrow. These assay conditions allow for the proliferation and differentiation of hematopoietic progenitors into mature cell types, which can then be enumerated and characterized based on their distinct morphology. Images were viewed under light microscope either at 4x or 10x magnification. Pictures on the left side are at 4x magnification and pictures on the right side are at 10x magnification. **(A)** colony forming unit-granulocyte (CFU-G), **(B)** colony forming unit-macrophage (CFU-M), **(C)** colony forming unit-granulocyte and macrophage (CFU-GM).

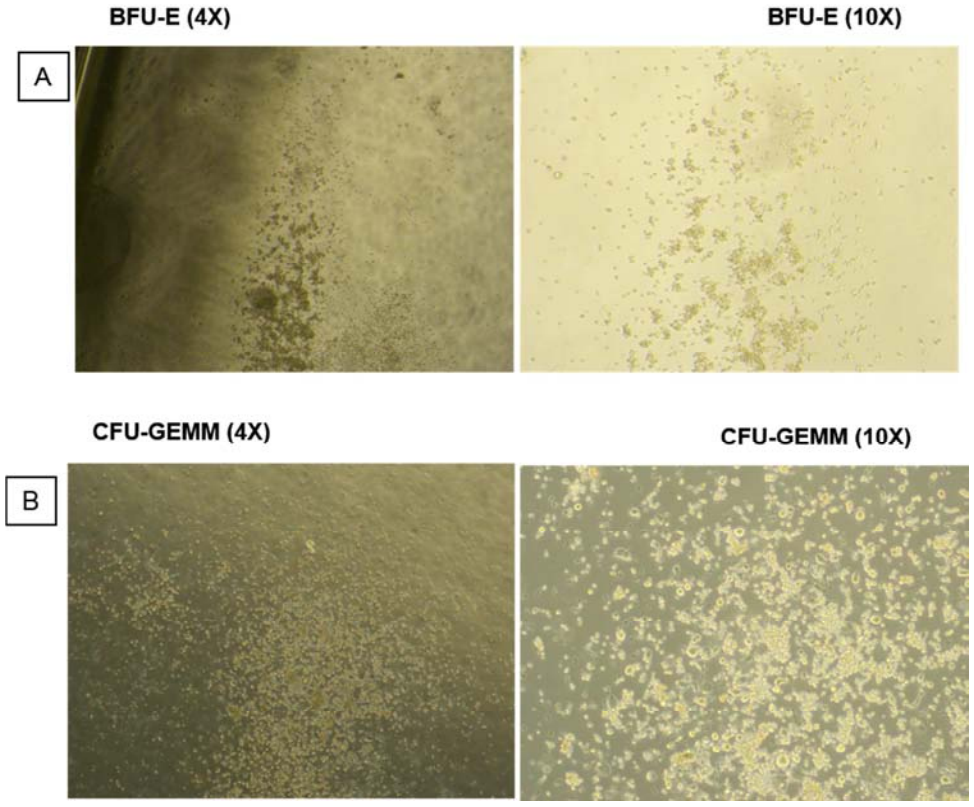

Appendix G 2

Examples of BFU-E and CFU-GEMM colonies enumerated during colony forming assays from bone marrow. These assay conditions allow for the proliferation and differentiation of hematopoietic progenitors into mature cell types, which can then be enumerated and characterized based on their distinct morphology. Images were viewed under light microscope either at 4x or 10x magnification. Pictures on the left side are at 4x magnification and pictures on the right side are at 10x magnification. **(A)** Erythroid burst-forming units (BFU-E) and **(B)** Multipotential colony-forming cells (CFU-GEMM)

Appendix H

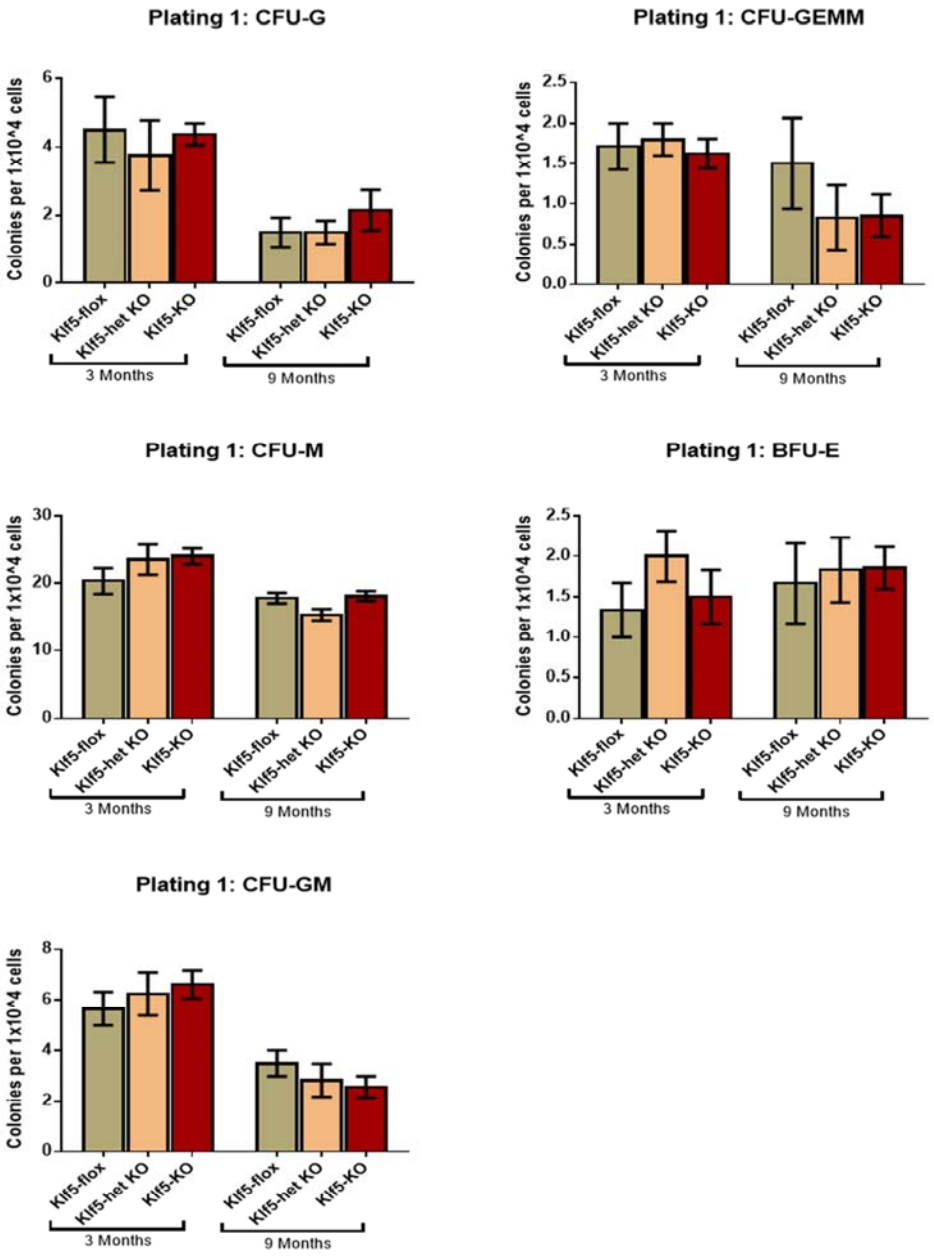

Appendix H 1

Different colonies were typed and scored individually on the first plating of CFU assay from bone marrow of 3 and 9 months old mice. Shown are mean values plus or minus SEM across the genotype grouped by age. **CFU-G**: colony forming unit granulocyte, **CFU-M**: colony forming unit macrophage, **CFU-GM**; colony forming unit granulocyte-macrophage, **BFU-E** burst forming unit erythroid and **CFU-GEMM**; Multipotential colony-forming cells.

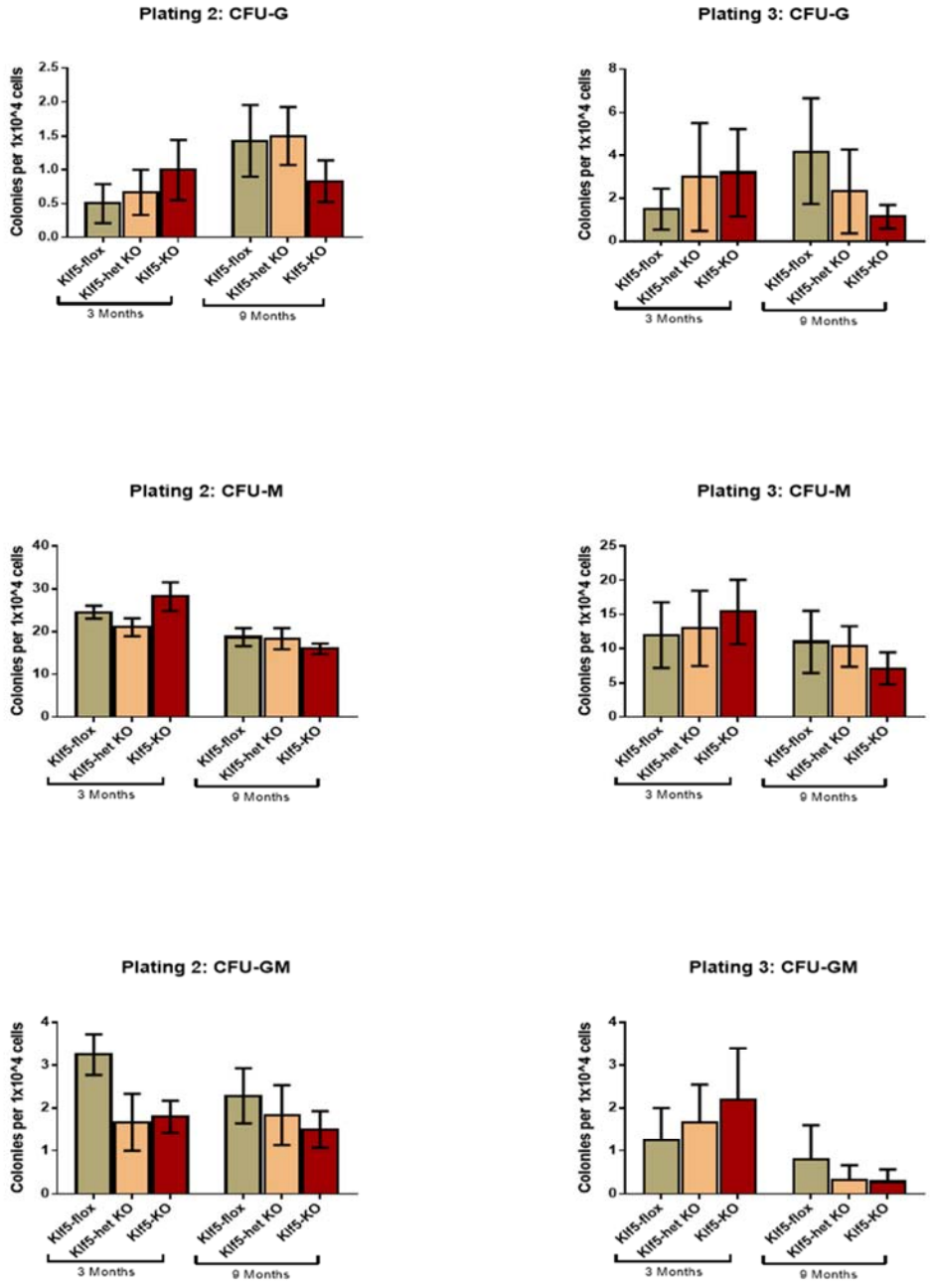

Appendix H 2

Different colonies were typed and scored individually on the serial re-plating of CFU assay from bone marrow of 3 and 9 months old mice. Shown are mean values plus or minus SEM across the genotype grouped by age. **CFU-G**: colony forming unit granulocyte, **CFU-M**: colony forming unit macrophage, **CFU-GM**; colony forming unit granulocyte-macrophage, **BFU-E** burst forming unit erythroid and **CFU-GEMM**; Multipotential colony-forming cells.

Appendix I

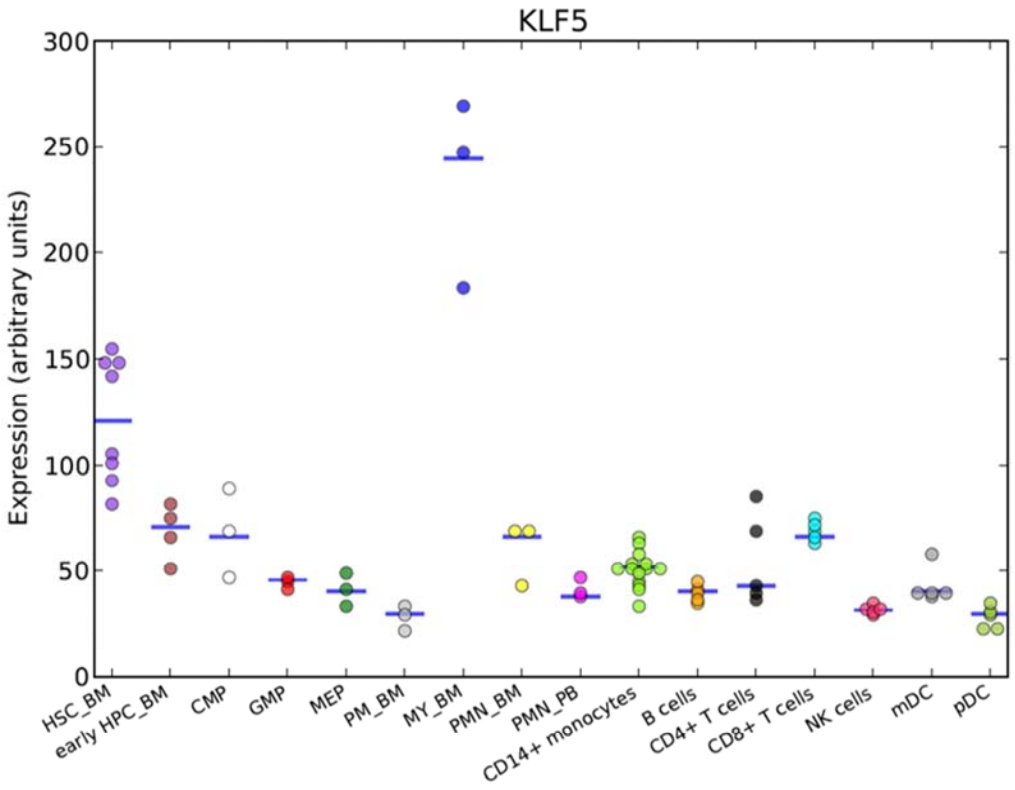

Appendix I 1

The HemaExplorer gene expression database where *KLF5* expression in human T-cells is relatively low compared to myeloid and HSC [327].

Appendix J

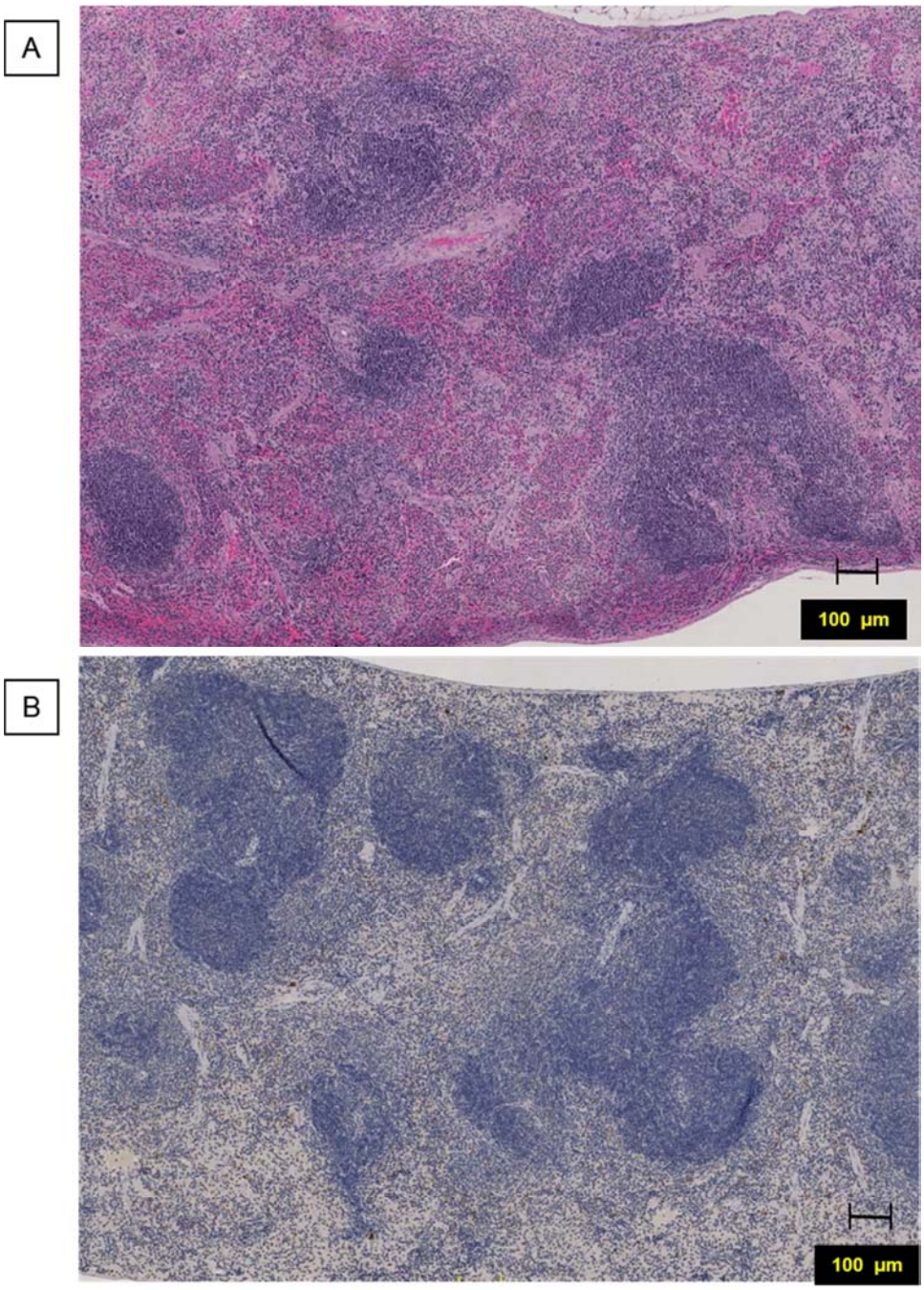

Appendix J 1(i): Spleen morphology of 3 months *Klf5*-flox mice

Mouse spleen from control littermate with age match were sectioned and stained with H&E or and anti-MPO antibody. **A)** Top panel is the *Klf5*$^{fl/fl}$ mice with H&E staining while **B)** the bottom picture shows the spleen section from *Klf5*$^{fl/fl}$ with MPO staining. Images captured at 5X using Nanozoomer DP.

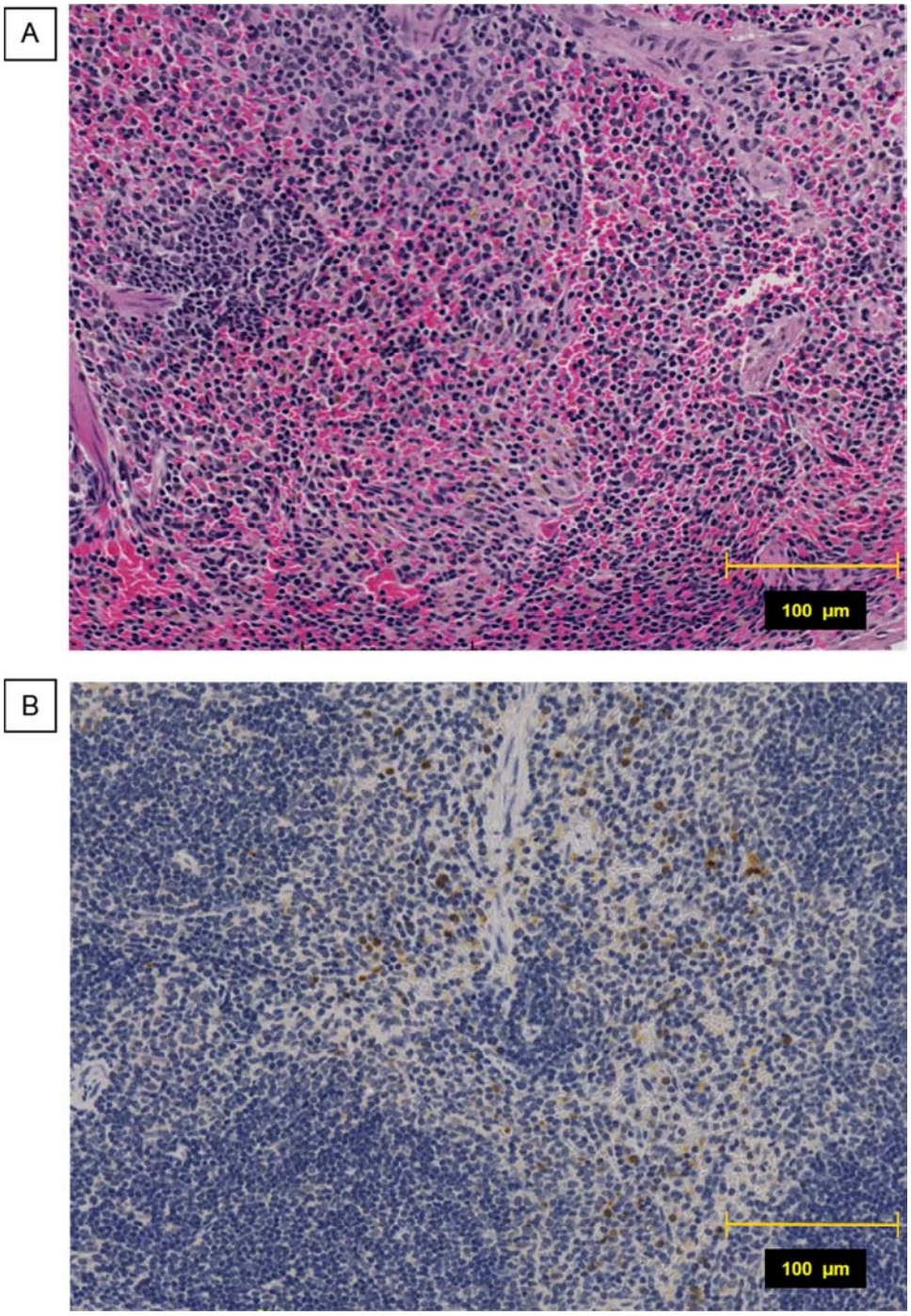

Appendix J 1(ii): Spleen morphology of 3 months *Klf5*-flox mice

Mouse spleen from control littermate with age match were sectioned and stained with H&E or an anti-MPO antibody. **A)** Top panel is the *Klf5*$^{fl/fl}$ mice with H&E staining while **B)** the bottom picture shows the spleen section from *Klf5*$^{fl/fl}$ with MPO staining. Images captured at 5X using Nanozoomer DP. Images captured at 20X using Nanozoomer DP.

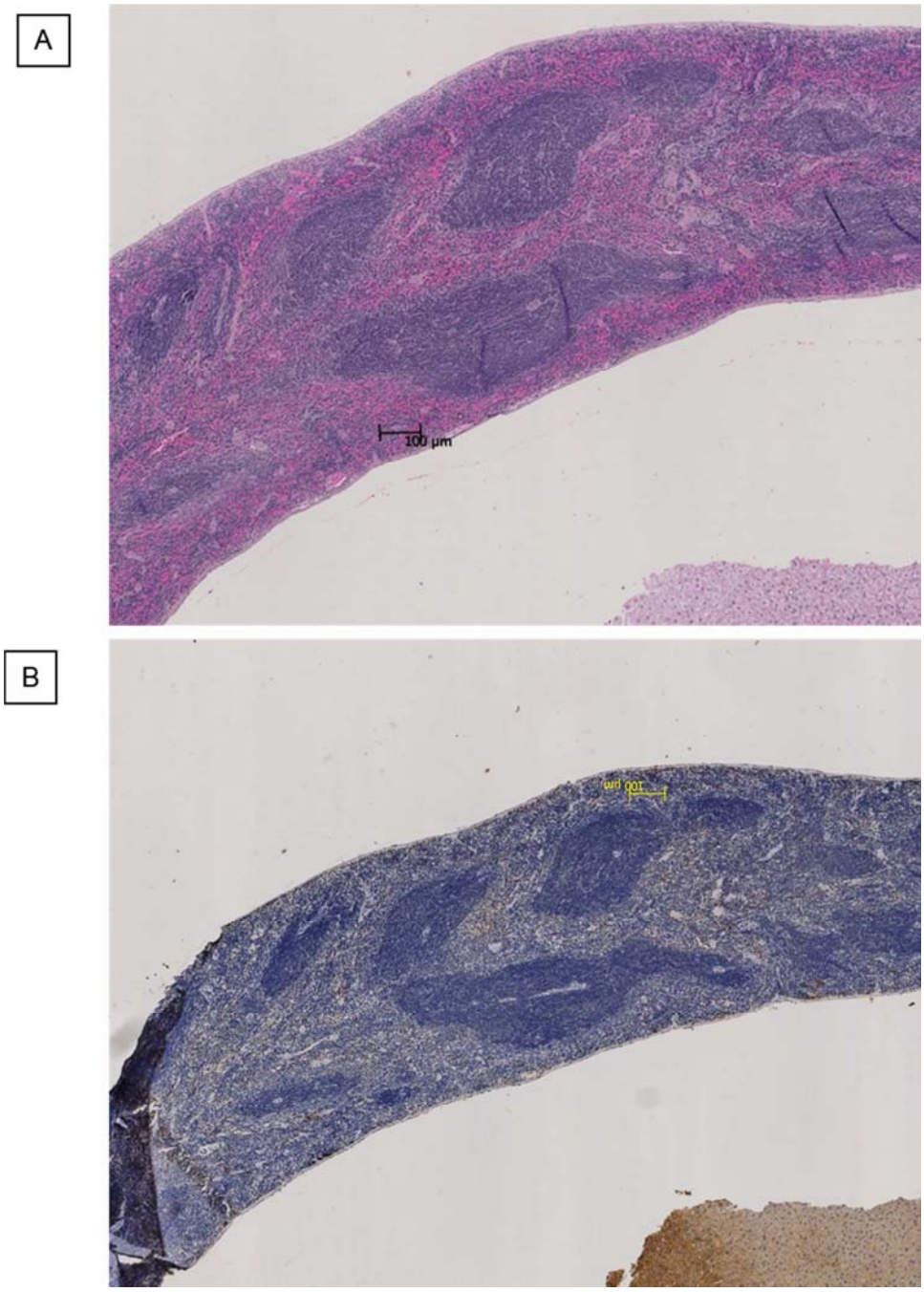

Appendix J 2(i): Spleen morphology of 3 months *Klf5*-flox mice

Mouse spleen from control littermate with age match were sectioned and stained with H&E or an anti-MPO antibody. **A)** Top panel is the *Klf5*$^{fl/fl}$ mice with H&E staining while **B)** the bottom picture shows the spleen section from *Klf5*$^{fl/fl}$ with MPO staining. Images captured at 5X using Nanozoomer DP. Images captured at 5X using Nanozoomer DP.

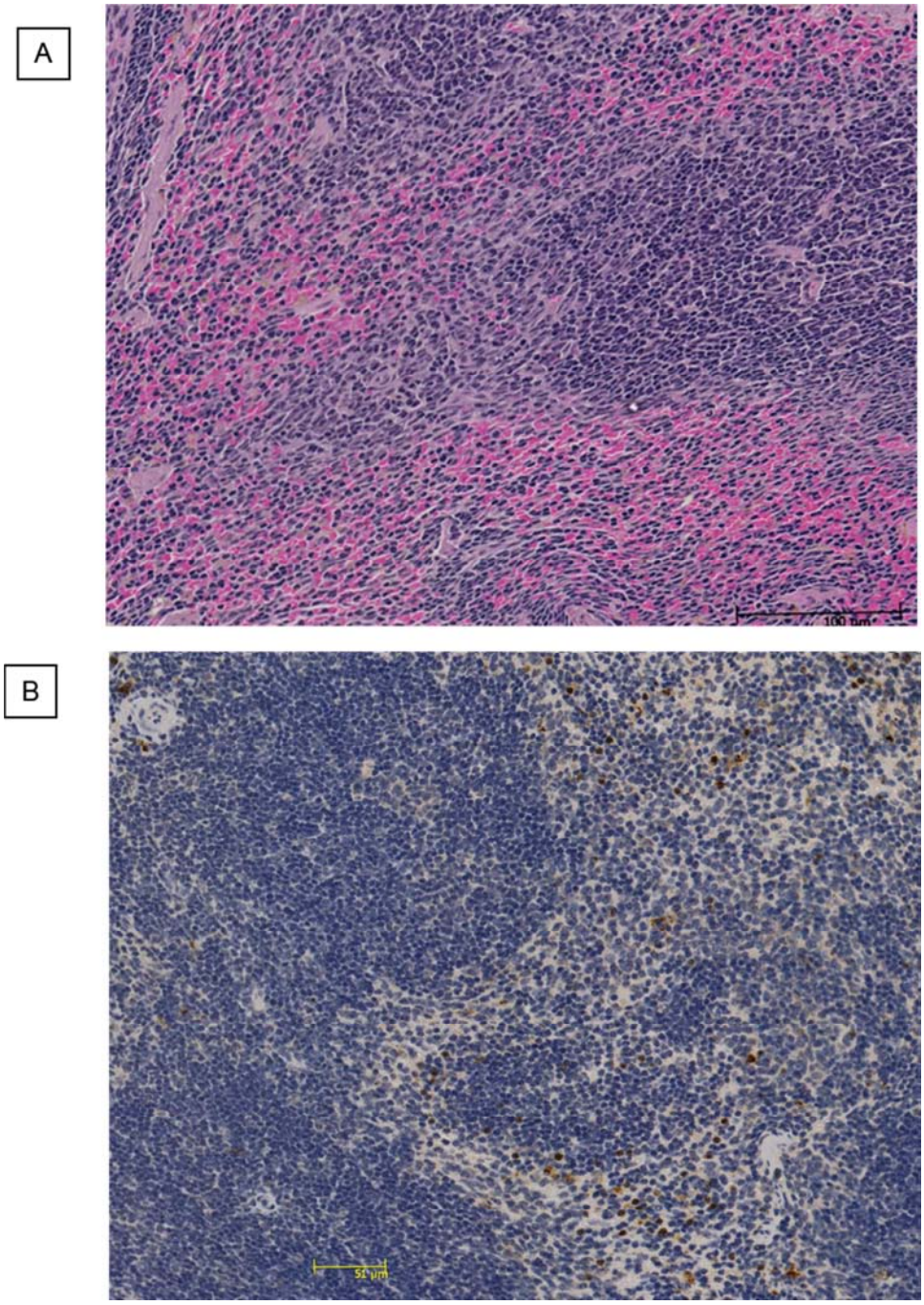

Appendix J 2(ii): Spleen morphology of 3 months *Klf5*-flox mice

Mouse spleen from control littermate with age match were sectioned and stained with H&E or an anti-MPO antibody. **A)** Top panel is the *Klf5*$^{fl/fl}$ mice with H&E staining while **B)** the bottom picture shows the spleen section from *Klf5*$^{fl/fl}$ with MPO staining. Images captured at 5X using Nanozoomer DP. Images captured at 20X using Nanozoomer DP.

Appendix K

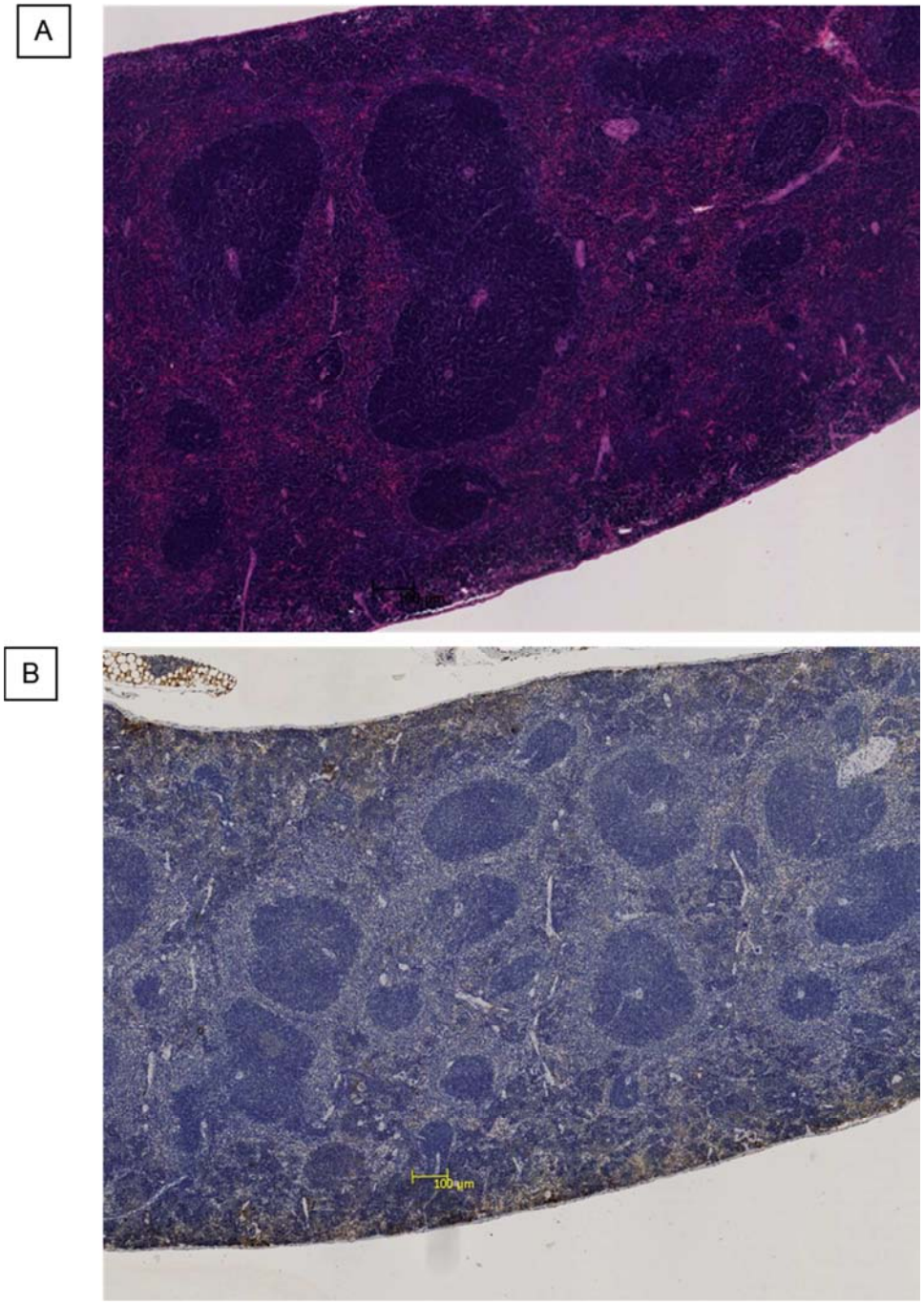

Appendix K 1(i): Spleen morphology of 3 months Klf5Δ/Δ mice

Mouse spleen from knockout mouse were sectioned and stained with H&E or an anti-MPO antibody. A) Top panel is the *Klf5*$^{\Delta/\Delta}$ mice with H&E staining while B) the bottom picture shows the spleen section from *Klf5*$^{\Delta/\Delta}$ with MPO staining. Images captured at 5X using Nanozoomer DP.

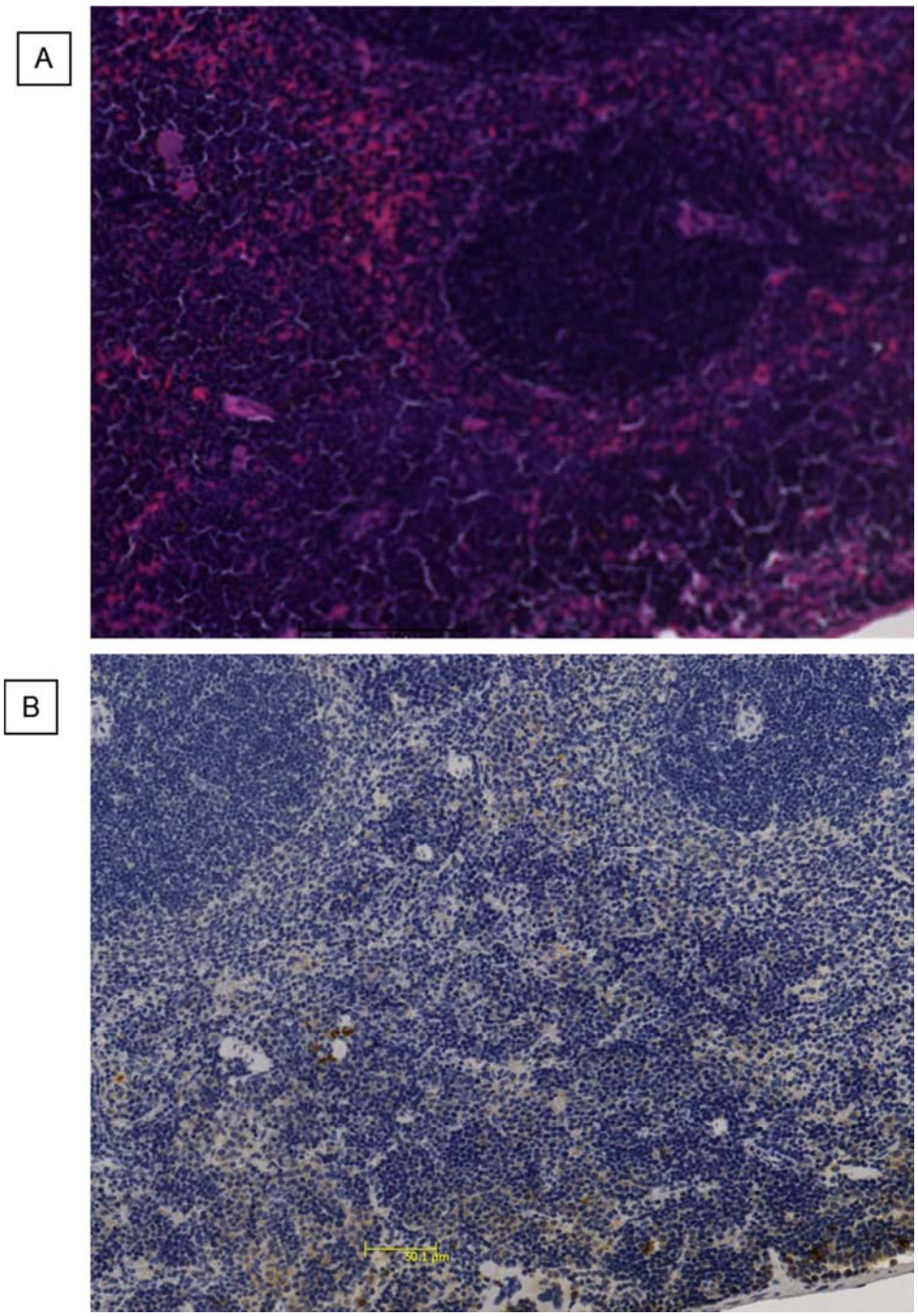

Appendix K 1(ii): Spleen morphology of 3 months *Klf5*$^{\Delta/\Delta}$ mice

Mouse spleen from knockout mouse were sectioned and stained with H&E or an anti-MPO antibody. A) Top panel is the *Klf5*$^{\Delta/\Delta}$ mice with H&E staining while B) the bottom picture shows the spleen section from *Klf5*$^{\Delta/\Delta}$ with MPO staining. Images captured at 5X using Nanozoomer DP.

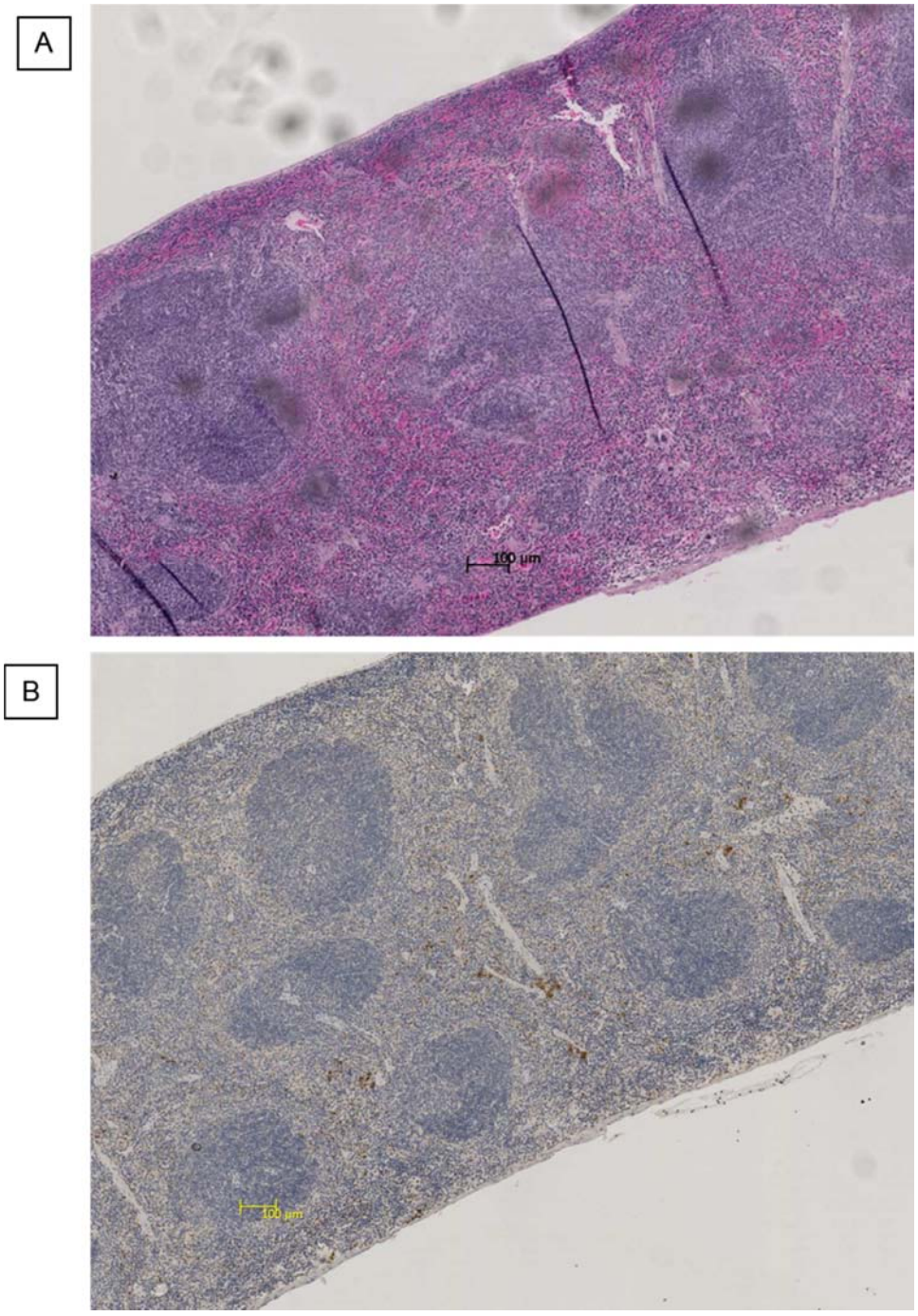

Appendix K 2(i): Spleen morphology of 3 months *Klf5*$^{\Delta/\Delta}$ mice

Mouse spleen from knockout mouse were sectioned and stained with H&E or an anti-MPO antibody. A) Top panel is the *Klf5*$^{\Delta/\Delta}$ mice with H&E staining while B) the bottom picture shows the spleen section from *Klf5*$^{\Delta/\Delta}$ with MPO staining. Images captured at 5X using Nanozoomer DP.

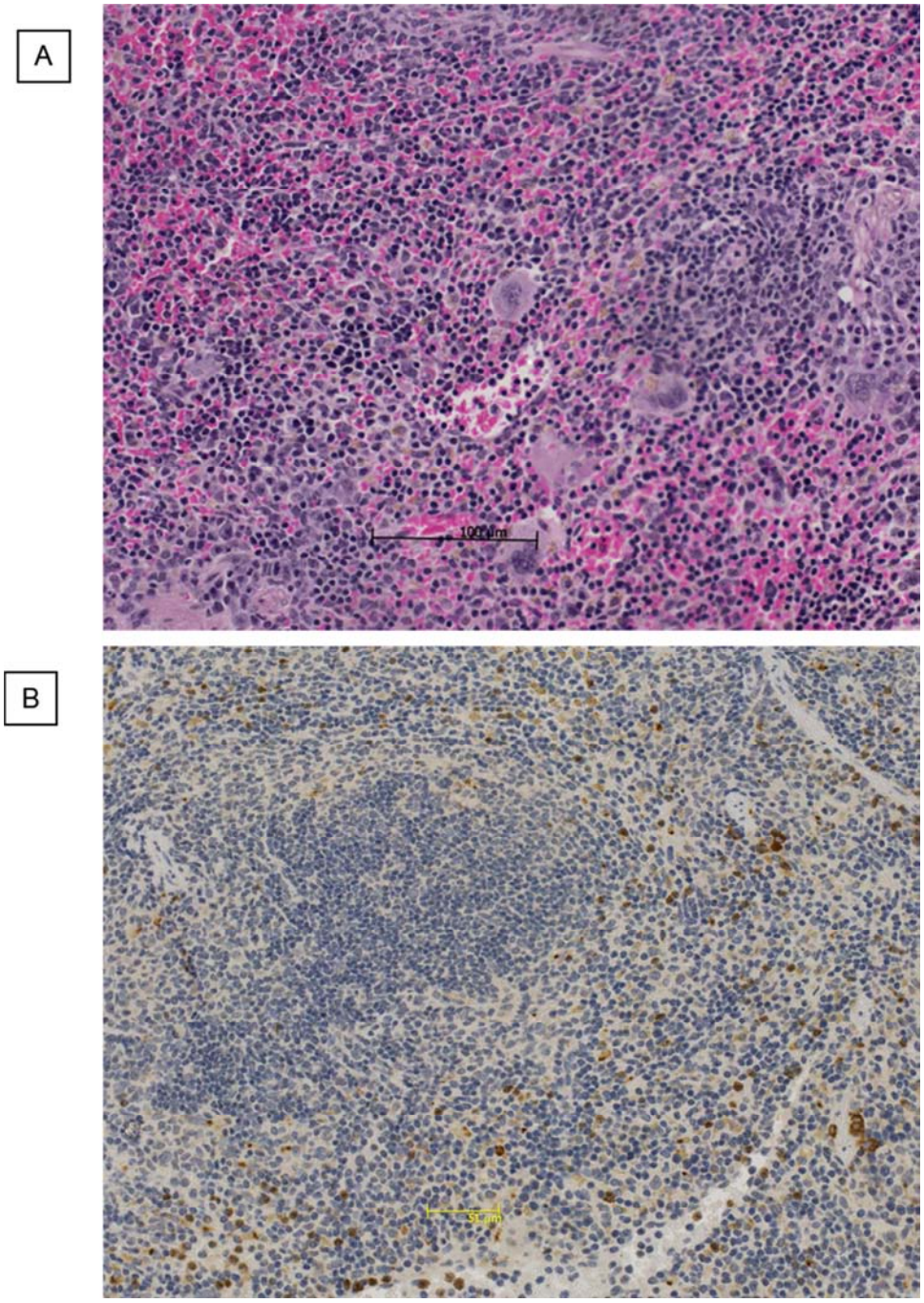

Appendix K 2(ii): Spleen morphology of 3 months *Klf5*$^{\Delta/\Delta}$ mice

Mouse spleen from knockout mouse were sectioned and stained with H&E or an anti-MPO antibody. A) Top panel is the *Klf5*$^{\Delta/\Delta}$ mice with H&E staining while B) the bottom picture shows the spleen section from *Klf5*$^{\Delta/\Delta}$ with MPO staining. Images captured at 20X using Nanozoomer DP.

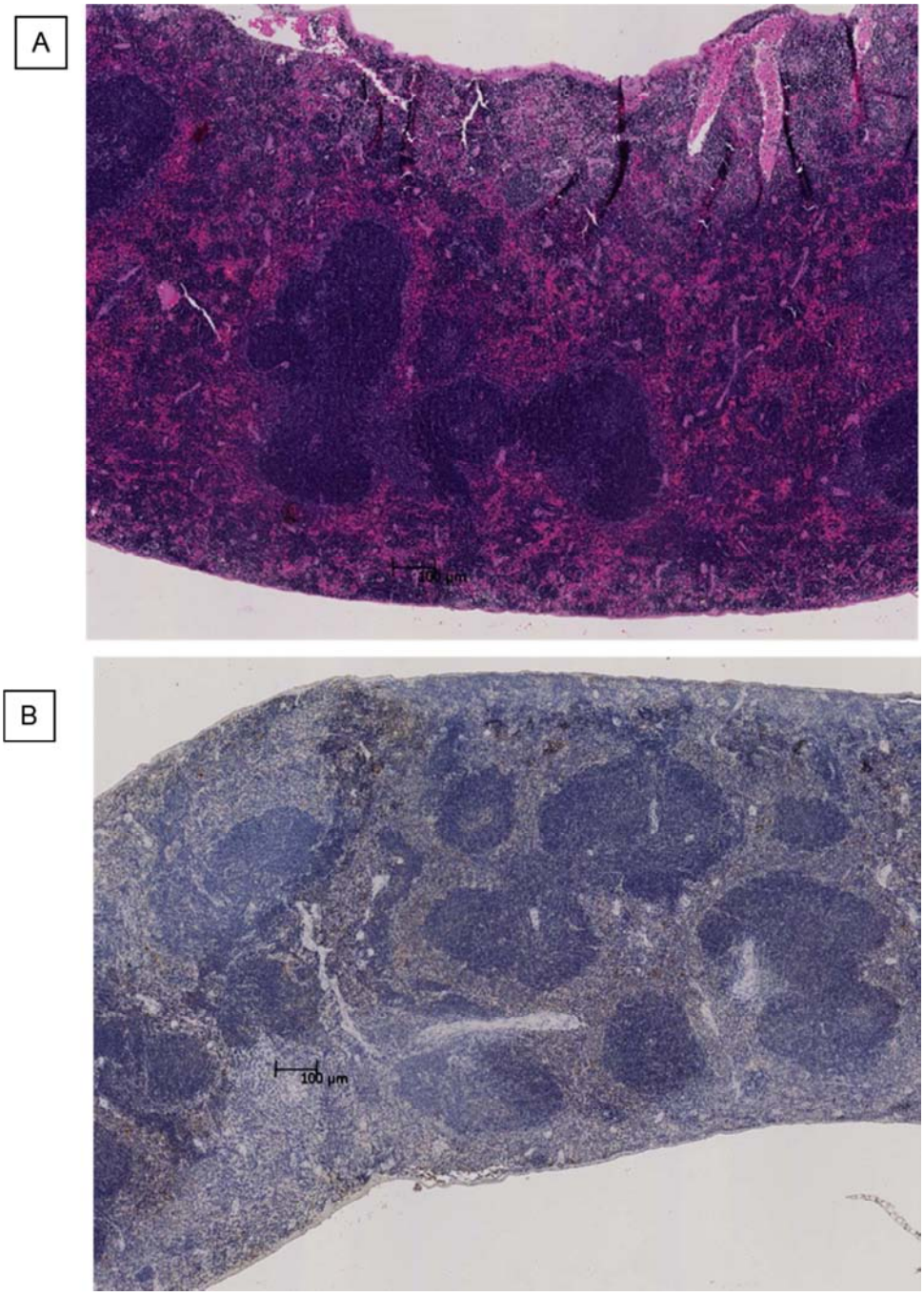

Appendix K 3(i): Spleen morphology of 3 months *Klf5*$^{\Delta/\Delta}$ mice

Mouse spleen from knockout mouse were sectioned and stained with H&E or an anti-MPO antibody. A) Top panel is the *Klf5*$^{\Delta/\Delta}$ mice with H&E staining while B) the bottom picture shows the spleen section from *Klf5*$^{\Delta/\Delta}$ with MPO staining. Images captured at 5X using Nanozoomer DP.

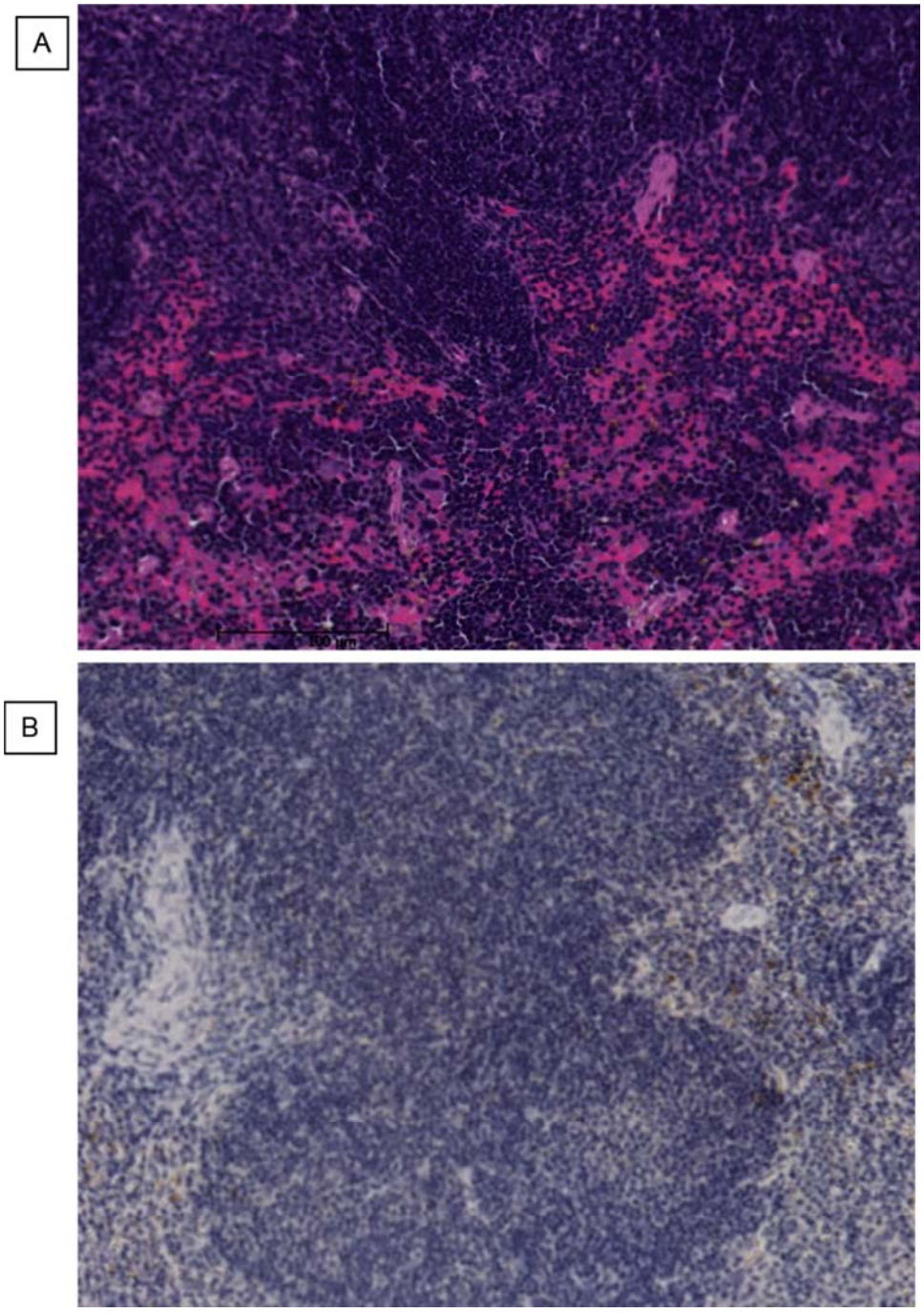

Appendix K 3(ii): Spleen morphology of 3 months *Klf5*$^{\Delta/\Delta}$ mice

Mouse spleen from knockout mouse were sectioned and stained with H&E or an anti-MPO antibody. A) Top panel is the *Klf5*$^{\Delta/\Delta}$ mice with H&E staining while B) the bottom picture shows the spleen section from *Klf5*$^{\Delta/\Delta}$ with MPO staining. Images captured at 20X using Nanozoomer DP.

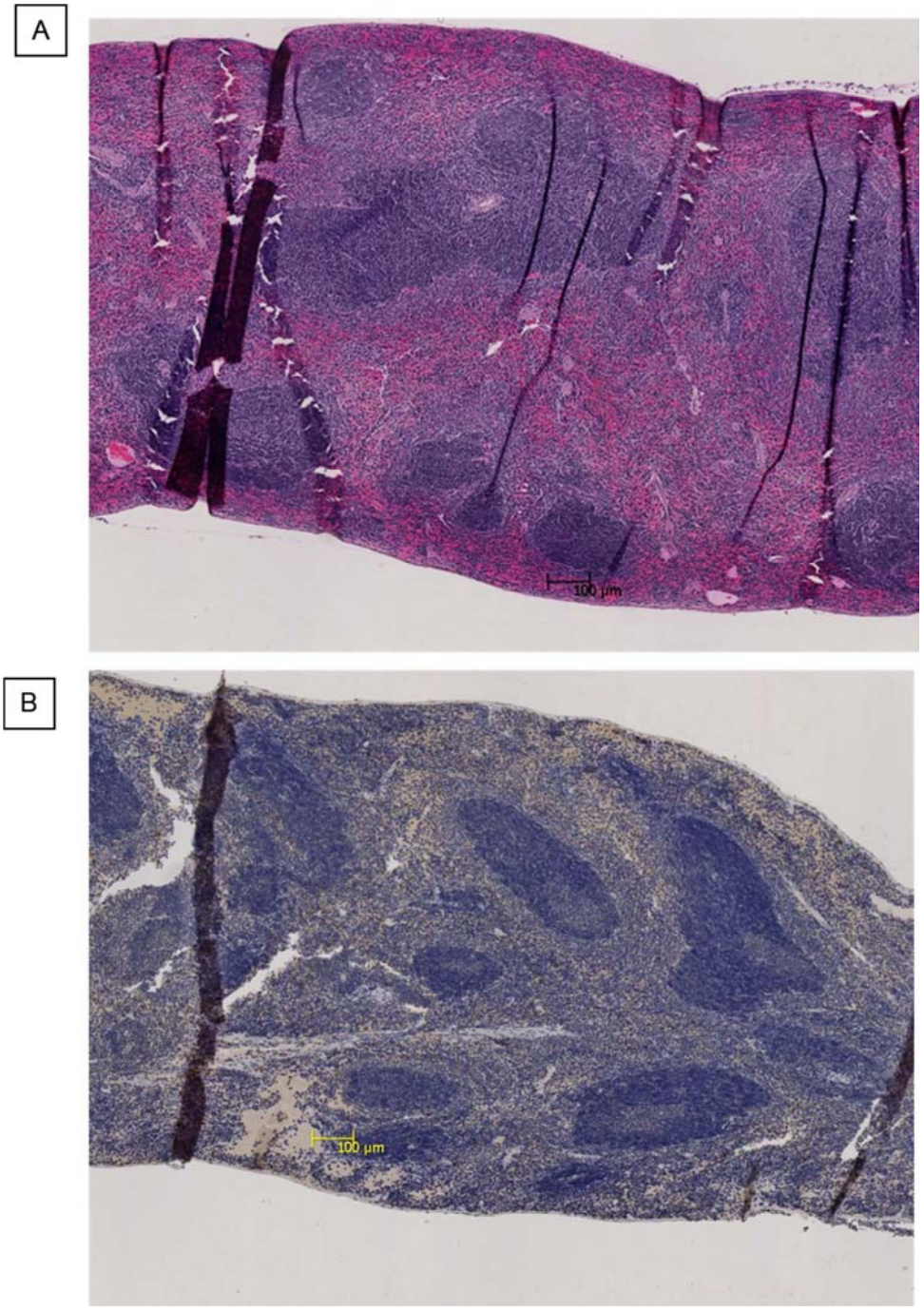

Appendix K 4(i): Spleen morphology of 3 months *Klf5*$^{\Delta/\Delta}$ mice

Mouse spleen from knockout mouse were sectioned and stained with H&E or an anti-MPO antibody. A) Top panel is the *Klf5*$^{\Delta/\Delta}$ mice with H&E staining while B) the bottom picture shows the spleen section from *Klf5*$^{\Delta/\Delta}$ with MPO staining. Images captured at 20X using Nanozoomer DP.

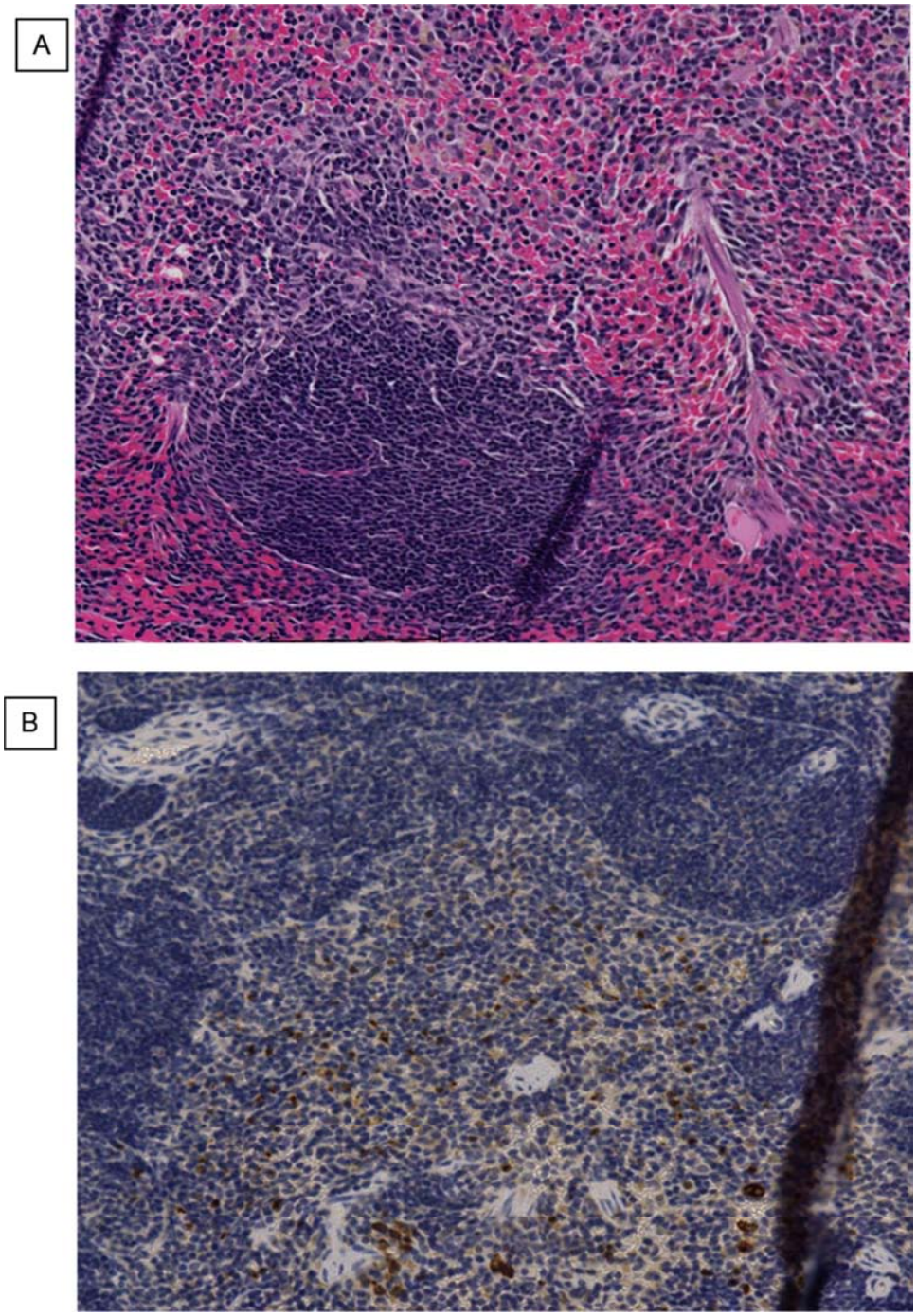

Appendix K 4(ii): Spleen morphology of 3 months *Klf5*$^{\Delta/\Delta}$ mice

Mouse spleen from knockout mouse were sectioned and stained with H&E or an anti-MPO antibody. A) Top panel is the *Klf5*$^{\Delta/\Delta}$ mice with H&E staining while B) the bottom picture shows the spleen section from *Klf5*$^{\Delta/\Delta}$ with MPO staining. Images captured at 20X using Nanozoomer DP.

Appendix L

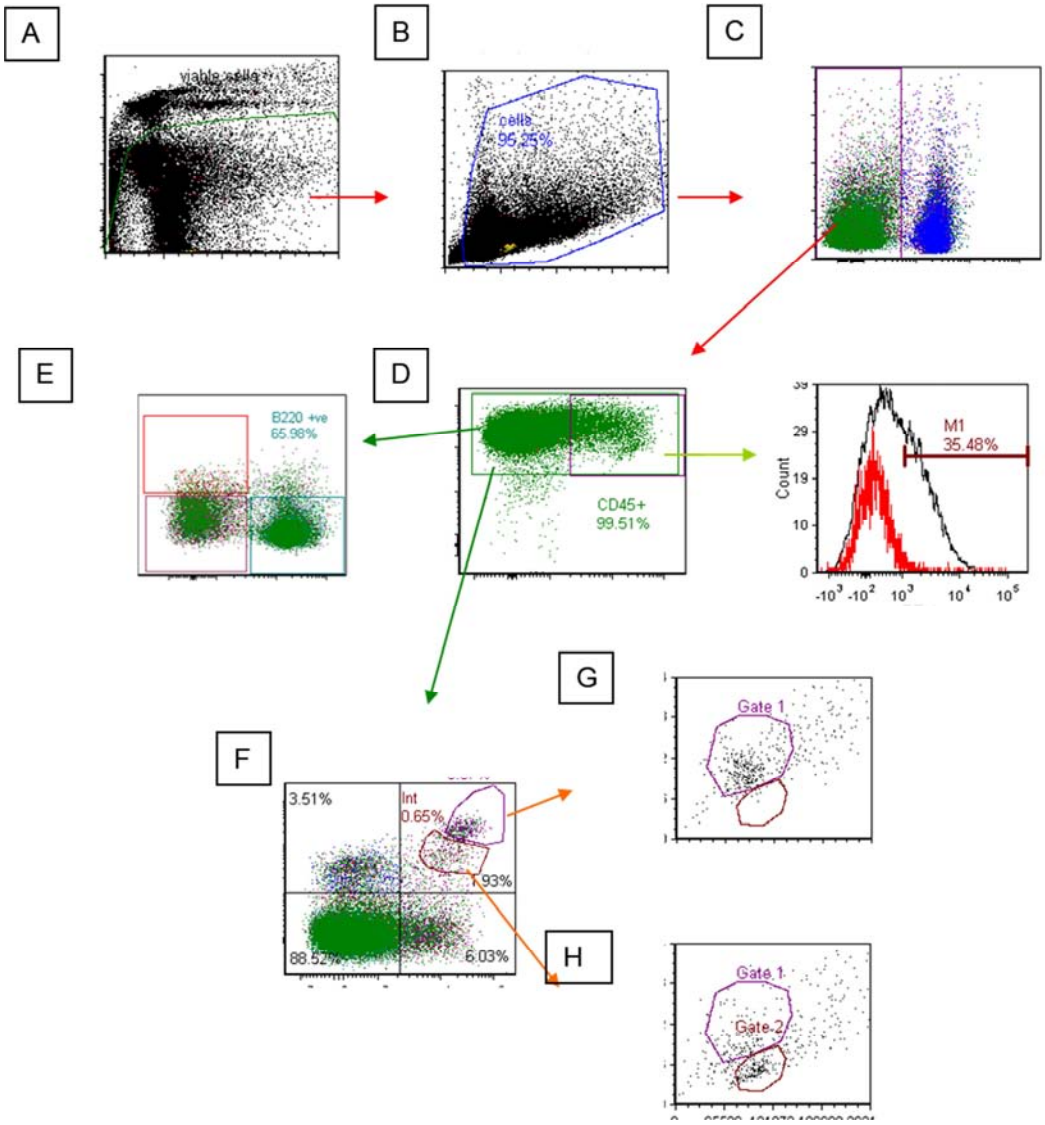

Appendix L 1

Flow cytometry analysis to assess mature cell types from the spleens of 9 month old mice. Plots showed are the representative of the gating strategy used for flow cytometry analysis of cell surface marker on mature myeloid and lymphoid cell types from spleen **(A)** Fluorogold negative cells were first gated as live cells **(B)** followed by purifying live cells based on the forward and side scatter. **(C)** Next, was to remove the TER119 positive cells (the red blood cell population) from the analysis. **(D)** The sequential panels was for the selection of CD45 positive cells which will then followed by plot to determine more specific define cell types, for example the plot with **(E)** CD3e and B220 marker for selection of mature lymphoid cells type and **(F)** Gr1 and Mac1 for mature myeloid cells population. The Gr1+Mac1+ have two different FS and SS character as shown above which can be defined as **(G)** The $Gr1^{hi}Mac1^{hi}$ cells and **(H)** $Gr1^{int}Mac1^{int}$ cells.

Appendix M

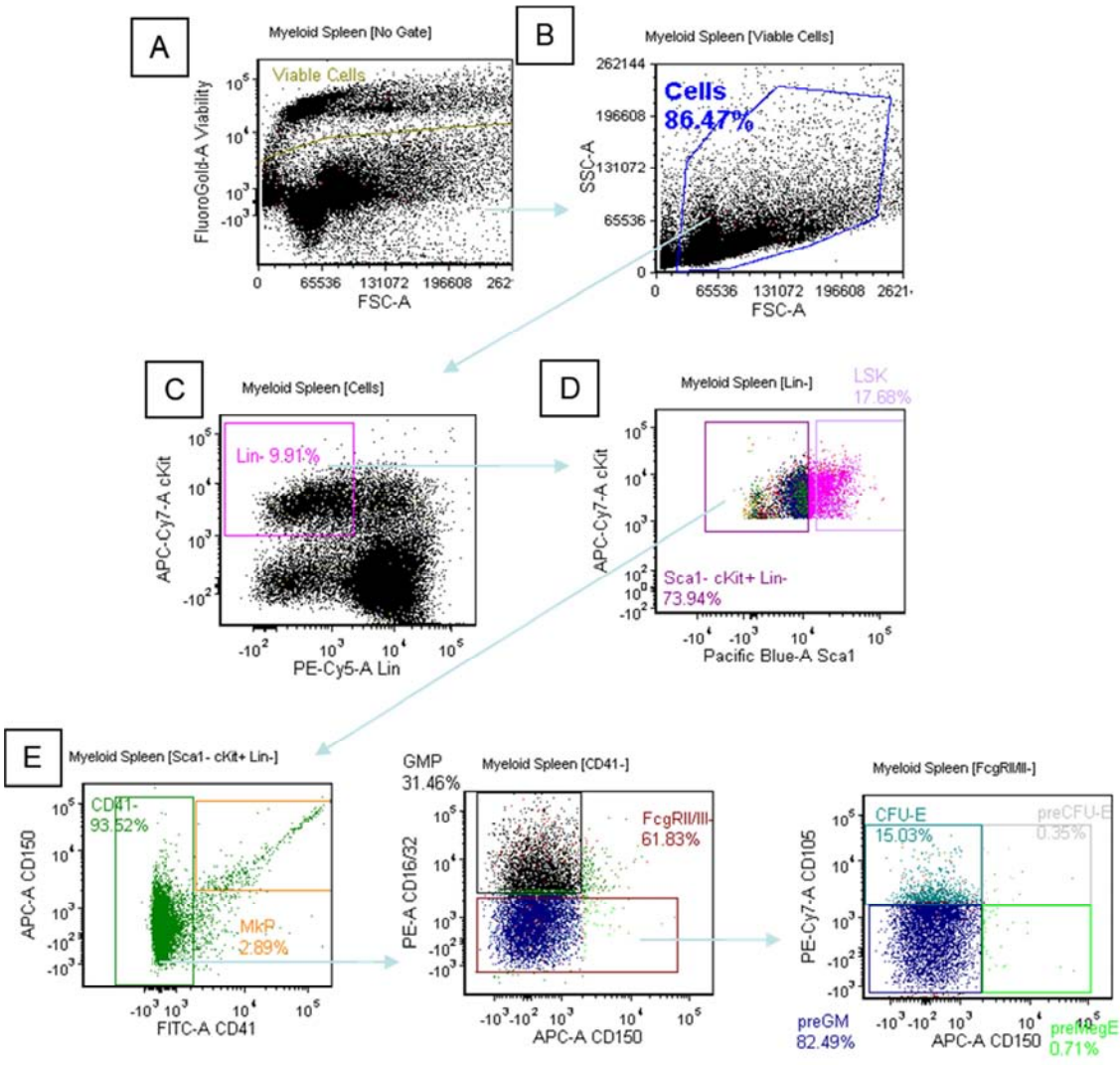

Appendix M 1

Flow cytometry analysis to assess myeloid progenitor from spleen cells of 9 months old mice. **(A)** Cells purification were started on gating the live cells, which are fluorogold negative **(B)** followed by eliminating unwanted particles including dead cells and debris based on the forward and side scatter to purify selected cells. **(C)** In order to increase the positive signals from immature cells type lineage negative and c-Kit positive cells were selected for the sequential plot. **(D)** Subsequent plot shows the gating on Sca-1 negative cells as for specific selection of myeloid progenitor cells. **(E)** Consecutively, the next three plots show the purified myelo-erythroid progenitor subsets including early bipotent progenitors for the erythroid/megakaryocyte lineages (preMegE), early monopotent erythroid (preCFU-E and CFU-E) and megakaryocyte progenitors (MkP), and primitive granulocyte/macrophage progenitors (preGM and GMP).

Appendix N

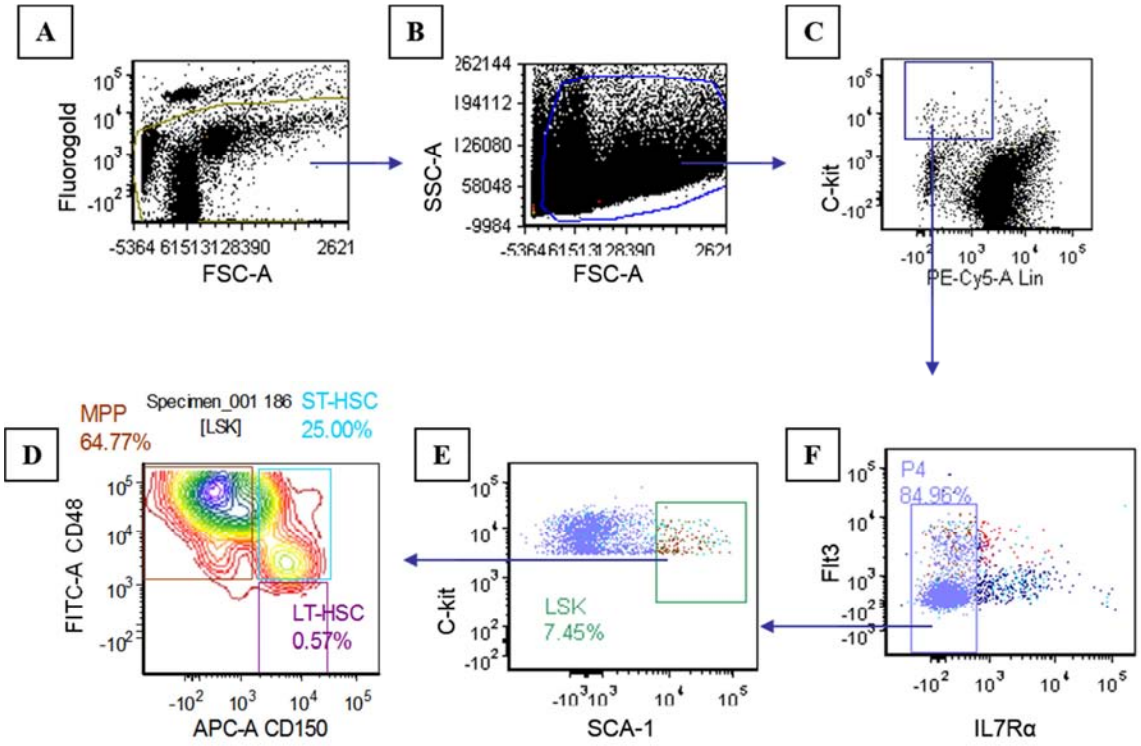

Appendix N 1

Flow cytometry analysis to assess stem cells compartment in the spleen of 12 months old mice. **(A)** Cells purification were started on gating the live cells, which are fluorogold negative **(B)** followed by eliminating unwanted particles including dead cells and debris base on the forward and side scatter to purify selected cells. **(C)** In order to increase the positive signals from immature cells type lineage negative and c-kit positive cells were selected for the sequential plot. **(D)** Subsequent plot shows the gating on IL7Rα negative cells as for specific selection for stem cells population. **(E)** Consecutively, the next plot were for Sca-1 positive cell selection. **(F)** Lastly, shown was the plot for specific stem cell selection which were long-term HSC (LT-HSC), short-term HSC (ST-HSC) and multi-potent progenitor (MPP).

Appendix O

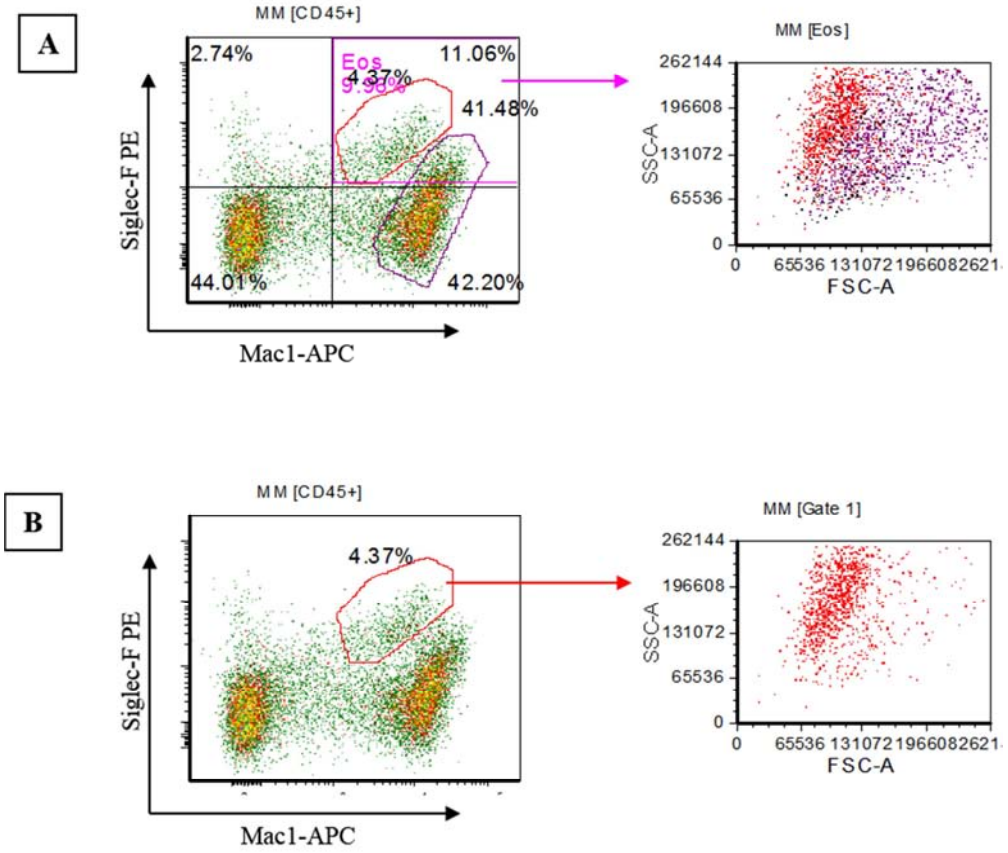

Appendix O 1

The gating strategy used to select for the eosinophil cell population in the peripheral blood and bone marrow. A) Total Sig-F^{+}, Mac-1^{+} double-positive gate will include some of the neutrophil cells as shown in the FS/SS plot. B) Eosinophil cells were determined as Sig-F^{+}, Mac1^{hi} population as shown in the red gate.

Appendix P

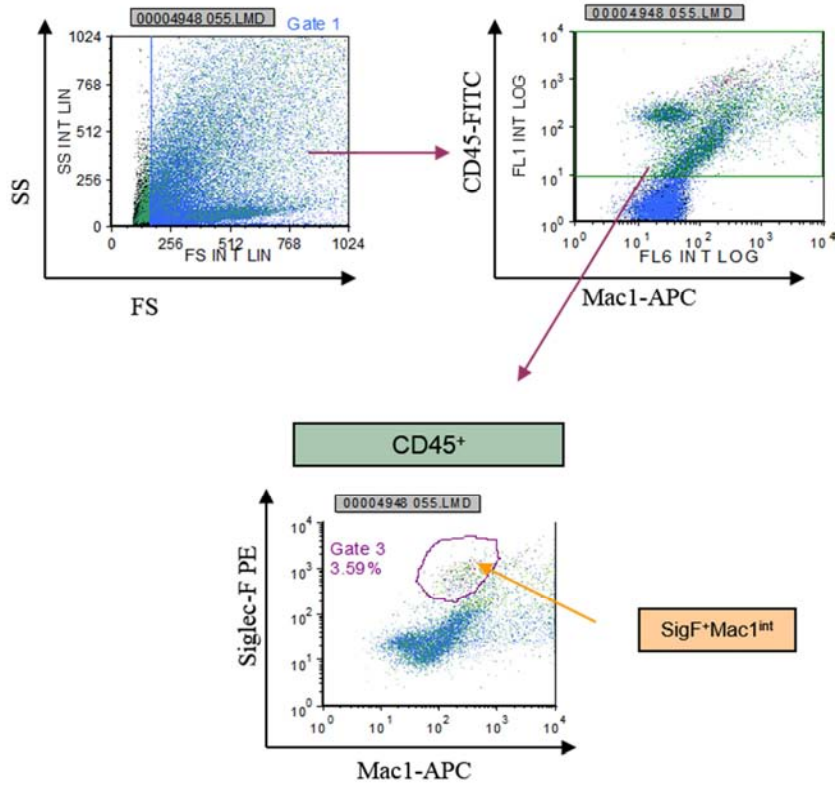

Appendix P 1

The gating strategy used to select for the eosinophil cell population in the lung. First plot shows the forward and side scatter with a gate to eliminate unwanted particles including debris and dead cells. Then, a gate was set on CD45 positive cells followed by gating on $Mac1^{int}$ and Siglec-F^{+}. Experiments were conducted on 6 mice from each genotype.

Thesis Amendment

Thesis Amendment as requested by reviewer 1

Chapter 1

No further information was requested for this chapter.

Chapter 2

No further information was requested for this chapter.

Chapter 3

Reviewer comment:

It is a little difficult to be sure how much of the data and figures presented in Chapter 3 were done by the student and how much were done by QIMR. The same applies for Appendices A-E. Any Figures generated by QIMR should have the appropriate acknowledgement. This should be clearly stated somewhere.

Respond to reviewer comment:

Page 82: Figure 3.4: "These steps were conducted by the QIMR transgenic facility" has been added in the figure legend to acknowledge the initial work done at QIMR.

QIMR provided the *Klf5*$^{+/fl}$*Flpe*$^{+}$ mice, hence I was directly involved in the subsequent steps of generating *Klf5*$^{fl/fl}$*VavCre*$^{+/-}$ mice including the

genotyping of *Klf5*$^{+/fl}$*Flpe*$^{+}$ mice when they first arrived in our facility. Hence no acknowledgement has been assigned in the subsequent Figures in Chapter 3.

Page 202: Appendix A: "This final cloning and targeting report was generated by the QIMR transgenic facility" has been added to acknowledge the initial work done at QIMR.

Page 203: Appendix A1: "This figure has been generated by the QIMR transgenic facility" has been added to acknowledge the initial work done at QIMR.

Page 208: Appendix B: "This Klf5 targeting transmission report has been generated by the QIMR transgenic facility" has been added to acknowledge the initial work done at QIMR.

Page 214 and 215: Appendices C and D: I generated these results and figures hence no acknowledgement has been added.

Reviewer comment:

The lack of complete loss of function model should be discussed somewhere at the end of Chapter 3. Does the student think a different cross to a different Cre driver might result in further knockdown of Klf5?

Respond to reviewer comment:

Page 97: Additional discussion has been added as follows:

While we cannot rule out that there is significant residual function of Klf5 in our knockout model, based on other reports of Klf5 conditional knockouts we believe that this 75% Klf5 protein reduction (Figure 3.10) observed by us is sufficient to reveal a loss of function phenotype. For example, *Xing et al.* have shown that approximately 80% Klf5 deletion in prostatic epithelial cells is enough to promote the development and severity of prostate tumorigenesis [312]. This Klf5 deletion was obtained by using a *PB-Cre4* transgenic strain where expression of Cre recombinase is driven by the prostatic epithelial specific probasin promoter [312]. In addition, another study has shown that conditional disruption of Klf5 derived by mating *Klf5-LoxP* and *Le-Cre* mice results in approximately 25% of Klf5 protein remaining and causes defective eyelids, malformed meibomian glands, abnormal cornea and loss of conjunctival goblet cells [311]. The most effective Klf5 knockout model so far is the inducible *Mx1-Cre;Klf5*$^{flox/flox}$ model as reported by *Ishikawa et al*. where approximately 10% of *Klf5* mRNA is expressed in the *Mx1-Cre;Klf5*$^{flox/flox}$ mice [275]. However, this system also allows partial gene inactivation in other tissues [313], which potentially results in indirect phenotype.

Chapter 4

Reviewer comment:

I have some technical concerns about the analysis of the HSC and progenitor cell populations (Figure 4.11). I am not sure the Sca-1 has worked properly. There seem

to be too many cells in the LSK gate in part D to me; 32% of the kit^{+} cells. In my experience normal marrow would have <3% in this gate using this method. Does the student have any explanation of why this looks so different to other published work?

Respond to reviewer comment:

In this study the LSK population, was determined as the percentage of the Sca-1^{+} gate from the c-Kit^{+}, Lin^{-} population (as mentioned in the text on page 102). In the literature, the LSK population is often alternatively defined by the Sca-1^{+}, c-Kit^{+} population from the Lin^{-} population, for example as shown by *Dolence et. al* and *Kunimoto et. al* [371, 372]. This is most likely the strategy that is being referred to by reviewer 1. We have used the strategy described by *Pronk et. al* (see page 103 of the thesis) for the detection of immature myelo-erythroid progenitor subsets from c-Kit^{+} enriched bone marrow cells. However, if we alter the analysis to determine LSK as a percentage of the Sca-1^{+}, c-Kit^{+} from the Lin^{-} population, the LSK percentage obtained for this specific sample shown in Figure 4.11 is 3.18% from total c-Kit^{+} enriched cells. Therefore we believe the discrepancy highlighted by review 1 is due only to this alternative analysis strategy and not a technical difference in staining or data collection.

Reviewer comment:

Can some comment be made about colony types in Figure 4.20?

Respond to reviewer comment:

No additional information is added: Different types of colonies were scored in the first plating and the subsequent replating and are shown in Appendix H. Comment was also made in Section 4.2.3.1, Chapter 4.

Chapter 5

Reviewer comment:

Again some idea about colony type might be useful. Was any FACS done for erythroid cells in the spleen?

Respond to reviewer comment:

No additional information is added: Different types of colonies were scored in this assay and shown in Figure 5.6. Comment was also made in Chapter 5, Section 5.2.2.1.

No FACS was conducted for erythroid cells in the spleen as part of this project, but it is agreed that this could be measured in future experiments.

Chapter 6

Reviewer comment:

Is 25% residual KLF5 protein enough for near normal function? What alternatives could be tried in the future? Another cross?

Respond to reviewer comment:

Refer page 97 in Chapter 3 and as comment above (page 242).

Reviewer comment:

Does the candidate think any molecular studies are worth considering in the future or is the phenotype too trivial for this to be considered a worthy to pursuit?

Respond to reviewer comment:

Page 177: Additional discussion has been added.

As such, a future experiment to examine the changes in gene expression by microarray analysis will be beneficial. This could be designed to compare the *Klf5*$^{fl/fl}$ and *Klf5*$^{\Delta/\Delta}$ haemopoietic transcriptomes in HSC, eosinophils and neutrophils from bone marrow specifically from 9 and 12 months old mice. This would identify the changes in gene expression associated with HSC, eosinophils and neutrophils.

Thesis Amendment as requested by reviewer 2

Chapter 1

This chapter has been proof read and the English grammar has been corrected as requested by reviewer 2.

Chapter 2

The changes in the scientific precision have been made as assigned by reviewer 2.

Chapter 3

The nomenclature of *Klf5*$^{fl/f}$, *VavCre*$^{+/-}$ has been changed to *Klf5*$^{fl/fl}$*VavCre*$^{+/-}$ for this Chapter.

Chapter 4

No further information was requested for this chapter.

Chapter 5

No further information was requested for this chapter.

Chapter 6

No further information was requested for this chapter.